Surface Modified Polymers for Controlled Macroscopic Functions



Shuyun Chng

Merton College

University of Oxford

A thesis submitted for the degree of

Doctor of Philosophy

Trinity 2016

Abstract

Surface Modified Polymers for Controlled Macroscopic Functions

Shuyun Chng, Merton College, University of Oxford

A thesis submitted for the degree of D.Phil, Trinity Term 2016

This thesis is concerned with the chemical modification of polymer surfaces to confer various functionalities for controlled macroscopic functions, and in particular, photochromic activity and drug delivery. In this collaboration project, the first two years spent in Oxford placed emphasis on the development of a versatile synthetic route for surface modification of polymers with proof of concept. The next two years were spent at the Singapore Institute of Manufacturing Technology (SIMTech) for translational research, which involved the application of the processes developed in Oxford for large area surface engineering, and testing of the surface modified polymers.

Different approaches to modify surface of polymer by chemical methods were investigated, and compared to analogous chemistry in solution. The best surface modification approach was then optimised to determine the most suitable system for translation. A library of polymers with variation in end group, and with expansion of substrate scope, was characterised in detail for chemical and macroscopic properties. In particular, drug delivery properties were investigated using hole-plate bioassays and HPLC-MS methods, and it was found that the antibiotic, Penicillin V, was still active after being loaded onto the polymer scaffolds, with surface modified polymers binding and releasing more drug than the corresponding controls. Incorporation of the spiropyran units on to the polymer surfaces also demonstrated good photochromic activities.

With the transfer of the technology to SIMTech, surface modification processes were re-designed and tested on a variety of 2D engineering polymers. Macroscopic function of photochromic activity, change in surface wettability and drug delivery were investigated.

Lastly, a surprising finding on adhesion function generated from the diaryldiazo compound is disclosed, with preliminary results of lap-shear and t-peel tests showing high levels of adhesion. Moreover, when tested with sol-gel coatings, enhanced adhesion of the coating was found.

Acknowledgement

Firstly, I would like to express my utmost gratitude to Professor Mark Moloney, who has always been the most understanding and encouraging. I greatly appreciate his kind words, immense patience, encouragement and guidance throughout these four years. It was his optimism that shaped my positive outlook and attitude in life and at work. I would also like to thank Dr Linda Wu very much for the kind and strong support, without whom I would not been able to initiate this collaboration project and have such a smooth transition of the project from Oxford to SIMTech.

I am very grateful to all the staff at the Oxford CRL, Merton College and SIMTech who have helped me in one way or another. Special thanks to Ms Wendy Sobey for the immense help with the bioassay agar plates preparation, Dr Ashley Shepherd for the XPS and BET measurements, Dr Robert Jacobs for the ATR-IR and diffused reflectance measurements, Mr Lingzhi Gong for the HPLC-MS setting up, Mr Min Hao Goh and Ms Hong Xie for surface characterisation and instrument booking at SIMTech, Mr Eugene Kok for the help with PDMS preparation and adhesion testing using the Instron Micro Meter, Ms Weiting Ang for all the assistance in the STG lab.

I am also very thankful to the past and present members of the Moloney group, especially to Emily and Alex for the informative discussion about my project, and to my two best friends in lab, Tharindi and Celine for the fruitful discussions, strong encouragement and awesome company throughout the four years. And to my bestie Xinying from SIMTech who have provided me with all the 2D polymers I needed for the project and the continuous encouragement, kindness and friendship.

My papa and mama, my sisters Shuhui and Shuting, and my friends have been the most supportive and understanding throughout. I am really grateful to have them and love them all very much.

Finally, this work would not have been possible without the generous funding from A*STAR Graduate Academy.

Table of Contents

ABBREVIATIONS ..... **I**

1 INTRODUCTION **1**

1.1 Surface Modification of polymers 1

1.2 Macroscopic Functions 12

1.3 Large Area Surface Engineering 21

1.4 Thesis outline 24

2 CHEMICAL MODIFICATION: METHODS AND STRATEGIES **25**

2.1 Introduction 25

2.2 Synthesis of Spiropyran 26

2.3 Direct Modification 27

2.4 Indirect Modification 33

2.5 Direct Modification versus Indirect Modification 35

2.6 Investigation of Chemistry in Solution 37

2.7 Conclusion 45

3 SURFACE MODIFICATION OF POLYMERS **46**

3.1 Introduction 46

3.2 Mod Ax: Pre-activation of polymer surface 48

3.3 Mod Bx': Diazonium salt variation 55

3.4 Mod Cx'': Spiropyran derivatization 63

3.5 Substrate Variation 68

3.6 Surface Engineering for Manufacturing 76

3.7 Surface Characterisation and Analysis 101

3.8 Conclusion 113

4 CONTROLLED MACROSCOPIC FUNCTIONALITIES **115**

4.1 Introduction 115

4.2 Photochromicity Study 115

4.3 DRUG DELIVERY 131
4.4 CONCLUSION 151
5 ADHESION ENHANCEMENT 153
5.1 INTRODUCTION 153
5.2 SUBSTRATE-TO-SUBSTRATE ADHESION 153
5.3 APPLICATION WITH SOL-GEL AS PRIMER 161
5.4 PROPOSED CAUSE OF ADHESION 163
5.5 CONCLUSION 165
6 CONCLUSIONS AND FUTURE WORK 166
7 EXPERIMENTAL 168
8 REFERENCES 204
APPENDIX A: LIST OF SURFACE MODIFIED POLYMERS I
APPENDIX B: COMBUSTION ANALYSIS CALCULATIONS AND RESULTS III
APPENDIX C: LIST OF ATR-IR PEAKS FOR ALL POLYMERS XVIII
APPENDIX D: UV-VIS SPECTRA ON DISC XXI
APPENDIX E: BET DATA AND ANALYSIS ON DISC XXI
APPENDIX F: WCA DATA AND ANALYSIS ON DISC XXI
APPENDIX G: XPS DATA XXII
APPENDIX H: BIOASSAY RESULTS XXV
APPENDIX I: HPLC-MS CALCULATIONS AND RESULTS XXIX

Abbreviations

The following abbreviations are used in this thesis:

aq	Aqueous
Ar	Aryl
ATR-IR	Attenuated total internal reflectance Infrared
Av	Avogadro's number (6.023×10^{23})
^{t}Bu	*tert*-Butyl
°C	Degree Celsius
conc.	Concentrated
E.coli	*Escherichia coli*
Eq.	Equivalents
ESI	Electrospray ionization
Et	Ethyl
FT-IR	Fourier transform infrared spectroscopy
g	Grams
HPLC	High-performance liquid chromatography
H	Hour
HRMS	High resolution mass spectrometry
IR	Infrared Radiation
L	Litres
Lit.	Literature
NBS	*N*-bromosuccinimide
n-BuLi	*n*-Butyllithium
m	Meta
M	Molar
M^{+}	Molecular ion
Me	Methyl
Min	Minute
Mol	Mole
M.P	Melting point
MS	Mass spectrometry
MW	Molecular weight

m/z	Mass to charge ratio
RBF	Round bottom flask
R_f	Retention factor
R.T	Room temperature
NMR	Nuclear magnetic resonance
o	Ortho
p	Para
Pen V	Penicillin V (Phenoxymethylpenicillin)
Ph	Phenyl
R	Alkyl
S. aureus	*Staphylococcus aureus*
Sat.	Saturated
TLC	Thin layer chromatography
Ts	Tosyl
UV	Ultra-violet
v/v	Volume per volume
WCA	Water Contact Angle
Wt	Weight
w/v	Weight per volume
XPS	X-ray photoelectron spectroscopy

Common Solvents abbreviations:

DCM	Dichloromethane
DMSO	Dimethyl sulfoxide
EA	Ethyl Acetate
EtOH	Ethanol
Petrol	Petroleum Ether (BP: 40-60°C)
MeCN	Acetonitrile
MeOH	Methanol
THF	Tetrahydrofuran

NMR abbreviations:

Δ_H	Chemical Shift for Protons
δ_C	Chemical Shift for Carbons

COSY	2-Dimensional Proton Correlation Spectroscopy
d	Doublet
dd	Doublet of doublet
ddd	Doublet of doublet of doublet
DEPT	Distortionless enhancement by polarization transfer
dt / td	Doublet of Triplet/ Triplet of Double
HSQC	Heteronuclear single quantum correlation
Hz	Hertz
J	Coupling Constants
m	Multiplet
ppm	Parts per million
s	Singlet
t	Triplet
tt	Triplet of Triplet

Common polymers abbreviations:

COC	Cyclic Olefin Copolymer
LDPE	Low Density Polyethylene
PC	Polycarbonate
PDMS	Polydimethoxysilane
PE	Polyethylene
PET	Polyethylene Terephthalate
PMMA	Poly(methyl methacrylate)
PP	Polypropylene
PS	Polystyrene
TPU	Thermoplastic Polyurethane
UHMWPE	Ultra High Molecular Weight Polyethylene

1 Introduction

1.1 Surface Modification of polymers

“Polymer” is a term that was first coined by Swedish Chemist Jöns Jakob Berzelius in 1833.[1] With the birth of petrochemical industry post World War II, resulting in the polymer revolution with the explosion of the plastic age, polymers have since found their way into numerous consumer products and industrial applications. With an annual production of plastic pellets of more than 250 billion pounds in weight from petroleum feedstock, synthetic polymers are the most widespread man-made material in the world.[2] While polymers are often utilized for their favourable bulk properties, such as mechanical strength, and unique phase behaviour for injection moulding and extrusion into desired shapes and forms, their surface properties are often less than ideal for the desired applications. This can result in many problems, such as delamination of an adhesive layer, biofouling of membranes, or bacteria growth on catheters.[3] The modification of the surface of polymers in order to control surface interactions and functions is one way of controlling these difficulties for particular applications.

1.1.1 Surface Modification Techniques

Since the surface of polymers can be relatively inert, a wide range of surface treatment techniques have been development and have evolved over the years. In general, surface modification techniques can be classified into three broad categories: physico-chemical, mechanical and biological methods.[3]

Physico-chemical methods can be further classified into:

a) Gas phase methods, which usually employ gases that contain active species such as free radicals, electrons, ions, or electromagnetic radiations. Examples include: Chemical Vapour Deposition (CVD); Plasma Vapour Deposition (PVD); and etching or oxidising using corona discharge or ion beam.

(b) Liquid and bulk phase methods, which involve physical desorption from a bulk phase, or chemical reactions at the surface. Examples include solution deposition of surface-assembled monolayers (SAMs), chemical treatments using oxidants, sulfonylation or acetylation to modify surface groups of polymers, or conjugation of molecules such as attaching silanating agents to surface groups.

(c) Combination of (a) and (b), which include graft or interpenetrating network (IPN) polymerisation with initiation using ionizing radiation or ozone, followed by polymerisation, or microlithography.

Although widely used and effective, many of these surface modification techniques suffer the drawbacks of requiring large infrastructures, very harsh reaction conditions, or high operation and equipment costs. Of interest in this thesis is the development of a wet chemistry method which requires simple infrastructure for surface modification of polymers.

1.1.2 Surface modification using diarylcarbenes

Diarylcarbenes has been extensively studied [4-6] and the Moloney group has made significant advances in using diarylcarbenes for the surface modification of various materials for various applications. This section examines the use of these diarylcarbenes for surface modification.

1.1.2.1 Reactivity of carbenes

Carbenes are neutral species containing a carbon atom with only six valence electrons. Often represented as **:**CH_2, carbenes can exist in two possible electronic structures - as a singlet or as a triplet. While a singlet carbene has a pair of electrons in a non-bonding sp^2 orbital and has an empty p orbital (**Figure 1.1**), a triplet carbene has two unpaired electrons, one in an sp^2 orbital, one in a p orbital, which resembles a di-radical (**Figure 1.2**).

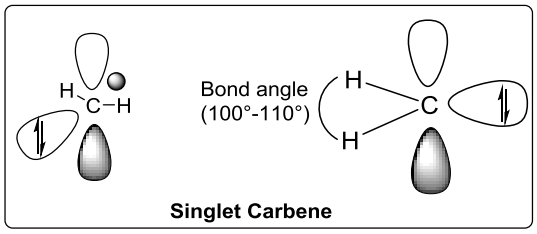


Figure 1.1. Structure of carbene in singlet state.[7]

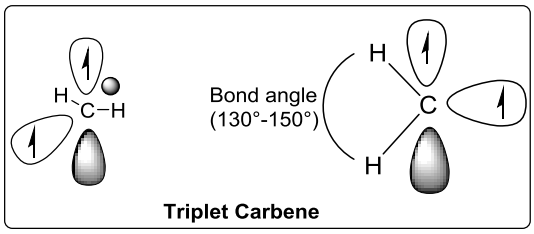


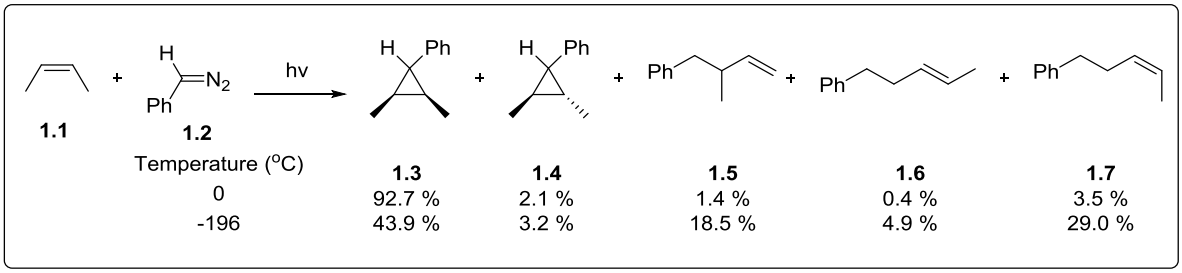
Figure 1.2. Structure of carbene in triplet state.[7]

According to Hund's rule, most carbenes are more stable in the triplet state as the energy gained by bringing the electron in the p orbital to the sp^2 orbital for more s character does not offset the repulsion that exists between the two spin-paired electrons in one orbital.

Reactivity in solution: The early study of carbene reactions by Woodworth and Skell suggested that characteristics of reaction of triplet carbenes would differ from those of the singlet carbene,[8, 9] and this is known as the Skell-Woodworth rule. While singlet carbene addition is a one-step, concerted reaction and is stereospecific, triplet carbene addition is step-wise and non-stereospecific. Therefore, the mechanism of the reaction would differ depending on whether the carbene is in singlet or triplet form. However, for carbenes with relatively small singlet-triplet gaps, interchanging of the singlet and triplet state is often faster than the reaction of

the triplet. When this happens, reactions may proceed via singlet forms even though only small amount of singlet forms exist in equilibrium with triplet forms.[10]

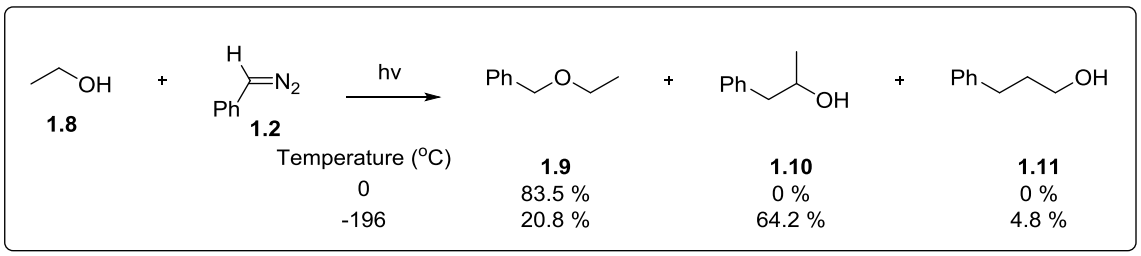
Reactivity in solid matrix: Of greater interest and relevance to the work in this thesis is carbene reactivity in a solid matrix. The work conducted by Moss *et.al.* revealed that reactions of arylcarbenes in solidified olefinic matrices are very different from those conducted in the solution phase.[11]



Scheme 1.1. Photolysis of phenyldiazomethane in cis-but-2-ene matrice.

Phenyldiazomethane (**1.2**) when photolysed to yield the corresponding carbene, reacted with *cis*-but-2-ene (**1.1**) to give *cis*-1,2-dimethyl-3-phenylcyclopropane **1.3** as the major product, thus, illustrating that the carbene reacted with the olefin predominantly in singlet form. However, when photo-irradiation of **1.2** was conducted at -196°C with **1.1** as a solid matrix, there was a change in product distribution, with significant increase in yields of 3-benzylbut-1-ene (**1.5**) and cis-5-phenylpent-2-ene (**1.7**). While **1.5** and **1.6** were the result of H-atom abstraction by the triplet carbene, **1.7** was suggested to be formed by allylic H-atom abstraction.

The work reported by Moss and co-workers[11-14] inspired Tomioka and his co-workers to explore reaction of phenylcarbenes in solidified alcohols.[15-18]



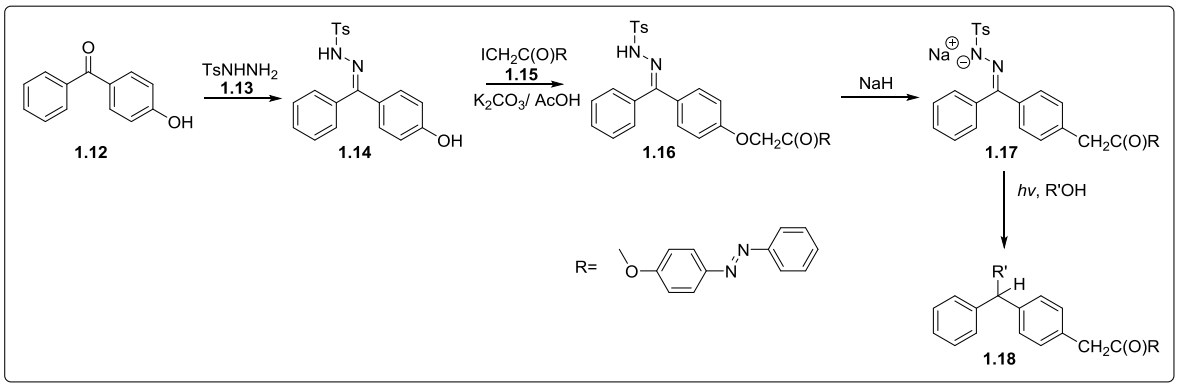
Scheme 1.2. Photolysis of phenyldiazomethane in ethanol matrice.

Tomioka and Izawa[16] found that reaction of the arylcarbene with solidified ethanol at -196°C differed from that of the reaction conducted in solution phase ethanol. The reaction in ethanol solution at 0°C yielded benzyl ethyl ether (**1.9**) as the sole product, whereas reaction with solidified ethanol resulted in 2-phenylpropan-2-ol (**1.10**) as the major product. While singlet carbenes are trapped efficiently by O-H bonds to yield ethers, triplet carbenes tend to undergo H-atom abstraction of C-H bonds to give product mixtures resulting from radical pair. This demonstrated that reaction of the arylcarbene with solidified ethanol at low temperature was more prevalent in the triplet form compared to singlet form.

Work done by Moss *et. al.* [11-14] and Tomioka *et. al*.[15-18] showed that triplet carbene reactions dominated in solidified organic matrices at low temperature. In his review about reactions of carbenes in solidified organic media at low temperature, Tomioka[19] concluded that H-atom quantum tunnelling to triplet carbene is the possible reason for the significant increase in C-H insertion products. For the work presented in this thesis, it can be expected that a series of diarylcarbene insertion reactions, particularly C-H insertion, would take place on the surface of the polymers leading to introduction of functionality onto the polymer surfaces. Whether insertion reactions takes place through the quantum tunnelling approach, or through classical mechanistic pathways, the overall outcome of irreversible covalent bond formed for functionalisation of the polymer surface is of greater importance and interest.

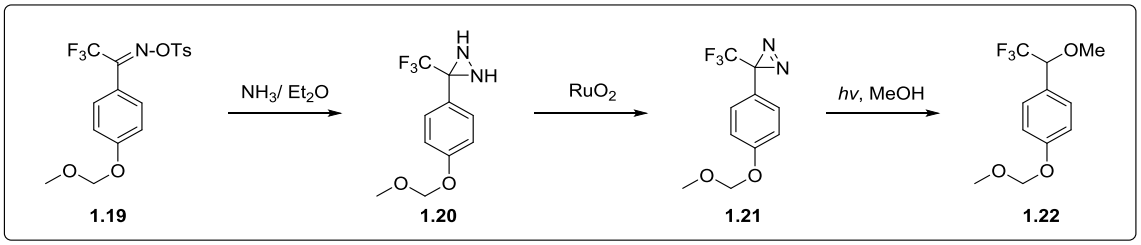
1.1.2.2 Generation of diarylcarbene

Diarylcarbenes can be easily generated via photolysis, and the presence of 2 aromatic rings allowed for greater convenience in functionalisation with other functional moieties. Moloney and Braybrook[20] demonstrated the preparation of diarylcarbenes as photoactivable reactive dyes from tosylhydrazone (**Scheme 1.3**).



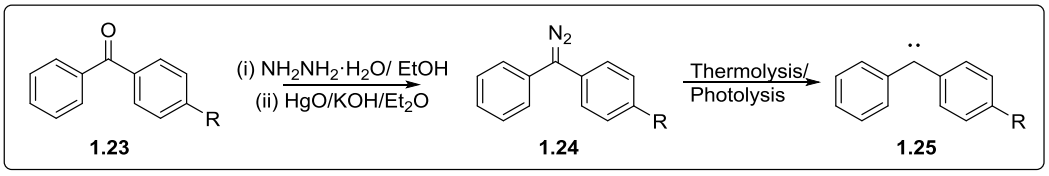
Scheme 1.3. Generation of diarylcarbene from tosylhydrazone, with reactive dye attached.

Treating *p*-hydroxybenzophenone (**1.12**) with 4-toluenesulfonyl hydrazine (**1.13**) yielded the tosylhydrazone (**1.14**), which was then further reacted with iodoacetylester (**1.15**) in basic conditions to give intermediate (**1.16**). Conversion of the tosylhydrazone to sodium salt (**1.17**), followed by photolysis in alcohol to generate the corresponding diarylcarbene, gave the desired photoproducts (**1.18**). However, this method suffered from low yields and sensitivity of the diarylcarbene reactivity to the nature of the solvent. Investigation of alternative diarylcarbene precursors was made.



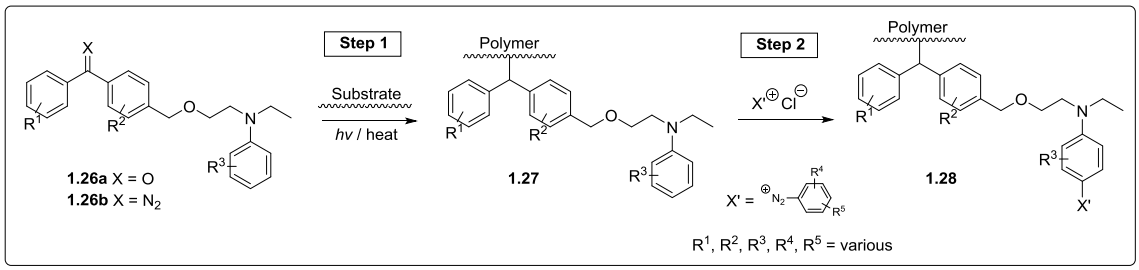
Scheme 1.4. Generation of diazirinyl-substituted photoactivable dye.

Moloney and Braybrook[20] modified a photoactive dye with a diazirinyl group (**Scheme 1.4**) to investigate diarylcarbene generation. The synthesis was somewhat more lengthy, and the yields of the photoproduct were again low. Moreover, the diaryl group proved to be difficult to further functionalise. Thus, this route of using diazirine to generate diarylcarbene was discontinued. However, Hayes *et.al.*[21] subsequently managed to photoinduce the attachment of a diazirine derivative onto nylon-6,6. Further work established by Moloney *et.al.*[22-26] demonstrated that diaryldiazo compounds are an excellent alternative to diazirines as diarylcarbene precursors.



Scheme 1.5. Generation of a diarylcarbene from diaryldiazo compound.

Diaryldiazo systems (**1.24**) can be readily prepared from the benzophenone (**1.23**) in a two-step synthesis via a hydrazone intermediate (**Scheme 1.5**). Diarylcarbenes (**1.25**), as highly reactive intermediates, can then be generated from the relevant diaryldiazo (**1.24**) via thermolysis or photolysis. This was first used for the irreversible dyeing of polymers, including PS, PE, nylon, silica and to some extent, PTFE.[24]



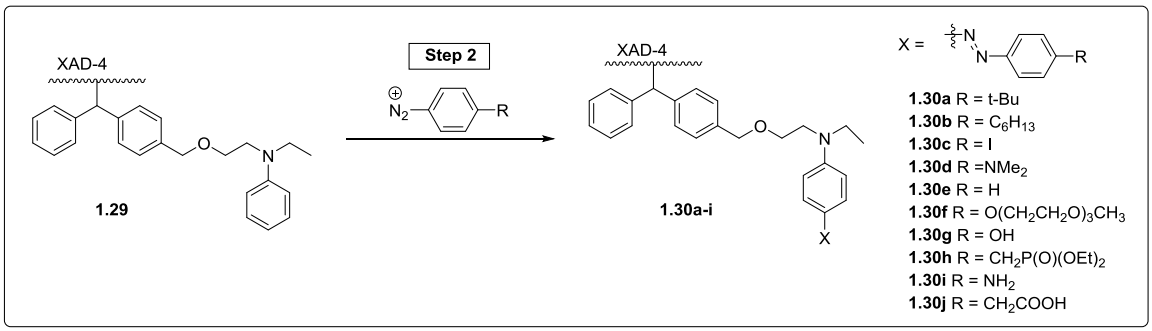
Scheme 1.6. Surface functionalisation of materials.

Surface of the polymer was first pre-activated with an electron-rich aryl group in **Step 1** via the highly reactive diarylcarbene intermediate, followed by post modification of the polymers using azo coupling with various azo dyes in **Step 2** (**Scheme 1.6**). The coloured products proved the effectiveness and efficacy of this surface modification process (see **Figure 1.3** below). Having demonstrated that this surface modification method is reliable and practical, further development using this method was explored.

1.1.2.3 Functionalisation of surfaces

Using the reaction route described in **Scheme 1.6** as the general surface modification method, the Moloney group further developed this approach to include various chemical moieties for valuable functions, some of which are briefly reviewed below.

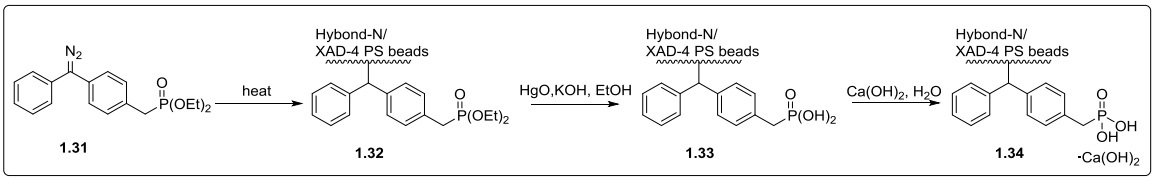
Protein binding: Instead of coupling with azo dyes, surface modified XAD-4 polystyrene beads were coupled with a variety of diazonium salts to investigate the effects these chemical moieties have on protein binding.[27]



Scheme 1.7. Surface modified XAD-4 bead for protein binding.

This investigation that was performed with bovine serum albumin (BSA) showed that **1.30a**, **b**, **d**, **i** and **j** gave high binding affinity, while **1.30e**, **f** and **g** gave protein binding lower than the control. A more recent work described the characterisation of these *in-situ* BSA protein adsorptions onto similarly surface modified polystyrene thin film using real-time quartz crystal microbalance with dissipation (QCM-D), providing direct evidence for the adherence at the surface.[28]

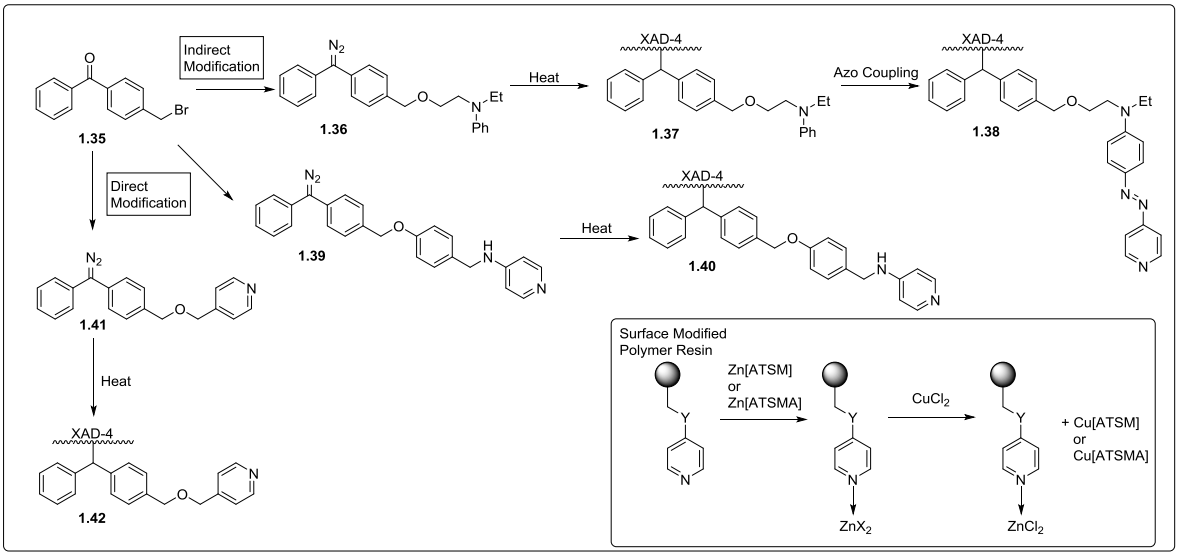
Biocompatibility: Using XAD-4 polystyrene beads and Hybond-N (a nylon membrane) as polymeric substrates, enhanced biocompatibility was observed when phosphonate residues were introduced onto the polymer surfaces (**Scheme 1.8**).[29]



Scheme 1.8. Surface modification of polymer with phosphonate group.

The diaryldiazo unit with the phosphonate derivative was first inserted onto the surface, which was further treated with calcium hydroxide to form the calcium phosphonate derivative. Testing of these surface modified polymers with MG63 human osteosarcoma cell line showed improved growth of the cells on the modified surface, indicating that enhanced biocompatibility can be tailored onto surface of polymers using a simple chemical method.

Metal Chelation: The surface of XAD-4 polystyrene beads can also be functionalised to be used to anchor metal chelating ligands.[30]

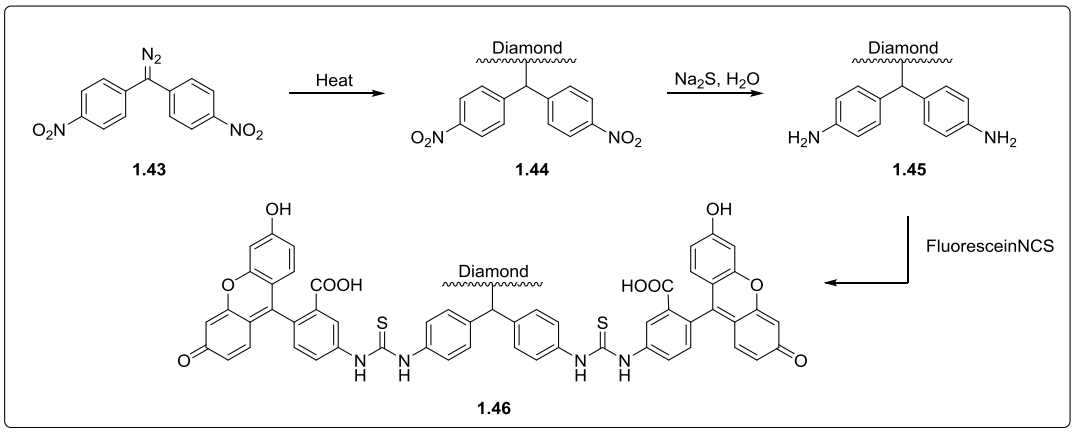


Scheme 1.9. Surface functionalisation of XAD-4 beads for metal chelation.

Using a common precursor (**1.35**), a multipronged approach was employed for functionalising the surface of XAD-4 polystyrene beads with pyridine residues. The surface of the polymer could first be pre-activated with an electron rich aromatic ring (**1.37**) followed by azo coupling reaction with the appropriate diazonium salt to confer the pyridine moiety onto the surface of the molecule (**1.38**). Alternatively, the pyridine residue could first be incorporated into the diaryldiazo (**1.39** and **1.41**), then functionalised onto the polymer surface (**1.40** and **1.42**). A library of polymers were evaluated and showed to be capable of binding Zn[ATSM] and Zn[ATSMA] ligands. Ligand exchange was demonstrated when immersed in a Cu^{2+} containing solution to generate Cu[ATSM] and Cu[ATSMA] in solution. This work not only demonstrated the ability of surface-functionalised polymers to act as anchoring agents to introduce metal-chelating ligands onto surface of polymers, but also showed the ability to quickly create a library of chelating polymers from a common precursor. As shown in **Scheme 1.9**, the approach to introduce chemical moieties

onto a polymer surface in order to confer functions can be done in two ways. One way is to incorporate the desired moiety into the diaryldiazo compound prior to surface modification, termed as direct modification. Alternatively, this can be done by post-surface modification, termed as indirect modification. Both direct and indirect modification methods are further investigated in Chapter 2.

Fluorescence activity: The surface modification technique developed was also demonstrated to be applicable to other materials.[31]



Scheme 1.10. Surface modification of CVD diamond for fluorescence activity.

As shown in Scheme **1.10**, the diarlycarbene derivative was generated from diarlydiazo 1.35 via thermolysis for the surface modification of diamond sample prepared by CVD. The NO_2 side group was then reduced to NH_2 for further reaction with fluorescein derivative for incorporation of fluorescent functional moiety on the surface of the diamond sample.

Fluorescence activity achieved upon surface modification of CVD diamond (see **Figure 1.4** below) not only demonstrated the ability of diarylcarbenes to modify a very inert surface, but also showed that this surface modification method can be used in combination with other surface modification methods.

Other than the above-mentioned surface functionalisation, the Moloney group also explored many other types of surface functionality that have been previously

introduced, including biocidal,[32] hydrophobic,[33] and end-group effects,[34, 35] onto a wide variety of substrates.[26, 36]



Figure 1.3. Highly coloured surface modified silica.[24]

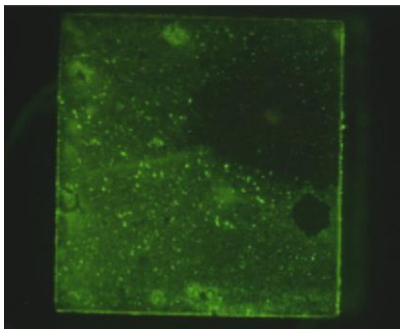


Figure 1.4. Fluorescence on CVD diamond sample.[31]

1.2 Macroscopic Functions

'Macroscopic' is defined as being visible to the eyes without the aid of magnifying tools, and 'function' means the activity to serve certain purpose. Therefore, the term 'macroscopic functions' simply means having activities that serve certain purposes that are visible to the eye. Various macroscopic functions such as dyeing,[24] metal chelation,[30] enhance biocompatibility,[29] fluorescence activity[31] and many others[27, 28, 32, 33, 36, 37] were explored by the Moloney group by means of surface functionalisation of polymers, as briefly reviewed in the previous section. The work in this thesis focuses on the introduction of a spiropyran residue for photochromic activity and possible drug delivery.

1.2.1 Photochromism

'Chromism' is defined as reversible change in colour, and by extension, a reversible change of other physical properties.[38] There are many forms of 'chromism', and these colour change phenomena are classified and named after the stimulus that resulted in the colour change, usually as the prefix.[39] For example, colour change brought about by heat is known as thermo-chromism, while colour change due to

electric current is known as electro-chromism. (See **Table 1.1** for list of chromic phenomena). In particular, photochromism is of interest in the study reported in this thesis due to ease and convenient alteration of physical properties through controlled use of UV or visible light radiation.

Table 1.1. Various colour change phenomena, their stimuli and application.[39]

Phenomena	Stimulus	Applications
Photochromism	Light	Ophthalmic lenses, novelty printing, security printing, cosmetics, optical data storage, memories and switches, sensors
Thermochromism	Heat	Thermochromic pigments, temperature indicators and thermometers, security and novel printing
Electrochromism	Electric current	Windows, mirrors, displays
Solvatochromism	Solvent polarity	Colour formers, thermal fax papers, indicators, metal ion detectors
Ionochromism	Ions	
Halochromism	pH changes	
Tribochromism	Mechanical friction	
Piezochromism	Mechanical pressure	

Photochromism can be defined as the reversible transformation of chemical species between two isomeric states having different absorption spectra, *i.e.* different colour.[40] This change is often accompanied by different physical and chemical properties, such as geometrical structures, oxidation-reduction potentials, dielectric constants, and refractive indices in the two isomers. Photochromic compounds have found applications in ophthalmic lenses and optoelectronic devices for optical data storage, memories and switches, sensors and holographic security printing (**Table 1.1**).[39] These dynamic materials also have great potential in emerging applications such as “smart” windows for energy-efficient buildings, self-healing coatings and reusable self-erasing paper.[41]

1.2.1.1 Classification of photochromic compounds

Ideal properties required from organic photochromic compounds include:[38]

1) rapid, strong colour development when irradiated with UV light;
2) controllable reversal to the colourless state;
3) having a wide range of colours across the visible spectrum;
4) having long life, with constant response or colour intensity throughout many irradiation cycles; and
5) having a rest state that has little or no colour.

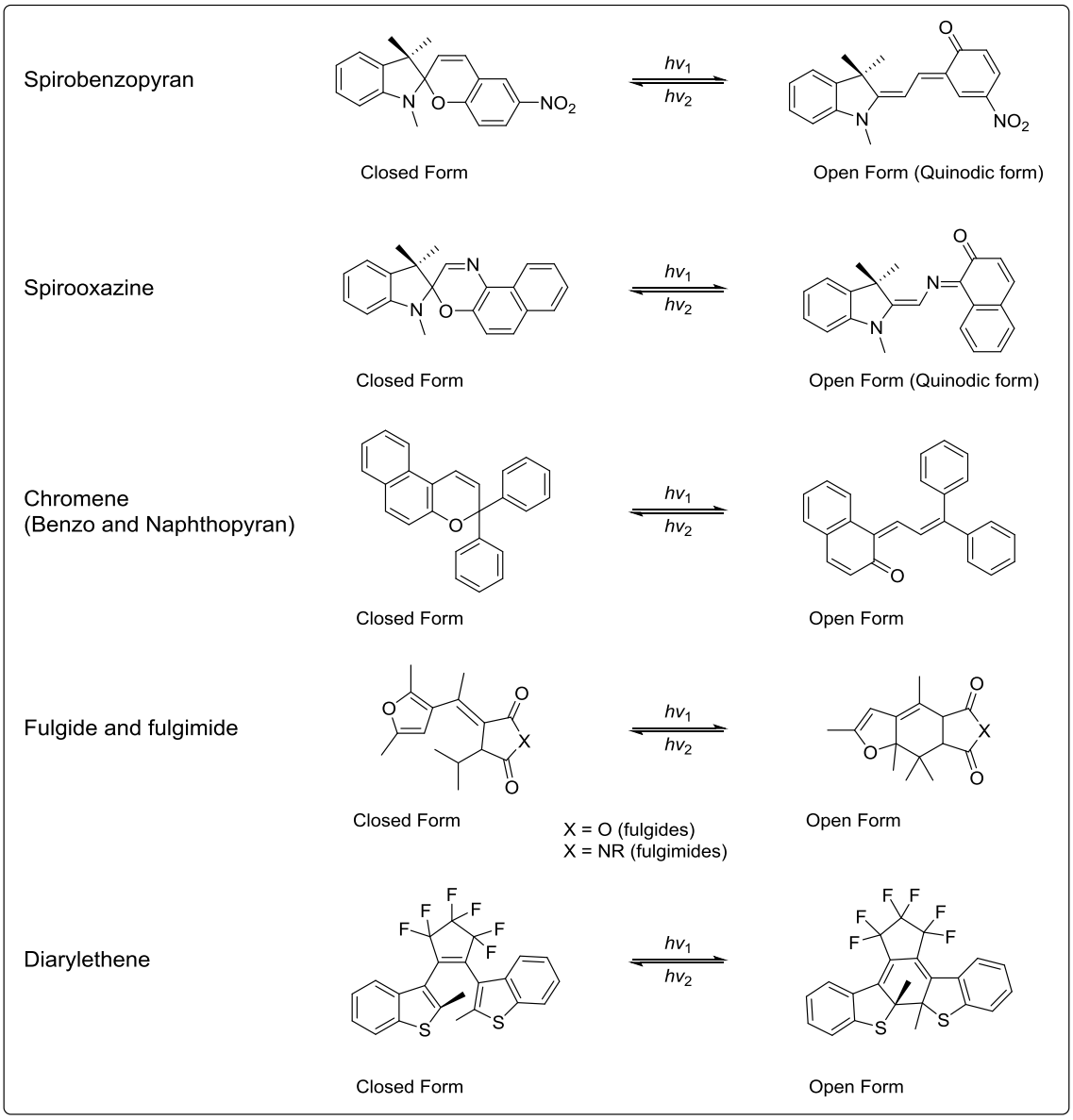


Figure 1.5. Different families of organic photochromic compounds. In all cases, $hv_2 < hv_1$.

Photochromic compounds can be classified according to their general structures. Five main common classes of photochromic compounds which approach these ideal requires are spiropyrans, in particular spirobenzopyrans and spirooxazines, chromenes, fulgides and diarylethenes (see **Figure 1.5**).[38] Other miscellaneous photochromic systems not included in **Figure 1.5** include spirodihydroindolizines, azo compounds, polycyclic aromatic compounds, anils and related compounds, polycyclic quinones, perimidinespirocyclohexadienones, viologens and triarylmethanes. There are also many biological systems that are photochromic, such as retinal proteins and phytochrome. However, very few of these compounds remain photochromic when isolated from living cells or systems. [38, 42]

As one of the most widely studied photochromic class of compounds,[40, 42-44] spiropyrans are of interest in this thesis, due to ease of controlling and switching forms, and hence, physical properties for various macroscopic functions, using UV irradiation of various wavelengths.

1.2.1.2 Spiropyran and its properties

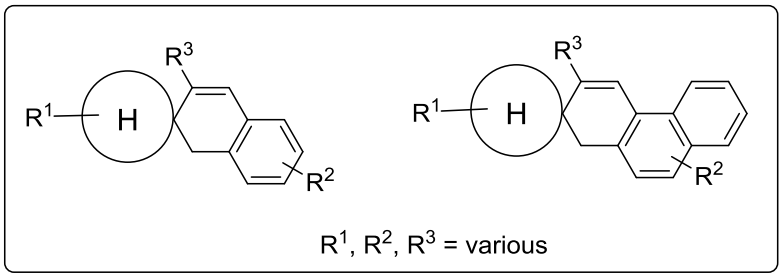
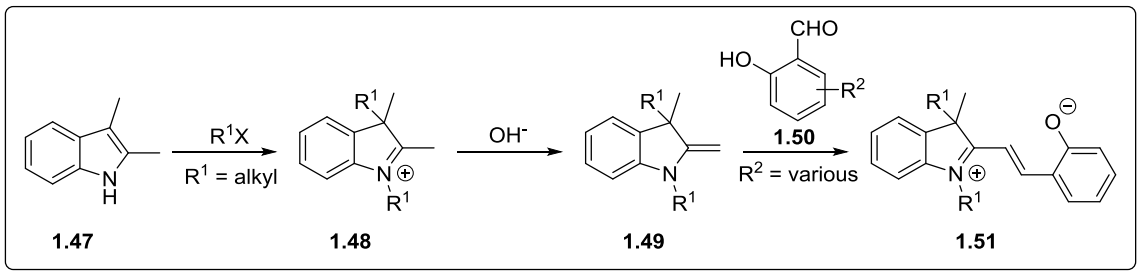


Figure 1.6. Heteroocyclic (H)-spiro-Benzopyran or Napthopyran.

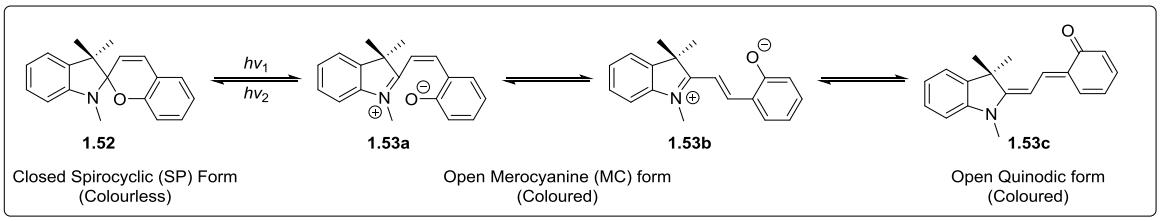
Spiropyrans are usually made up of two heterocyclic parts linked together by a sp^3 carbon. Varying the components of the spiropyran gave numerous possibilities of the structures; the heterocylic part (labelled 'H' in **Figure 1.6**) can be made up of azaheterocyclics ranging from indoline, benzothiazoline to pyrrolidine, quinoline, or non-azoheterocylics such as xanthene or dithiole, while the pyran ring is either be a

benzo or naphthopyran. Many other different chemical moieties (R) or can also be attached to these heterocyclic ring systems.[45]



Scheme 1.11. General synthetic route of spirobenzopyran and its derivatives.

A general synthetic pathway for the synthesis of spirobenzopyran is shown in **Scheme 1.11**; by condensation of a Fischer's base **1.49** with salicylaldehyde **1.50**, the desired spirobenzopyran **1.51** can be synthesized. Indolinium compound with different alkyl groups R^1, or salicylaldehydes with different side groups R^2, can be used as well. However, the condensation reaction usually requires long hours of reflux, and purification of the spirobenzopyran through flash column usually results in loss of product.



Scheme 1.12. Photochromic interconversion of spiropyran.

While thermochromism of spiropyrans was noted in 1921, photochromism of this class of compounds was only observed later in 1952 by Fischer and Hirshberg.[46] UV irradiation of the closed spirocyclic (SP) form at about 365 nm give rise to the open-ring merocyanine (MC) form. Extensive investigation showed that this ring opening is a first order process[47] and the photoisomerism begins with the cleavage of the C_{spiro}-O bond, to give cis-MC,[48] followed by rotation about the C-C bond[49] to yield trans-MC (**Scheme 1.12**). Non-polar solvent would generally stabilise the

quinoidal form.[50] The reverse photoisomerism from MC to SP form is usually a first-order spontaneous process, which can be accelerated by visible light.

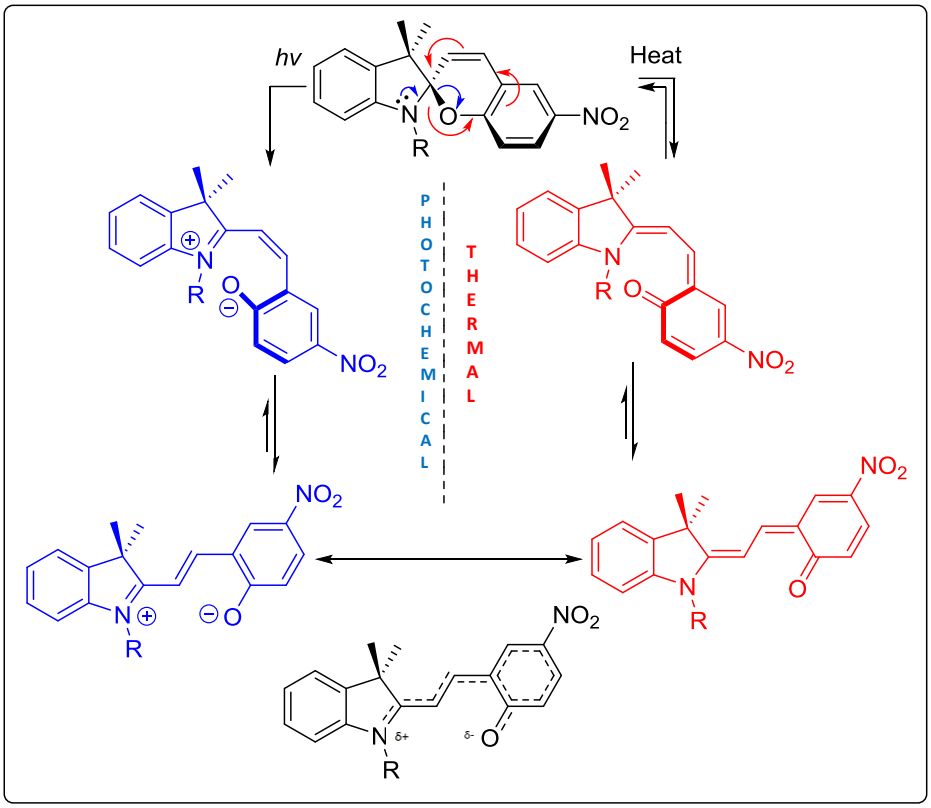


Figure 1.7. Proposed mechanism for photochemical and thermal ring opening of spiropyran.[41]

The ring opening reaction can either be due to heterolytic cleavage of the C_{spiro}-O bond, or via a 6 π electrocyclic ring-opening mechanism. While the former is related to the mechanism for photochromism and the latter is linked to thermochromism of spiropyrans (see **Figure 1.7**),[41] investigation performed by Swansburg and co-workers[51] demonstrated that solvent polarity also affect the ring-opening mechanism. The "polar mechanism" involves the C_{spiro}-O bond cleavage with anchimeric assistance by the nitrogen from indoline moiety, whereas the "non-polar" electrocyclic ring-opening mechanism does not involve anchimeric assistance by the indoline nitrogen. As the work in this thesis focuses on the photochromism of the spiropyran, ring-opening mechanism was deemed to be more closely associated with the C_{spiro}-O bond cleavage.

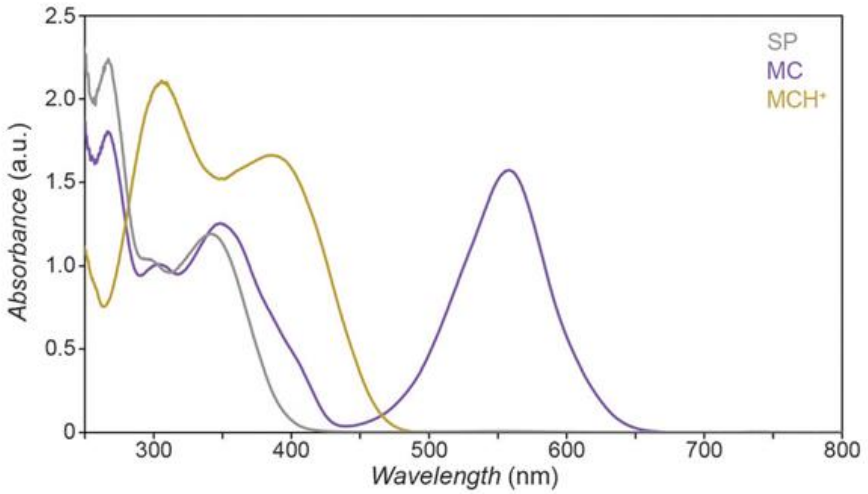


Figure 1.8. Typical photochromic UV-Vis spectra of Spiropyran in spirocyclic (SP) form, merocyanine (MC) form, and protonated merocyanine (MCH^+) form.[41]

In the closed SP form, the two heterocyclic halves are orthogonal and electronically isolated. However, upon UV-irradiation, heterolytic cleavage of the C_{spiro}-O bond results in the molecule adopting a virtually planar geometry. This allows for the overlapping of π electrons of both heterocyclic rings, thus resulting in the open MC form having electronic transition in the visible region and exhibiting colour.[52] Generally, the colourless form absorbs more strongly than the coloured form at around 250 nm, whereas the coloured form absorbs strongly at around 320 – 400 nm, and 450 – 600 nm (see **Figure 1.8**).[41] However, as the open forms are usually thermally unstable, it was necessary to use a rapid scanning spectrophotometer to measure absorption spectra of the coloured forms.[42] While spiropyrans are thermochromic, Hirshberg and Fischer[53, 54] observed that the absorption spectra of several open form MCs changed significantly with varied temperatures. These effects were attributed to a change in position of the thermal equilibrium of the coloured species, which may include formation of dimers and higher aggregates. On the other hand, spiropyrans and their aggregates can also exhibit strong solvatochromism, as the spectra undergo hypsochromic shifts with increase in solvent polarity.[55]

1.2.1.3 Spiropyran on solid surfaces

While spiropyrans are not photochromic when in solid form, they can still display phototchromism when dissolved or dispersed in gels, films, plastic resins or solids.[52] Compared to spiropyrans in solvents, it was noted that immobilisation of spiropyran onto a surface was able to reduced photodegradation of the photochromic compound,[56] and tailor the photochromic switching behaviour better.[57] It was also observed that immobilisation affects the isomerisation kinetics; the coloured merocyanine form is more stable when immobilised on surface, with coloured form lasting up to hours, whereas dissolved merocyanine converts back to colourless spirocyclic form within seconds.[58] More importantly, it is necessary for the spiropyran to be covalently attached to various supports so that the spiropyran unit can be sufficiently robust and be able to meet requirements of practical applications.

Extensive work had been done by various groups to immobilise spiropyrans on various supports for a variety of purposes. Sumaru *et. al*.[59-61] have pioneered the incorporation of spiropyrans into crosslinked hydrogels to be used as light-actuated microvalves in microfluidic chips. Davis and co-workers[62] incorporated spiropyran into chain of bulk polymers and subjected the polymer to tensile strength tests to demonstrate the piezochromism of spiropyran. Interestingly, spiropyran-functionalised biopolymers were found to be useful for the photocontrol of polypeptide conformations and,[63, 64] enzymatic activities.[65, 66] Transport through proteins can also be photocontrolled using spiropyran by increasing binding selectivity of selected proteins.[67, 68] Immobilisation of the spiropyran moieties on solid supports enabled tailored control of macroscopic properties such as surface wettability, surface binding of metal ions and other surface properties. [41] A review

by Klajn[41] discussed the immobilisation of spiropyran on various supports in greater detail.

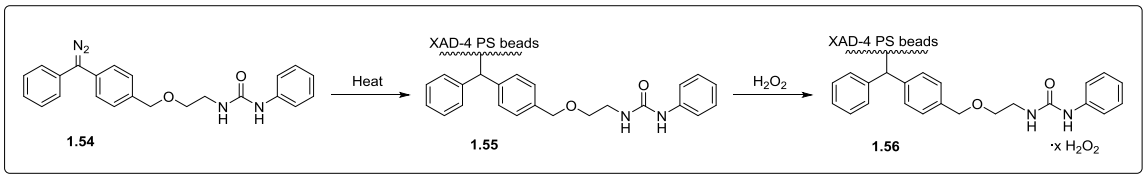
It was of interest of this thesis to demonstrate the possible control of surface macroscopic function though the photochromism of spiropyran immobilised on polymer surface through surface modification of the polymers.

1.2.2 Drug delivery

The increased resistance of antibiotics is of increasing concern worldwide, and indiscriminate use is of antibiotics is one of the major causes of this.[69, 70] While various organisations, such as the World Health Organisation, have endeavoured to improve the current situation through policy formulation,[71] there are increasing calls for more investment into new antibiotics research.[72, 73] In this work, the term 'drug delivery' is simply defined as the ability of the material to bind and release drugs, in particular, antibiotics such as penicillin, and is concerned with using minimal amount of antibiotics for samples preparation for drug delivery via surface modification.

1.2.2.1 Drug binding and release: bulk vs surface

Most approaches for incorporation of drugs into polymer for site-specific drug delivery include blending the drug into the polymer bulk,[74] so that the drug would usually be released either through slow or controlled diffusion,[75-77] controlled morphologies of the polymer,[78] or by burst release through degradation of the polymer.[79, 80] However, sample preparation using these methods usually requires significant amounts of the drugs for good dispersion and subsequent diffusion from the bulk. The investigation for biocidal activity performed by the Moloney group used a different approach, and demonstrated that hydrogen peroxide can be bound on the surface-modified polymer for biocidal activity.[32]



Scheme 1.13. Surface modification of polymer for binding of hydrogen peroxide.

As hydrogen peroxide exists in a stable urea complex, introducing urea and thiourea group in the diaryldiazo enabled the urea group to be functionalised onto the surface of a polymer. The surface-modified polymer was then loaded with hydrogen peroxide and tested by bioassays. These surface-modified polymers were found to have very effective activity against both Gram-positive and Gram-negative bacteria. Therefore, it was of interest for the work in this thesis to investigate if surface modification on a polymer could also bind and release drugs, in particular, using very small amount of drugs for topical drug delivery.

1.3 Large Area Surface Engineering

As a discipline founded by Tom Bell in the 1980s,[81, 82] surface engineering refers to a wide range of technologies and processes designed to modify the surface and near surface regions of a material to introduce functions that are different from the bulk of the materials.[83] These technologies can be broadly categorised into two classes, namely surface coating and surface modification.[84] While surface modification discussed in the section above is a subset of surface engineering, the latter focuses more on feasible technology for large scale processes and manufacturing applications. The complexity is greater when considering surface engineering for manufacturing, for which cost and process upscaling become very important.[85]

1.3.1 Greater emphasis on 'Lab-to-Market' translational research

Despite reports of numerous innovative surface modification methods, few of these have been put into industrial uses. While researchers generally aim to prove a hypothesis or concept, issues such as economies of scale were usually not taken into consideration. This usually resulted in the innovation having high degree of complexity in its fabrication and processes.[86] Thus, synthesis route or surface modification steps could not be easily translated into scalable process that can be readily streamlined into a manufacturing process. With increasing emphasis for industries to embark on strategic change to further develop new capabilities to customers in the high value manufacturing sector,[87] these industries are turning to academic research and development for novel solutions. The need for the strategic partnership between universities and industries is intensified with the rise of a global knowledge economy.[88] Consequently, there is an increasing focus on 'Lab-to-Market' translational research, with more industrial research collaborations aiming to bridge the gaps between research and development performed at laboratory scale.

Some of the work described in this thesis is a collaboration project between the Singapore Institute of Manufacturing Technology (SIMTech) and the Moloney group. The first two years were spent at the University of Oxford in the Moloney group in attempt to devise and optimise synthetic chemical routes most suitable for feasible upscaling surface modification of polymers for various macroscopic functions. The next two years encompassed research undertaken at SIMTech endeavouring to translate this research from fundamental laboratory scale synthesis to a feasible process for large area processing.

1.3.2 Choice of polymers

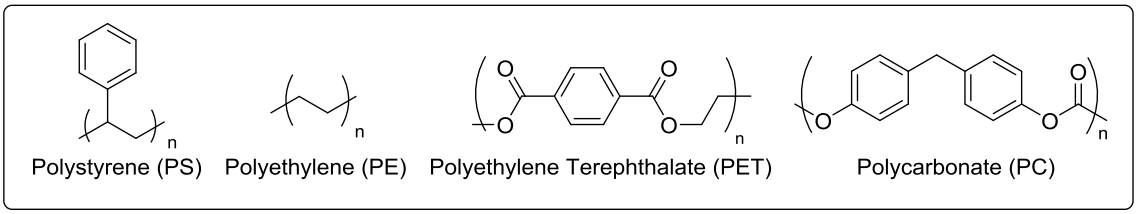


Figure 1.9. Choices of polymers.

Developed by Rohm and Haas Company, Amberlite® XAD-4 beads were chosen as the model material for the study for the development and optimisation of the synthesis and surface modifications, because they are safe to work with, well characterised and readily available commercially. These highly crosslinked polystyrene-type polymeric beads are solvent resistant and porous, with surface area of 725 m^2/g, 50 Å of mean pore size, 0.35 – 1.18 mm particle size.[89, 90] XAD-4 beads were favourable for this optimisation study because of their high surface area and ease of handling. They were also a good representation of typical non-polar hydrocarbon polymer containing only crosslinked by unsubstituted aryl groups and saturated hydrocarbon chains. This allowed for the demonstration of the functionalisation of surfaces of relatively inert polymers using the chemical modification method developed. Comprising about 80% of the chemical industry output worldwide,[91] engineering and commodity polymers such as polyethylene (PE), polyethylene terephthalate (PET), polystyrene (PS), polycarbonate (PC) and polypropylene are more challenging substrates from a chemical perspective, but would be useful in demonstrating the versatility of the surface modification method developed, and for this reason were included in later development work.

1.4 Thesis outline

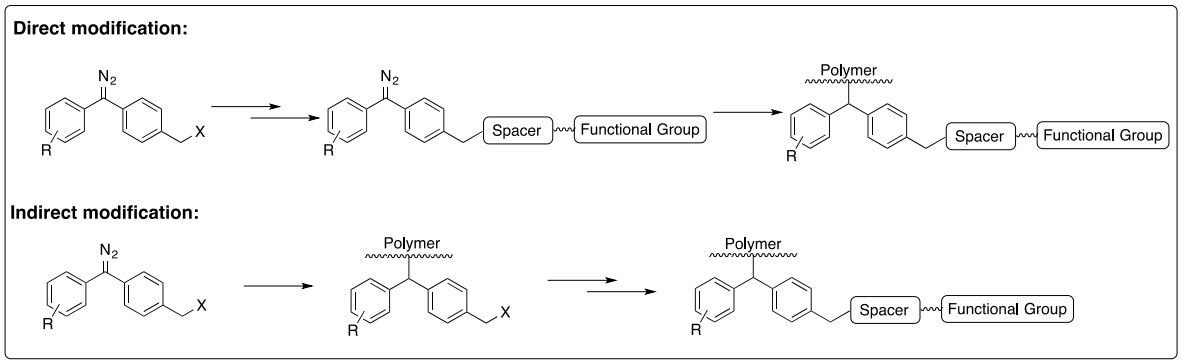
This thesis is concerned with the development and optimisation of organic synthetic routes and processes that are versatile and scalable for translational surface modification of polymers, with the incorporation of functional moieties suitable for macroscopic functions of photochromic activity and drug delivery.

Two different approaches to modify surface of XAD-4 PS beads were examined in **Chapter 2** to determine the preferred method; the direct modification method, which incorporated desired functional moiety into a diaryldiazo structure prior to generation of diarylcarbene for surface modification, or indirect modification method, which uses post surface modification azo-coupling to confer functionalities. Analogues of surface modification were synthesized for investigation of the chemistry of the surface modification. **Chapter 3** covers the surface modification of polymers. from the optimisation of proposed surface-modification route using XAD-4 PS beads, and polymer substrate variation to the development of surface modification processes for translation into feasible large area surface engineering. Various surface characterisation methods and their limitations were also discussed. The controlled macroscopic functions of the surface-modified polymers were then examined in **Chapter 4,** for their photochromic activity and drug delivery capabilities, with comparison to analogues synthesized. Finally, a surprising discovery of enhanced adhesion was examined with preliminary findings reported in **Chapter 5**.

2 Chemical Modification: Methods and Strategies

2.1 Introduction

In the Introduction, it was shown that the surfaces of polymers can be modified chemically to tailor desirable functions and applications while retaining the favourable bulk properties of the polymers. This chapter focuses on the exploration of carbene chemistry developed in the Moloney group for the functionalisation of polymer surfaces. A key goal has been to transfer the fundamental synthesis and surface modification techniques to further translational application, in particular using the expertise and facilities at SIMTech (Singapore).

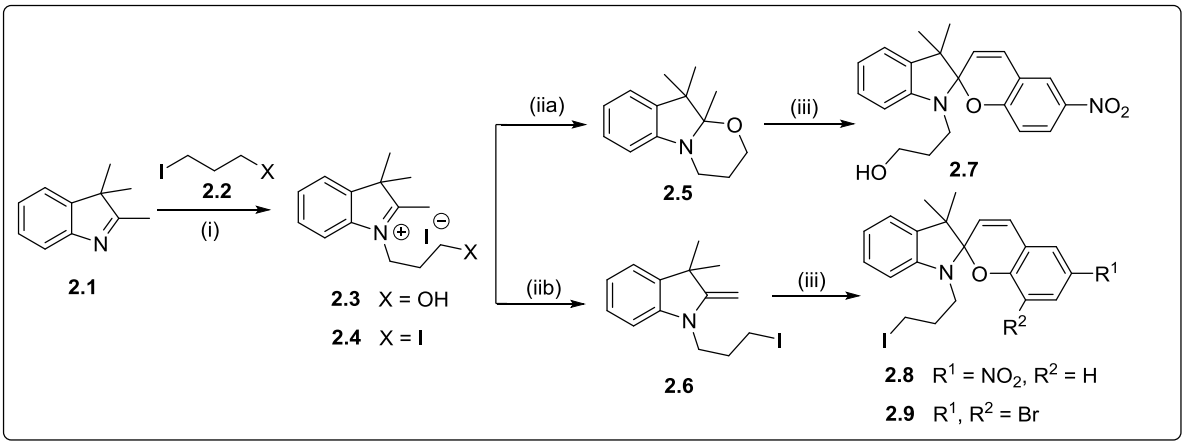


Scheme 2.1. General strategies for direct and indirect surface modification.

Surface functionalisation developed in the Moloney group using diarylcarbene reactive intermediates[22, 23] can be achieved through two main strategies, namely direct and indirect modification.[36] In this context, direct modification refers to the use of diazo compounds with the desired surface-modifying chemical functional group already incorporated into the molecule, while indirect modification refers to a two-stage process using firstly, carbene modification to introduce electron-rich functionality, followed by a second post modification of the polymer to introduce the

desired functional group (**Scheme 2.1**). The work in this chapter focuses on the introduction of a spiropyran residue, using both direct and indirect methods, although many other types of surface functionality have been previously introduced in Chapter 1, with a typical loading of the diarylmethyl unit onto the material surface of the order of 3 x 10^{14} molecules per cm^2.[25]

2.2 Synthesis of Spiropyran



Scheme 2.2. Synthesis of Spiropyrans. Conditions: (i) I-$CH_2CH_2CH_2$-X (**2.2** X = OH, I), $CHCl_3$, reflux 50-72h (**2.3** = 95%, **2.4** = 51%); (iia) KOH, H_2O, 3h R.T (**2.5** = 47%); (iib) NaOH, H_2O, 1h R.T (**2.6** = 80%); (iii) 5-nitrosalicyaldehyde or 3,5-dibromosalicyaldehyde, EtOH, 1h sonication, R.T (**2.7** = 80%, **2.8** = 58%, **2.9** = 54%).

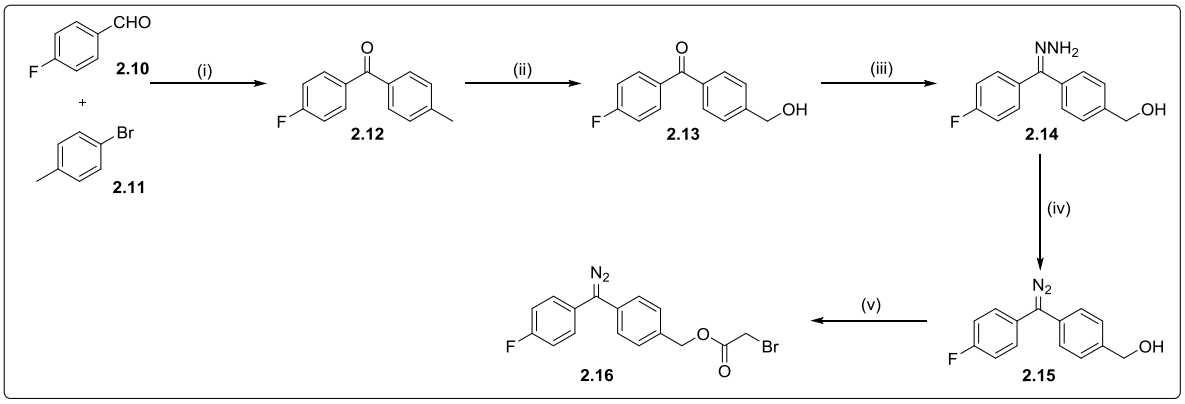
The syntheses of the required spiropyrans are shown in **Scheme 2.2**; although derived from a literature route,[92, 93] considerable optimisation was required to achieve a reliable and scalable procedure. Thus, commercially available 2,3,3-trimethylindolenine **2.1** was refluxed with iodide **2.2** (X = OH or I) to give iminium salts **2.3** and **2.4**; it was found that prolonging the reaction time of step (i) improved the yield of **2.4** significantly. With **2.3** and **2.4** in hand, their reaction under alkaline conditions gave **2.5** and **2.6** respectively, but with better yields when the reaction time was shortened, relative to the literature report.[92, 93] Further reaction with respective salicyaldehydes gave corresponding spiropyrans **2.7**, **2.8** and **2.9**; it was noteworthy that increasing the sonication time of the step (iii) from 1 min to 1 h

resulted in a significant increase in yield for **2.7** from 10% to 80%. Sonication is widely used to enhance rates of reactions and hence, shortening reaction time for many traditional reactions, primarily due to formation of highly reactive species during cavitation, promoting of mixing, enhancement in mass and heat transfer.[94] It was likely that continuous sonication (ultrasound) used in reaction (iii) allowed for more intimate mixing of the reactants and hence, enhanced both the rate of reaction as well as yields. Spiropyrans **2.7**, **2.8** and **2.9** with either a terminal hydroxyl group or iodo group were synthesized for their use either as a nucleophile or electrophile in subsequent reactions. Other functional groups were chosen to assist with surface characterisation; the -NO_2 functional moiety of **2.7** and **2.8** was chosen with the aim to give characteristic IR absorption bands when modified onto polymers, while the -Br moiety of **2.9** would give indicative presence on the polymers when characterised using combustion analysis. This will be discussed in greater detail in the following sections.

2.3 Direct Modification

Direct modification requires the chemical synthesis of a diazo compound with the desired functional moiety incorporated into the molecule prior to thermolysis or photolysis for the generation of the corresponding carbene, for insertion onto polymer surface. Depending on the functions to be conferred, and hence the functional groups to be attached onto the polymer surfaces, syntheses of the functionalised diazo derivatives can be lengthy and challenging, requiring careful consideration of the stability and sensitivity of the diazo functional group to the reactions. For this reason, systems stabilized by electron withdrawing groups were examined, using work done previously by Apichat Aphaiwong in the Moloney Group as a starting point.[95]

2.3.1 Synthesis of functionalised diazo



Scheme 2.3. Preparation of functionalised stable diazo 2.16. Conditions: (i) n-BuLi, 2h, R.T, followed by I_2, K_2CO_3, ^tBuOH, reflux 3h (**2.12** = 78%); (ii) Benzoyl peroxide, NBS, $CHCl_3$, reflux 24h in light, followed by $CaCO_3$, 1,4-dioxane, H_2O, reflux 24h (**2.13** = 33%); (iii) $NH_2NH_2{\cdot}H_2O$, EtOH, reflux 24h (**2.14** = 83%); (iv) MnO_2, KOH, MeOH, 24h R.T in dark (**2.15** = 81%); (v) Bromoacetyl bromide, Et_3N, DCM, 0°C, 4h.

The synthesis of the stabilized diazo precursor is shown in **Scheme 2.3;** though the synthesis had been previously reported,[95] it was found to be tedious and lengthy with low yields. 4-Fluorobenzaldehyde (**2.10**) was added to the lithiated species, obtained from a mixture of 4-bromotoluene (**2.11**) and n-BuLi in dry THF at low temperature, to yield the corresponding alcohol intermediate, which was then oxidized by I_2 under basic conditions to give **2.12** in good yield. This was followed by bromination of **2.12**, by refluxing with NBS in chloroform, and then base treatment, which gave **2.13** in low yield. Refluxing the functionalised benzophenone **2.13** with hydrazine monohydrate in ethanol gave the corresponding hydrazone **2.14**, and oxidation with manganese dioxide under basic conditions afforded the diazo **2.15**. Further reaction of **2.15** with bromoacetyl bromide yielded functionalised diazo **2.16**, however, while the strong electron withdrawing effect of the *p*-fluoro system was expected to stabilize its corresponding hydrazone **2.14**, and diazo-derivative **2.15** and **2.16**, these proved difficult to purify by flash column chromatography as the hydrazone and diazo functionality were not sufficiently stable on silica. As a result, NMR characterisation was very difficult. Though

hydrazone **2.14** was contaminated with impurities, full characterisation of the compound and NMR assignment was possible, and the presence of E and Z isomers was evident from the HSQC spectrum. However, after oxidizing hydrazone **2.14** to diazo **2.15**, the NMR spectrum was very unclear. At best, it could be inferred from the HSQC that the conversion of E and Z isomers of the hydrazone into the diazo-derivative had occurred as only one cross peak instead of two was seen for the benzylic protons (-CH_2), due to the loss of asymmetry of the molecule. In addition, the IR spectrum of the compound showed a strong band at 2043 cm^{-1} for diazo functionality (**Figure 2.3**), clearly indicative of the diazo functional group being formed.

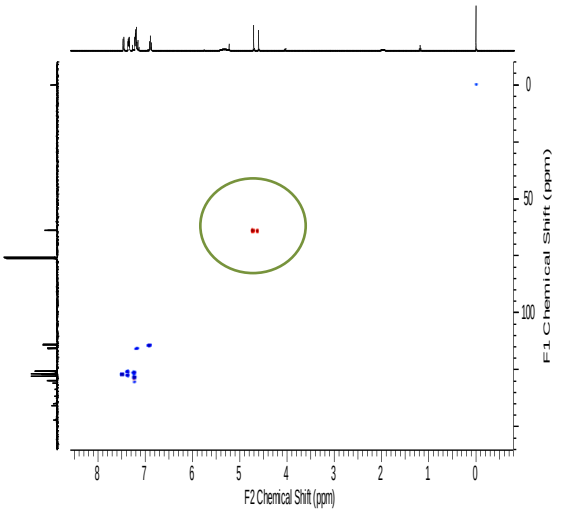


Figure 2.1. HSQC of hydrazone 2.14.

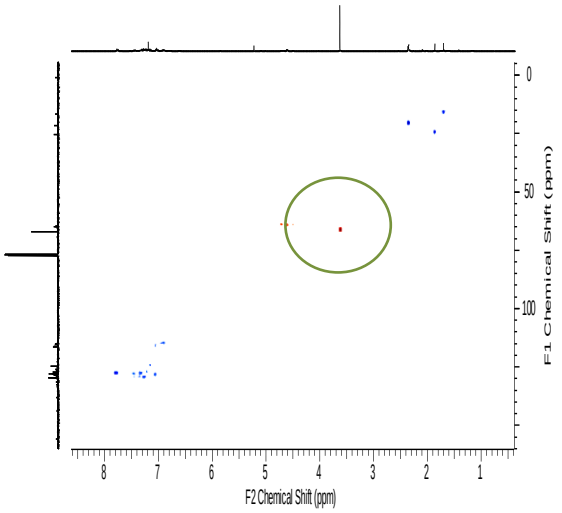


Figure 2.2. HSQC of diazo 2.15.

Successful conversion to diazo **2.16** was indicated by the presence of the diazo functional group at around 2046cm^{-1} in the IR spectrum (**Figure 2.4**). A strong absorption band due to the carbonyl of the ester group was also observed at 1741 cm^{-1}.

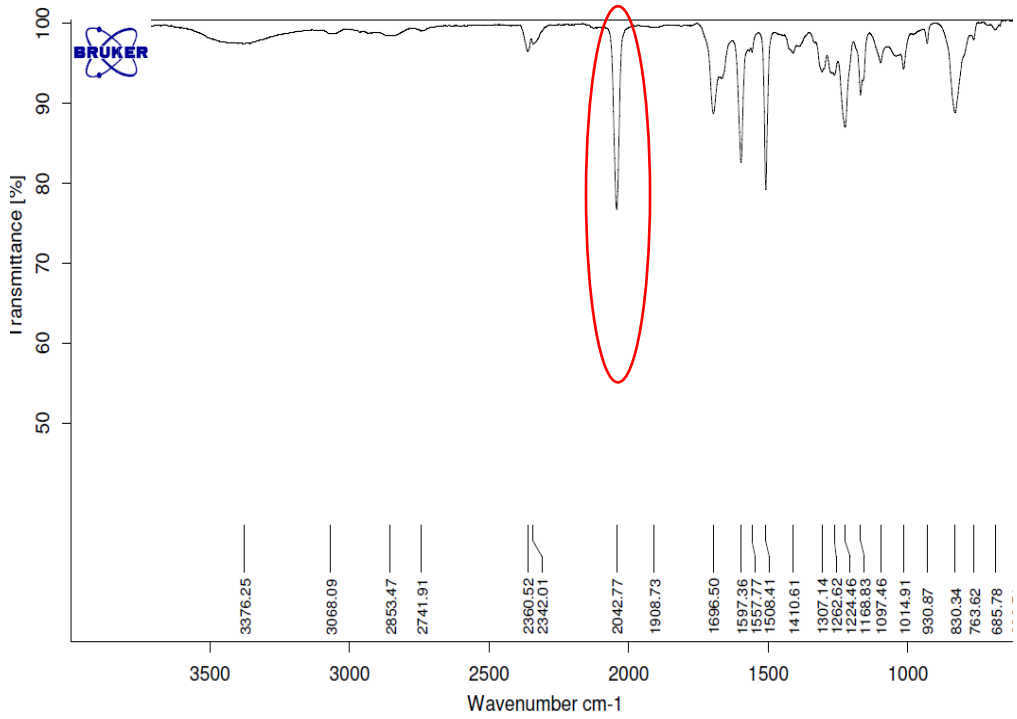


Figure 2.3. FTIR spectrum for diazo 2.15.

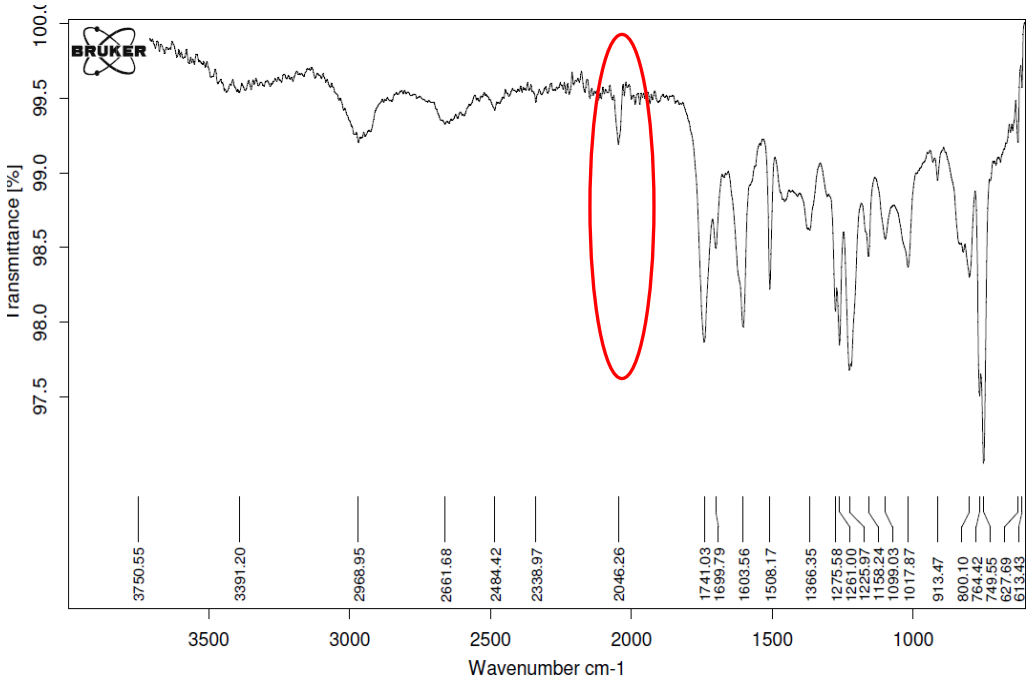
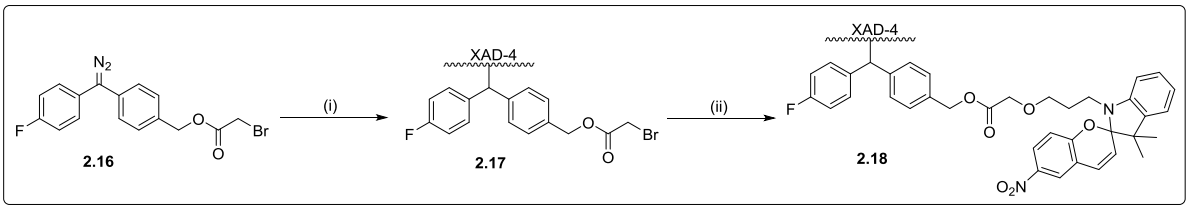


Figure 2.4. FTIR spectrum for diazo 2.16.

This work showed that the diazo derivatives **2.15** and **2.16** could be synthesized, but overall yields and purity were clear limiting factors to this direct modification approach. Nonetheless, given the work put into developing this system, surface modifications using it were examined.

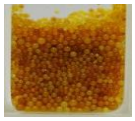
2.3.2 Surface functionalisation using direct modification



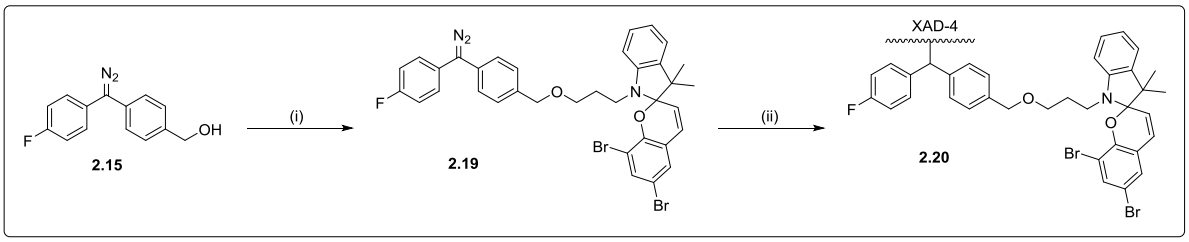
Scheme 2.4. Surface modification of XAD-4 PS beads with diazo 2.16. Conditions: (i) XAD-4 PS beads, Et_2O, heat at 120°C; (ii) K_2CO_3, spiropyran **2.7**, MeCN, R.T.

Diazo-derivative **2.16** was dissolved in diethyl ether and XAD-4 PS beads were added into the solution. Careful removal the solvent *in vacuo* resulted in a thin coating of the diazo compound on the beads by physisorption. Upon heating for 30 min at 120°C, the diazo system collapsed to the corresponding carbene via thermolysis, and was expected to insert onto polymer surface, giving an irreversible surface modification while retaining the bulk properties of the polymer. Modified polymer **2.17** was then derivatized with spiropyran **2.7** to give **2.18**.

Table 2.1. Characterisation of polymers 2.17 and 2.18.

Sample	Appearance	Combustion Analysis/ % Found	Combustion Analysis Surface Modifications/ {mol / g of polymer} [molecules. per cm^2] (% Surface Coverage)	ATR-IR	XPS Atomic Ratio	
					Found	Expected
2.17		C: 86.19 ± 0.30 H: 7.77 ± 0.30 N: 0.12 ± 0.026 Br: 0.87 ± 0.19	Br: {(1.1 ± 0.2) x10^{-4}} [(9.0 ± 2.0) x10^{12}] (6.6 ± 1.5)	1726 (C=O), 1603 (C=C), 1506 (C=C)	N/C: 0.0610 O/C: 0.253 Br/C: 0.000921 F/C: 0.000658	N/C: 0.00 O/C: 0.125 Br/C: 0.0625 F/C: 0.0625
2.18		C: 85.7 ± 0.30 H: 7.76 ± 0.30 N: 0.09 ± 0.30 Br: 0.19 ± 0.042	N: {(3.2 ± 0.7) x10^{-5}} [(2.7 ± 0.6) x10^{12}] (2.6 ± 0.6) Br: {(2.4 ± 0.5) x10^{-5}} [(2.0 ± 0.4) x10^{12}] (1.4 ± 0.3)	1725 (C=O), 1603 (C=C), 1510 (NO_2, C=C), 1357 (NO_2)	-Nil-	-Nil-

From ATR-IR spectroscopic analysis of modified material, it was possible to identify the characteristic –C=O absorption bands of modified polymers **2.17** and **2.18** at around 1724 cm^{-1}. However, it was not possible to identify the $–NO_2$ group for **2.18** as the peaks were hidden under broad peaks at 1357 and 1510 cm^{-1}.



Scheme 2.5. Surface modification of XAD-4 PS beads with diazo 2.19. Conditions: (i) K_2CO_3, spiropyran **2.9**, MeCN, RT; (ii) XAD-4 PS beads, Et_2O, heat at 120°C.

In an alternative, the approach used shown in **Scheme 2.5** was to first integrate the spiropyran unit into the diaryldiazo molecule prior to diarylcarbene formation. Similarly to diazo-derivative **2.15**, the purification of **2.19** by flash column chromatography was not possible, due to instability of the diazo functionality. Nonetheless, a distinct IR absorption band due to the diazo functionality was still observed at 2039 cm^{-1} for **2.19**, which appeared as a navy blue coloured gum. Surface modification of Blank XAD-4 PS beads with **2.19** gave material **2.20**.

Table 2.2. Characterisation of polymer 2.20.

Sample	Appearance	Combustion Analysis/ % Found	Combustion Analysis Surface Modifications/ {mol / g of polymer} [molecules. per cm^2] (% Surface Coverage)	ATR-IR	XPS Atomic Ratio	
					Found	Expected
2.20		C: 89.97 ± 0.30 H: 8.02 ± 0.30 N: <0.10 Br: 0.55 ± 0.12	Br: {(3.4 ± 0.3)x10^{-5}} [(2.9 ± 0.3) x10^{12}] (2.6 ± 0.3)	1604 (C=C), 1511 (NO_2), 1486 (C=C) 1446 (C=C) 1357 (NO_2)	N/C: 0.0734 O/C: 0.249 Br/C: 0.00199 F/C: 0.00199	N/C: 0.0286 O/C: 0.0571 Br/C: 0.0571 F/C: 0.0286

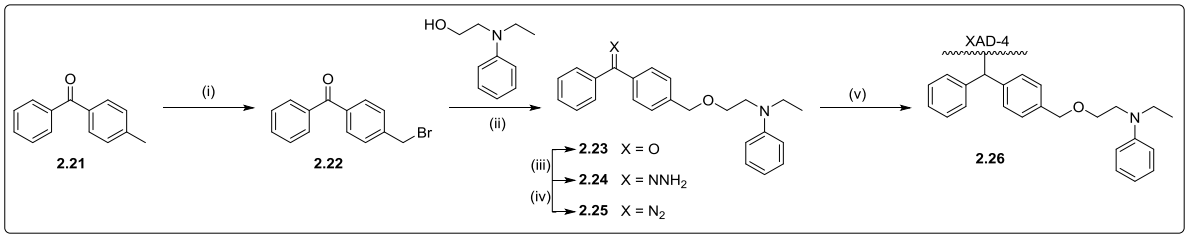
Combustion analysis of modified XAD-4 beads **2.20** detected the presence of Br, indicative of successful surface modification, with an estimated surface coverage of approximately 2.6% (**Table 2.2**). XPS also clearly indicated the detection of F and Br, with the ratio of Br to C found to be 0.00199. With the expected ratio calculated to be 0.0286, the surface coverage of the modification could be approximated to be 3.5%. Combining results from both XPS and combustion analysis, the surface modification coverage ranges between 2.6 to 3.5%. Both surface characterisation methods are further discussed in Chapter 3.

In all, despite the difficult synthesis and characterisation of the functionalised diazo system, the synthesis of a diaryldiazo with a *p*-fluoro substituent, successful derivatization with the spiropyran unit and immobilisation onto polystyrene XAD-4 beads was achieved for surface modification, but difficulties with synthesis and characterisation provided clear limitations to this approach, and suggested that indirect modification might be more efficient.

2.4 Indirect Modification

Indirect modification involved firstly, the post-modification of the polymer surface with an electron-rich aromatic system, followed by introduction of the desired functional moiety onto the polymer via a second azo coupling of a suitable diazonium salt.

2.4.1 Pre-activation of polymer surface

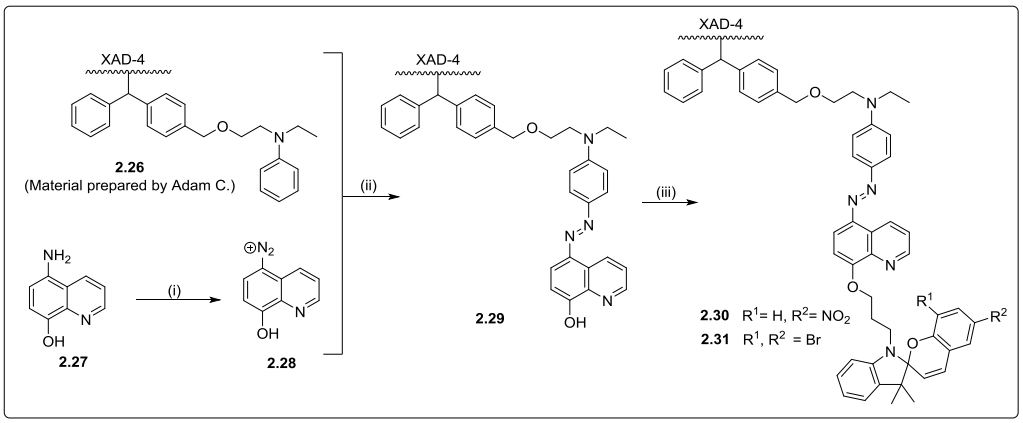


Scheme 2.6. Pre-activation of XAD-4 PS beads surface. Conditions: (i) NBS, $CHCl_3$, followed by reflux; (ii) $PhN(Et)CH_2CH_2OH$, NaH, THF, R.T; (iii) $NH_2NH_2.H_2O$, EtOH, reflux; (iv) MnO_2, KOH, THF, R.T (dark).

The required pre-activated XAD-4 PS beads were prepared by Mr. Adam Creamer by modification of 4-methylbenzophenone using a published strategy.[24] Thus, 4-methylbenzophenone **2.21** first underwent allylic bromination to give **2.22**, followed by a nucleophilic substitution reaction with 2-(*N*-Ethylanilino)ethanol to give **2.23**. Reflux of **2.23** with hydrazine monohydrate yielded hydrazone **2.24**, which upon oxidation with manganese dioxide afforded diazo **2.25**. The diarylcarbene derived

from **2.25** was generated via thermolysis for functionalisation of XAD-4 beads, accomplishing the pre-activation of the polymer surface.

2.4.2 Post-modification of polymer



Scheme 2.7. Azo coupling of diazonium salt 2.28 to surface modified polymer 2.26, followed by derivatization with spiroyran. Conditions: (i) THF, H_2O, $NaNO_2$, HCl, 0°C, 30min in dark; (ii) 0°C – R.T, 18hr; (iii) Spiropyran **2.8** or **2.9**, K_2CO_3, MeCN, 18h, R.T.

Following **Scheme 2.7**, post-modification of pre-activated XAD-4 PS beads **2.26** included first, an azo-coupling reaction using diazonium salt **2.28**, followed by derivatization with spiropyran **2.7** or **2.8** via nucleophilic substitution reaction. Primary aromatic amine **2.27** was diazotized with $NaNO_2$ and HCl in cold H_2O and THF to generate diazonium salt **2.28,** which was used *in situ* for azo coupling to the electron rich aromatic ring on the polymer surface of **2.26**. (Diazonium salt synthesis and azo coupling reactions are explored and discussed in greater detail below in Section 2.6)

Table 2.3. Characterisation of modified polymers 2.29, 2.30, 2.31.

Sample	Appearance	Combustion Analysis/ % Found	Surface Modifications/ {mol / g of polymer} [molecules. per cm^2] (%Surface Coverage)	ATR-IR	XPS Atomic Ratio		UV-Vis λ_{max} / nm
					Found	Expected	
2.29		C: 89.69 ± 0.30 H: 7.73 ± 0.30 N: 0.46 ± 0.10	N: {(8.2 ± 1.8) x10^{-5}} [(6.8 ± 1.5) x10^{12}] (7.4 ± 1.6)	3383 (-OH), 1603 (C=C), 1511 (C=C), 1487 (C=C).	-Nil-	-Nil-	349, 406, 620
2.30		C: 89.5 ± 0.30 H: 7.56 ± 0.30 N: 0.42 ± 0.09	N: {(5.0 ± 1.1) x10^{-5}} [(4.2 ± 0.9) x10^{12}] (4.5 ± 1.0)	1604 (C=C), 1511 (C=C, NO_2) 1486 (C=C) 1343 (NO_2)	-Nil-	-Nil-	371

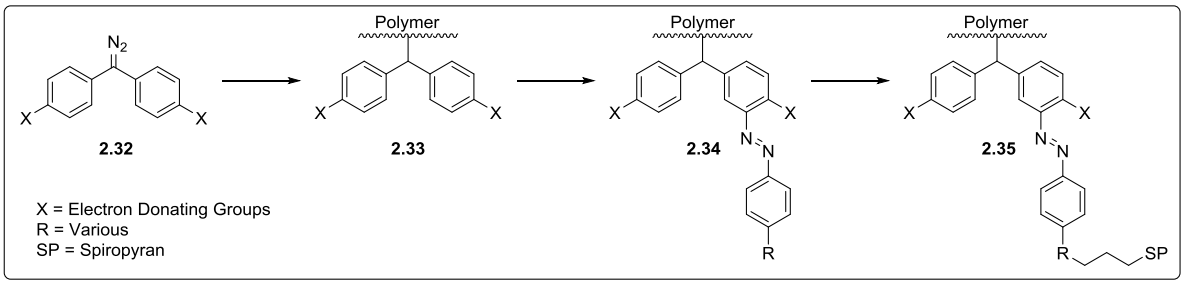
2.31		C: 89.79 ± 0.30 H: 7.63 ± 0.30 N: 0.28 ± 0.06 Br: 1.96 ± 0.43	N: {(4.0 ± 0.9) x10^{-5}} [(3.3 ± 0.7) x10^{12}] (3.6 ± 0.8) Br: {(1.2 ± 0.3) x10^{-4}} [(1.0 ± 0.2) x10^{13}] (11 ± 2)	1604 (C=C), 1511 (C=C), 1486 (C=C), 1446 (C=C).	N/C: 0.0737 O/C: 0.245 Br/C: 0.00291	N/C: 0.0909 O/C: 0.0364 Br/C: 0.0364	361, 601

ATR-IR analysis of material **2.30** showed a strong band at 1343 cm^{-1} while the other characteristic band of $–NO_2$ at around 1510 cm^{-1} was hidden. Combustion analysis of **2.31** showed the presence of the bromine on the polymers, estimated as approximately 11% surface coverage of the polymer, thus indicating the successful modification of the polymer surface with the desired functional moiety. From XPS results, with the ratio of Br to C found to be 0.00291 and since the expected value is 0.0364, surface coverage can also be estimated to be approximately 8.0%. Thus, combining results from both combustion analysis and XPS, the surface coverage of the modification for **2.31** was estimated to be a range of 8.0% to 11%.

2.5 Direct Modification versus Indirect Modification

Considering both methods of surface modification of polymers, while keeping in mind the feasibility of transferring such technology to SIMTech in Singapore to be translated into viable process for large area processing, indirect modification was the preferred method compared to direct modification for various reasons. Firstly, in terms of ease of synthesis and modification, indirect modification proved to be of greater convenience and ease compared to direct modification. Compared to the direct modification method, where the final diazo before surface modification could not be obtained in pure form, indirect modification required a shorter synthesis before the group was inserted onto polymer surface, and gave purer and more stable synthetic intermediates, and this gave greater confidence in the chemistry. Secondly, in terms of loading, indirect modification seemed to perform better than

the direct method, with surface coverage of approximately 8.0 - 11% compared to 2.6 – 3.5% as estimated from combustion analysis and XPS. With the limitation of characterisation methods available for surface analysis, and working at the detection limits of these characterisation techniques, having greater confidence and greater loading was considered to be a strong advantage. Finally, as the facilities available at SIMTech were mainly for translational research geared towards manufacturing technology, rather than elaborate chemical synthesis, a facile yet versatile synthesis was preferred. The indirect modification method is therefore much preferred over the direct modification method. However, the indirect modification method discussed in this Chapter still has many drawbacks. In order to have a modification method that is feasible for translation into large area surface engineering process, a shorter route with higher yields was necessary. In addition, to increase the efficiency of the azo coupling of the diazonium salt, a more electron-rich system is much preferred. As such, another method to further pre-activate the surface for azo coupling with diazonium salt was examined.



Scheme 2.8. Proposed alternative indirect surface modification route.

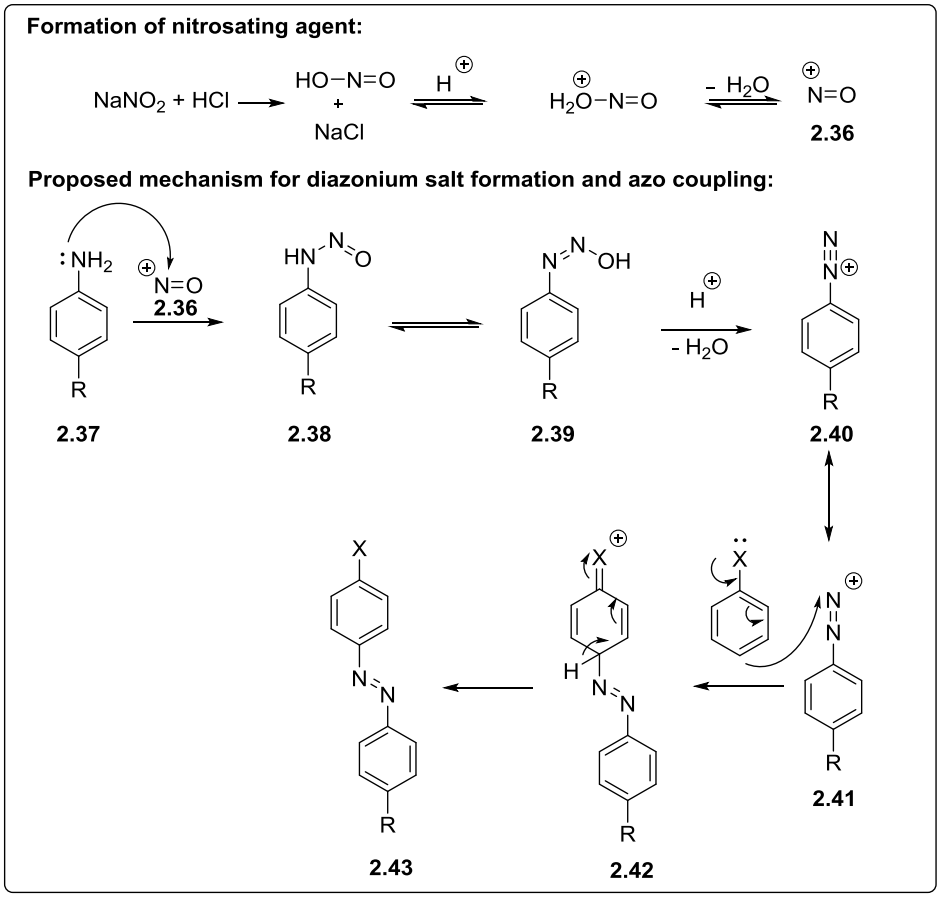
It was essential for X in **Scheme 2.8** to be a strong electron-donating group for two purposes; firstly, it creates a more reactive diazo compound for increased insertion efficiency and therefore loading onto polymer surface, and secondly, it facilitates a more efficient azo coupling with diazonium salt. An additional advantage is the flexibility that this approach gives; R can be any functional group as long as the

diazonium salt can be synthesized and coupled onto the electron-rich aromatic ring that was inserted onto the polymer surface in the first step. Thus, it is easily possible to confer any functionality onto any polymer for any desired applications. Compared to the synthetic route used previously, it was anticipated that this proposed alternative route would be more suitable; the starting materials would be commercially available benzophenone-type derivatives, and only a straightforward 2-step reaction would be required to achieve the desired diaryldiazo derivative for formation of the relevant diarylcarbene for surface modification. Subsequent post-modification could then be easily achieved without tedious purification process.

2.6 Investigation of Chemistry in Solution

A critical process in the indirect modification approach is azo coupling, and it is necessary to have full confidence that this step is reliable. Therefore, investigation of the azo-coupling process in solution using dimethylaniline, phenol and anisole as model systems was conducted. Moreover, as seen in the previous section, characterisation of the modified polymers can be very challenging as the loading of the functional groups onto the polymer surface tends to be rather low, with analyses often requiring working at the detection limits of various characterisation methods. Therefore, it was considered that the synthesis of analogues of the compounds would be helpful to understand the underlying solution chemistry.

Aromatic azo compounds are widely used in the chemical industry as dyes and pigments,[96, 97] food additives[98] and indicators[99], and azo coupling is one of the classical methods used to prepare these compounds. This method is based on the initial diazotization of an aromatic primary amine at low temperature to form the corresponding diazonium salt, which then reacts with an electron-rich nucleophile.

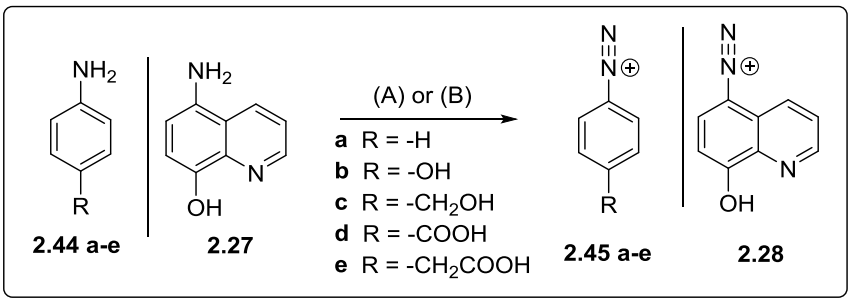


Scheme 2.9. Proposed reaction mechanism for diazonium salt formation and azo coupling. [100]

As seen in **Scheme 2.9**, acid, to form nitrous acid from $NaNO_2$, is necessary for the formation of the diazonium salt from a primary amine. Further protonation followed by H_2O elimination provides the nitrosating agent (+N=O) **2.36**. Reaction of the nitrosating agent with the amine **2.37** leads to the *N*-nitroso derivative **2.38**, which tautomerises to give the diazohydroxide **2.39**. A second protonation and H_2O elimination affords the diazonium salt **2.40** that is stabilized by resonance.[100, 101] After the diazonium salt is formed, several mechanisms have been proposed for the azo coupling step.[101] Currently, the most widely accepted mechanism is an electrophilic aromatic substitution of the electron rich aromatic starting material (where X is an electron donating group) with the electrophilic nitrogen of the diazonium salt.[100] While these reactions are well known, literature analysis suggested that they had not been examined in detail in recent years, and it was of

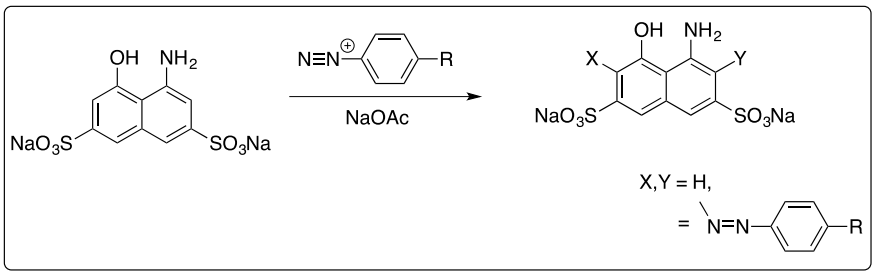
importance in the work described in this thesis to have some information about the efficiency and rate of coupling.

2.6.1 Synthesis of diazonium salt



Scheme 2.10. Syntheses of diazonium salts from aromatic amines. Conditions: (A): $NaNO_2$, HCl, THF, H_2O; (B): Isopentyl nitrite, HBF_4, EtOH.

A range of diazonium salts **2.28** and **2.45 a-e** was synthesized from their respective aromatic amines (see General Method A in Chapter 6). Diazonium salts are known to be unstable above 0°C and can be explosive when dry.[100] As such, they were not isolated, but used directly *in situ* for the subsequent azo coupling reactions. A colourimetric H-acid test was used to confirm the successful formation of the diazonium salts prior to the diazonium salt being used for subsequent azo coupling reactions.[102] (see General Method B in Chapter 6)

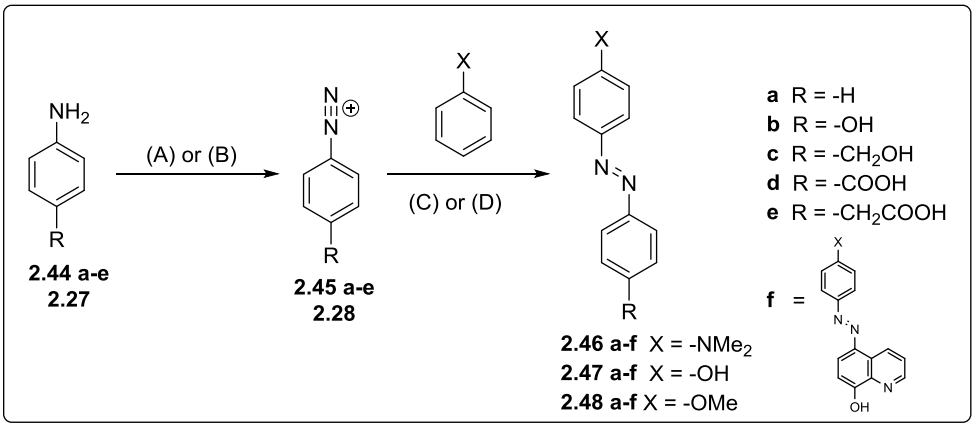


Scheme 2.11. H-acid test.

The H-acid test was conducted by first mixing a small aliquot of sample from the reaction mixture with a little sodium acetate, then adding this mixture to a small sample of 4-amino-5-hydroxy-2,7-naphthalene disulfonic acid powder, also known as H-Acid. The presence of the salt was indicated by the formation of a dark purple

colour. Alternatively, the reaction for the formation of the diazonium salt could also be monitored using mass spectrometry, to track the loss of the ion peak for the primary aromatic amine, and formation of the diazonium salt ion peak.

2.6.2 Azo coupling reaction



Scheme 2.12. Azo coupling reaction. Conditions: (A): $NaNO_2$, HCl, THF, H_2O; (B): Isopentyl nitrite, HBF_4, EtOH; (C): without NaOAc; (D), with NaOAc.

Table 2.4. List of azo coupling reactions performed.

Entry	X	R	Conditions	Yields / %
1	-NMe_2	-H	(A) + (C)	40
2	-NMe_2	-H	(A) + (D) [a]	98
3	-NMe_2	-H	(B) + (C)	20
4	-NMe_2	-H	(B) + (D) [a]	67
5	-NMe_2	-OH	(A) + (D) [a]	Complex mixture [c]
6	-NMe_2	-CH_2OH	(A) + (D) [a]	96
7	-NMe_2	-COOH	(A) + (D) [a]	97
8	-NMe_2	-CH_2COOH	(A) + (C)	Complex mixture [c]
9	-NMe_2	-CH_2COOH	(A) + (D) [a]	Complex mixture [c]
10	-NMe_2	-8-hydroxyquinoline	(A)	Complex mixture
11	-NMe_2	-8-hydroxyquinoline	(A) + (D) [a]	Complex mixture
12	-OH	-H	(A) + (C)	34
13	-OH	-H	(A) + (D) [a]	82
14	-OH	-H	(A) + (D) [b]	95
15	-OH	-OH	(A) + (C)	Complex mixture [c]
16	-OH	-OH	(A) + (D) [a]	Complex mixture [c]
17	-OH	-CH_2OH	(A) + (C)	12
18	-OH	-CH_2OH	(A) + (D) [a]	77
19	-OH	-CH_2OH	(A) + (D) [b]	87
20	-OH	-COOH	(A)	Impure
21	-OH	-COOH	(A) + (D) [a]	70
22	-OH	-COOH	(A) + (D) [b]	88

23	-OH	-CH_2COOH	(A) + (C)	Complex mixture [c]
24	-OH	-CH_2COOH	(A) + (D) [a]	Complex mixture [c]
25	-OH	-CH_2COOH	(A) + (D) [b]	Complex mixture [c]
26	-OH	-8-hydroxyquinoline	(A)	Complex mixture
27	-OH	-8-hydroxyquinoline	(A) + (D) [a]	Complex mixture
28	-OH	-8-hydroxyquinoline	(A) + (D) [b]	Complex mixture
29	-OMe	-H	(A) + (D) [b]	Little / No reaction
30	-OMe	-OH	(A) + (D) [b]	Little / No reaction
31	-OMe	-CH_2OH	(A) + (D) [b]	Little / No reaction
32	-OMe	-COOH	(A) + (D) [b]	Little / No reaction
33	-OMe	-CH_2COOH	(A) + (D) [b]	Little / No reaction
34	-OMe	-8-hydroxyquinoline	(A) + (D) [b]	Little / No reaction

[a] Using 1 equiv of NaOAc.
[b] Using 2 equiv of NaOAc.
[C] Mass spectrometry spectrum showed that $[M+H]^+$ or $[M-H]^-$ was base peak.

Entries **1 – 4** demonstrated the optimization of the conditions for the azo coupling reaction with *N*,*N*-dimethylaniline. Diazonium salts could be generated from either conditions A or B as indicated in **Scheme 2.12**. However, comparing entries **1** with **3**, and **2** with **4**, the azo coupling reaction gave better yields with condition A, using $NaNO_2$ with HCl in THF and H_2O, compared to condition B, using isopentyl nitrite with HBF_4 in EtOH. This could be due to the counter ion of the diazonium salt, since the non-nucleophilic tetrafluoroborate (BF_4^-) anion enhances the stability the diazonium salt compared to nucleophilic chloride (Cl^-) anion.[103, 104] However, greater stability could also mean weaker reactivity, and thus, a plausible cause for lower yields of 20 – 30% in this case.

Furthermore, as seen from the results in

Table 2.4, the azo coupling reactions were pH dependent. Addition of 1 equivalent of NaOAc to neutralize the reaction mixture to about pH 4 – 5 resulted in a significant 47 – 65 % increase in yields. An additional 1 equivalent of NaOAc could also make a difference of about 10 – 18% increase in yields. By neutralizing the pH of the mixture to about pH 4 – 5, protonation of phenol or *N,N*-dimethylaniline was prevented, which could inhibit the coupling reaction. However, not all diazonium

salts reacted cleanly with phenol or aniline to give the desired compound. Complex mixtures resulted from the coupling with diazonium salts **2.45b**,**e** and **2.28**. Though it was not possible to purify and isolate the products **2.46b,e** and **2.47b,e**, mass spectra of the reaction mixtures indicated the presence of the desired azobenzene, with the molecular ion (as $[M+H]^+$ or $[M-H]^-$) being the base peak. However, the molecular ion was not observed for azo coupling reaction with diazonium salt **2.28.**

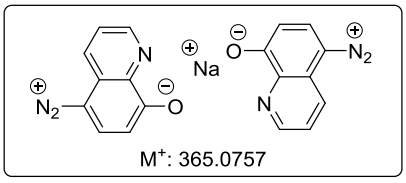


Figure 2.5. Suggested structure corresponding to m/z of 365.0768.

Further probing of the reaction using mass spectrometry showed that the desired diazonium salt **2.28** was formed, with measured m/z of 172.0503. Measured m/z of 194.0324 showed that diazonium salt **2.28** could also conjugate with sodium ion with hydroxyl oxygen, giving dimeric species corresponding to measured m/z of 365.0768. (See **Figure 2.5** and **Figure 2.6**)

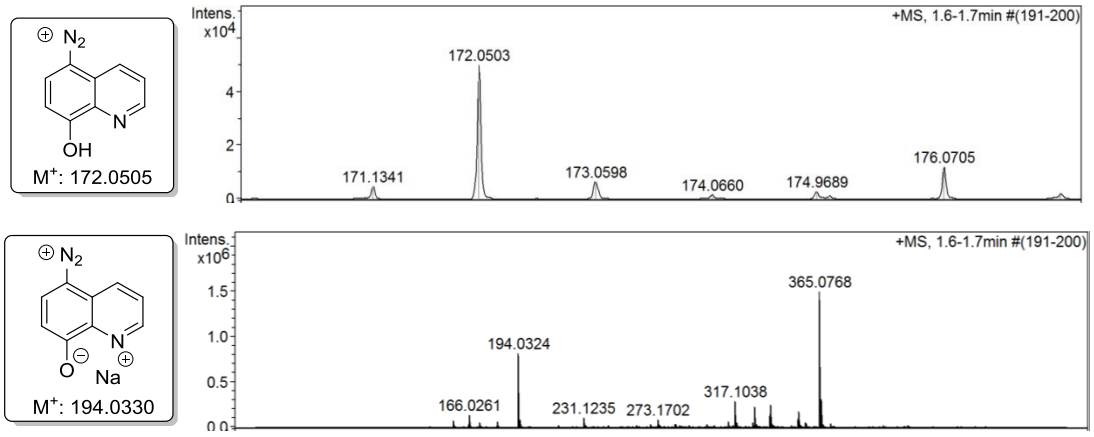


Figure 2.6. High Resolution Mass Spectrometry Spectra for diazonium salt 2.28 with possible species formed in solution.

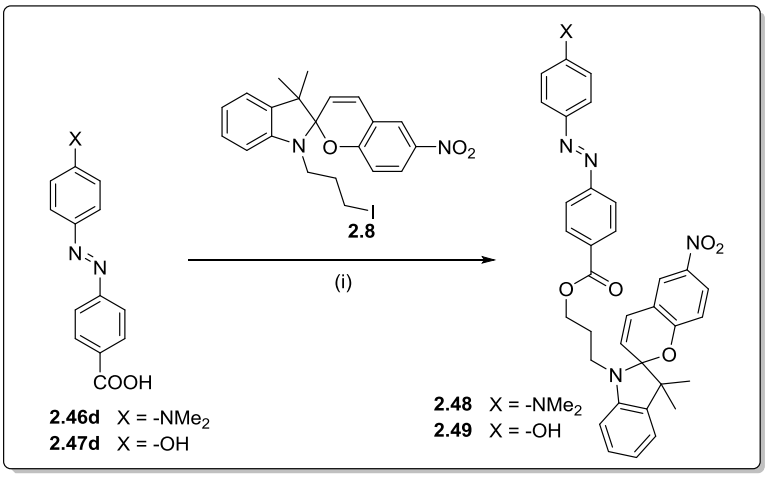
It was noted that there was little or no reaction of the diazonium salts with anisole in entries **29** -**34**. According to the literature, neutral species are not sufficiently nucleophilic for the azo coupling reaction to take place.[100] However, this was contradictory to some reports which mentioned that when a more electrophilic

diazonium salt is used,[105-107] or when there are solid supports used in the reaction to act as acid/base catalyst,[108] the azo coupling reaction with anisole would still proceed. The feasibility of azo coupling of para-substituted diazonium salts with the anisole-type system on solid support was also demonstrated in this thesis, which is discussed later in Chapter 3.

This solution work indicated that diazonium couplings with good efficiency could be expected for phenol and dimethylaniline type systems, although less so for anisole type systems. Overall, a strategy using this coupling approach appeared to be feasible.

2.6.3 Derivatization with spiropyran

Appropriate azobenzenes **2.46d**, **2.47d** were derivatized with the spiropyran **2.8** to synthesize the analogue **2.48** and **2.49**.



Scheme 2.13. Derivatization of azobenzene 2.46d and 2.47d with spiropyran 2.8. Conditions: (i) K_2CO_3, solvent, R.T, 5 h. [X = -NMe_2 (79%), X = -OH (72%)]

Table 2.5. Reaction of azobenzene with spiropyran in different solvents.

Entry	X	Solvent	Yield/%
1	-NMe_2	THF	Incomplete reaction
2	-NMe_2	Acetone	Incomplete reaction
3	-NMe_2	MeCN	Incomplete reaction
4	-NMe_2	DMSO	79
5	-OH	DMSO	72

Solvent selection was found to be crucial in this reaction. When THF, acetone and MeCN were used, the reaction was not able to go to completion as the azobenzene **2.46d** and **2.47d** precipitated out of the reaction mixture within an hour. When DMSO was used, the azobenzene **2.46d** and **2.47d** was able to remain soluble throughout the reaction and gave good yields of 79% and 72 % for analogues **2.48** and **2.49** respectively. The compounds were fully characterised by NMR spectroscopy and HRMS.

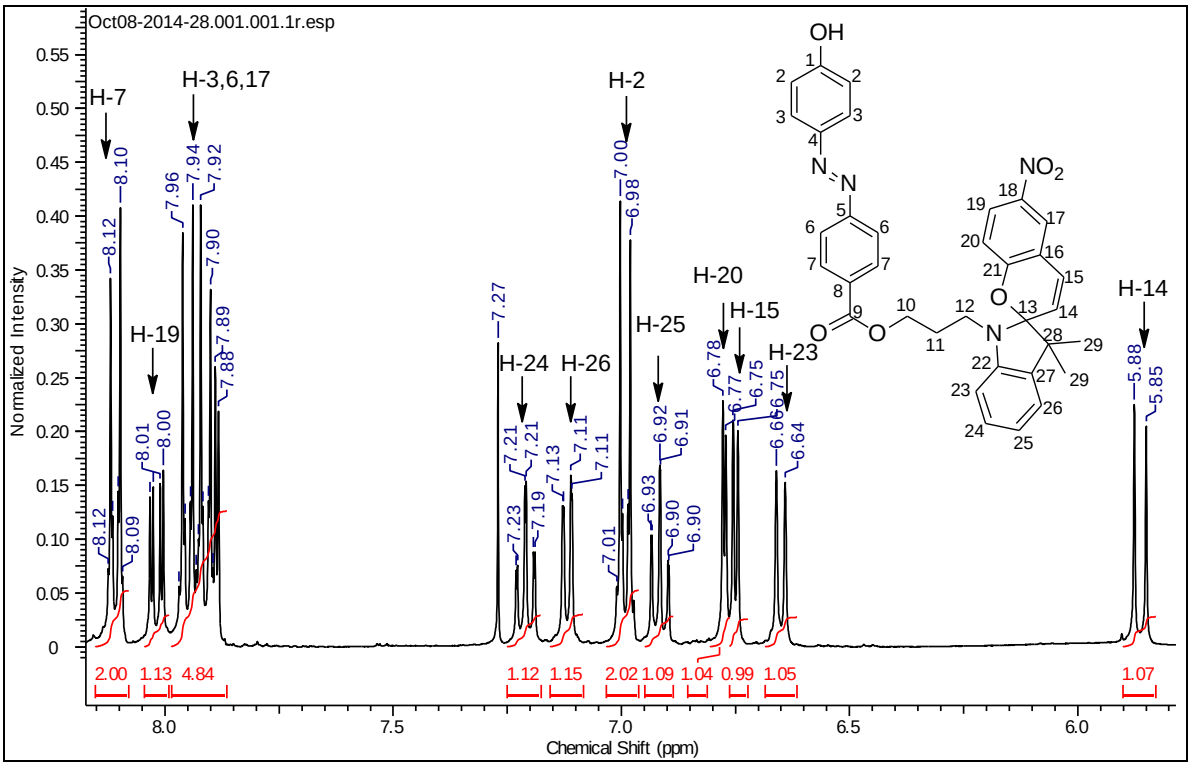


Figure 2.7. Expanded NMR view of compound 2.49 in $CDCl_3$.

The coupling constant of the vinyl protons H-14 and H-15 in **Figure 2.7** was 10.5 Hz, indicating that they were in *cis* form as expected, and this data is consistent with the fact that spiropyrans are usually more stable in their spirocyclic closed ring form.[40, 44, 109, 110] In addition, the *J* coupling for H-2 and H-7 were both 8.8 Hz, clearly indicating that both aromatic rings were joined by the azo functionality at the para position, and were not ortho or meta coupled.

The successful synthesis of analogue **2.49** was crucial in this work; it demonstrated the feasibility and reliability of both the azo-coupling reaction to an electron-rich aromatic ring, and the subsequent derivatization of the azobenzene with a spiropyran. It was important to know that the desired nucleophilic substitution reaction between the iodo group of the spiropyran and the acid group of the azobenzene had taken place, instead of other possible side reactions, such as ring opening reaction of the spiropyran at spiro-carbon by the nucleophilic group etc. The analogues were also important in comparing solution studies to surface modified polymer studies in applications as explored in greater detail later in Chapter 4.

2.7 Conclusion

In all, the work described in this chapter has shown that indirect surface modification was more effective than direct surface modification. In addition, in view of the need to transfer the technology for further translation in SIMTech, the indirect modification method was chosen over direct modification for its ease and efficiency. A proposed synthetic route to further refine the indirect method was found to be feasible for translation. The proof of chemistry of the proposed synthetic route was achieved by solution model studies of analogues of the compounds to be modified onto the surface. The next chapter explores the optimization of the proposed route, and surface modification of various polymers using the proposed synthesis.

3 Surface Modification of Polymers

3.1 Introduction

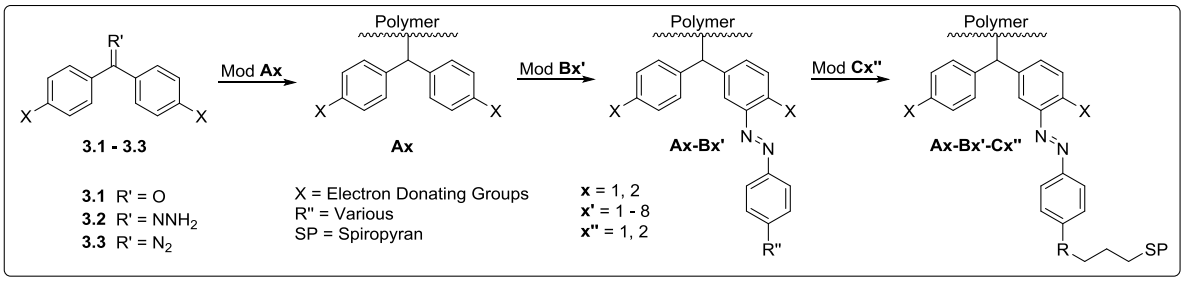
With the indirect modification method decided as the preferred option, and the proposed strategy established, this chapter reports work which explores the surface modification of polymers in greater depth and scope. The optimisation of each synthesis and surface modification step, followed by the expansion of scope for the diazonium salts and polymeric substrates used, is reported. Challenges arose from characterisation methods for modified polymers, and endeavours to translate the modification methods into feasible large-scale surface engineering processes are discussed.

3.1.1 Optimisation

Synthesis of various diaryldiazo intermediates for surface modification,[22, 23, 26, 36] and azo coupling using diazonium salts to modify polymer surfaces[27, 28, 30, 36] have been performed by previous members of the Moloney Group as discussed in Chapter 1. However, there was a need to refine and optimise the synthesis and systems; firstly, to establish a general method with shorter synthesis steps suitable for wider variety of substituted benzophenone precursors; secondly, to improve yields and simplify purification methods to make the synthesis suitable for upscaling; and lastly, to determine the most suitable system to be investigated and be transferred to Singapore for surface engineering process development.

The aim of modifying polymer surfaces with various chemical groups was to confer properties onto the surfaces to enable the polymers to achieve desired macroscopic functions, such as photochromism and drug delivery. Therefore, it was necessary to

vary diazonium salts so as to modify the polymer surfaces with different functional moieties, and examine which side group worked best for derivatization with a spiropyran to achieve photochromism, or for drug delivery.



Scheme 3.1. General reaction scheme for surface modification of polymers.

The general outline to modify the surface of the polymers with various chemical functional groups is shown in **Scheme 3.1** Using a commercially available substituted benzophenone **3.1** as starting material, optimisation was required for the synthesis of the relevant hydrazone **3.2** and diazo **3.3**. Thereafter, modification A (Mod **Ax**) for the pre-activation of the polymer surface to make **Ax**, in preparation for the subsequent azo-coupling (Mod **Bx'**) of diazonium salt to give **Ax-Bx',** was planned. Lastly, modification C (Mod **Cx''**) involved derivatization of the polymer surface with spiropyran to bring about the desired photochromism by formation of **Ax-Bx'-Cx''**. The optimisation and modification steps are discussed in greater detail in the following sections.

3.1.2 Labelling of surface modified polymers

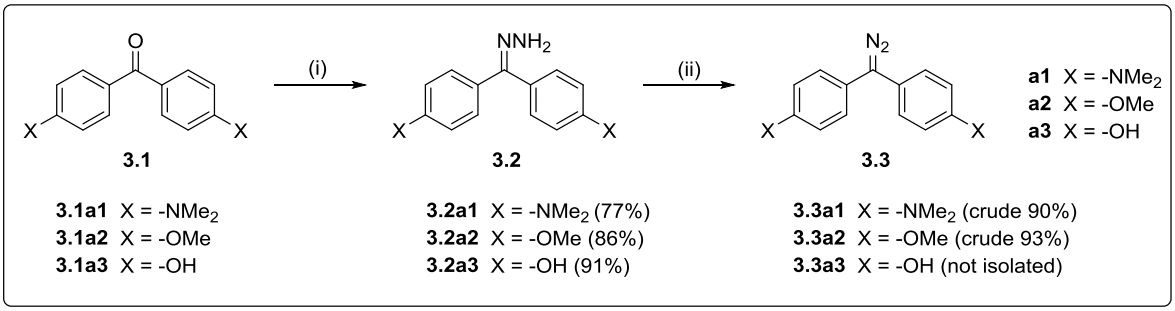
The general labelling of compound was presented in **Scheme 3.1**. However, with X being variable electron donating groups, R'' representing various functional moieties and SP representing spiropyrans with different side groups, the labelling of the compounds can be very complex and confusing, and especially so when different polymers were used. As such, the following method for labelling of surface modified polymers from this section forward was adopted; with modification made on the

polymer surface is labelled after the type of polymer and the modification step. For example, a sample labelled **XAD4.A1** would indicate that the XAD-4 PS beads (XAD4) sample had undergone surface modification **A1**, and the general structure would look like **Ax** in **Scheme 3.1**. A sample labelled as **LDPE.A2-B4** would signify that the LDPE polymer (LDPE) surface has first went through modification **A2**, followed by modification **B4**, with general structure of **Ax-Bx'** shown in **Scheme 3.1**. A sample labelled as **PETp.6A1-B5-C2** would indicate that the PET pellets (PETp) surface had first undergone modification **A1**, followed by modification **B5** and finally derivatized with spiropyran **C2**. (See **Appendix A** for list of surface modified polymers labelling) Individual modifications with the corresponding side groups are indicated in the relevant schemes in the sections below.

3.2 Mod Ax: Pre-activation of polymer surface

3.2.1 Synthesis of diaryldiazo reactive intermediates

As discussed in Chapter 2, and as seen from **Scheme 3.1** above, pre-activation of the polymer surface with electron rich aromatic rings is necessary for efficient azo coupling onto the polymer surface. Commercially available electron rich derivatives of benzophenones, with X being OH, NMe_2 and OMe, were chosen for their variable electron donating ability. Hydroxyl groups, with a labile proton, would be able to be deprotonated, while NMe_2 and OMe are electron donating.



Scheme 3.2. General reaction scheme for synthesis of diaryldiazo. Conditions: (i) $NH_2NH_2 \cdot H_2O$, EtOH, reflux 24-48 h; (ii) MnO_2, KOH, THF, Na_2SO_4, 3h R.T in dark.

A considerable amount of effort went into the optimisation of reactions in **Scheme 3.2** to establish it as a general reaction scheme that is suitable for upscaling; the amount of hydrazine monohydrate was varied to optimise reaction time without compromising yields, different methods and conditions were tested to crystallise the hydrazone for easy purification, and both manganese dioxide and mercury (II) oxide were examined as preferred conditions to oxidise hydrazone to diazo.

Following general reaction **Scheme 3.2**, the relevant benzophenone **3.1** was first refluxed with hydrazine monohydrate in ethanol for up to 48 hours to yield the corresponding hydrazone **3.2**. It was noted that when fresh hydrazine monohydrate was used, at 15 equivalents with **3.2a1**, or 10 equivalents for **3.1a2** or **3.1a3**, 24 h of reflux in ethanol was sufficient to convert all of the starting material into the relevant hydrazone. However, when the hydrazine monohydrate had aged, up to 48 h of reflux was required. The reaction progress could be tracked using low resolution mass spectrometry. Pure products could be easily obtained by first adding a small amount of water to the crude reaction mixture when it was still hot from reflux, followed by removal of some ethanol from the mixture *in vacuo* until the mixture turned slightly chalky, then crystallizing out the hydrazone in an ice bath. Hydrazone **3.2** was then stirred with manganese dioxide in THF for 3 hours to afford the desired diazo **3.3**. Manganese dioxide was preferred over mercury (II) oxide as it is

less toxic than the latter, and was able to complete the oxidation reaction within a shorter time.

As seen from **Scheme 3.2**, all 3 types of benzophenones used **3.1** (X = -NMe_2, -OMe, -OH) were able to be converted to the respective hydrazones. Purification by crystallisation gave clean products, with yields varying from a good 77% for **3.2a1**, to excellent for **3.2a2** and **3.2a3** with 86% and 91% respectively. However, when oxidized, **3.3a3** with the free OH substituent was too unstable and reactive to be isolated for characterisation and further reaction. It was observed that the green product turned almost instantaneously to yellow upon exposure to light. On the other hand, both **3.3a1** and **3.3a2** were sufficiently stable to be used for further reaction, with **3.3a1** being relatively more reactive than **3.3a2**.

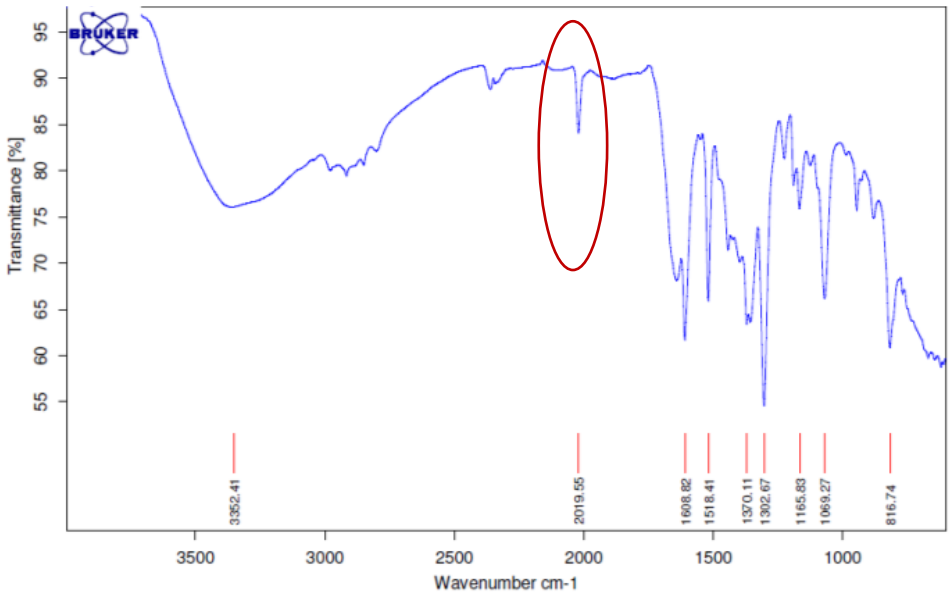


Figure 3.1. IR spectrum of 3.3a1.

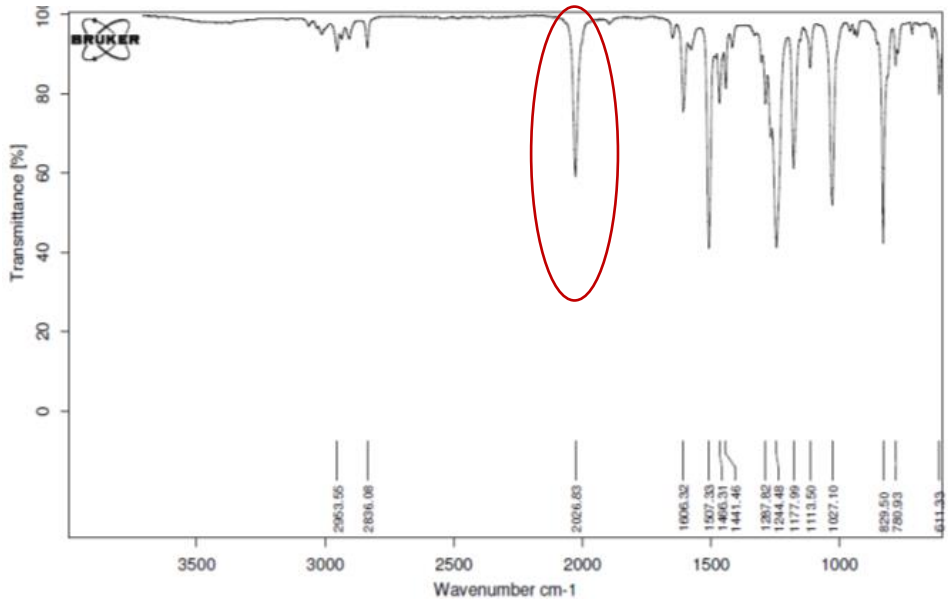
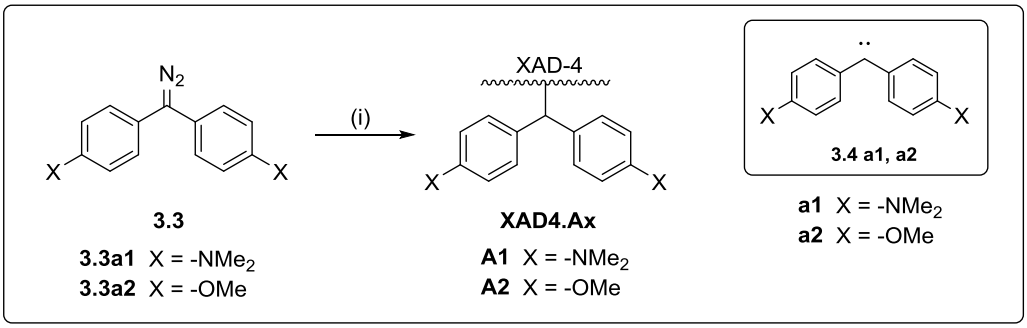


Figure 3.2. IR spectrum of 3.3a2.

Visual observation for changes of the two diazo compounds under room light was noted; **3.3a1** changed colour rather rapidly from green to yellow when exposed to room light, while **3.3a2** took some time to change from purple to yellow when exposed to the same room light. Nonetheless, characterisation by FTIR was still possible for both **3.3a1** and **3.3a2**. FTIR spectra (**Figure 3.1** and **Figure 3.2**) showed that the absorption band corresponding to the diazo group were **3.3a1** at 2020 cm^{-1} compared to **3.3a2** at 2027 cm^{-1}, clearly confirming the presence of the diazo function. In addition, **3.3a1** was not sufficiently stable for good NMR characterisation, while a relatively clean proton spectrum was obtained for **3.3a2**.

Diazo **3.3a1** was expected to be more reactive and light sensitive than **3.3a2** due to better activating effect of the nitrogen, and this is consistent with the experimental data. It was also observed that **3.3a2** could be kept up to six months and remained purple when kept in the freezer and shielded from light. However, it was best to use **3.3a1**, within a few days as it would discolour within two weeks even when it was kept in freezer and shielded from light. In both cases, the XAD-4 PS beads were surface modified with freshly prepared diazo for the best results.

3.2.2 Surface modification using diaryldiazo reactive intermediates



Scheme 3.3. Surface modification of XAD-4 PS beads. Conditions: (i) XAD-4 PS beads, Et_2O, heat at 120°C.

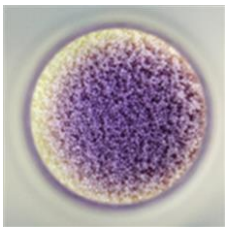


Figure 3.3. Modification A2 by heat in RBF.

The diazo **3.3** was dissolved in Et_2O and XAD-4 PS beads were poured into the solution. Careful removal the solvent *in vacuo* in the dark resulted in a thin coating of the diazo on the beads by physisorption. The beads were dried and then heated for approximately 30 to 45 min. A change in colour from green (for **3.3a1**) or purple (for **3.3a2** –see **Figure 3.3**) to yellow indicated the completion of the modification. The change in colour was due to the loss of N_2 and formation of the corresponding diarylcarbene by thermolysis. The surface modified beads were then washed with copious amount of acetone and water, and dried thoroughly on a sintered funnel.

Table 3.1. Characterisation of Mod A XAD-4 polystyrene beads.

Sample	Appearance	Combustion Analysis/ % Found	Surface Modifications/ {mol / g of polymer} [molecules. per cm^2] (%Surface Coverage)	ATR-IR	XPS Atomic Ratio		UV-Vis λ_{max} / nm
					Found	Expected	
XAD4. Blank		C: 86.47 ± 0.30 H: 7.99 ± 0.30 N: 0.18 ± 0.04	-Nil-	1602 (C=C) 1511 (C=C) 1486 (C=C)	N/C: 0.0509 O/C: 0.170	N/C: 0.00 O/C: 0.00	288
XAD4.A1		C: 89.71 ± 0.30 H: 7.98 ± 0.30 N: 0.68 ± 0.15	N: {(2.5 ± 0.6) x10^{-4}} [(2.1 ± 0.5) x10^{13}] (16 ± 4)	1603 (C=C), 1512 (C=C), 1487 (C=C), 1445 (C=C), 1349 (C-N)	N/C: 0.0436 O/C: 0.418	N/C: 0.118 O/C: 0.00	380
XAD4.A2		C: 90.90 ± 0.30 H: 8.21 ± 0.30 N: 0.14 ± 0.03	-Nil-	1603 (C=C), 1512 (C=C), 1246 (C-O), 1173 (C-O).	N/C: 0.0127 O/C: 0.248	N/C: 0.00 O/C: 0.133	349

Unexpectedly, nitrogen content was detected on the **XAD-4.Blank** (unmodified XAD-4 PS beads) when analysed using combustion elemental analysis and XPS. Nitrogen contents from the unmodified XAD-4 PS beads could have originated from the cross-linkers or initiators used in manufacturing of the beads, or other possible impurities. In addition, high porosity of the beads could lead to significant adsorption of nitrogen containing impurities. With chemical modifications and extensive post-modification washing of the beads with acetone and water, nitrogen content often remained significant, consistent with surface modification. However, for some samples (e.g **XAD4.A2**) the detected level of nitrogen dropped to close to the detection limit, and this could be due either to wash out of the nitrogen impurities or surface modification but only at a level close to the nitrogen detection limit.

From **Table 3.1**, it was evident from the combustion analysis and noticeable colour change from white to yellow that surface modification had occurred for **XAD4.A1,** with an estimate of 16% surface coverage of the modification. XPS atomic ratio estimated a much higher surface area of 37%, with N to C ratio found to be 0.0436. Characterisation by ATR-IR was not as straightforward as the peak for C-N was hidden among the peaks which correspond to the bulk polymer as seen in **Figure 3.4** below.

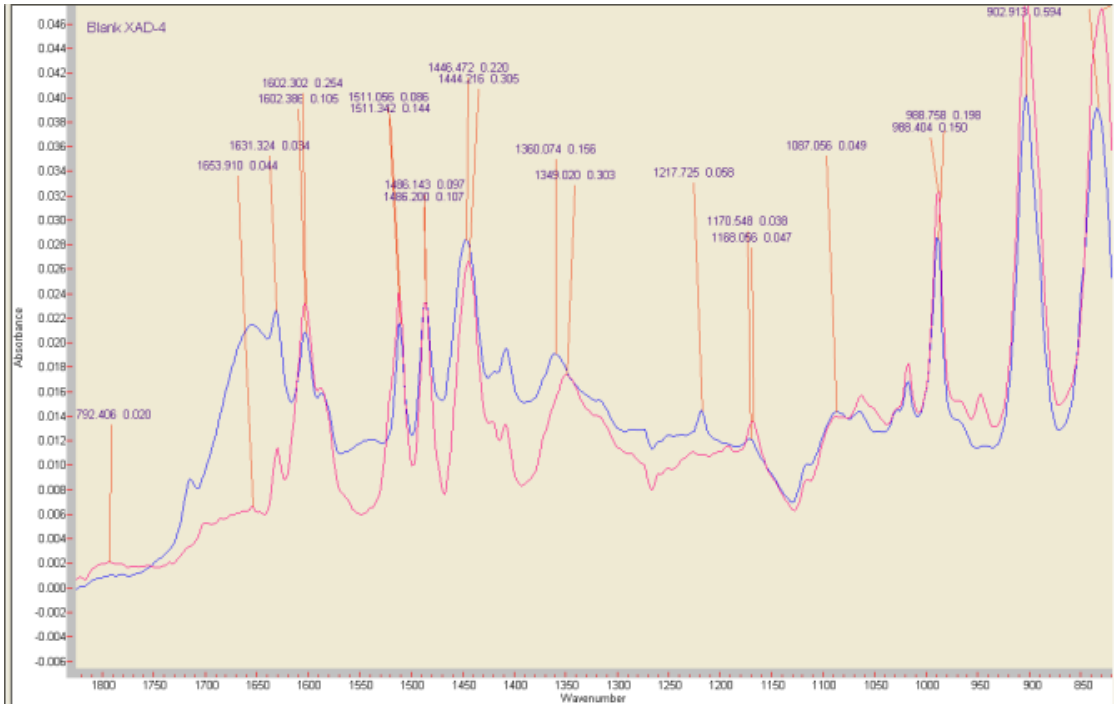


Figure 3.4 . IR spectrum of XAD4.Blank (blue) and XAD4.A1 (red) at fingerprint region.

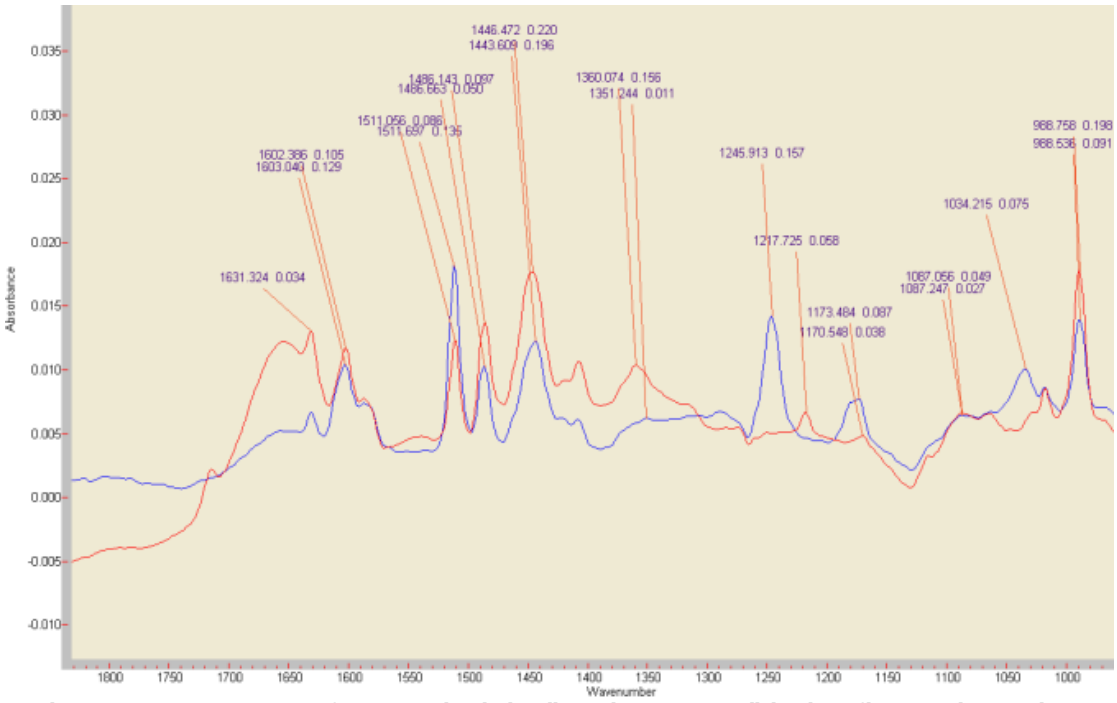


Figure 3.5. IR Spectra of XAD4.Blank (red) and XAD4.A2 (blue) at fingerprint region.

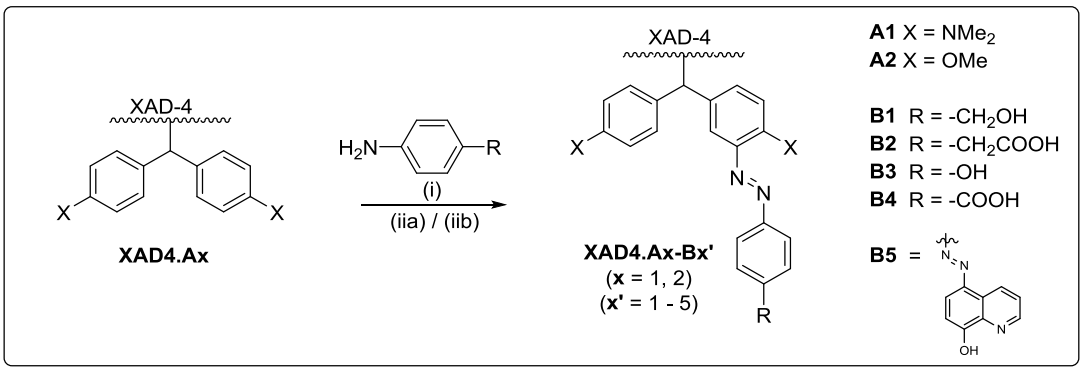
Obviously, surface coverage of **XAD4.A2** could not be estimated from combustion analysis or XPS due to the lack of nitrogen. The change in colour of the beads was not apparent either. However, successful modification was evident from the IR spectrum as seen in **Figure 3.5**, where the new peak at 1246 cm^{-1} and 1173 cm^{-1} corresponding to the C-O bond modified onto the surface was observed. Atomic

ratios found using XPS also indicated an increase in O to C ratio, and a decrease in N to C ratio, relative to **Blank XAD-4**. This was indicative that the surface of the polymer was partially covered by the modification **A2**, resulting in detection of more O from OMe group of the modification. However, as the surface modification was not of 100% coverage, some of the N that was detected could have been from the unmodified surface of the polymer.

This study was vital in deciding the best system to be transferred to Singapore for further development, in terms of ease of synthesis, and stability of system for handling and process development. Taking into consideration that the system has to be replicated in Singapore under humid conditions without molecular characterisation available, and the need to later develop the modification process for large area modification, the OMe system using **3.1a2** as starting material was preferred. Moreover, starting material **3.1a2** is much less toxic than **3.1a1** (Michler's ketone), which is a suspected carcinogen and germ cell mutagen.[111]

3.3 Mod Bx': Diazonium salt variation

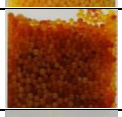
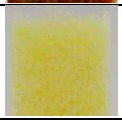
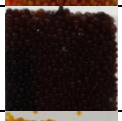
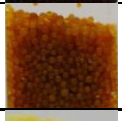
A variety of diazonium salts were experimented to demonstrate the ability to confer various chemical functional groups onto pre-activated polymer surface.

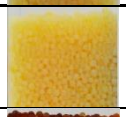
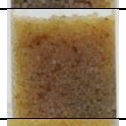


Scheme 3.4. Azo-coupling of XAD4.Ax with a variety of diazonium salts. Conditions (i): $NaNO_2$, THF:H_2O = 1:1, 3M HCl, 0C. (iia) 0°C – R.T. (iib) 0°C – R.T, NaOAc.

Following **Scheme 3.4**, diazonium salts were generated from the required amines by stirring with $NaNO_2$ in THF: H_2O = 1:1 in acidic conditions at 0°C for 30 min, and were used *in situ* (see General Reaction A). Two conditions were investigated to determine if NaOAc was necessary for effective azo coupling to occur on a solid surface. For condition (iia), beads **XAD4.Ax** were poured directly into the solution of diazonium salt, whereas for condition (iib), NaOAc was added into the solution of freshly prepared diazonium salt and stirred for 5 min prior to the addition of the beads into the solution. The beads were then left to stand for 18 h in both conditions, followed by washing with copious amount of acetone and water and dried on a sintered funnel. Controls (**XAD4.Ctrl-Bx'**) were made using same conditions as (iib), except that blank XAD-4 PS beads were used.

Table 3.2. Surface Modified XAD-4 samples.

Sample	Appearance	Combustion Analysis/ % Found	Surface Modifications/ {mol / g of polymer} [molecules. per cm^2] (%Surface Coverage)	ATR-IR	XPS Atomic Ratio		UV-Vis λ_{max} / nm
					Found	Expected	
XAD4. A2-B1 (iia)		C: 90.1 ± 0.30 H: 7.72 ± 0.30 N: 0.25 ± 0.06	N: {(8.9 ± 2.0) x10^{-5}} [(7.4 ± 1.6) x10^{12}] (8.8 ± 1.9)	-Nil-	-Nil-	-Nil-	389
XAD4. A2-B1 (iib)		C: 89.71 ± 0.30 H: 7.75 ± 0.30 N: 0.32 ± 0.07	N: {(1.1 ± 0.2) x10^{-4}} [(9.5 ± 2.1) x10^{12}] (11 ± 2.4)	1604 (C=C), 1511 (C=C), 1246 (C-O), 1173 (C-O)	-Nil-	-Nil-	426
XAD4. Ctrl-B1		C: 91.3 ± 0.30 H: 8.21 ± 0.30 N: 0.17 ± 0.04	N: {(6.1 ± 1.3) x10^{-5}} [(5.0 ± 1.1) x10^{12}] (4.3 ± 0.9)	-Nil-	-Nil-	-Nil-	402
XAD4. A2-B2 (iia)		C: 89.69 ± 0.30 H: 7.68 ± 0.30 N: 0.43 ± 0.09	N: {(1.5 ± 0.3) x10^{-4} [(1.3 ± 0.3) x10^{13} (16 ± 3)	-Nil-	-Nil-	-Nil-	418
XAD4. A2-B2 (iib)		C: 87.42 ± 0.30 H: 7.48 ± 0.30 N: 1.07 ± 0.24	N: {(3.8 ± 0.8) x10^{-4}} [(3.2 ± 0.7) x10^{13}] (40 ± 9)	1701 (C=O), 1604 (C=C), 1512 (C=C), 1487 (C=C)	N/C: 0.107 O/C: 0.249	N/C: 0.136 O/C: 0.182	496
XAD4. Ctrl-B2		C: 90.63 ± 0.30 H: 7.94 ± 0.30 N: 0.30 ± 0.07	N: {(1.1 ± 0.2) x10^{-4}} [(8.9 ± 2.0) x10^{12}] (7.9 ± 1.7)	-Nil-	-Nil-	-Nil-	407
XAD4. A2-B3 (iia)		C: 90.18 ± 0.30 H: 7.84 ± 0.30 N: 0.27 ± 0.06	N: {(9.6 ± 2.1) x10^{-5}} [(8.0 ± 1.8) x10^{12}] (9.3 ± 2.0)	-Nil-	-Nil-	-Nil-	349, 412
XAD4. A2-B3 (iib)		C: 89.81 ± 0.30 H: 7.78 ± 0.30 N: 0.40 ± 0.9	N: {(1.4 ± 0.3) x10^{-4}} [(1.2 ± 0.3) x10^{13}] (14 ± 3)	1603 (C=C), 1512 (C=C), 1487 (C=C), 1444 (C=C)	-Nil-	-Nil-	422

XAD4. Ctrl-B3		C: 90.92 ± 0.30 H: 7.92 ± 0.30 N: <0.1	-Nil-	-Nil-	-Nil-	-Nil-	350, 409
XAD4. A2-B4 (iia)		C: 89.98 ± 0.30 H: 7.76 ± 0.30 N: 0.32 ± 0.07	N: {(1.1 ± 0.2) x10^{-4}} [(9.5 ± 2.1) x10^{12}] (12 ± 3)	-Nil-	-Nil-	-Nil-	349
XAD4. A2-B4 (iib)		C: 88.75 ± 0.30 H: 7.60 ± 0.30 N: 0.47 ± 0.10	N: {(1.7 ± 0.4) x10^{-4}} [(1.4 ± 0.3) x10^{13}] (17 ± 4)	1744 (C=O), 1604 (C=C), 1512 (C=C), 1487 (C=C)	N/C: 0.0899 O/C: 0.221	N/C: 0.143 O/C: 0.190	441
XAD4. Ctrl-B4		C: 90.83 ± 0.30 H: 7.93 ± 0.30 N: <0.1	-Nil-	-Nil-	-Nil-	-Nil-	402
XAD4. A2-B5 (iia)		C: 90.49 ± 0.30 H: 8.29 ± 0.30 N: 0.24 ± 0.05	N: {(5.7 ± 1.3) x10^{-5}} [(4.8 ± 1.1) x10^{12}] (3.9 ± 0.9)	-Nil-	-Nil-	-Nil-	397
XAD4. A2-B5 (iib)		C: 90.94 ± 0.30 H: 8.35 ± 0.30 N: 0.24 ± 0.05	N: {(5.7 ± 1.3) x10^{-5}} [(4.8 ± 1.1) x10^{12}] (3.9 ± 0.9)	1603 (C=C), 1512 (C=C), 1246 (C-O), 1178 (C-O).	N/C: 0.0633 O/C: 0.357	N/C: 0.125 O/C: 0.125	377
XAD4. Ctrl-B5		C: 90.66 ± 0.30 H: 8.02 ± 0.30 N: <0.1	-Nil-	-Nil-	-Nil-	-Nil-	333
XAD4. A1-B4		C: 88.49 ± 0.30 H: 7.72 ± 0.30 N: 1.03 ± 0.23	N: {(1.8 ± 0.4) x10^{-4}} [(1.5 ± 0.3) x10^{13}] (15 ± 3)	1734 (C=O), 1603 (C=C), 1509 (C=C), 1270 (C-O)	N/C: 0.0843 O/C: 0.185	N/C: 0.167 O/C: 0.0833	522
XAD4. A1-B5		C: 89.82 ± 0.30 H: 8.14 ± 0.30 N: 0.70 ± 0.15	N: {(1.0 ± 0.2) x10^{-4}} [(8.3 ± 1.8) x10^{12}] (8.2 ± 1.8)	1603 (C=C), 1511 (C=C), 1445 (C=C), 1352 (C-N)	N/C: 0.0215 O/C: 0.131	N/C: 0.192 O/C: 0.0385	408, 655

ATR-IR spectroscopic analysis was not always conclusive of surface modification due to hidden or overlapping peaks and in particular was not very useful for **XAD4.A2-B1**, **XAD4.A2-B3**. However, IR spectra of **XAD4.A2-B2** and **XAD4.A2-B4** indicated the presence of C=O functional group at around 1701 cm^{-1} and 1744 cm^{-1}, and thus, indicative of successful modification.

From the results summarised in **Table 3.2**, it was noted that NaOAc was indispensable for better azo coupling efficiency. However, the extent of improvement in coupling efficiency due to addition of NaOAc differed for different diazonium salts. There was a slight increase of 2.2% estimated surface coverage for **XAD4.A2-B1**, a 5% increase for **XAD4.A2-B4**, and a significant increase of 24% for **XAD4.A2-B2**. However, surface coverage for **XAD4.A2-B5** was calculated to be the same of 3.9%, with or without NaOAc. It appeared that, be it for samples using

the same diazonium salt with different reaction conditions, or across samples of same conditions with different diazonium salt, the increase in azo coupling efficiency, and hence, surface coverage, was also reflected in the increase in colour intensity of the modified XAD-4 PS beads as seen from the photos of the beads in **Table 3.2**. The colours of the beads were quantified using diffused reflectance UV-Vis (absorbance mode).

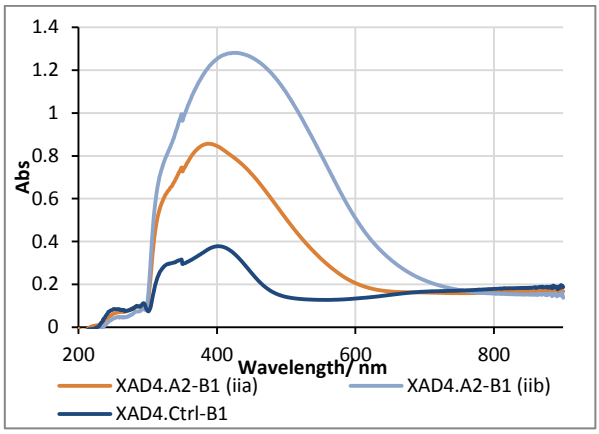


Figure 3.6. UV-Vis spectra of surface modified beads XAD4.A2-B1 (iia) and (iib), and their control Ctrl-B1.

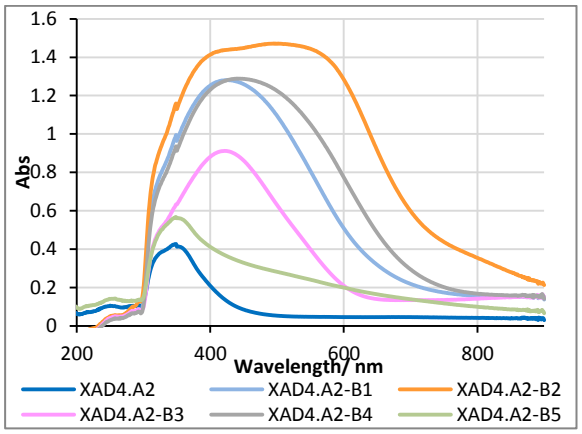


Figure 3.7. UV-Vis spectra of surface modified beads XAD4.A2-B1 to B5 (iib).

As seen from **Figure 3.6,** using the same diazonium salt species to give modification **B1**, there was increase in intensity of absorption from **XAD4.Ctrl-B1** to **XAD4.A2-B1 (iia)** to **XAD4.A2-B1 (iib)**. This correlates with the increase in azo coupling efficiency from control to samples without NaOAc in azo coupling, to samples with NaOAc in azo coupling, as verified using combustion analysis. This trend was similar for all the samples (see Appendix D for UV-Vis spectra of other samples). In general, the effect brought about by NaOAc was similar to the solution investigation discussed in Chapter 2; NaOAc was necessary to increase the pH to prevent protonation of the OMe group, and thus, increasing electron density of the aromatic ring for enhanced azo coupling.

It was previously shown both in the solution chemistry investigation (Chapter 2) and reported in the literature that the anisole-type system did not react with any of the diazonium salts as it was not sufficiently nucleophilic.[100, 112] However, as seen from the results in **Table 3.2**, all the controls (**XAD4.Ctrl-B1** – **XAD4.Ctrl b5**) indicated much lower nitrogen content relative to the samples with pre-activated surfaces. **Figure 3.6** also showed that **XAD4.Ctrl-B1**, which used Blank XAD-4 PS beads for azo-coupling, has lower UV-Vis absorbance compared to azo coupling with polymers that has pre-activated surfaces. This not only illustrated that it was necessary for the pre-activation of the polymer surface for good azo coupling efficiency, but also confirmed that azo coupling could take place with OMe type system, contrary to the results in solution investigation. However, the underlying reason for the difference in solution and solid interface type chemistry remained unclear.

As seen from **Figure 3.7**, the absorption intensity was the highest for **XAD4.A2-B2**, followed by **XAD4.A2-B4**, then **XAD4.A2-B1**, and **XAD4.A2-B3**, and lastly **XAD4.A2-B5**. This is almost consistent with results from combustion analysis, with **XAD4.A2-B2** having highest surface coverage, followed by **XAD4.A2-B4**, and **XAD4.A2-B5** having lowest nitrogen content. Different side groups attached to the diazonium salt resulted in the difference in electrophilicity of the diazonium salt, and hence, the different extent and efficiency of azo coupling onto the polymer surface. In general, an isolated chromophore of the azo group (R-N=N=R) with $n \rightarrow \pi^*$ transition would have λ_{max} around 340 nm.[113] However, when azo-coupled with the aromatic ring, the extent of conjugation increased, resulted in bathochromic shift to longer wavelength as seen in **Figure 3.7**, with all the samples of **XAD4.A1-bx'** having λ_{max} due to the azo moiety greater than 340 nm. Increased conjugation

resulted in the electronic levels of the chromophore moving closer together, thus, the energy required to produce a transition from an occupied electronic level to an unoccupied electronic level decreases, causing the wavelength of the UV-Vis absorbed to be longer. An increase in intensity, hyperchromicity, was also observed, consistent with a greater density of chromophores at the polymer surface. Despite the difference in bathochromic shift due to different substituent side groups, and thus λ_{max}, absorbance intensity is reflective of efficiency of azo coupling.

According to Beer-Lambert Law:

$$A = \log(\frac{Io}{I}) = \varepsilon cl \text{ , where}$$

A = Absorbance,

Io = Intensity of incident light,

I = intensity of light leaving sample

c = concentration of the surface modification,

l= path length,

ε = molar absorption coefficient

Since there is a similar main chromophore and only different with side group, ε was assumed to be similar for all the samples. This assumption is valid from consideration of **Figure 3.9**, which shows that analogous azo coupling in solution exhibit similar UV-Vis spectra, implying similar ε value. Taking l to be constant, absorbance would be directly proportional to concentration c, which translates to extent of azo coupling on the polymer surface when evaluating polymers with the same modification **A1** or **A2**.

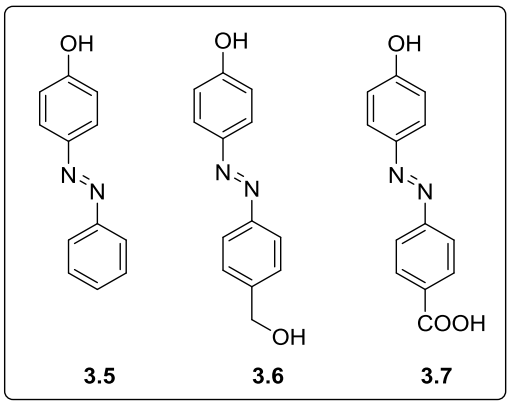


Figure 3.8. Analogues of surface modification.

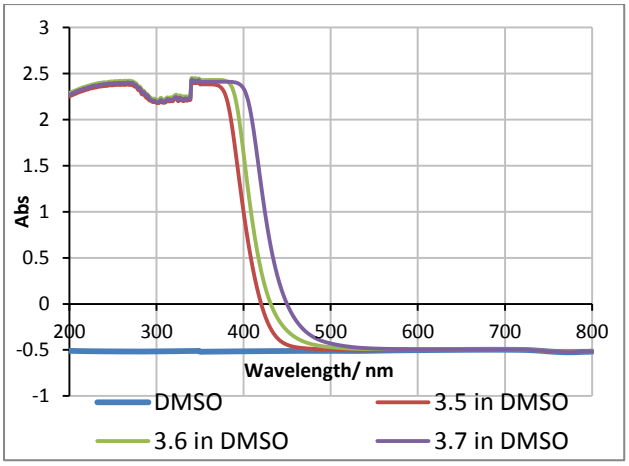


Figure 3.9. UV-Vis absorption spectra of analogues in DMSO.

Samples **XAD4.A2-B2**, **XAD4.A2-B4** and **XAD4.A2-B5** were of particular interest. According to the solution studies in Chapter 2 where analogues to modifications on surface were synthesized, modification **B2** gave a complex mixture, even though molecular ion peak of azo coupled product appeared as base peak in the low resolution mass spectrum, modification **B4** gave the best yields with desired product isolated, and modification **B5** gave complex mixtures even though it was confirmed that the diazonium salt was formed using high resolution mass spectrometry. For sample **XAD4.A2-B2**, similar to the solution studies, there were black impurities formed. The samples were cleaned by extensive washing with water and acetone with intermittent ultrasonication. The identity of the black impurities remained unknown. On the other hand, excluding results of **B2**, modification **B4** still performed the best compared to other diazonium salts, with estimated surface coverage of 17%. Although **B5** performed the worst with estimated surface coverage of only 3.8%, results still indicated that there was azo coupling reaction onto the surface of XAD-4 beads.

With materials on hand, beads **XAD4.A1** were examined using modification **B4**, with the best performing diazonium salt with the benzoic acid moiety, and

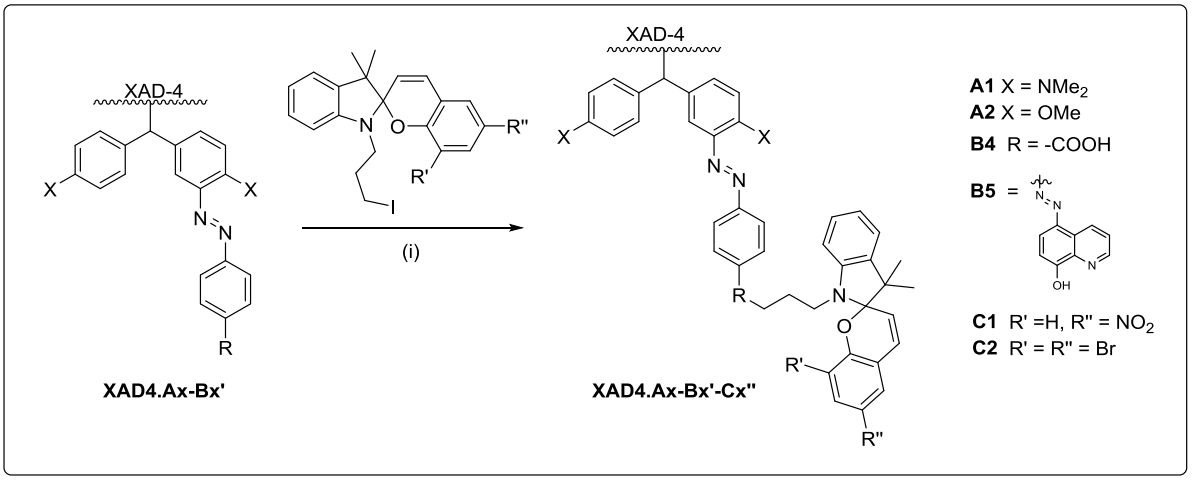
modification **B5,** with the worst performing diazonium salt with the 8-hydroxyquinoline side group. As seen from the results in **Table 3.2**, combustion analysis showed that the surface coverage of the modification was indeed better for **B4** than **B5**, with 15% and 8.2% respectively. This is also consistent with the XPS data which showed that the N to C ratio found for **XAD4.A1-B4** was 0.0843, while that for **XAD4.A1-B5** was 0.0215, with the former being higher due to better coupling efficiency.

It was expected for beads **XAD4.A1** to have better azo coupling than beads **XAD4.A2** due to the more activated aromatic ring system. However, this is inconsistent with the experimental data collected. Both modifications **B4** using **XAD4.A1** and **XAD4.A2** resulted in similar extent of azo coupling, with estimated surface coverage of 15% and 17% for beads **XAD4.A1-B4** and **XAD4.A2-B4** respectively. This unexpected result suggested that surface coverage of modification **A2** was higher than that of **A1**, thus, leading to a similar extent of azo coupling (Mod B) despite **A2** having a less activated surface than **A2**. On the other hand, the difference seemed to be of significance in the case of modification **B5**, where extent of azo coupling was low. With **XAD4.A1-B5** and **XAD4.A2-B5** having a low surface coverage of 3.9% and 8.2% respectively, a difference of 4.3% would seem substantial.

In general, it was concluded that the best performing diazonium salt was **B4** with the benzoic acid moiety, while **B5** with the 8-hydroxyquinoline moiety showed the worst coupling efficiency. Despite showing very high nitrogen content in combustion analysis and XPS measurement, and therefore estimated surface coverage, it was uncertain if **B2,** with the phenylacetyl moiety, was a good candidate for diazonium salt coupling as it resulted in side products which could not be characterised, and

uncertainty of the underlying chemistry. Nonetheless, alongside with all other surface modified sample, it was tested for drug delivery properties, which is explored in Chapter 4.

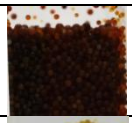
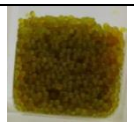
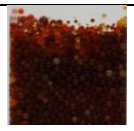
3.4 Mod Cx'': Spiropyran derivatization



Scheme 3.5 . Derivatization of XAD4.Ax-Bx'' with spiropyran. Conditions: (i) Reflux in MeCN with K_2CO_3, 3h.

Materials on hand were subjected to further post-modification by inserting a spiropyran moiety. Following **Scheme 3.5**, refluxing the surface-modified beads **XAD4.Ax-Bx'** with K_2CO_3 and the corresponding spiropyrans in MeCN, would afford the surface-modified beads **XAD4.Ax-Bx'-Cx''**. Other than being able to confer desired functional moiety **R** using azo coupling of diazonium salt via modification **Bx'**, an additional step in this whole modification route would enable more complex functionalities, such as photochromic spiropyrans, to be modified onto polymer surfaces. XAD-4 PS beads with modifications **B4** and **B5** were chosen, with **B4** being the best performing and **B5** the worst.

Table 3.3. List of polymers with surface derivatized with spiropyrans.

Sample	Appearance	Combustion Analysis/ % Found	Surface Modifications/ {mol / g of polymer} [molecules. per cm^2] (%Surface Coverage)	ATR-IR	XPS Atomic Ratio		UV-Vis λ_{max} / nm
					Found	Expected	
XAD4. A1-B4-C1		C: 88.33 ± 0.30 H: 7.66 ± 0.30 N: 1.03 ± 0.23	N: {(1.2 ± 0.3) $x10^{-4}$} [(1.0 ± 0.2) $x10^{13}$] (12 ± 3)	1734 (C=O), 1603 (C=C), 1362 (NO_2), 1271 (C-O)	N/C: 0.0679 O/C: 0.169	N/C: 0.133 O/C: 0.111	524
XAD4. A1-B5-C1		C: 90.13 ± 0.30 H: 7.75 ± 0.30 N: 0.79 ± 0.17	N: {(8.1 ± 1.8) $x10^{-5}$} [(6.7 ± 1.5) $x10^{12}$] (7.9 ± 1.7)	1603 (C=C), 1511 (C=C, NO_2), 1486 (C=C), 1445 (C=C), 1343 (NO_2 , C-N)	N/C: 0.0429 O/C: 0.155	N/C: 0.149 O/C: 0.0851	406
XAD4. A1-B5-C2		C: 89.72 ± 0.30 H: 8.28 ± 0.30 N: 0.49 ± 0.11 Br: 0.97 ± 0.21	N: {(5.8 ± 1.3) $x10^{-5}$} [(4.8 ± 1.1) $x10^{12}$] (5.7 ± 1.3) Br: {(6.0 ± 1.3) $x10^{-5}$} [(5.0 ± 1.1) $x10^{12}$] (5.9 ± 1.3)	1605 (C=C), 1512 (C=C), 1488 (C=C), 1446 (C=C), 1351 (C-N).	N/C: 0.0729 O/C: 0.161 Br/C: 0.00222	N/C: 0.128 O/C: 0.0426 Br/C: 0.0426	342, 600
XAD4. A2-B4-C1		C: 87.60 ± 0.30 H: 7.71 ± 0.30 N: 0.60 ± 0.13	N: {(1.1 ± 0.2) $x10^{-4}$} [(8.0 ± 1.8) $x10^{12}$] (11 ± 2)	1702 (C=O), 1604 (C=C), 1511 (C=C, NO_2), 1338 (NO_2), 1173 (C-O)	N/C: 0.0384 O/C: 0.189	N/C: 0.0930 O/C: 0.163	450
XAD4. A2-B5-C1		C: 89.41 ± 0.30 H: 8.21 ± 0.30 N: 0.23 ± 0.05	N: {(3.2 ± 0.7) $x10^{-5}$} [(2.7 ± 0.6) $x10^{12}$] (2.8 ± 0.6)	1604 (C=C), 1512 (C=C, NO_2), 1341 (NO_2), 1246 (C-O).	N/C: 0.0893 O/C: 0.224	N/C: 0.111 O/C: 0.133	349, 524, 555, 653
XAD4. A2-B5-C2		C:90.77 ± 0.30 H: 7.64 ± 0.30 N: 0.23 ± 0.05 Br: 0.49 ± 0.11	N: {(4.1 ± 0.9) $x10^{-5}$} [(3.4 ± 0.7) $x10^{12}$] (3.5 ± 0.8) Br: {(3.1 ± 0.7) $x10^{-5}$} [(2.6 ± 0.6) $x10^{12}$] (2.6 ± 0.6)	1604 (C=C), 1512 (C=C), 1246 (C-O), 1173 (C-O).	N/C: 0.114 O/C: 0.236 Br/C: 0.00176	N/C: 0.0889 O/C: 0.0889 Br/C: 0.0444	349, 560
XAD4. Ctrl C1		C: 90.71 ± 0.30 H: 7.93 ± 0.30 N: <0.1	-Nil-	-Nil-	-Nil-	-Nil-	358, 556

Modification A1 vs A2: As seen from **Table 3.3,** both samples **XAD4.A1-B4-C1** and **XAD4.A2-B4-C1** have similar estimated surface coverage of 12% and 11% respectively. On the other hand, samples **XAD4.A1-B5-C1** and **XAD4.A2-B5-C1** registered a difference in estimated surface coverage of 5.1%. Likewise for samples **XAD4.A1-B5-C2** and **XAD4.A2-B5-C2**, the estimated surface coverage differed by up to 3.3%. This is consistent with the discussion above, where the extent of modification **Bx'** was dependent on the extent of modification **Ax**, while modification **B4** showed a similar extent of modification but **B5** had greater discrepancies for the

different pre-activated surface. This, in turn, affected modification **Cx"**, as seen from the results above, with **XAD4.Ax-B4-C1** having similar results, but **XAD4.Ax-B5-C1** or **XAD4.Ax-B5-C2** having greater difference in surface coverage. This showed the difference in extent of modification was likely to further propagate with each step.

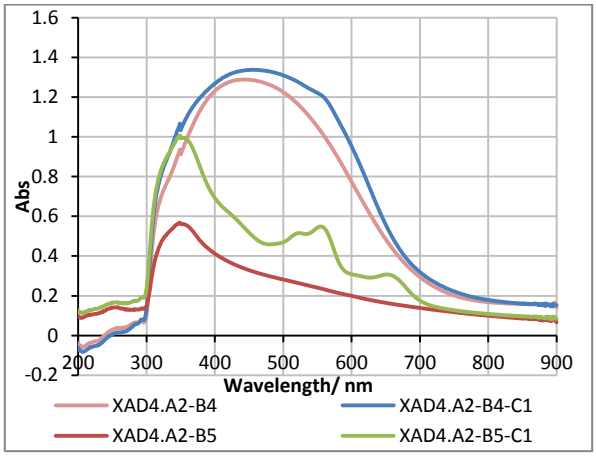


Figure 3.10. UV-Vis spectra for surface modified beads XAD4.A2-B4 and XAD4.A2-B5, before and after surface modification C1.

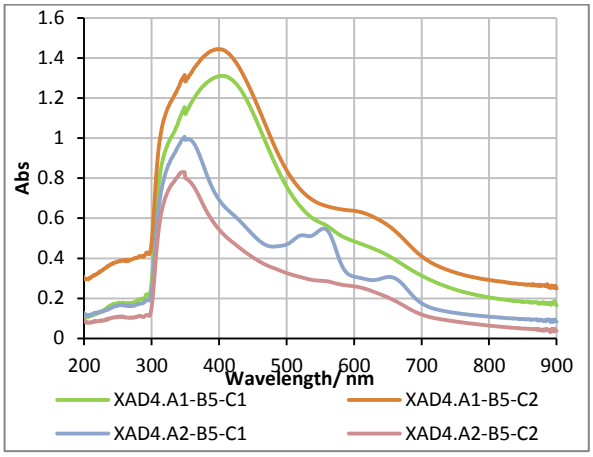


Figure 3.11. UV-Vis spectra for surface modified beads with modification B5.

Modification B4 vs B5: Colour change due to derivatization with spiropyran (Modification **Cx"**) was not significant for **XAD.A2-B4-C1** as the beads were already intensely coloured prior to the derivatization. However, as the XAD-4 beads with modification **B5** were relatively lightly coloured, after modification **C1** and **C2**, the change in colour of the beads was more apparent. This was especially noticeable for sample **XAD4.A2-B5-C1**. As seen in **Table 3.3**, where **XAD4.A2-B5** changed from light brown to pink when derivatized with spiropyran to give **XAD4.A2-B5-C1**. This is also reflected in the UV-Vis data collected. As seen in **Figure 3.10**, the change in absorbance intensity from **XAD4.A2-B4** to **XAD4.A2-B4-C1** was only a slight 0.05 at 450nm, whereas that for **XAD4.A2-B5** to **XAD4.A2-B5-C1** was about 0.42 at 350nm. However, different from the above discussion in Section 3.3, the increase in absorbance is not an indication of efficiency of modification. The

increase in absorbance from **XAD4.A2-B4** to **XAD4.A2-B4-C1** was very little as both polymers were near limit of absorbance measurement.

$$A = \log (I_0/I),$$

where

A = Absorbance

I_0 = Intensity of incidence light

I = Intensity of light leaving cell

Graph 3.1. Percentage of light absorbed by sample against absorbance unit.



As seen from **Graph 3.1**, the absorbance follows a logarithmic function; with an absorbance nearing 1.5, it means that about 97% the light is being absorbed by the sample. Therefore, the addition of a new chromophore in sample **XAD4.A2-B4-C1** would not have a large increase in absorbance due to the new chromophore as seen in sample **XAD4.A2-B5-C1** as the former already has almost all the light absorbed.

However, the absolute absorbance value for **XAD4.A2-B4-C1** and **XAD4.A2-B5-C1** still does reflect that the surface coverage of modification for the former was higher than that of latter. With a different in the side group only, they are likely to have similar molar extinction coefficient ε, making comparison valid as discussed in **Section 3.3**. This is different from the previous case, due to **XAD4.A2-B4-C1** nearing the limit of maximum absorbance such that the absorbance value no longer has direct correlation to concentration, and hence, the extent of surface modification. Therefore, the absolution absorbance value could only give a rough indication of which sample has higher surface modification coverage.

Modification c1 vs c2: With different side groups on the spiropyran, the colour conferred on the XAD-4 PS beads differs as well. Surface modification with spiropyran containing the NO_2 moiety (**C1**) gave a more purplish-pink colouration whereas modification with the spiropyran containing the di-bromo moieties (**C2**) gave a greenish-blue colouration. This is reflected in the UV-Vis spectra of the samples as seen in Figure 3.11. The peaks due to modification **C1** were very apparent in the UV-Vis spectra of sample **XAD4.A2-B5-C1**, appearing at 524 nm, 555 nm and 653. According to **Table 3.4**, the colour observed for these peaks should be a combination of red-violet and violet. This corresponded to the picture of the sample shown in **Table 3.3**. Similarly, samples **XAD4.A1-B5-C2** showed peak at 600 nm that corresponded to the blue-green colour observed.

Table 3.4. Relationship between the observed colour and colour absorbed at their corresponding wavelength.[113]

Colour Observed	Wavelength Absorbed / nm	Colour Absorbed
Yellow	400	Violet
Orange	450	Blue
Red	500	Blue-green
Red-Violet	530	Yellow-green
Violet	550	Yellow
Blue-green	600	Orange-red
Green	700	Red

Derivatization efficiency was defined as:

$$\frac{\text{Surface coverage of mod C polymer}}{\text{Surface coverage of mod B polymer}} \times 100\%$$

Table 3.5. Modification C1 derivatization efficiency.

	A1 (NMe_2)	**A2 (OMe)**
Ax-B4	12/15 = 80%	11 / 17 = 65%
Ax-B5	7.9 / 8.2 = 96%	2.8 / 3.9 = 72%
Yields of analogues	79% (**2.48**)	72% (**2.49)**

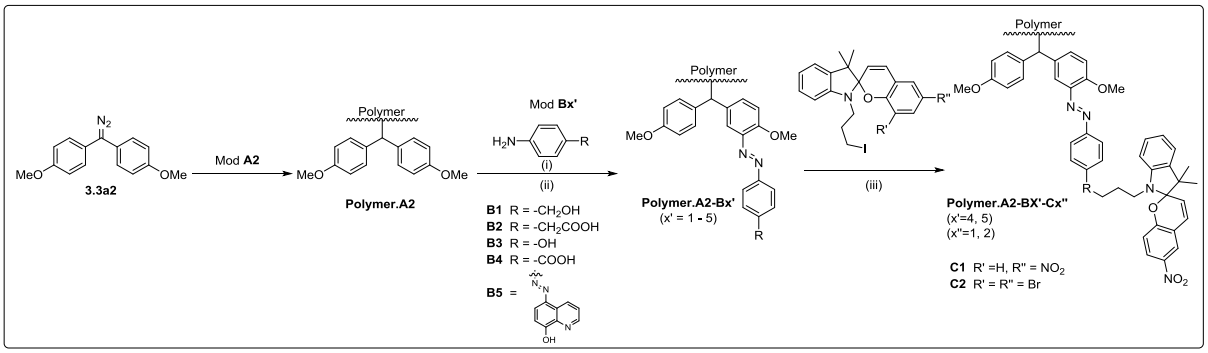
The derivatization efficiency calculated as shown in **Table 3.5** showed that derivatization with spiropyran on the surface of the XAD-4 PS beads had efficiency similar to that seen in the solution investigation. With the photochromic spiropyran moiety attached to the surface of the XAD-4 PS beads, the beads displayed light responsive photochromic properties. This is discussed in Chapter 4.

3.5 Substrate Variation

With the general surface modification system determined, and the conditions for each step of the diaryldiazo synthesis and surface modification optimized and finalized (**Scheme 3.6**), the substrate scope was expanded. It was necessary to test the versatility of the system with various varieties of polymeric substrates, prior to attempts to translate the modification process from a lab process to a feasible large-scale surface engineering process, to ensure that the synthetic and surface modification route established so far works for other polymer substrates. A variety of polymers, including PET pellets (PETp), LDPE pieces (LDPE) to UHMWPE powders (UHMW) were tested. With polymers of different forms and bulk chemical structures, the expansion of substrate scope would enable better understanding of the advantages and limitations of the surface modification method established for different types and forms of polymers. The surface area of each material was determined by BET analysis shown in **Table 3.6**.

Table 3.6. BET data of various polymers measured.

	PET pellets	LDPE powder	UHMWPE powder
BET measurement/ m^2/g	0.998± 0.265	0.136 ± 0.019	1.91 ± 0.04



Scheme 3.6. General scheme for surface modification of polymers. Conditions (i): $NaNO_2$, THF:H_2O = 1:1, 3M HCl, 0°C. (ii) 0°C – R.T, NaOAc. (iii) Spiropyran **2.8** or **2.9**, K_2CO_3 in reflux 3 h in MeCN.

Table 3.7. Surface modification of various polymers.

Sample	Appearance	Combustion Analysis/ % Found	ATR-IR	XPS Atomic Ratio		UV-Vis λ_{max} / nm
				Found	Expected	
Blank PETp		C: 44.32 ± 0.30 H: 3.11 ± 0.30 N: <0.1	1714 (C=O), 1506 (C=C), 1240 (C-O).	-Nil-	-Nil-	277
PETp. A2		C: 44.03 ± 0.30 H: 3.09 ± 0.30 N: <0.1	1607 (C=C), 1507 (C=C), 1242 (C-O), 1173 (C-O)	-Nil-	-Nil-	277, 369
PETp. A2-B1		C: 45.06 ± 0.30 H: 3.87 ± 0.30 N: <0.1	1611 (C=C), 1506 (C=C), 1243 (C-O)	-Nil-	-Nil-	277, 369
PETp. A2-B2		C: 44.71 ± 0.30 H: 3.62 ± 0.30 N: 0.18 ± 0.04	1714 (C=O hidden under C=O for substrate), 1609 (C=C), 1507 (C=C)	-Nil-	-Nil-	277, 369
PETp. A2-B3		C: 44.09 ± 0.30 H: 4.47 ± 0.30 N: <0.1	1608 (C=C), 1506 (C=C)	-Nil-	-Nil-	277, 369
PETp. A2-B4		C: 44.15 ± 0.30 H: 4.30 ± 0.30 N: <0.1	1714 (C=O), 1608 (C=C), 1506 (C=C),	-Nil-	-Nil-	277, 369
PETp. A2-B4-C1		C: 43.32 ± 0.30 H: 3.84 ± 0.30 N: 0.27 ± 0.06	1715 (C=O), 1612 (C=C), 1507 (C=C), 1341 (NO_2), 1242 (C-O).	-Nil-	-Nil-	277, 369
PETp. A2-B5		C: 44.6 ± 0.30 H: 3.09 ± 0.30 N: <0.1	1606 (C=C), 1506 (C=C), 1241 (C-O), 1173 (C-O)	-Nil-	-Nil-	277, 369
PETp. A2-B5-C1		C: 43.42 ± 0.30 H: 3.12 ± 0.30 N: 0.52 ± 0.11	1610 (C=C 1507 (C=C, NO_2), 1341 (NO_2), 1243 (C-O)	-Nil-	-Nil-	277, 369, 562

Sample	Appearance	Combustion Analysis/ % Found	ATR-IR	XPS Atomic Ratio		UV-Vis λ_{max} / nm
				Found	Expected	
PETp. A2-B5-C2		C: 44.15 ± 0.30 H: 3.08 ± 0.30 N: 0.57 ± 0.13 Br: 0.15 ± 0.03	1613 (C=C), 1506 (C=C), 1243 (C-O) 1175 (C-O)	-Nil-	-Nil-	277, 369
PETp. Ctrl-C1		C: 44.23 ± 0.30 H: 3.87 ± 0.30 N: 0.21 ± 0.05	-Nil-	-Nil-	-Nil-	296, 358
Blank LDPE		C: 85.19 ± 0.30 H: 14.77 ± 0.30 N: <0.1	2916, 2849, 1473	N/C: 0.000838 O/C: 0.0464	N/C: 0.00 O/C: 0.00	283
LDPE. A2		C: 85.16 ± 0.30 H: 14.66 ± 0.30 N: <0.1	1603 (C=C), 1507 (C=C), 1245 (C-O)	N/C: 0.00262 O/C: 0.0457	N/C: 0.00 O/C: 0.133	283, 351
LDPE. A2-B1		C: 85.55 ± 0.30 H: 14.75 ± 0.30 N: <0.1	1604 (C=C), 1507 (C=C), 1246 (C-O)	-Nil-	-Nil-	292, 356
LDPE. A2-B2		C: 83.78 ± 0.30 H: 14.00 ± 0.30 N: 1.21 ± 0.27	1742 (C=O), 1606 (C=C), 1253 (C-O)	-Nil-	-Nil-	259, 356, 490
LDPE. A2-B3		C: 85.59 ± 0.30 H: 14.63 ± 0.30 N: <0.1	1604 (C=C), 1507 (C=C), 1245 (C-O)	-Nil-	-Nil-	243, 293, 348
LDPE. A2-B4		C: 85.59 ± 0.30 H: 14.09 ± 0.30 N: <0.1	1604 (C=C), 1507 (C=C), 1245 (C-O)	N/C: 0.0146 O/C: 0.0916	N/C: 0.143 O/C: 0.190	295, 348
LDPE. A2-B4-C1		C: 85.14 ± 0.30 H: 14.50 ± 0.30 N: <0.1	1247 (C-O), 1175 (C-O)	N/C: 0.0172 O/C: 0.0670	N/C: 0.0930 O/C: 0.163	295, 348, 563
LDPE. A2-B5		C: 85.37 ± 0.30 H: 14.41 ± 0.30 N: <0.1	1604 (C=C), 1247 (C-O)	-Nil-	-Nil-	283, 351
LDPE. A2-B5-C1		C: 85.5 ± 0.30 H: 14.56 ± 0.30 N: <0.1	2020, 1472, 1261	-Nil-	-Nil-	283, 351
LDPE. A2-B5-C2		C: 85.51 ± 0.30 H: 14.65 ± 0.30 N: <0.1 Br: <0.1	1978, 1473, 1261	-Nil-	-Nil-	283, 351
LDPE. Ctrl-C1		C: 85.26 ± 0.30 H: 14.71 ± 0.30 N: <0.1	-Nil-	-Nil-	-Nil-	213, 255, 299, 348, 563
Blank UHMW PE		C: 84.64 ± 0.30 H: 15.17 ± 0.30 N: <0.1	2915, 2848, 1472	-Nil-	-Nil-	286

Sample	Appearance	Combustion Analysis/ % Found	ATR-IR	XPS Atomic Ratio		UV-Vis λ_{max} / nm
				Found	Expected	
UHMW. A2		C: 83.28 ± 0.30 H: 14.78 ± 0.30 N: <0.1	1249 (C-O), 1171 (C-O)	-Nil-	-Nil-	234, 286, 343
UHMW. A2-B1		C: 84.19 ± 0.30 H: 14.62 ± 0.30 N: <0.1	1511 (C=C), 1247 (C-O)	-Nil-	-Nil-	203, 235, 277, 348
UHMW. A2-B2		C: 83.65 ± 0.30 H: 14.62 ± 0.30 N: 0.66 ± 0.15	1713 (C=O), 1606 (C=C), 1509 (C=C), 1246 (C-O)	-Nil-	-Nil-	349, 496
UHMW. A2-B3		C: 83.53 ± 0.30 H: 14.62 ± 0.30 N: <0.1	1511 (C=C), 1246 (C-O)	-Nil-	-Nil-	203, 235, 277, 348
UHMW. A2-B4		C: 84.81 ± 0.30 H: 14.37 ± 0.30 N: <0.1	1609 (C=C), 1511 (C=C), 1247 (C-O)	-Nil-	-Nil-	203, 235, 277, 348
UHMW. A2-B4-C1		C: 84.74 ± 0.30 H: 14.50 ± 0.30 N: <0.1	1720 (C=O), 1247 (C-O)	-Nil-	-Nil-	234, 276, 341, 564
UHMW. A2-B5		C: 84.05 ± 0.30 H: 14.97 ± 0.30 N: <0.1	1248 (C-O), 1172 (C-O)	-Nil-	-Nil-	234, 286, 343
UHMW. A2-B5-C1		C: 84.85 ± 0.30 H: 15.35 ± 0.30 N: <0.1	1175 (C-O)	-Nil-	-Nil-	234, 286, 343
UHMW. A2-B5-C2		C: 85.00 ± 0.30 H: 14.93 ± 0.30 N: <0.1 Br: 0.46 ± 0.10	1174 (C-O)	-Nil-	-Nil-	234, 286, 343
UHMW. Ctrl-C1		C: 84.47 ± 0.30 H: 14.89 ± 0.30 N: <0.1	-Nil-	-Nil-	-Nil-	204, 246, 336

As surface area data was not available from the polymer manufacturers, BET measurements of these polymer substrates were performed. Compared to the porous XAD-4 PS beads that were used previously, there was a significant reduction of surface area for PET pellets, LDPE and UHMWPE powders as seen from the BET results obtained in **Table 3.6**. This directly affected the elemental combustion analysis characterisation. As seen from **Table 3.7**, most of the samples have N content below detection limit of 0.1%. As such, no conclusive data can be

drawn from this method of characterisation. The low surface area also rendered the mathematical model used to calculate the surface modification coverage invalid with erroneous analysis results being obtained for some of the PET pellets and LDPE powder samples. This is further discussed later in section 3.7.1. Nonetheless, it was observed that different forms of the polymers were good for different characterisation. XPS data collected for LDPE powder was useful to estimate surface coverage of the modification. As seen from **Table 3.7**, **Blank LDPE** and **LDPE.A2**, which had surface modification **A2**, contained only traces of N. The XPS atomic ratio for **LDPE.A2-B4** and **LDPE.A2-B4-C1** gave N to C ratio that estimated to surface coverage of approximately 10.2% and 18.5 % respectively. It is important to note that 1% surface coverage of XAD-4 beads is not equivalent to 1% of LDPE as the surface area of XAD-4 is much higher. While 1% of XAD-4 would mean a surface coverage of about 7.25 m^2/g, 1% of LDPE would correspond to 0.001 m^2/g. Hence, even though both polymers may have 1% surface modification coverage, the surface modified material with higher surface area would have been more sensitive to characterisation methods.

Though it was not possible to approximate surface coverage of **LDPE.A2** due to lack of a heteroatom, the ATR-IR spectrum of **LDPE.A2** as seen in **Figure 3.12** indicated successful surface modification **A2**, with peaks corresponding to the surface modification clearly visible in contrast to the blank polymer. ATR-IR characterisation was also useful in indicating successful azo coupling for **LDPE.A2-B2** and **LDPE.A2-B4** with clear C=O peaks observed at as seen in **Figure 3.13** and **Figure 3.14** at around 1742 cm^{-1} and 1695 cm^{-1} respectively.

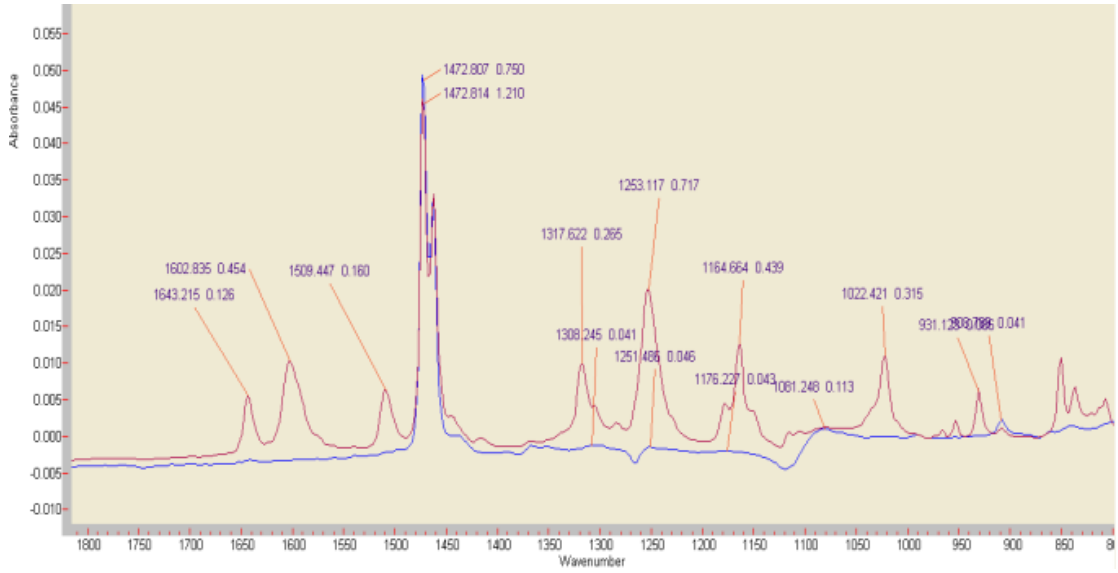


Figure 3.12. ATR-IR spectra of LDPE Blank (blue) and LDPE.A2 (red) at fingerprint region.

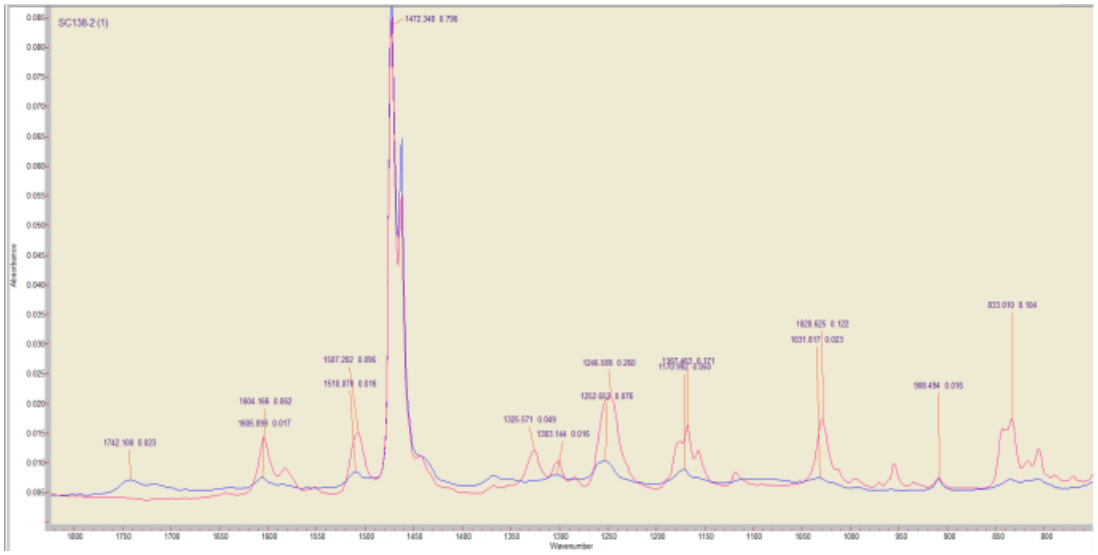


Figure 3.13. ATR-IR spectra of LDPE.A2 (blue) and LDPE.A2-B2 (red) at fingerprint region.

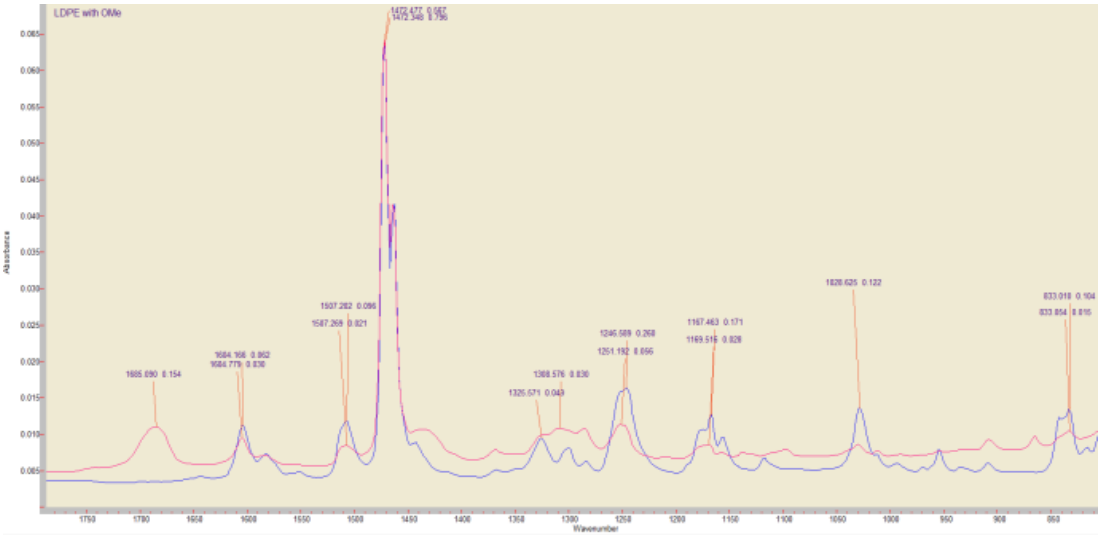


Figure 3.14. ATR-IR spectrum of LDPE.A2 (blue) and LDPE.A2-B4 (red) at fingerprint region.

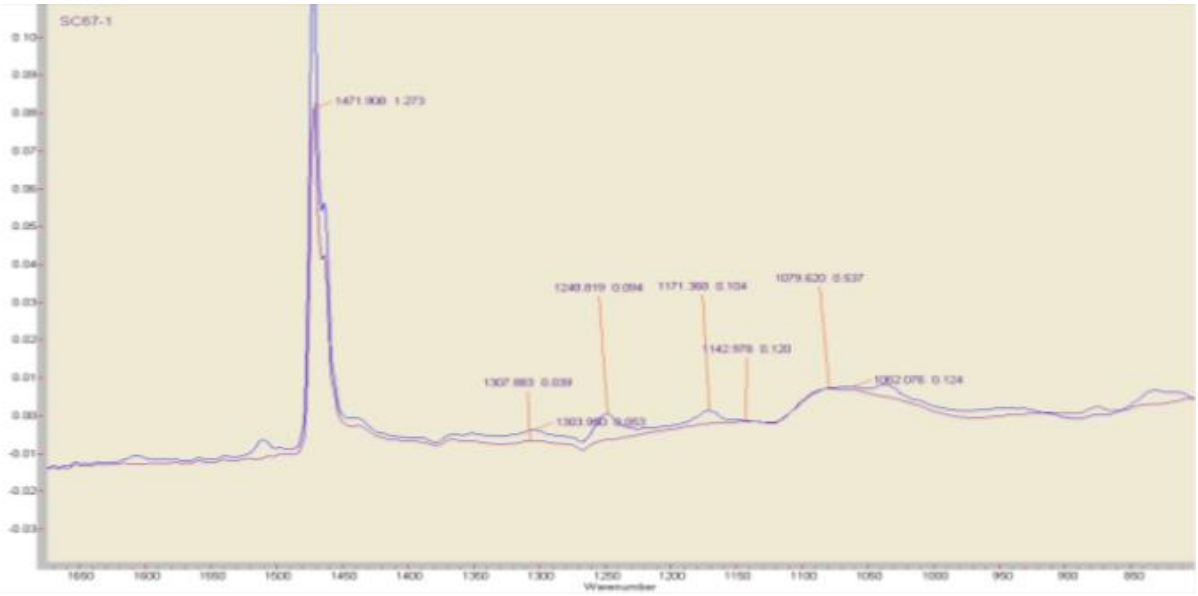


Figure 3.15. ATR-IR spectrum of Blank UHMWPE (purple) and UHMW.A2 (blue) at fingerprint region.

Unlike LDPE, UHMWPE powders were not useful for ATR-IR characterisation as seen in **Figure 3.15**, as the IR absorption peaks due to the surface modification were not apparent like those for the LDPE samples. However, UHMWPE samples were very useful in diffused reflectance UV-Vis characterisation as the nature of the sample suits this characterisation method best (this is further elaborated in Section 3.7.4 below).

Figure 3.16 below shows that all diazonium salts have similar azo coupling efficiency onto UHMWPE powder surface, except for **UHMW.A2-B2** which used the diazonium salt with a phenylacetic acid moiety. All samples showed a peak at around 350nm, which corresponded to the azo chromophore.

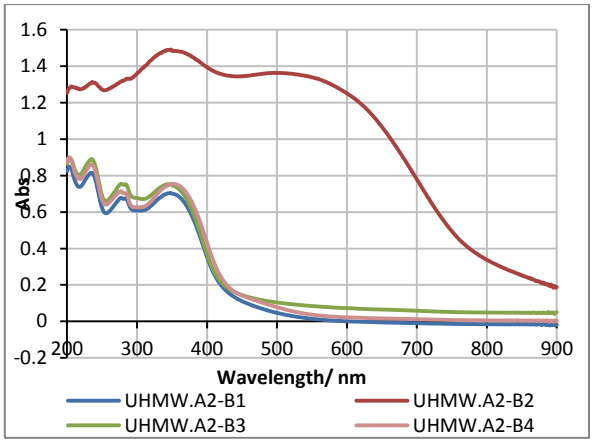


Figure 3.16. UV-Vis spectra for UHMWPE powder samples with varying diazonium salts.

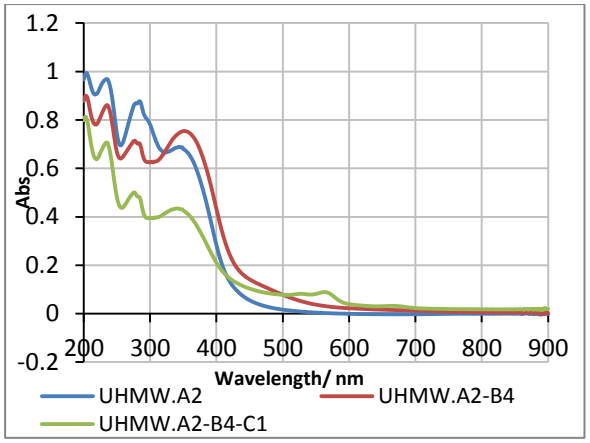


Figure 3.17. UV-Vis spectra for UHMW.A2, UHMW.A2-B4 and UHMW.A2-B4-C1.

Figure 3.17 shows the change in UV-Vis spectra of surface modified UHMWPE powders as they underwent surface modification from **A2** to **B4** and finally to **C1**, to give **UHMW.A2**, **UHMW.A2-B4** and **UHMW.A2-B4-C1** respectively. Other than the peak at around 350nm that arose due to azo chromophore, the slight peak at around 560nm for sample **UHMW.A2-B4-C1** was due to the spiropyran.

PET pellets (PETp) were difficult to characterise by both ATR-IR spectroscopy and UV-Vis spectrophotometry. For ATR-IR, the peaks that corresponded to the surface modification coincide with the bulk polymer peaks, thus, making it difficult to identify new peaks formed due to modifications. The pellet form of the polymer substrate made characterisation by UV-Vis unfavourable. However, it was the easiest to handle for hole-plate bioassay testing (see discussion in Chapter 4).

With the expansion of polymeric substrate scope, more pros and cons of the modification methods surfaced. Firstly, a drastic reduction in surface area resulted in significant reduction in surface modification loading, causing characterisation of these surface modified polymers to be challenging at the analytical detection limits. Secondly, compared to polystyrene bulk of XAD-4 PS beads, UHMWPE and LDPE with only saturated hydrocarbon units, are even more inert and thus more difficult to

surface modify. Nonetheless, it was found that different forms were good for different characterisation methods as compared to XAD-4 beads. UHMWPE powders were excellent for UV-Vis characterisation. LDPE was useful for ATR-IR characterisation due to the fact that the bulk substrate does not have peaks within fingerprint region. PET was easy for subsequent handling for bioassay testing.

Throughout this study, it was confirmed that the surface modification route established was viable for other polymeric substrates, including relatively more inert PE types. Despite the low surface modification loading, macroscopic properties due to the surface modifications were still observed and this is further demonstrated and elaborated in Chapter 4. With these goals met, this surface modification system and technology was ready to be moved to Singapore for further development.

3.6 Surface Engineering for Manufacturing

With the move of the project to Singapore Institute for Manufacturing Technology (SIMTech), challenges of the project differed from those encountered in Oxford as the focus of the project shifted. Considerations for manufacturing are mostly applications driven. Therefore, the aim of the project was to devise general surface modification methods that can easily be applied or altered for various on-demand applications, such as surface engineering for Roll-to-Roll application, or batch production, while retaining the ability to perform macroscopic functions. In this section the focus is mainly on the translation of the surface modification system established in Oxford, from the laboratory methods developed and experimented previously, to feasible processes for potential manufacturing scale. With these objectives set, more issues to consider arose.

3.6.1 From 3D to 2D substrates

Instead of beads, pellets and powders, industrial requirements for surface engineering are often for regular or irregular flat surfaces. Therefore, the form of polymers used was changed from 3D to 2D flat substrates. In addition, a wider variety of commodity polymers and engineering materials would need to be tested so as to develop a robust surface modification method suitable for wider scope of polymeric substrates. Materials such as flat PS, PC, PP and COC were produced by injection moulding in SIMTech. PET sheets were available readily from the Roll-to-Roll machine. TPU pieces were made by dissolving the resin in THF, followed by casting onto large petri dish and drying off the solvent. PDMS sheet was made by using commercial kit Sylgard® 184, and casted onto silicon wafer (details of various substrates used are given in Chapter 6).

3.6.2 Process development

Unlike beads and pellets used previously that could be handled and modified easily using simple laboratory glassware, flat substrates required development of processes suitable for each step of modification. Therefore, there was a need to re-design the process for each surface modification step. When considering the need to make the modification process a scalable one, apparatus for surface modification could no longer be limited to simple laboratory glassware, especially for substrates that are large in size. Simple laboratory processes like heating in silicon oil and reflux in solvents required alternatives as well. This is examined in the following sections.

3.6.2.1 Mod Ax: Pre-activation of flat polymer surface

For the pre-activation of polymer surface (Mod **Ax**), unlike beads or pellets or powders that could be coated on the surface easily with diaryldiazo **3.3a2** by suspension in solution and drying *in vacuo*, coating methods needed to be devised for coating the diaryldiazo **3.3a2** onto the flat substrates. Both dip coating and spray coating methods were examined. Purple diaryldiazo **3.3a2** was dissolved in diethyl ether and this solution was then either poured into a container or into a spray bottle in preparation for dip coating and spray coating respectively.

Dip Coating

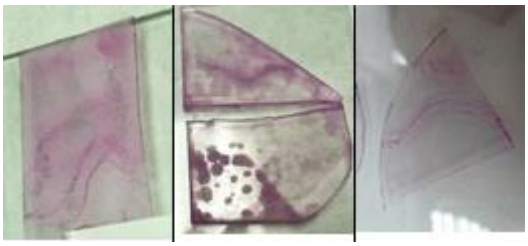


Figure 3.18. PET, PDMS and TPU pieces dip-coated with 3.3a2.

Spray Coating



Figure 3.19. PET, PDMS and TPU pieces spray-coated with 3.3a2.

Dip Coating: The polymer piece was first clamped on a dip coater, followed by immersion into the solution for about 10 s before being withdrawn at a constant speed. A thin layer of the solution was deposition on the surface when the polymer was pulled up. While dip coating enabled both surfaces of the flat substrate to be coated, it suffered drawbacks such as irregular coverage. Surface wettability of some of the polymers was not always compatible with diethyl ether, resulting in poor wetting. As such, when excess liquid drained from the surface after the polymer was pulled up from the solution, some diaryldiazo **3.3a2** was partially drawn away from the surface. Irregular drying of the diethyl ether also resulted in irregular deposition of **3.3a2** on the polymer surface as seen in **Figure 3.18**.

Spray Coating: There are diverse methods of spray coating and there are many factors that can affect the quality of the deposition layers, such as selection of nozzle for different spray pattern, spray impact, angle and drop size, speed of carrier gas and more.[114] However, for simplicity, a simple spray bottle with simple round orifice spray nozzle was used. Compared to the dip coating method which requires a container full of coating solution in order to submerge the polymer substrates entirely, much less coating solution was required for spray coating, thus, saving materials. Moreover, as seen from **Figure 3.19**, the coverage of **3.3a2** was more uniform. When sprayed, only a minimal amount of solvent was deposited onto the surface and since this dried almost instantaneously, good coverage of the surface was achieved. As such, wettability was not of major concern. Therefore, spray coating method was preferred over dip coating method even though it could only cover one side at a time.

Thermolysis or Photolysis: With the substrates coated with diaryldiazo **3.3a2**, the next step involved the generation of the carbene either via thermolysis or photolysis, for the pre-activation of the polymer surface by carbene insertion. Heating of the coated flat substrates to generate the carbenes via thermolysis could be achieved by using an oven furnace. However, the polymers could undergo warping when there is differential thermal expansion and shrinkage of the material when heating and cooling down during the modification process.[115] Some polymers with low glass transition temperatures can also undergo physical changes. Therefore, generation of carbene via thermolysis is not as favourable in this context.

Alternatively, diaylcarbenes could also be generated from the diaryldiazo via photolysis. Photolysis for quick carbene generation required high intensity UV. Normal bench-top UV lamps did not work efficiently due to their low intensity.

Moreover, heating due to the high intensity UV could hasten evaporation of solvent residue on the polymer surface during the coating process and aid in carbene generation.



Figure 3.20. Conveyor belt fitted with high intensity UV.



Figure 3.21. PDMS Pieces spray coated with 3.3a2 before and after UV irradiation for Mod A.

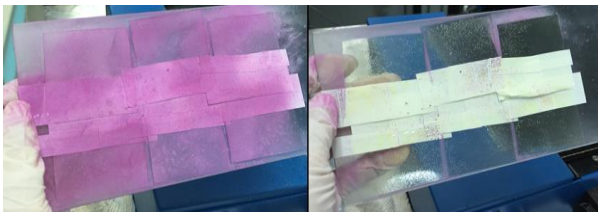


Figure 3.22. PET sheet spray coated with 3.3a2 before and after UV irradiation.

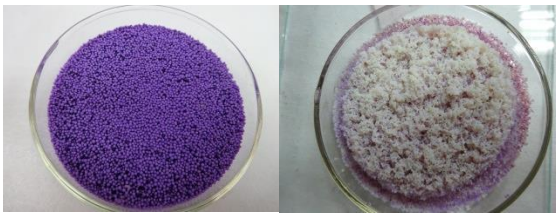


Figure 3.23. XAD-4 beads coated with 3.3a2 in petri dish before and after UV irradiation

Using a high intensity UV with a conveyor belt system shown in **Figure 3.20**, diarylcarbene generation using photolysis for surface modification could be achieved. As seen from **Figure 3.21** and **Figure 3.22**, completion of modification **A2** could be observed by a change from opaque purple coating to a clear yellow tinted colour. The speed of the belt was set to expose the coated substrate for up to 40 s. Prolonged exposure was prevented as the high intensity UV could generate significant heating of the substrates, which could damage the polymers. The substrates were then washed with water and ethanol. Acetone was not used as it would damage most of the commodity polymers such as PC and PS.

However, there are drawbacks of this method as well. As seen in **Figure 3.23**, the photolysis method is not suitable for beads and pellets. Only the top layer of the XAD-4 PS beads was modified as only the top layer was exposed to UV irradiation, whereas the bottom layer remained unmodified. In addition, UV irradiation only

allowed for single side to be modified at a time, as such, substrates coated with diaryldiazo **3.3a2** using dip coating method were not suitable. If both sides of the flat substrates require surface modification, the spray coating and UV-irradiation process has to be done twice. Nonetheless, photolysis method was preferred as it only took a few seconds for the completion of modification **A2**, compared to heating which required about 30 min.

3.6.2.2 Mod Bx': Azo coupling on flat polymer surface

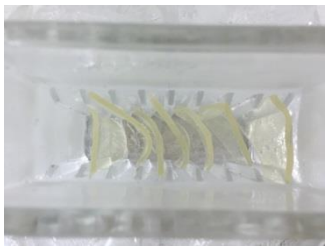


Figure 3.24. Glass container with slots holding flat PDMS samples.



Figure 3.25. Substrates contained in glass holder immersed in cold diazonium salt solution.

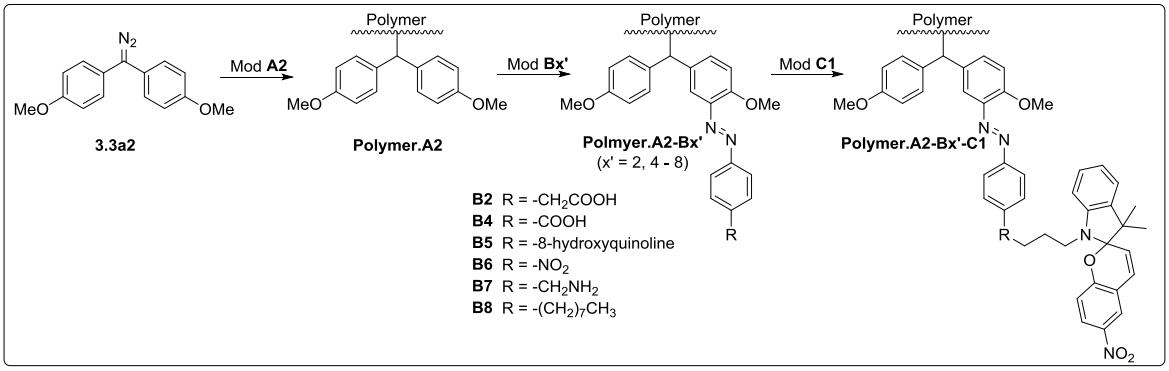
Previously for modification **Bx'**, beads or pellets were left to stand in diazonium salt solution in the round bottom flask at 0°C and warm up gradually to room temperature over 18 h. Instead of using round bottom flask, special containers with slots were used for modification of the flat substrates. Diazonium salts were synthesized in ethanol rather than a mix of THF and water as some polymer substrates may be susceptible to damage by THF. Freshly prepared diazonium salt in cold solution was poured into the container fitted with the substrates to be surface modified and left to stand in ice bath for 18 h. The substrates were then washed with water and ethanol. This is a scalable process as a larger slotted container with more tightly fitted slots could be used for larger samples. Should the samples be irregular sized, a simple container without slots can be used instead for immersion of the sample.

3.6.2.3 Mod Cx'': Derivatization with spiropyran on flat polymer surface

Previously, modification **Cx''** on the surface of the polymers was performed via reflux conditions. However, reflux is not a very scalable process and not suitable for

flat substrates. As such, there was a need to change the process and conditions of modification C to a simple and scalable process. Conditions similar to the solution studies were employed, where the substrates were stirred in the aprotic polar solvent, DMSO, instead of refluxing in MeCN. Therefore, instead of refluxing for 3 h in MeCN, the reaction time was lengthened to 5 h or longer, but employing less harsh conditions and a simpler method. The set-up for this modification step is similar to modification Bx' (**Figure 3.24** and **Figure 3.25**). Flat polymer samples were fitted into containers with slots, and a mixture of spiropyran and K_2CO_3 in DMSO was poured in. A stir bar was placed at the bottom of the container for stirring. After 5 h of immersion, the flat substrates were washed with copious amount of water and ethanol.

3.6.3 Surface modification of flat commodity polymers

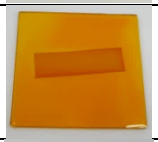
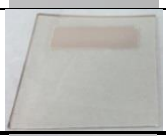


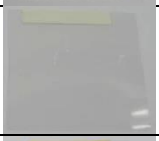
Scheme 3.7. Surface modification of flat polymer substrates.

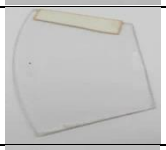
A variety of flat polymers were tested using the process developed. Previously, it was noted that combustion analysis would not be useful for characterisation of polymer samples with a low surface area as the low surface modification loading would result in the heteroatom measurement below detection limit. As such, this characterisation method was omitted for the flat substrates. Water contact angle (WCA) was introduced as flat samples would be suitable for this characterisation

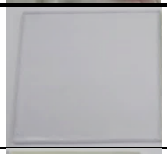
method. It acts as a useful indication of surface wettability. In addition, UV-Vis was measured in transmittance mode instead of reflectance mode.

Table 3.8. List of surface modified polymer made in SIMTech.

Sample	Appearance	ATR-IR	XPS Ratio		Water Contact Angle
			Found	Expected	
PDMS.Blank		2962, 1446, 1412, 1257, 1010, 788	N/C: 0.00 O/C: 0.564	N/C: 0.00 O/C: 0.500	112.5 ± 0.2
PDMS.A2		1607 (C=C), 1511 (C=C)	N/C: 0.00 O/C: 0.430	N/C: 0.00 O/C: 0.133	112.3 ± 0.5
PDMS.A2-B2		1607 (C=C), 1512 (C=C)	N/C: 0.00842 O/C: 0.613	N/C: 0.0870 O/C: 0.174	110.9±1.1
PDMS.A2-B4		1700 (C=O), 1608 (C=C), 1512 (C=C)	N/C: 0.00557 O/C: 0.553	N/C: 0.0909 O/C: 0.182	109.0 ± 10.5
PDMS.A2-B5		1606 (C=C), 1510 (C=C),	N/C: 0.00 O/C: 0.670	N/C: 0.125 O/C: 0.125	111.5±0.9
PDMS.A2-B6		1608 (C=C), 1512 (C=C)	N/C: 0.00961 O/C: 0.599	N/C: 0.143 O/C: 0.190	112.3±1.0
PDMS.A2-B7		1611 (C=C), 1512 (C=C)	N/C: 0.00934 O/C: 0.589	N/C: 0.136 O/C: 0.0909	112.7±0.9
PDMS.A2-B8		1608 (C=C), 1510 (C=C),	N/C: 0.00200 O/C: 0.570	N/C: 0.0690 O/C: 0.0690	114.0±0.8
PDMS.A2-B2-C1		1606 (C=C), 1510 (C=C)	N/C: 0.00907 O/C: 0.715	N/C: 0.0909 O/C: 0.159	110.7±0.9
PDMS.A2-B4-C1		1606 (C=C), 1509 (C=C)	N/C: 0.00585 O/C: 0.451	N/C: 0.0930 O/C: 0.162	114.6 ± 0.7
PC.Blank		1769 (C=O), 1602 (C=C), 1503 (C=C), 1219 (C-O)	N/C: 0.0250 O/C: 0.201	N/C: 0.00 O/C: 0.214	84.8±0.4

PC.A2		1605 (C=C), 1584 (C=C), 1505 (C=C)	N/C: 0.0197 O/C: 0.243	N/C: 0.00 O/C: 0.133	97.2±1.5
PC.A2-B2		1770 (C=O), 1605 (C=C), 1503 (C=C)	N/C: 0.0408 O/C: 0.219	N/C: 0.0870 O/C: 0.174	93.0±2.6
PC.A2-B4		1700 (C=O), 1604 (C=C), 1505 (C=C)	N/C: 0.0555 O/C: 0.245	N/C: 0.0909 O/C: 0.182	89.5±1.7
PC.A2-B7		1604 (C=C), 1506 (C=C)	N/C: 0.0418 O/C: 0.282	N/C: 0.136 O/C: 0.0909	89.0±2.5
PC.A2-B8		1604 (C=C), 1503 (C=C)	N/C: 0.0226 O/C: 0.286	N/C: 0.0690 O/C: 0.0690	96.0±2.2
PC.A2-B2-C1		1601 (C=C), 1503 (C=C),	-Nil-	-Nil-	95.2±2.8
PET.Blank		1714 (C=O), 1505 (C=C), 1409 (C=C), 1245 (C-O)	N/C: 0.0230 O/C: 0.262	N/C: 0.00 O/C: 0.00	74.2±2.1
PET.A2		1606 (C=C), 1578 (C=C)	N/C: 0.0323 O/C: 0.266	N/C: 0.00 O/C: 0.133	82.4±1.6
PET.A2-B2		1713 (C=O) , (C=C)	N/C: 0.0213 O/C: 0.296	N/C: 0.0890 O/C: 0.174	76.8±1.9
PET.A2-B4		1713 (C=O), 1604 (C=C), 1578 (C=C)	N/C: 0.0154 O/C: 0.370	N/C: 0.0909 O/C: 0.181	76.9±4.3
PET.A2-B6		1603 (C=C), 1506 (C=C)	N/C: 0.0449 O/C: 0.337	N/C: 0.143 O/C: 0.190	92.1±2.9
PET.A2-B7		1603 (C=C), 1506 (C=C)	N/C: 0.0512 O/C: 0.315	N/C: 0.136 O/C: 0.0909	86.5±5.1
PET.A2-B2-C1		1505 (C=C), , 1386 (NO_2),	N/C: 0.0232 O/C: 0.288	N/C: 0.0909 O/C: 0.159	87.2±3.5
PET.A2-B4-C1		1715 (C=O), 1505 (C=C)	N/C: 0.0176 O/C: 0.249	N/C: 0.0930 O/C: 0.162	79.9±1.5

TPU.Blank		3330 (N-H), 1700 (C=O), 1596 (C=C),	N/C: 0.00371 O/C: 0.173	N/C: 0.118 O/C: 0.176	81.0±6.4
TPU.A2		1600 (C=C), 1510 (C=C)	N/C: 0.00873 O/C: 0.188	N/C: 0.00 O/C: 0.133	80.4±1.5
TPU.A2-B2		1700 (C=O), 1596 (C=C)	N/C: 0.0243 O/C: 0.171	N/C: 0.0890 O/C: 0.174	61.9±2.1
TPU.A2-B2-C1		1596 (C=C), 1527 (NO_2), 1358 (NO_2)	N/C: 0.0198 O/C: 0.178	N/C: 0.0909 O/C: 0.159	95.7±2.1
TPU.A2- B4		1700 (C=O) , 1596 (C=C)	N/C: 0.0122 O/C: 0.203	N/C: 0.0909 O/C: 0.182	59.0±7.3
TPU.A2- B4-C1		1701 (C=O), 1597 (C=C)	N/C: 0.0138 O/C: 0.203	N/C: 0.0930 O/C: 0.162	85.4±1.8
COC.Blank		2866, 1455, 1359, 1294, 1155, 1039	N/C: 0.0110 O/C: 0.111	N/C: 0.00 O/C: 0.00	97.8±1.7
COC.A2		1606 (C=C), 1510 (C=C), 1253 (C-O), 1172 (C-O)	N/C: 0.0144 O/C: 0.118	N/C: 0.00 O/C: 0.133	90.1±5.1
COC A2-B2		1607 (C=C), 1508 (C=C)	N/C: 0.0135 O/C: 0.129	N/C: 0.0890 O/C: 0.174	84.0±2.3
COC.A2-B4		1455, 1359, 1294	-Nil-	-Nil-	76.2±1.8
COC.A2-B2-C1		1360 (NO_2), 1254 (C-O)	N/C: 0.00770 O/C: 0.176	N/C: 0.0909 O/C: 0.159	54.5±7.3
PMMA.Blank		1769 (C=O), 1602 , 1503, 1465, 1409, 1387, 1219	-Nil-	-Nil-	74.5±2.1
PMMA.A2		1605 (C=C), 1505 (C=C)	-Nil-	-Nil-	81.6±3.2
PMMA.A2-B2		1723, 1637, 1483 (C=C), 1240 (C-O)	-Nil-	-Nil-	70.0±8.6

PMMA.A2-B2-C1		-Nil-	-Nil-	-Nil-	-Nil-
PS.Blank		3025, 2920, 1869, 1801, 1746, 1601, 1542, 1451	-Nil-	-Nil-	90.4±1.1
PS.A2		1601 (C=C), 1583 (C=C)	-Nil-	-Nil-	87.2±3.8
PS.A2- B2		1601 (C=C), 1583 (C=C)	-Nil-	-Nil-	112.2±8.6
PS.A2-B4		1603 (C=C), 1507 (C=C), 1243 (C-O)	-Nil-	-Nil-	100.8±2.1
PS A2- B7		1603 (C=C), 1508 (C=C)	-Nil-	-Nil-	111.1±4.3
PS.A2-B8		1604 (C=C), 1507 (C=C), 1242 (C-O)	-Nil-	-Nil-	111.4±5.3
PS.A2- B2-C1		1559 (C=C), 1508 (C=C), 1252 (C-O)	-Nil-	-Nil-	115.1±4.0
PP.Blank		2950, 2917, 1457, 1376, 1167, 998, 973, 841	-Nil-	-Nil-	99.6±2.2
PP.A2		1608 (C=C), 1510 (C=C), 1250 (C-O)	-Nil-	-Nil-	101.1±1.2
PP.A2-B2		1609 (C=C), 1509 (C=C), 1255 (C-O)	-Nil-	-Nil-	98.6±2.1
PP.A2-B2-C1		1609 (C=C), 1250 (C-O)	-Nil-	-Nil-	99.5±1.6

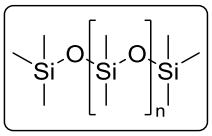


Figure 3.26. Chemical structure of PDMS.

PDMS: Polydimethoxysilane (PDMS), commonly referred to as silicone, is a common silicon-based organic elastomer that is widely used in many microfluidic[116-118], biomedical[119] and cosmetics[120] applications as it is a biocompatible material.[121]

XPS results showed that no nitrogen (N) was detected for **PDMS.Blank** and **PDMS.A2** samples. This was expected due to the absence of N from PDMS bulk structure (as seen in **Figure 3.26**) and modification **A2**. There was not much change in the WCA from **PDMS.Blank** to **PDMS.A2**, with average angle of 112.5° and 112.3° respectively. Nonetheless, successful modification was indicated clearly in the IR spectrum of **PDSM.A2**. As seen from **Figure 3.27**, the newly modified peaks were observed at 1608 cm^{-1} and 1511 cm^{-1}, corresponding to the phenyl C=C modified onto the surface, which was previously absent.

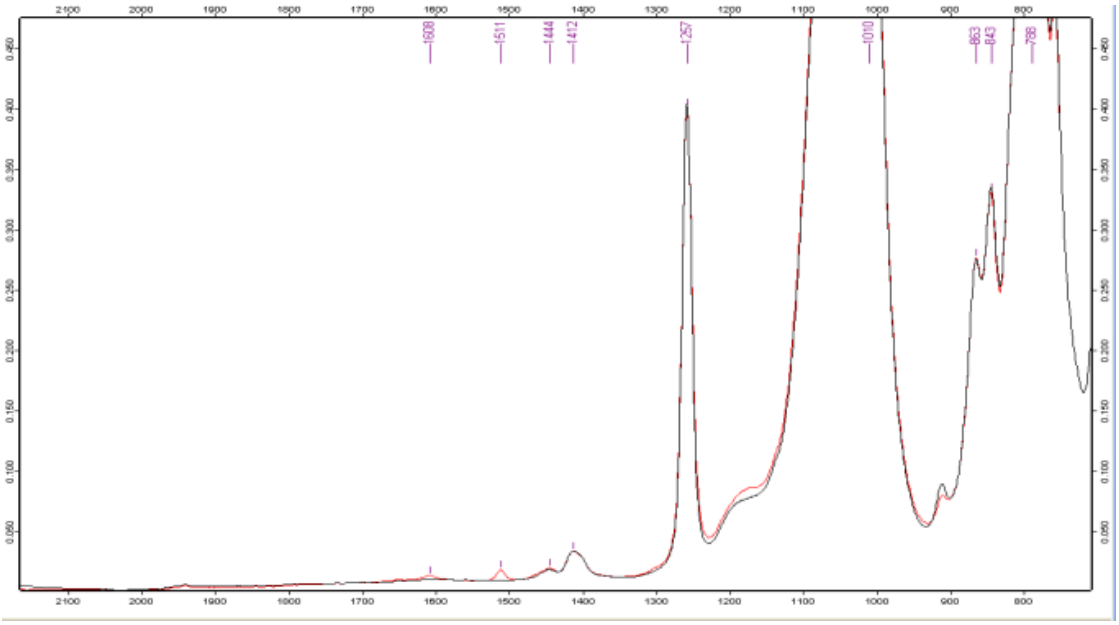


Figure 3.27. ATR-IR spectra of PDMS.Blank (Blue) + PDMS.A2 (Red).

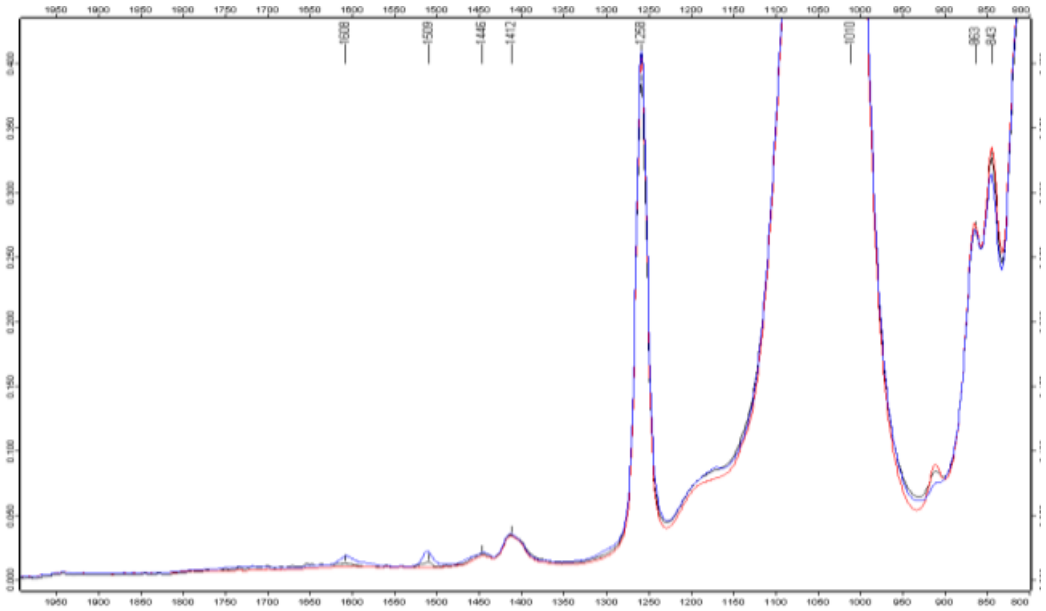


Figure 3.28. ATR-IR Spectra of PDMS.Blank (red) + PDMS.A2 (Blue) + PDMS.A2-B4 (Black).

Traces of N detected using XPS for both **PDMS.A2-B2** and **PDMS.A2-B4**, with N to C ratio of 0.00557 and 0.00842, which estimated to be about 6.4% and 9.7% surface coverage respectively. It was also observed that there were slight decrease in WCA of 1.4° and 3.3° respectively. However, it was noted that the confidence interval for the WCA of **PDMS.A2-B4** was large (10.5°). This was due to the non-uniformity of the surface modification. With some part of the sample modified, the WCA would be low, but when tested on an unmodified area, the WCA would be large, thus, giving a large variability. On the other hand, characterisation using ATR-IR for modification **Bx'** was not useful as the spectra appear to be very similar to that of **PDMS.A2** as seen in **Figure 3.28**. This suggested that the extent of azo coupling (Mod **Bx'**) was below the detection limit of the ATR-IR instrument.

Modification **B6**, with a nitro side group, was expected to have good azo coupling as the nitro moiety would render the diazonium salt more electrophilic for better azo coupling. This is reflected in **PDMS.A2-B6** having higher N to C ratio of 0.00961 gathered from XPS analysis, estimating a surface coverage of 6.7%.

PDMS Mod B5 and **PDMS Mod B8** showed a colour change after azo coupling. However, **PDMS Mod B5** gave no trace of N detected from XPS, and the WCA was similar to that of the **PDMS.Blank** and **PDMS.A2**, thus, indicating very low surface modification. XPS of **PDMS Mod B8** gave N to C ratio of 0.00200, which estimated a low surface coverage of 2.9%. It was uncertain what caused the colour change given the low surface coverage. Therefore, Atomic Force Microscopy (AFM) was used further probe the surface of selected PDMS polymers in attempt to better understand possible reasons for these observations.

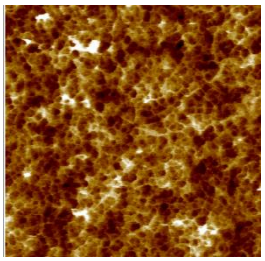


Figure 3.29. AFM picture of Blank.PDMS.

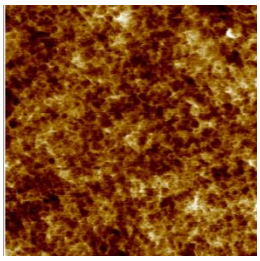


Figure 3.30. AFM picture of PDMS.A2.

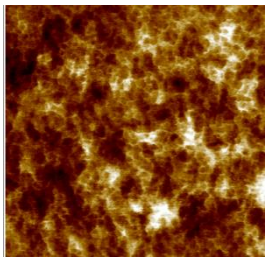


Figure 3.31. AFM picture of PDMS.B4.

As seen from **Figure 3.29**, the surface of **PDMS.Blank** was rather porous. With further modification, there was increasing surface coverage of the pores on the surface, but most of the pores remain visible under the AFM. With the pore being hydrophobic, the strong colouration in **PDMS.A2-B5** and **PDMS.A2-B8** modified PDMS could be due to absorption of strongly coloured hydrophobic impurities or compounds from side reactions into the pores during the immersion of the diazonium salt solutions.

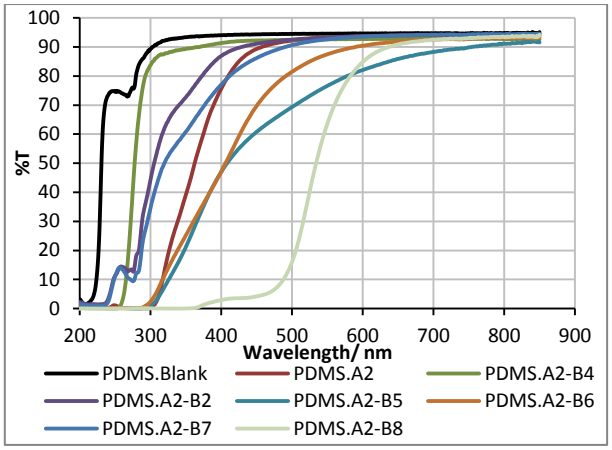


Figure 3.32. UV-Vis spectra of PDMS.Blank, PDMS.A2 and PDMS.A2-B1 to B6.

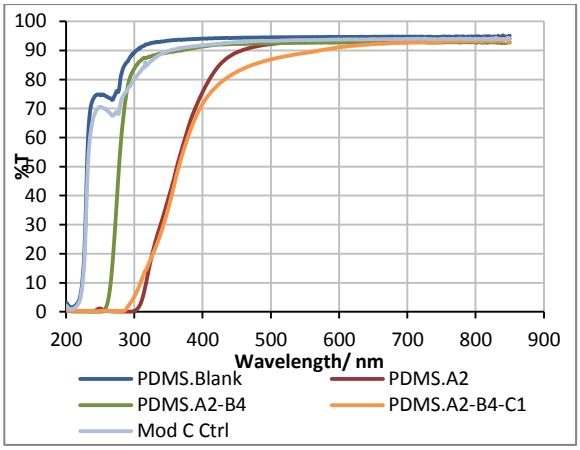


Figure 3.33. UV-Vis spectra of PDMS/Blank, PDMS.A2. PDMS.A2-B1, PDMS.A2-B4-C1 and PDMS.Ctrl-C1.

As seen from **Figure 3.32**, **PDMS.A2** saw a decrease in %T after the pre-activation step, but %T improved after Mod **B1**. Visually, it was observed that after washing freshly modified **PDMS.A2**, the substrate appeared slightly chalky on the surface. However, when in contact with water or ethanol, the sample would become clear, but fogged up again when exposed to air after drying. Upon prolonged immersion in diazonium salt-ethanol solution, the sample became clear and transparent even after drying in air. It was uncertain what caused the opaqueness in **PDMS.A2**, but it was likely that prolonged exposure in ethanol solvent dissolved or washed away the loose layers on the sample during modification **Bx'**, leaving only a very thin layer of the surface modification. **PDMS.A2-B4-C1** and saw a large decrease in %T between 250 nm to 600 nm as seen from **Figure 3.33** even though it remained transparent and clear visually with a tint of pink.

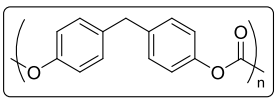


Figure 3.34. Chemical structure of PC.

PC: Polycarbonate (PC) is a type of engineering plastic with varied industrial applications in electronics, automotive, optics, medical and more.[122] With increasing commercial importance, PC is expected to achieve high annual global demand of 1.5 million tons.[122]

PC polymer bulk has many peaks in the IR fingerprint region, rendering IR spectroscopy not as useful for characterisation of the subsequent modifications. There was N detection of the **PC.Blank**, likely to be due to additives or cross-linkers used in the injection moulding process when producing these flat polymer samples.

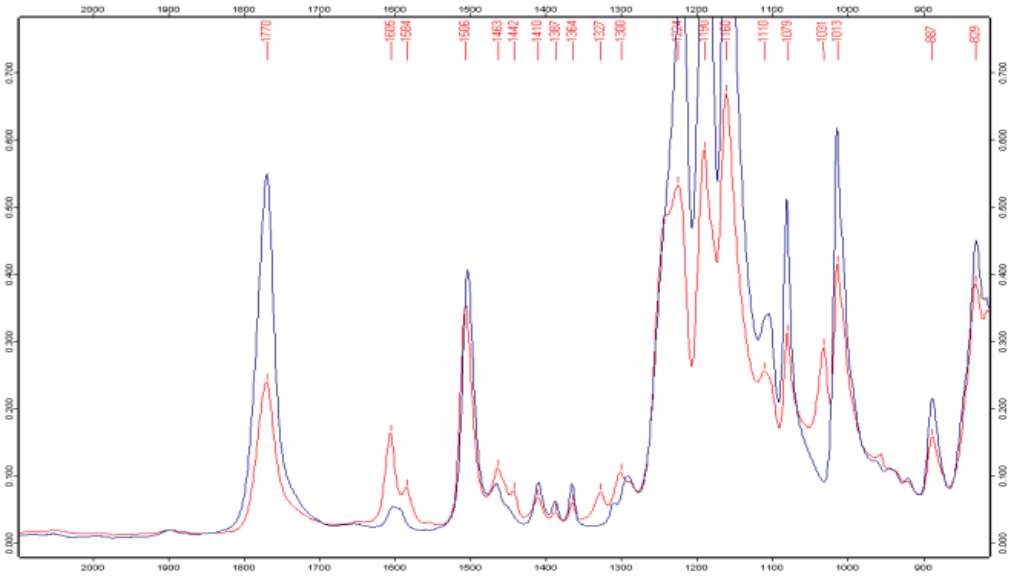


Figure 3.35. ATR-IR spectra of PC.Blank (blue) + PC.A2 (red)

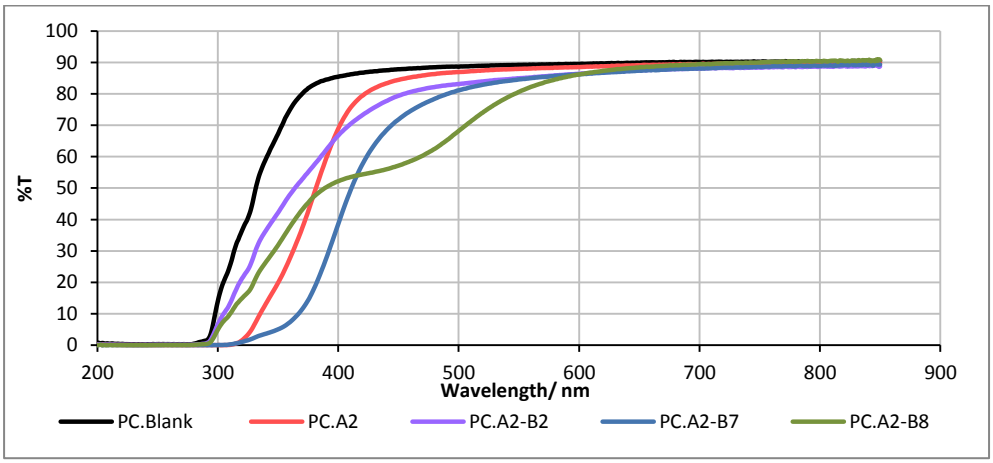


Figure 3.36.UV-Vis spectra of PC surface modified substrates.

There was slight decrease in N to C ratio, and an increase in O to C ratio measured using XPS for **PC.A2**. This could be caused by modification **A2** covering the surface which reduced the detection of N from the blank polymer surface, and the increase in O could be due to the introduction of aryl-OMe group from modification **A2**. In addition, an increase in WCA could be due to modification of the surface with more

hydrophobic aryl-OMe compared to relatively hydrophilic carbonyl. Samples of PC with modifications **B2**, **B4** and **B7** observed an apparent increase of N to C ratio from modification **A2**. Although the increase in N to C ratio was indicative of modification **Bx'**, due to non-uniformity in surface coverage, the extent of surface modification could not be determined as some of the N detected might have been due to blank rather than modification **Bx'**. Nonetheless, due to introduction of more polar side groups, an apparent decrease of 4.1° - 8.2° in WCA was observed. XPS analysis of **PC.A2-B8** saw N to C ratio similar to that of **PC.Blank** and **PC.A2**. WCA of the **PC.A2-B8** was also similar to **PC.A2**, thus, suggesting very little extent of modification **B8**.

Mod **C1** was not suitable for PC substrates as both DMSO and MeCN were not compatible to PC and would damage the surface as seen in **Table 3.8**.

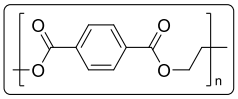


Figure 3.37. Chemical structure of PET.

PET: Polyethylene Terephthalate (PET) is a polyester-based engineering thermoplastic. In recent years, PET sheets are widely used in printed lighting and electronics, and other Roll-to-Roll research in SIMTech.

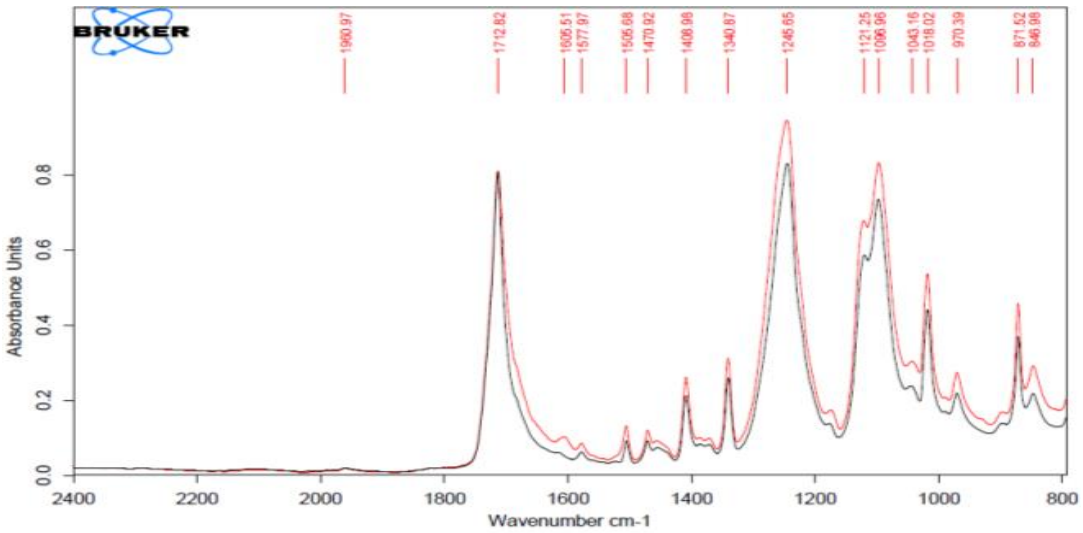


Figure 3.38. ATR-IR spectra of PET.Blank (black) + PET.A2 (red).

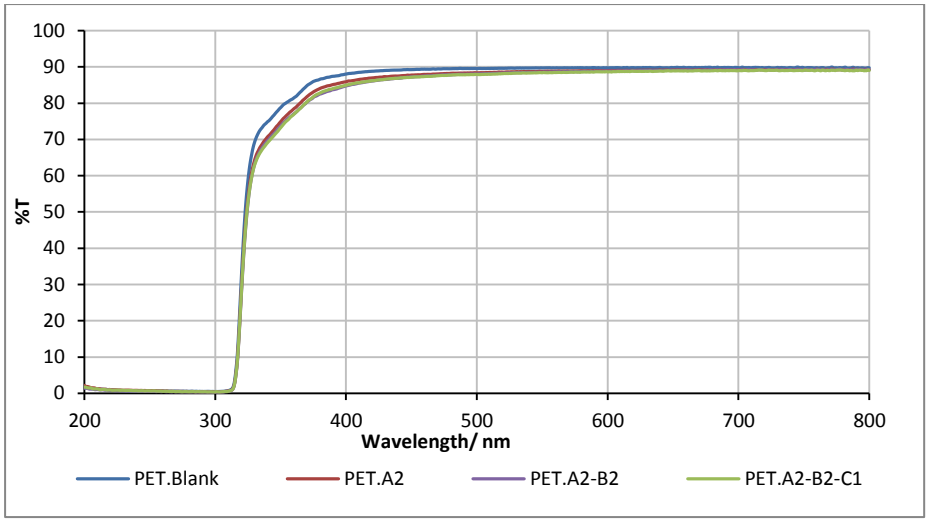


Figure 3.39. UV-Vis spectra of PET Modified Polymers

ATR-IR was not useful for characterisation for PET as the IR peaks due to the bulk polymer overlapped with the peaks due to the surface modifications. Nonetheless, IR peak due to modification **A2** was still slightly visible at 1607 cm^{-1} and 1578 cm^{-1} as seen from **Figure 3.38**. XPS results of both the **PET.Blank** and **PET.A2** detected N, likely to be due to nitrogen-containing additives used in production.

For **PET.A2-B2** and **PET.A2-B4**, the C=O peak was hidden below the bulk. XPS analysis gave inconclusive surface modification coverage as the N to C ratio was much lower than that of the **PET.Blank** and **PET.A2**, likely to be due to low surface modification loading. Colour changes from **PET.A2** to **PET.A2-B2** or **PET.A2-B4** were not apparent. Nonetheless, due to the addition of polar COOH groups onto the polymer surfaces, a decrease of about 5.6° for WCA was measured for both **PET.A2-B2** and **PET.A2-B4**. This showed that despite low surface loading, the extent of modification of mod **B2** and **B4** onto PET polymer surface was still sufficient to bring about a macroscopic change in property such as surface wettability. For **PET.A2-B6** and **PET.A2-B7**, an increase in N to C ratio was measured by XPS. This was expected as N content would have increased due to azo, and amine or nitro functionalities.

As the PET sheets were very thin and transparent, any colour change to the surface was not observable by eye. However, characterisation using UV-Vis was sufficiently sensitive to detected changes. As seen from **Figure 3.39**, the UV-Vis spectra indicated very slight decrease in %T between 300 – 500 nm after each modification. However, the change in %T was not as obvious for **PET.A2-B2-C1** as its spectrum overlay closely with that of **PET.A2-B2**.

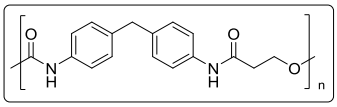


Figure 3.40. Chemical structure of TPU.

TPU: Polyurethane can be in the form of thermoplastic or thermoset material. Thermoplastic Polyurethane (TPU) is a form of thermoplastic elastomer that is usually flexible, clear and elastic, with wide applications in automotive, medical and electronics.[122]

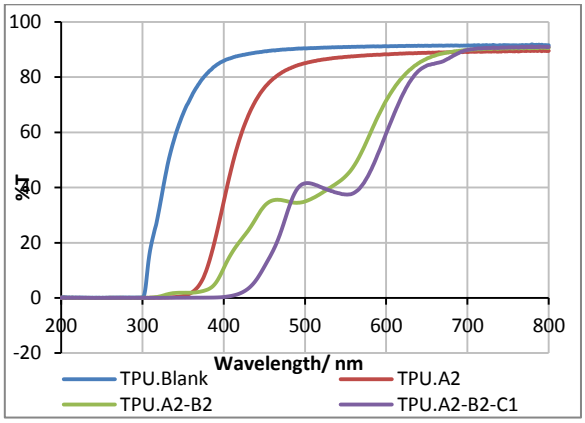


Figure 3.41. UV-Vis Spectra of surface modified TPU.

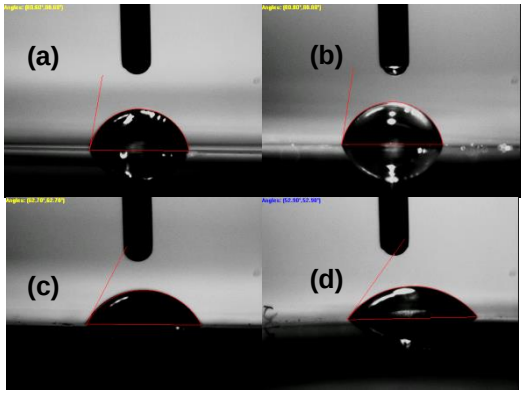


Figure 3.42. Water contact angle of surface modified TPU. (a) TPU.Blank. (b) TPU.A2. (c) TPU.A2-B2. (d) TPU.A2-B4

Pellets of TPU contain plasticisers, hence, when solvent casted with THF to give flat substrate, **TPU.Blank** and **TPU.A2** have traces of N detected from XPS analysis. Though both **TPU.Blank** and **TPU.A2** have similar WCA, and ATR-IR spectrum of **TPU.A2** did not give clear indications of successful surface modification as the peaks due to the surface modification were overlapped or hidden peaks by the polymer bulk at fingerprint region, the colour change due to the various modifications was apparent, and even more so for modification **Bx'**, as seen from **Table 3.8**. This is also reflected in the UV-Vis spectra as seen in **Figure 3.41**.

WCA of **TPU.A2-B2** and **TPU.A2-B4** as seen in **Table 3.8** showed apparent change for Mod **B2** and **B4** with a decrease in angle of 21.4° and 18.5° respectively, due to the introduction of polar COOH group onto the polymer surface. XPS analysis also measured an increase in N to C ratio due to introduction of the azo group.

As **TPU.A2-B2** was already intensely coloured, change in colour due to further modification **C1** to give **TPU.A2-B2-C1** became less apparent. Nonetheless, modification of **TPU.A2-B2** to give **TPU.A2-B2-C1** saw an increase in WCA as the COOH groups on the TPU surface were further derivatized with spiropyrans that are not as polar when exist in their closed-ring form. The increase in WCA varied from 26.4° to 33.8° for both **TPU.A2- B2-C1** and **TPU.A2-B4-C**.

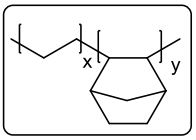


Figure 3.43. Chemical structure of COC.

COC: Cyclic olefin copolymer (COC) is a relatively new class of thermoplastics compared to commodity polymers like PE and PP.[123] They have a wide variety of applications, including packaging films, lenses, displays and medical devices.[122] COC pellets were injection moulded into microfluidic chips and discs in SIMTech for microfluidic research, and these were cut into pieces and used in this study.

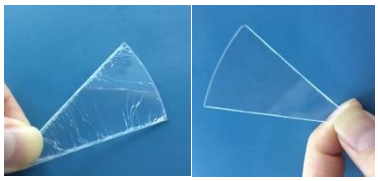


Figure 3.44. COC sample after immersing in diethyl ether (left) or acetone (right).

Instead of diethyl ether, acetone was used for modification **A2** of COC. It was observed that the use of diethyl ether resulted in the formation and propagation of brittle cracks in COC as seen in **Figure 3.44**, but acetone did not affect the polymer. Therefore, the diaryldiazo **3.3a2** was dissolved in acetone and spray coated onto the flat COC samples for photolysis via high intensity UV irradiation.

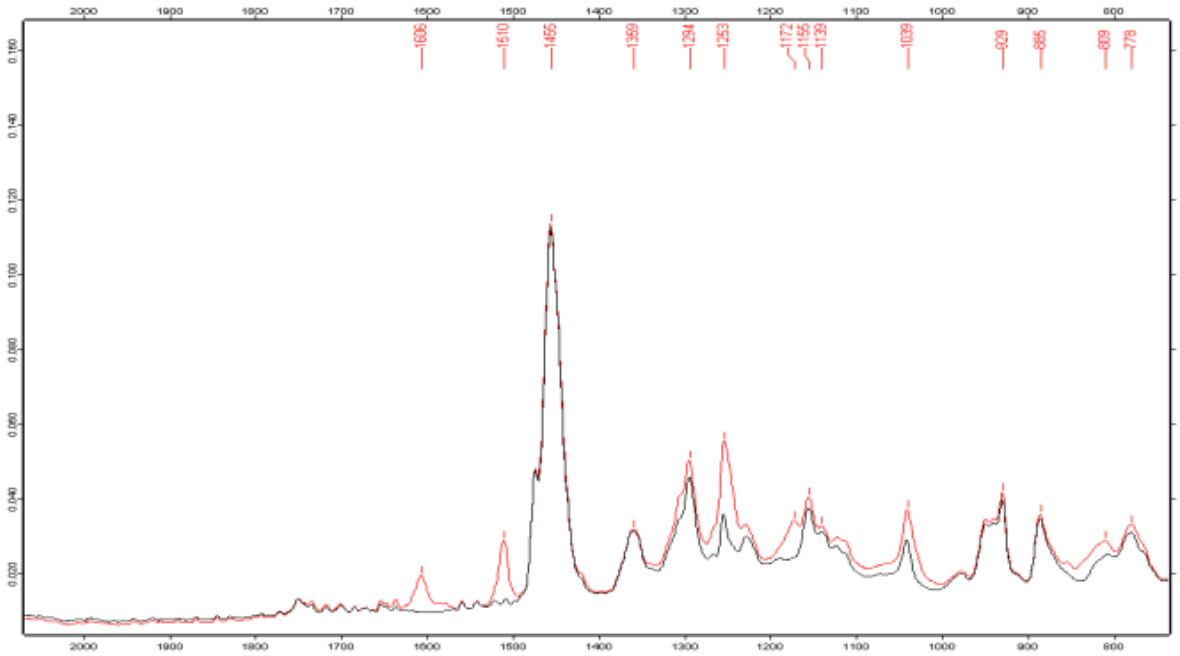


Figure 3.45. ATR-IR spectra of COC.Blank (Blue) and COC.A2 (red).

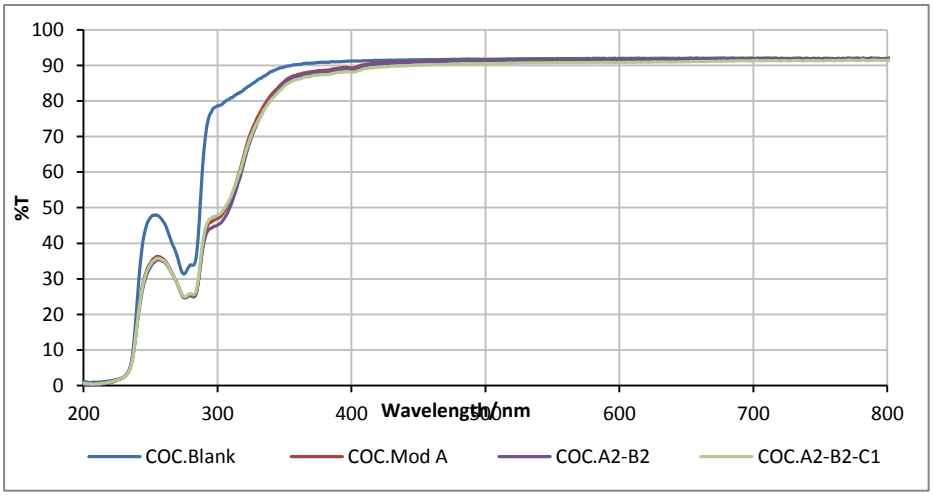


Figure 3.46. UV-Vis spectra for surface modified COC.

Successful modification **A2** was clearly indicated in IR spectrum (**Figure 3.45**) where new peaks due to the surface modification were observed at 1606 cm^{-1}, 1510 cm^{-1} and 1172 cm^{-1}. Though no change in colour was observed, a clear decrease in %T between 245 nm to 400 nm was observed from the UV-Vis spectra in **Figure 3.46**. Even though UV-Vis spectra remained similar to that of **COC.A2**, surface modified **COC.A2-B2** and **COC.A2-B4** saw a clear decrease of 13.9° and 6.1°

respectively in WCA, indicative of successful modification **Bx'** for macroscopic properties change.

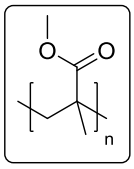


Figure 3.47. Chemical structure of PMMA.

PMMA: Poly(methyl methacrylate) (PMMA), commonly known as acrylic or acrylic glass, is a transparent thermoplastic that is often use as alternative to glass.[124] Other than being used widely as substitute to transparent glass, PMMA was also widely used as medical devices and implants as it has moderate biocompatibility.[125] There is also emerging application research for lab-on-a-chip microfluidic devices.[126] However, as seen from **Table 3.8**, PMMA is highly susceptible to solvent damage; treating the polymer with diethyl ether was fine, but immersion of **PMMA.A2** samples in ethanol solution of diazonium salt for surface modification **B2** overnight resulted in damaged surface. Further immersion in DMSO with spiropyran overnight caused the whole piece of polymer sample to be damaged. More solvent and process optimisation was required for PMMA.

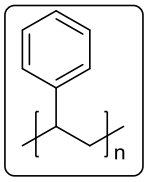


Figure 3.48. Chemical structure of PS.

PS: Polystyrene (PS) is a thermoplastic that is one of the most widely used plastics in the world, with an annual production of several billion kilograms.[127] The pellets of PS can be easily converted to different forms, for different applications. However, different from the highly cross-linked XAD-4 PS beads that were used in the previous studies, the flat PS substrates produced by injection moulding in SIMTech have surfaces that are highly susceptible to surface damage by solvent.

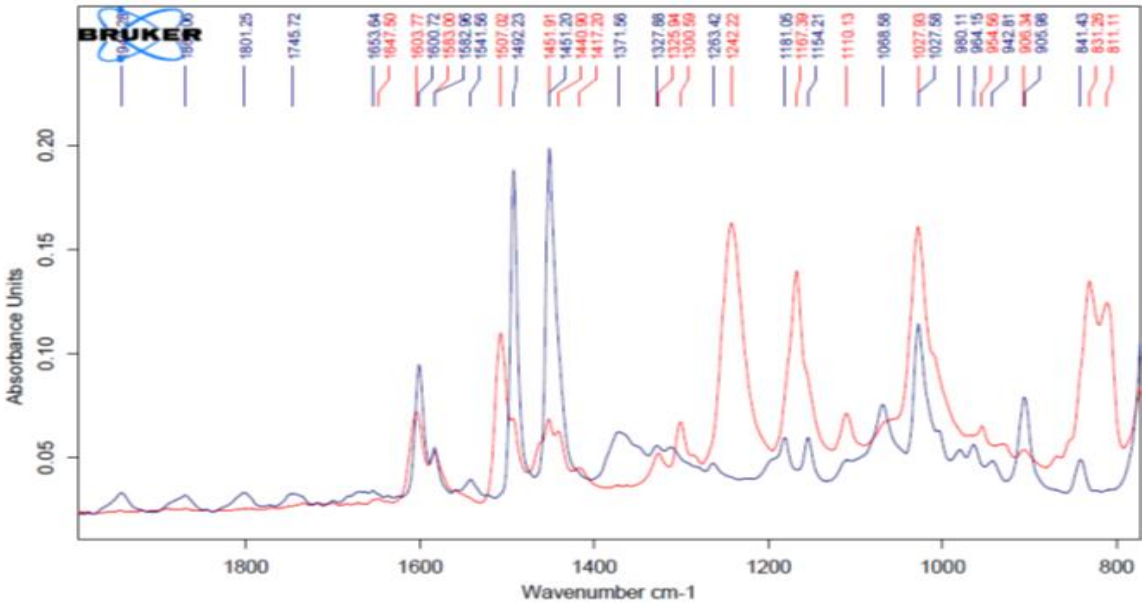


Figure 3.49. AIR-IR spectra of PS.Blank (Blue) and PS.A2 (Red).

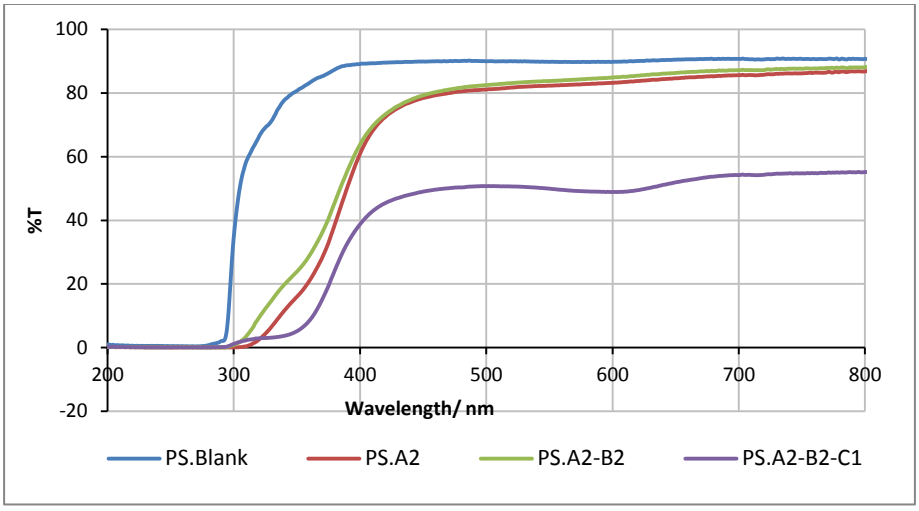


Figure 3.50. UV-Vis spectra of surface modified PS.

Clear indication of surface modification **Ax** was observed from the IR spectrum of **PS.A2** in **Figure 3.49**, with new peaks due to the surface modification observed at 1300 cm^{-1}, 1242 cm^{-1}, 1167 cm^{-1} and 1110 cm^{-1}. However, the use of diethyl ether in the surface pre-activation step resulted in slight fogging of the surface. This was reflected in the transmittance UV-Vis spectra where there is a significant decrease in %T of **PS.A2** between 300 – 800nm. The drop in %T was the greatest at about 350nm where %T for PS Mod A dropped from 80% to about 10%.

On the other hand, modification **Bx'** saw further roughening of the surface as reflected in the general increase in WCA PS sample with modifications **B2, B4**, **B7** and **B8**. The IR spectra of these samples also became unclear in the fingerprint region. This suggested that prolonged immersion in ethanol solution of diazonium salt affects the surface of the PS substrates. Prolonged immersion of **PS.A2-B2** into a solution of DMSO and spiropyran caused the surface of the PS substrate to be damaged as seen in **Table 3.8**, where the UV-Vis spectrum of **PS.A2-B2-C1** showed a great decrease in %T between 400 nm to 800 nm, from 80% to 50%. XPS analysis was not performed for these PS polymers as they were too thick and difficult to be cut into smaller sizes for characterisation by XPS.

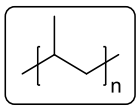


Figure 3.51. Chemical structure of PP.

PP: Polypropylene (PP) is a thermoplastic that is relatively lightweight, with excellent heat and chemical resistance.[122] It has such wide variety of applications and industrial uses that revenues of its sales are expected to exceed US$145 billion by 2019.[128]

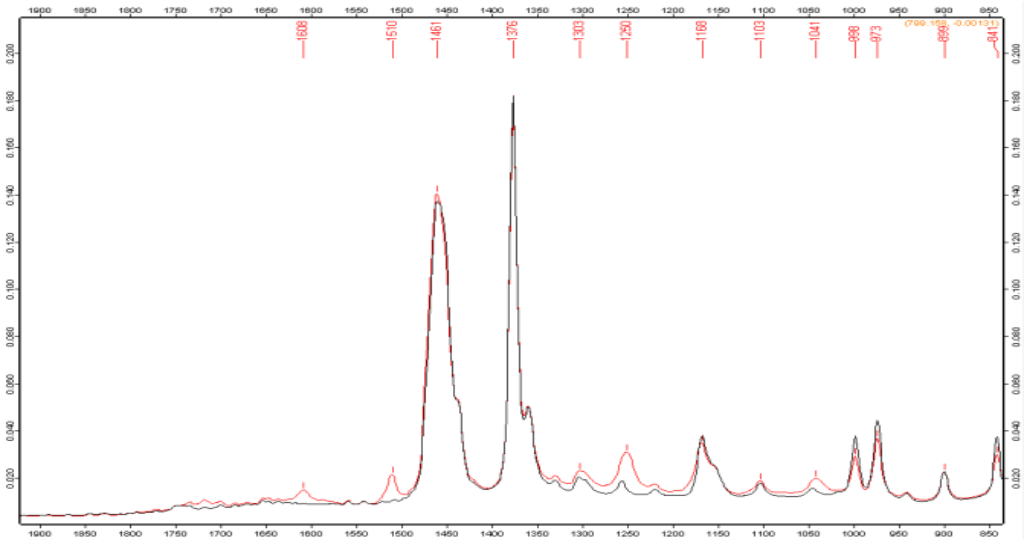


Figure 3.52. ATR-IR spectrum of PP.Blank (Black) and PP.A2 (red).

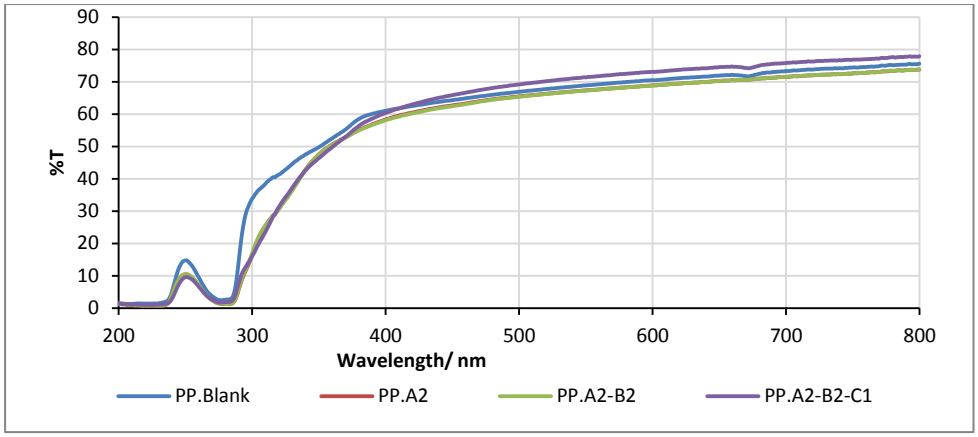


Figure 3.53. UV-Vis spectra of surface modified PP.

The physical appearance of all the PP samples remained unchanged throughout the modifications as seen in **Table 3.8**, thus, there was no visual indication of successful surface modifications or changes. Nonetheless, new absorption peaks of **PP.A2** at 1606 cm^{-1}, 1510 cm^{-1} and 1250 cm^{-1} due to the addition of aryl and OMe moieties onto the surface in the surface pre-activation step (Mod **A2**) were clearly shown in the ATR-IR spectrum as seen in **Figure 3.52**, indicating successful modification despite the polymer surface being relatively inert. Subsequent modification **B2** and **C1** was only indicated through slight changes in UV-Vis spectra as seen in **Figure 3.53.** There was a slight decrease in WCA by about 2.5° with the addition of the phenylacetic acid group onto the polymer surface, and a slight increase by 0.9° when further modified with spiropyran.

In all, different flat polymers showed different extent of surface modification, characterised by visual indication, transmittance UV-Vis spectrophotometry, ATR-IR or WCA. Polymers with surfaces functionalised with spiropyran moieties were examined for photochromic activity, and selected samples were tested for drug delivery. This is further discussed in the next chapter.

3.7 Surface Characterisation and Analysis

For the work discussed so far in this thesis, characterisation has always been very challenging, even more so when analysing samples with much lower surface loading. Throughout this study, while working on the edge of detection limits of various characterisation methods, a better understanding of the various characterisation methods was established, and which material form works best for which method was better comprehended. In this section, the characterisation methods used are discussed in greater detail.

3.7.1 Combustion elemental analysis

Combustion elemental analysis was conducted for all of the beads, pellets and powdered modified polymers. It is a very important characterisation method in this work, giving the indications of successful modifications by detection of N and other heteroatoms, and results from this analysis enabled estimation of surface coverage for XAD-4 PS beads. However, as seen from **Table 3.1, 3.2**, **3.3, 3.7** and **3.8**, combustion analysis only seemed to work best for XAD-4 PS beads, as combustion analysis of other polymers types usually gave heteroatom content below the detection limit.

While working at the detection limits of the instrument, it was important to understand how combustion elemental analysis was conducted to better understand the limitations of the data collected. Samples were burned entirely by dynamic flash combustion to be converted to their relevant combustion products, and were detected by a thermal conductivity detector (TCD) which then gave an output signal proportional to the concentration of the individual components of the mixture.[129] However, with only the surface modified and the bulk remaining unchanged, the

percentage of N detected would be much lower than that of C and H which usually makes up the bulk of the polymer. As such, surface coverage calculations based on results of this analysis method were deemed to give a lower limit estimate of the actual surface coverage. However, for PET pellets, LDPE and UHMWPE powder, the estimated calculations of surface coverage were considered to be highly unreliable as a result of the BET surface area measurement and the mathematical model, rather than the combustion analysis method. (See Appendix B for all combustion analysis data and calculation.)

3.7.1.1 BET

The Brunauer, Emmett and Teller (BET) method was used to estimate the specific surface area of the PET pellets, LDPE and UHMWPE powders. Conducted at the temperature of liquid nitrogen, the amount of gas adsorbed onto the surface of a solid can be measured, and treating the data collected with the BET adsorption isotherm equation gives the specific surface area. However, when measuring samples of PET pellets, LDPE pieces and UHMWPE powder, the measurements were highly inaccurate. The BET method was more commonly used for measurement of surface area of highly porous substrates, or substrates with relatively high surface area (>1 m^2/g).[130] According to the literature, to use BET measurement for low surface area substrates, argon or krypton should be used instead for better precision.[130, 131] However, as neither argon nor krypton gas was available, the BET experiment conducted using nitrogen gas instead. Despite being flawed, these BET results were used in the mathematical model for an estimated calculation of surface modification coverage, though highly unreliable estimations of surface coverage for PET pellets, LDPE and UHMWPE powder samples were sometimes observed. (See Appendix E for full BET data)

3.7.1.2 Mathematical Model used for Combustion Analysis

The mathematical model used for estimated calculation of surface modification coverage from combustion analysis was based on the assumption that the surface was sufficiently large that sampling error is minimal. Therefore, the mathematical model collapses when polymer substrates of much smaller surface area were used. Firstly, combustion analysis data collected would yield much higher error than perceived for low surface area materials. This is because sampling for substrate with high surface area would have much higher probability of getting a more uniform sample than samples with low surface area.

The error is further propagated when converting the calculation of molecules per square cm. This step is a form of mathematical averaging. However, without taking into consideration of the probability of uniformity of the sample when sampling, it introduces errors and uncertainties. For samples with large surface area, this step of averaging would not yield much error. However, for samples with low surface area and hence, surface loading, such averaging will be rendered highly erroneous and invalid.

While this model has its own limitations, it is still useful for estimated calculations of surface modification loading for a polymer with high surface area. (See Appendix B for combustion analysis calculation method and full data of all samples)

3.7.2 XPS

X-ray photoelectron spectroscopy (XPS) is another important surface characterisation tool. It enabled the measurement of the elemental composition up to 10nm depth of the surface layer, which approximated to be up to 30 atomic

layers.[132] Using the new XPS facility available in SIMTech, the beam was able irradiate samples at a focused 500µm diameter [See Appendix G for all XPS data]

3.7.2.1 Limitations due to nature of XPS analysis

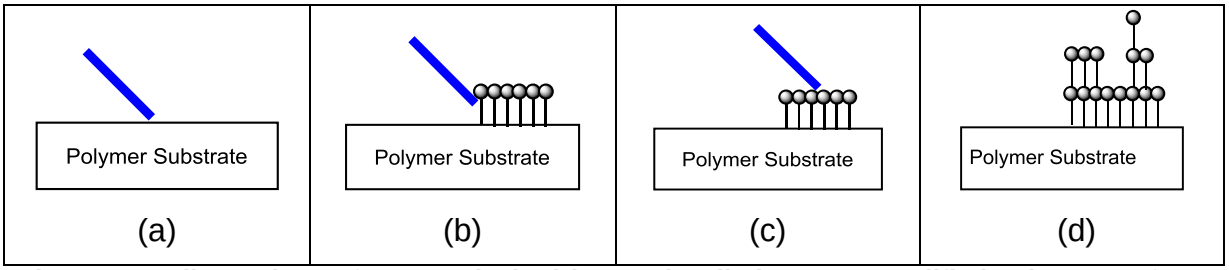


Figure 3.54. Illustrations of XPS analysis. (a) X-ray irradiation on unmodified polymer surface. (b) X-ray irradiation on both unmodified and modified surface of polymer. (c) X-ray irradiation on modified surface of polymer. (d) Multilayer surface modification on polymer substrate.

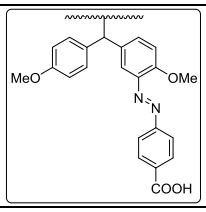
Figure 3.54 (a), **(b)** and **(c)** illustrated the possibilities of X-ray irradiation on the polymer sample surface when conducting XPS analysis. As the surface modifications of the samples were not uniform, when the focused beam was irradiated onto the polymer surface, it could either be irradiated onto the unmodified area **(a)**, or the modified area **(c)**, or a mix of both **(b)**. This would result in irregularities in the elemental composition measured. Take, for example, the results for flat PET samples; as the blank PET sheet had nitrogen-containing additives, when conducting XPS analysis for the surface modified samples, it was difficult to pin-point whether the nitrogen content detected was due to the polymer bulk, or was it from the new surface modification, or from both and to what extent.

Furthermore, the surface modifications may not be a monolayer. They were likely to exist as multilayer forms as illustrated in **Figure 3.54 (d)** and this would affect the elemental composition detected, and affect and calculation of the expected XPS atomic ratio as discussed below.

3.7.2.2 Expected atomic ratio calculation

The expected atomic ratio for XPS analysis can be calculated using two different methods.

Method 1: Taking into consideration only the molecule modified onto surface in question. For example:

	Chemical formula: $C_{22}H_{19}N_2O_4$ Expected atomic ratio: N/C: 2/22 = 0.0909 O/C: 4/22 = 0.182

This was the conventional method used in the group, and was used for the calculation for expected XPS atomic ratio throughout this work for its simplicity to give a rough estimation of surface coverage, in corroboration with combustion analysis results. However, a more detailed analysis and calculation was later established when working with substrates of low surface area.

Method 2: Taking both the molecule and the substrate into consideration, the expected (theoretical) atomic ratio is substrate dependent. Using this method, the expected ratio is calculated based on the maximum possible loading of the modification on a particular surface. This would be dependent on the minimum and maximum projected surface area of the substrate molecule.

For example, while a modification molecule covers up to 2 repeat units of PET, the same modification molecule may cover at least 7 repeat units of PE. In addition, atomic concentration data captured using XPS could reflect both the surface modification and the substrate. Using computational studies (www.chemicalize.org), it is possible to determine the approximate minimum projection area of the modification, as well as the minimum and maximum projected area of the substrate, and therefore, determine how many repeat units to use in our calculations. Using

minimum projected area of modification is to approximate maximum loading possible on the substrate.

As seen in **Table 3.9** below, the minimum projected area of most of the modifications fall between 50 -80 Å^2. **Table 3.10** gives the range of projected area for the polymers with different repeat units. The most suitable number of repeat units (n) for each type of

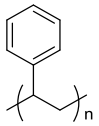
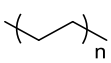
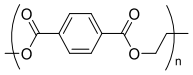
polymer is indicated on the right column of **Table 3.10**, marked with 'x'.

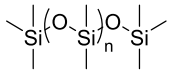
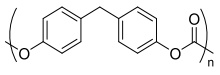
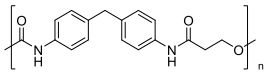
Table 3.9. Computed areas of modifications from simulation.

Modification	Min Projected area/ Å^2
A2 (-OMe)	45.77
A2-B2	62.48
A2-B2-C	83.01
A2-B4	58.72
[a]A2-B4-C	80.31
A2-B5	63.13
[a]A2-B5-C	73.98
A2-B6	58.12
A2-B7	58.12
A2-B8	66.15

[a] Limits of programme. An under-estimated value.

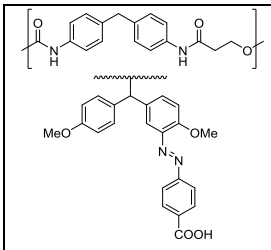
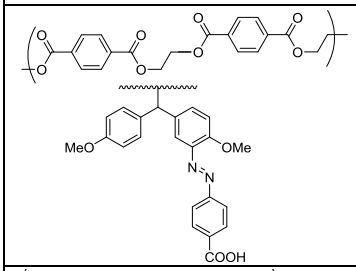
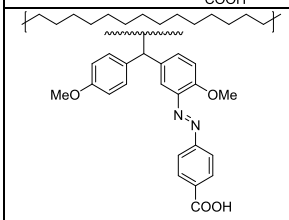
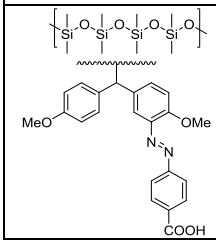
Table 3.10. Computed Sizes of materials from computation

Material	n	Min Projected area/ Å^2	Max Projected area/ Å^2	Choice
Polystyrene 	1	24.99	42.38	
	2	43.19	70.31	
	3	67.44	92.25	X
	4	78.24	114.08	
	5	85.58	136.83	
PE 	1	14.96	17.93	
	3	22.53	41.22	
	5	28.45	64.42	
	7	31.71	99.56	X
PET 	1	24.56	65.61	
	2	55.65	106.68	X
	3	83.51	160.04	

PDMS 	1	43.68	66.41	
	2	46.33	81.59	X
	3	55.25	96.37	
PC 	1	41.67	66.74	
	2	65.13	120.51	X
	2.5a	81.73	159.77	
TPU 	1	51.96	82.40	X
	2	75.40	159.63	

[a] Limits of the programme.

Table 3.11. Expected ratio calculation for XPS using method 2.

	n = 1 (1 repeat units of TPU) Chemical formula: TPU + Modification = $C_{38}H_{35}N_4O_5$ Expected ratio: N/C: 0.105 O/C: 0.131
	n = 2 (2 repeat units of PET) Chemical formula: PET + Modification = $C_{44}H_{42}N_2O_{12}$ Expected ratio: N/C: 0.0455 O/C: 0.273
	n = 7 (7 repeat units of PE) Chemical formula: PE + Modification = $C_{36}H_{48}N_2O_4$ Expected ratio: N/C: 0.0556 O/C: 0.111
	n = 2 (2 repeat units of PDMS) Chemical formula: PDMS + Modification = $C_{30}H_{43}N_2O_8Si_4$ Expected ratio: N/C: 0.0667 O/C: 0.267

Despite being a more thorough approach for calculating the expected XPS atomic ratio, this method was not used in this work for several reasons. Firstly, the calculation for this method is much more complex than the previous method; each modification of the molecule requires a new computation for projected minimum size, and each substrate requires computation of the minimum and maximum projected

surface area. This means that for each modification step, one needs to re-calculate the number of repeating units the modified molecule will cover, in order to establish the new expected ratio. Thus, the analysis of all of the surface-modified substrates can be very tedious, just to yield a number for use as an approximation of surface coverage, that can be rather similar to that obtained from method one that is simple and straightforward. Secondly, this method is only suitable for substrates that are non-porous with a low surface area, based on the assumption that the modification is made on a flat and chemically uniform substrate at the molecular level, and that the surface modification is a monolayer. However, from previous studies, it was noted that the pre-activation step would be forming a thin film rather than a monolayer.[25] In addition, it was unclear to what extent the XPS would penetrate the polymer substrate base with different degree of surface modification.

In addition, the computational software used is fairly simple, with only projected minimum and maximum areas and without indication of the preferred spatial orientation, stacking and alignment, whether the polymer exists as repeat units, or when certain groups are modified onto polymer surface. With the information available, the model was established at two-dimensional level, without consideration of the third dimensional spatial orientation of how the polymer substrate would accommodate and orientate the molecule modified onto its surface, thus, introducing error.

In all, despite the many limitations and uncertainties, results from XPS analysis, together with combustion analysis, could give a rough estimation of surface modification loading, and thus, by establishing the efficiency of the modification methods, determine extent of modification required for a macroscopic function to be observed.

3.7.3 ATR-IR

Attenuated Total Reflectance (ATR) refers to the sampling method used in conjunction with the Infrared (IR) spectroscopy, and thus is ATR-IR. This method was used to throughout this work to characterise the surface of the modified polymers by providing information of the expected functional group attached onto the surface, thus, is indicative of the success of the desired surface modification. However, this characterisation method suffered drawbacks when peaks due to bulk substrate overlap with, or cause the desired peaks to be hidden. In addition, when attempting to characterise modified polymers with a lower loading of surface modification, ATR-IR was not sufficiently sensitive for detection of the new modifications. Nonetheless, this characterisation method was very useful for polymers with little or no absorption peaks at the IR fingerprint regions, and was very effective in the surface characterisation of XAD-4 bead samples, and in showing peaks due to surface modification **A2** in most of the samples, and also modification **Bx** in some of the samples. (See Appendix C for all ATR-IR data.)

3.7.4 UV-Vis

UV-Vis is an extremely sensitive method used throughout the work in this thesis for quantification of colour. For beads, pellets and powder samples, the diffused reflectance method was used, while for the flat substrates, the transmittance mode was employed. Diffused reflectance measures the relative change in the amount of light reflected off a surface. This method was most suitable for the beads and powder samples as light could not pass through these samples, where conventional absorbance and transmittance UV-Vis mode could not be used. Characterisation of the materials was measured using a specially designed Pike Veemac Diffuse IR

accessory which uses a very small round cup of about 0.5 cm in diameter and less than 0.5 cm in height to hold the samples. This method was most suitable for powder samples rather than pellets because of the way the experiment was conducted and the scattering of the light off the sample forms. Powder samples can be packed neatly into the sample holder to give a relatively flat top surface in the sample holder. Therefore, light can still reflect off the flat surface relatively well. However, for PET pellets and LDPE bits, the samples cannot be packed neatly into the sample holder. This resulted in incident light shining on a highly irregular surface at the top of the sample holder, resulting in irregular surface reflectance, due to the nature of the sample. This was reflected in the UV-Vis spectra collected where UHMWPE powder samples gave the most detailed and clear UV-Vis spectra, followed by XAD-4 beads which could pack relatively well into the sample holder, but UV-Vis spectra collected for PET pellets were rather messy. A silver mirror was used as baseline for the diffused reflectance measurements. The raw data collected from the samples were processed using the blank polymer as the reference. Such conversion of raw to processed data was done so that peaks seen were due to modification, not bulk polymer. (See Appendix D for UV-Vis data)

3.7.5 Water Contact Angle (WCA)

Surface wettability studies usually involve a contact angle measurement as the preliminary investigation, giving the degree of wetting when the solid surface and the liquid interact. The technique used in this study to measure contact angle is a form of direct optical method, known as Drop Shape Analysis. Contact angles measured from a sessile drop can be further used to calculate the solid surface tension, which quantifies the wetting characteristics of the surface, using Young's

Equation, with the assumptions that the solid surface is rigid, smooth, homogenous and inert to the test liquid.[133]

However, such detailed calculations were not used for two main reasons. Firstly, the general interest of this work was for the observation of a change macroscopic properties arising from the surface functionalisation, and thus, a change in contact angle measured would be sufficient. Secondly, as mentioned in the discussion in the previous section, the assumptions required for the Young's Equation to be valid do not hold true; the surface-modified polymers do not have their surface uniformly modified, and some substrates, like PS, saw an increase in roughness after the surface modification.

Ultrapure water was used as the test liquid for the drop shape analysis to give an indication of the water surface wettability of the surface-modified flat polymers. 5 measurements, using 1.00 µL per drop, were taken for each polymer sample, and confidence interval was calculated using t-distribution. Some samples as seen in **Table 3.8** had large ± error limits. This could be attributed to the non-uniformity of the surface modification coverage. If the point measured was on the part polymer that were modified, there would be a change in WCA, while if the point measurement was done on the part of the polymer that remained unmodified, then there would be little or no change to the WCA. (See Appendix F for WCA data)

3.7.6 Error calculations

As the sample size was relatively small, t-distribution was used for calculating the confidence interval, for both the combustion analysis and water contact angle. However, the basis of calculations for both characterisation methods differ.

For combustion analysis, the percentage error for heteroatoms was calculated based on data collected from **XAD.A1** and approximated for all other samples. 5 samples of beads **XAD4.A1** were sent for combustion analysis to obtain 5 values of %N. This was to approximate t-distribution with 95% confidence to obtain a mean of 0.68%N with a 2-tailed confidence interval of ±0.15%. 0.15%N was estimated to be 22% of 0.68%N. Therefore, subsequent %N for other samples was assumed to take a 22% error of the analysed data. This generalisation arose as it was not possible to have every sample measured at least three to five times just to obtain a highly reliable error estimate for each sample due to the expense and time cost incurred.

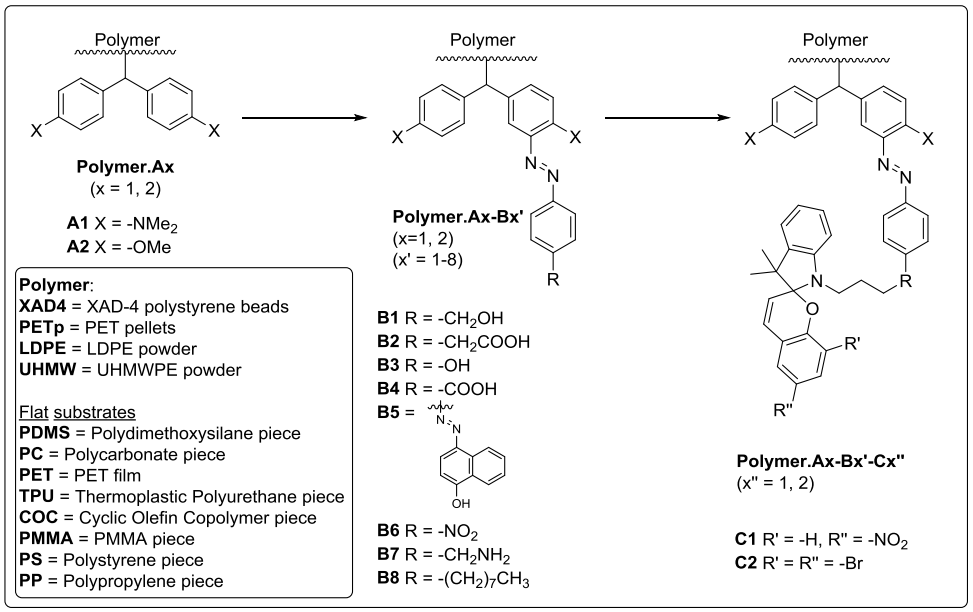
Combustion analysis results of beads **XAD4.A1** were chosen as the basis for the error calculation for 2 reasons: firstly, this was from the first step of the whole surface modification, thus, subject to less variability compared to samples from subsequent modifications; And secondly, the surface modification of beads **XAD4.A1** contained heteroatom N, suitable for combustion analysis.

WCA error calculation was based on individual samples. WCA can be conducted with greater ease and convenience compared to combustion analysis, and each sample can vary extensively; different materials used for substrate would show a very different extent of surface modification and surface wettability, and with low surface area and thus surface loading, the variability would be more pronounced. Therefore, compared to combustion analysis error calculation that was used for only one material XAD-4 PS beads that have a large surface area, it was necessary for error calculations of WCA to be based on individual samples.

Similarly, five WCA measurements were calculated for their mean and confidence interval using a two-tailed t-distribution at 95% confidence level. The final WCA

value was quoted as an average of the five measurements, along with the confidence interval calculated.

3.8 Conclusion



Scheme 3.8. Overall general scheme for all surface modified polymers.

In all, this chapter summarizes all of the surface modification experiments for polymers experiments involved in this thesis (**Scheme 3.8**). The synthesis of the diaryldiazo intermediates for pre-activation of surface for azo coupling was optimised, followed by expansion the scope of diazonium salts and polymeric substrates to decide the most appropriate synthesis to be transferred to SIMTech for further development. After transferring the project to Singapore, a scalable process for large area surface engineering was developed, first with modification process optimisation, followed by variation of different commodity and engineering polymers to examine the modification method.

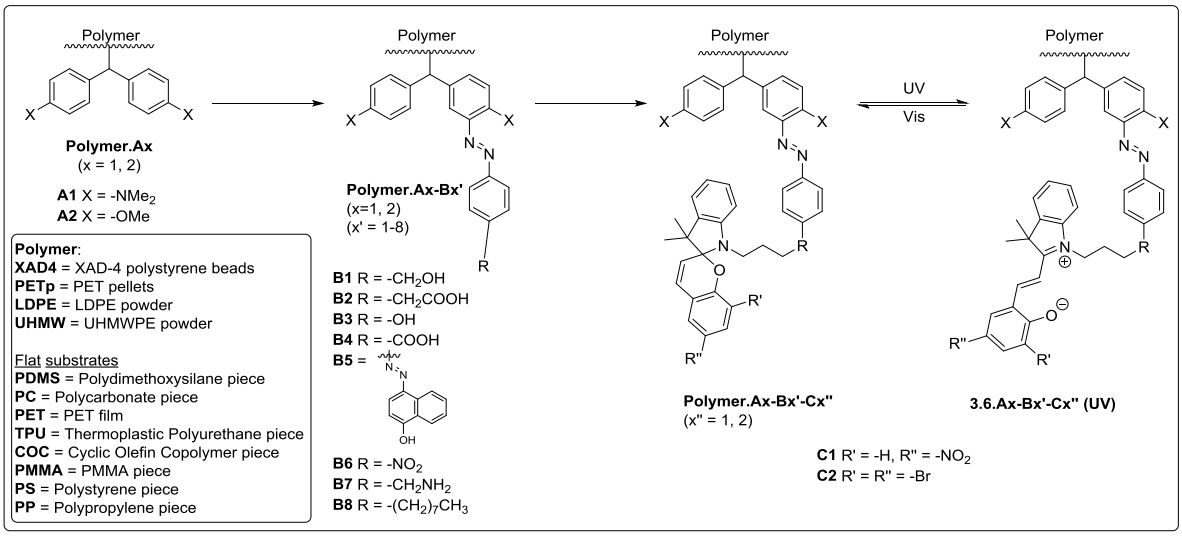
While different polymers gave varying extents of modification, most of the polymer substrates with relatively more inert surface such as PE, COC and PP saw very low surface modification loading that was lower than the detection limits of some

characterisation methods. Despite this limitation in surface coverage, macroscopic changes in properties like water contact angle were still observed. Further applications of these surface modified polymers for macroscopic functions are described in greater detail in the next chapter.

4 Controlled Macroscopic Functionalities

4.1 Introduction

The aim of modifying surfaces of polymers was to alter the surface properties for specific applications while retaining favourable bulk properties of the polymers. The previous chapter discussed the preparation, surface modifications and subsequent surface characterisation of a range of polymers. This chapter explores the applications of these surface-modified polymers for controlled macroscopic functions, and in particular, surface photochromism and drug delivery.



Scheme 4.1. Overall general scheme for all surface modified polymers.

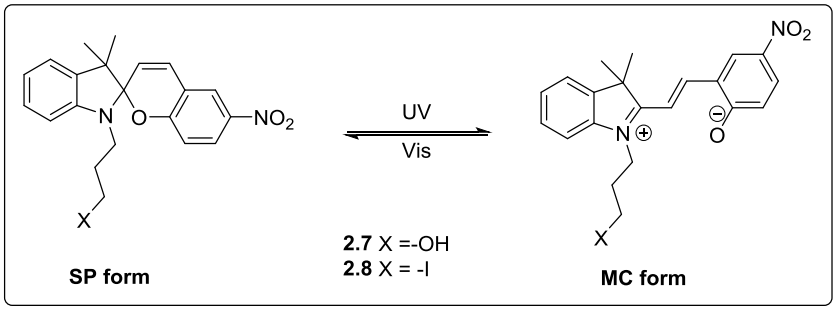
4.2 Photochromicity Study

Chapter 2 described the synthesis of spiropyran units and their derivatives which are analogous to those used for surface modifications on various polymers as reported in Chapter 3. This section investigates the photochromic behaviour of the

spiropyran and its derivatives in solution, compared to photochromic behaviour when immobilised onto polymeric surfaces.

4.2.1 Spiropyran analogues in solution

The synthesis of the spiropyran unit and analogues for use with surface modification was discussed previously in Chapter 2 and Chapter 3. This section explores the photochromic activity of the spiropyran molecule, as well as its derivatives.



Scheme 4.2. Spirocyclic (SP) close-ring form and Merocyanic (MC) open-ring form of spiropyran 2.7 and 2.8.



Figure 4.1. Appearance of spiropyran 2.7 in various solvents before (top) and after (below) UV-irradiation. (Across: AcOH, DCM, MeCN, THF, $CHCl_3$, EA)

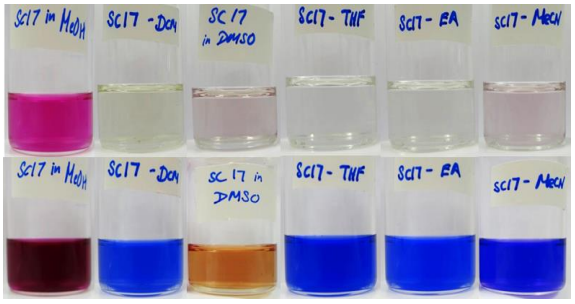


Figure 4.2. Appearance of spiropyran 2.8 in various solvents before (top) and after (bottom) UV-irradiation. (across: MeOH, DCM, DMSO, THF, EA, MeCN)

After dissolving the spiropyrans **2.7** or **2.8** in various solvents, and irradiating the solution with UV light, changes in colour were observed, which were quantified using UV-Vis spectrophotometry. The photochromic behaviour is due to the reversible change in structure from the spiropyran to the merocyanine form.

Photochromism: **Figure 4.1** and **Figure 4.2** show the appearance of spiropyran **2.7** and **2.8** in various solvents before and after UV-irradiation. Before UV-irradiation, most samples appeared pale or colourless. After UV-irradiation, they change to an intensely coloured solution, mostly blue or purple. This change in colour was also reflected in their UV-Vis spectra.

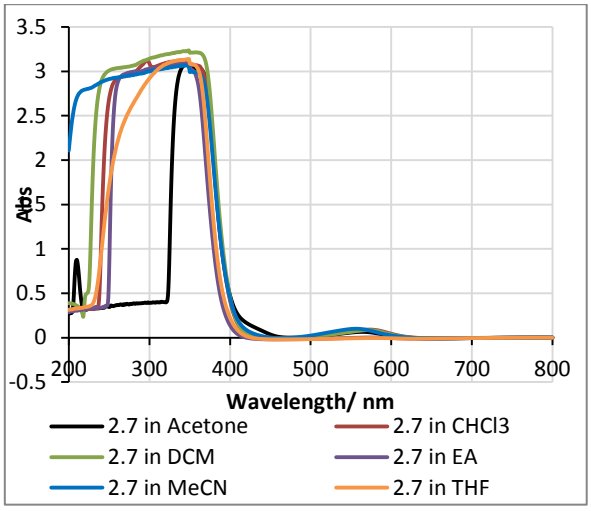


Figure 4.3. UV-Vis spectra of spiropyran 2.7 in various solvent before UV irradiation.

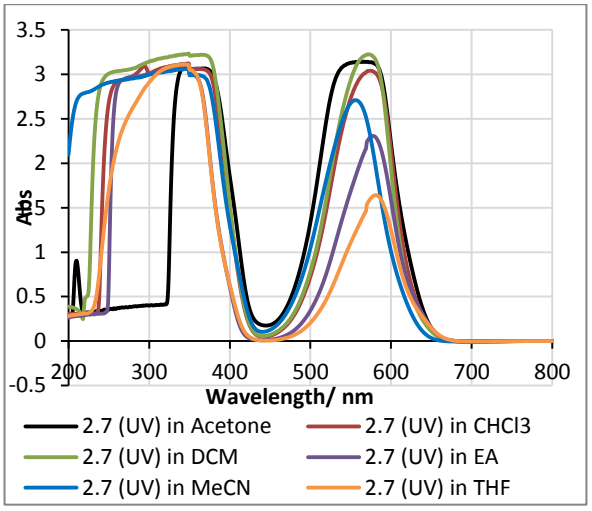


Figure 4.4. UV-Vis spectra of spiropyran 2.7 in various solvent after UV irradiation.

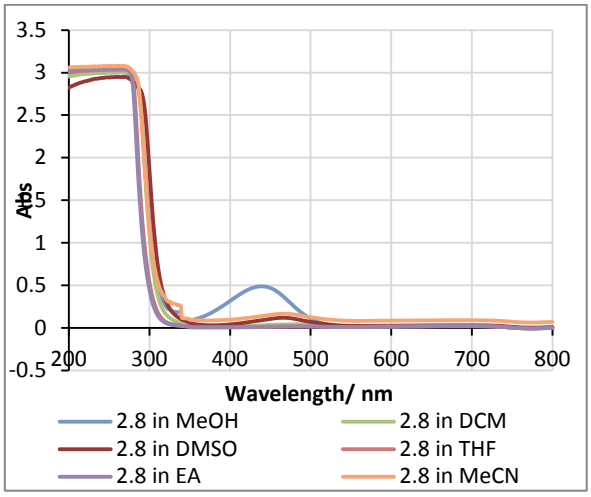


Figure 4.5. UV-Vis spectra of spiropyran 2.8 in various solvent before UV irradiation.

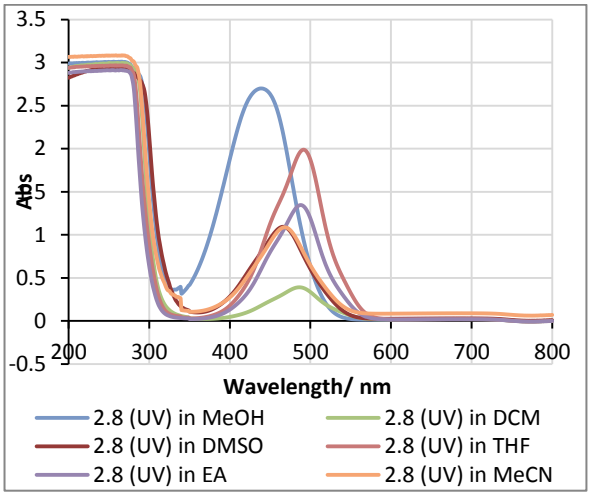


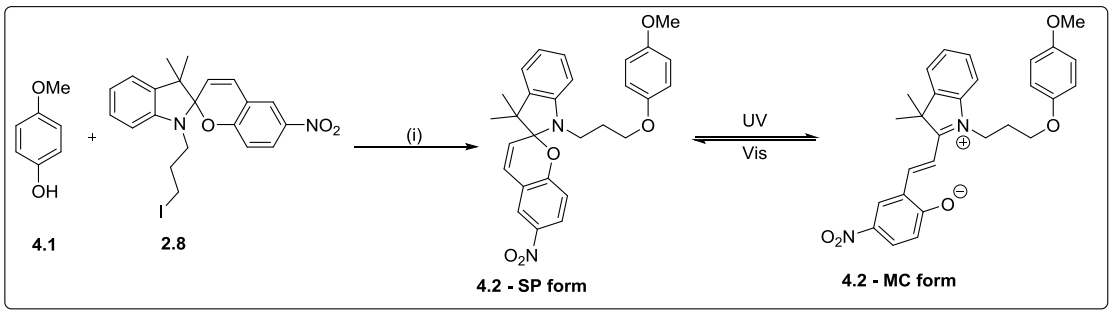
Figure 4.6. UV-Vis spectra of spiropyran 2.8 in various solvent after UV irradiation.

Comparing UV-Vis spectra in **Figure 4.3** to **Figure 4.4**, there was a sharp increase in absorbance for **2.7** at around 530 – 590 nm after UV irradiation, but the change in absorption spectra for **2.8** came at around 440 – 500 nm (**Figure 4.5**); for both, there was a noticeable difference in their absorption spectra after UV-irradiation, in

both the λ_{max} and Abs_{max}. For example, in DCM, λ_{max} for **2.7** in MC form was at around 584 nm, with absorbance of about 3.17, whereas for **2.8**, λ_{max} appeared at 495 nm, with absorbance of about 0.37. This decrease in λ_{max} and absorbance was also observed for other solvents such as $CHCl_3$, THF and EA even though they appear to be all blue in colour after UV-irradiation for both **2.7** and **2.8**. Similarly, UV-Vis spectra for both species differ at around 200 – 300 nm.

On the other hand, the UV-Vis spectra for both species remained similar before and after UV-irradiation at around 200 – 380nm and 200 -300nm for **2.7** and **2.8** respectively, thus, indicating that transformation from SP to MC form by UV-irradiation only affected the absorption spectra at around 450 – 600 nm for the isolated spiropyran unit.

Solvent effects: As seen from both **Figure 4.4** and **Figure 4.6**, different solvents gave different λ_{max} for **2.7** and **2.8**. For example, **2.7** in MeCN had λ_{max} at around 564 nm, while in DCM had λ_{max} at around 581 nm. Similarly, **2.8** saw λ_{max} at 450 nm for MeOH, and max at 495 nm for DCM. The transformation of the spirocyclic form transformed into the merocyanine form gives a zwitterionic product, which is more likely to be affected by the polarity of any solvent in which it is dissolved. Thus, an increase in solvent polarity causes λ_{max} to decrease as the molar coefficient (ε) of the compound decreases; this is known as negative solvatochromism, and corresponds to a hypsochromic shift (blue shift). Correspondingly, a bathochromic shift (red shift) would be termed positive solvatochromism. While solvatochromic effects have resulted in a change in λ_{max} and ε_{max}, the change in solvents could also affect the position of the equilibrium between the closed-ring SP form and the open-ring MC form and thus affect the observed UV-Vis spectra.



Scheme 4.3. Derivatization of 4-hydroxyanisole (4.1) with spiropyran 2.8. Condition: (i) K_2CO_3 in MeCN, reflux for 5 h.

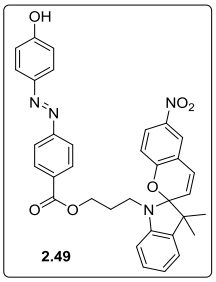


Figure 4.7. Structure of compound 2.49.

Spiropyran **2.8** was further reacted with 4-hydroxyanisole (**4.1**) to give derivative **4.2**, as seen in **Scheme 4.3** above. Another spiropyran-derivatized compound, **2.49** (**Figure 4.7**) was previously described in Chapter 2, and was used to further study how more complex systems could affect photochromic behaviour of the spiropyran. The compounds were dissolved in solution and UV-irradiated. The colour of the compounds before and after UV-irradiation was quantified using UV-Vis spectrophotometry.



Figure 4.8. Appearance of 4.2 (top) and 2.49 (bottom) in DMSO before (left) and after (right) UV-irradiation.

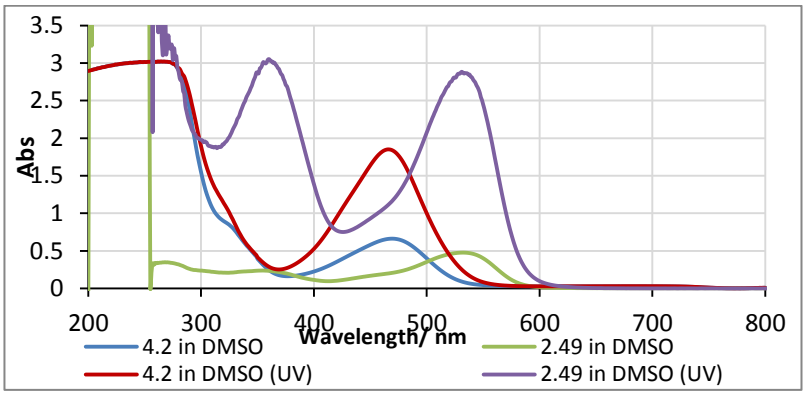


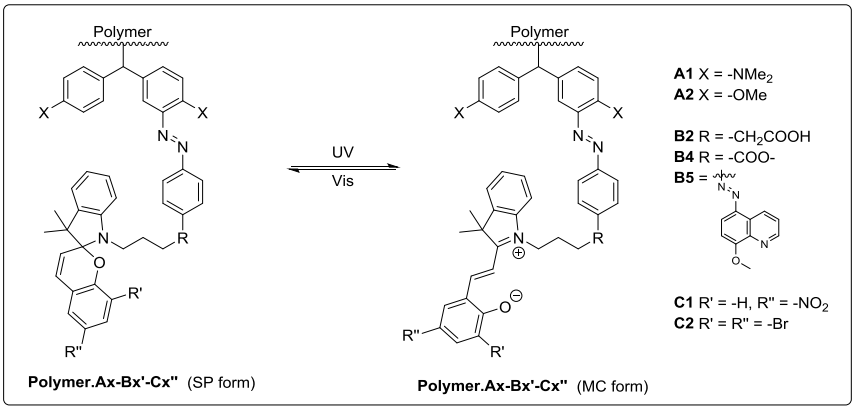
Figure 4.9. UV-Vis spectra of 4.2 and 2.49 in DMSO before and after UV-irradiation.

As seen from **Figure 4.9**, the absorption spectra of both compounds **4.2** and **2.49** changed after UV-irradiation, corresponding to the change in colour as seen in **Figure 4.8**. Similar to UV-Vis spectra of spiropyran **2.8** in **Figure 4.6**, there was a large increase in absorbance at around 467 nm for compound **4.2**. However, it was also noted there is slight difference in the spectrum at around 315 nm.

On the other hand, the absorption spectrum of **2.49** in **Figure 4.9** saw a drastic change, with significant increase in absorbance at 358 nm and 531 nm. While the increase in absorbance at 531 nm was similar to that of spiropyran **2.7** in **Figure 4.4**, likely to correspond to the change in structure of the spiropyran moiety, the peak at 358 nm was not present in the isolated spiropyran unit **2.7** or **2.8**. The peak at around 272 to 296 nm is usually due to the $\pi - \pi^*$ electronic transition in the indoline part of the spiropyaran, whereas band at around 323 – 351 is attributed to the chromene group.[134]

In summary, photochromic phenomena of both the spiropyran and derivatized systems in solution have been investigated using UV-Vis spectrophotometry. However, it was unlikely that these spectra correspond to a single MC open form. This is because most forms in solution thermally fade at a rate significant compared to the time required to capture the data on the UV-Vis spectrophotometer.[42] In addition, it was also visually observed that these spiropyran compounds decolourise rapidly in presence of light. Nonetheless, the UV-Vis data collected was sufficient to gather information such as λ_{max} for comparison to photochromic action on polymer surface.

4.2.2 Light responsive surfaces

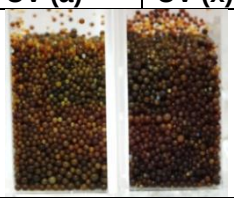
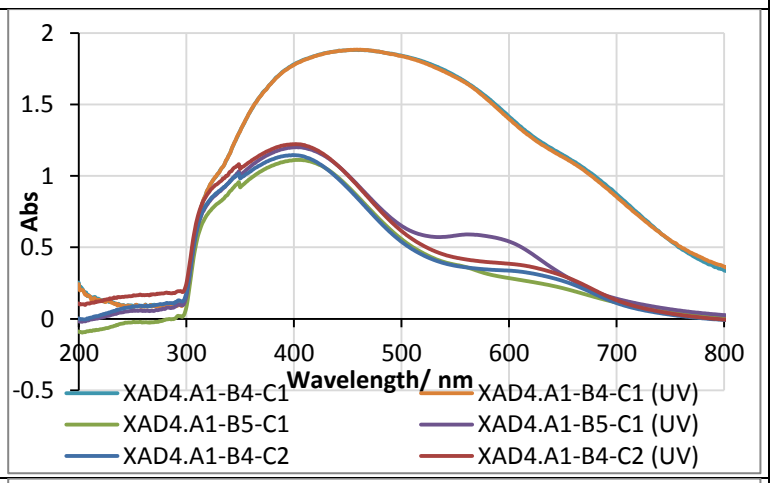
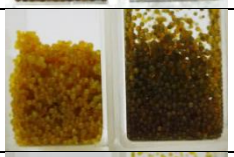
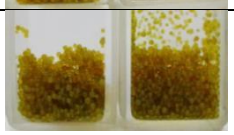
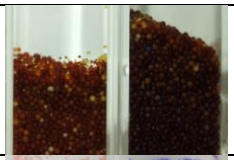
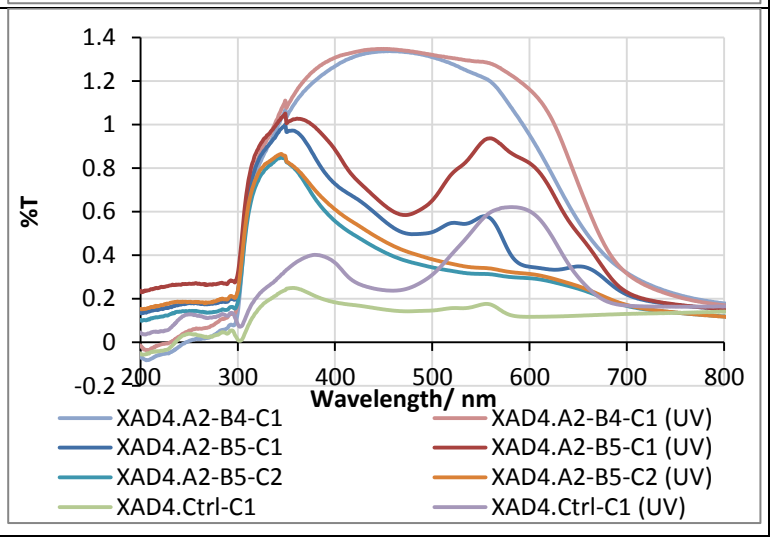
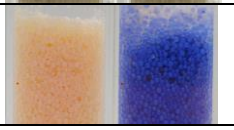


Scheme 4.4. SP and MC form of spiropyran on surface modified polymers.

In the previous chapter, the process and characterisation of surface modification of polymers were discussed. In this section, polymers with surface modified photochromic spiropyran were further investigated for photochromic activity. These light responsive surfaces (made in Oxford), ranging from high surface XAD-4 beads, to lower surface area pellets and powders, were characterised using Diffused-reflectance UV-Vis method. The analogous photochromic flat substrates prepared in SIMTech Singapore were characterised and studied using Transmittance mode of the UV-Vis spectrophotometer.

4.2.2.1 XAD-4 PS Beads

Table 4.1. Surface modified photochromic XAD-4 beads and their UV-Vis spectra.

Sample	Before UV (a)	After UV (x)	UV-Vis Spectra
XAD4.A1-B4-C1[a]			
XAD4.A1-B5-C1			
XAD4.A1-B5-C2			
XAD4.A2-B4-C1[a]			
XAD4.A2-B5-C1			
XAD4.A2-B5-C2			
XAD4.Ctrl-C1			

[a] Photo was taken under strong flash light for better colour distinction.

As seen from **Table 4.1**, XAD-4 PS bead samples with surface modification **A1** (sample **XAD4.A1-B4-C1**, **XAD4.A1-B5-C1**, and **XAD4.A1-B5-C2**) showed little change in colour before and after UV-irradiation. As seen from the corresponding UV-Vis spectra of the XAD-4 beads, absorption spectra of **XAD4.A1-B4-C1** appeared to be very similar before and after UV-irradiation, indicating very little change in colour of **XAD4.A1-B4-C1**, consistent with appearance of the beads. Prior to UV-irradiation, the beads were already intensely coloured, thus, any photochromic changes would not be observed or detected, even around the photochromic region of 400 – 600 nm, as the absorbance of beads in the UV-Vis spectra approached the limit of the UV-Vis detection method.

In contrast, **XAD4.A1-B5-C1** was relatively lighter coloured than **XAD4.A1-B4-C1**. As such, after UV-irradiation, a change in colour was observed as seen in **Table 4.1**. This change was also reflected in the UV-Vis spectra of **XAD4.A1-B5-C1**, with increase in absorbance at the region 500 – 650 nm, and λ_{max} at around 575 nm. On the other hand, even though the samples of **XAD4.A1-B5-C2** looked very similar before and after UV-irradiation, the absorption spectra of **XAD4.A1-B5-C2** still showed very slight change, demonstrating the high sensitivity of characterisation by UV-Vis spectrophotometer. This also indicated that spiropyran with the NO_2 side group works more efficiently than the Br side group in bringing about a visible photochromic change.

The visible colour change was more apparent for systems with modification **A2** (sample **XAD4.A2-B4-C1**, **XAD4.A2-B5-C1**, **XAD4.A2-B5-C2**) as seen from **Table 4.1**. **XAD4.A2-B4-C1** still appeared to darken slightly after UV-irradiation even though the beads were already rather intensely coloured prior to UV-irradiation. This change was reflected in the absorption spectra with slight increase in absorbance at

around 395 nm and 600 nm. The change in colour for **XAD4.A2-B5-C1** was the most apparent, with a clear transformation from pink to blue after UV-irradiation, and significant change in absorption spectra, indicated by significant increase in absorbance at around 353 nm and 560 nm. In a manner similar to **XAD4.A1-B5-C2**, although the appearance of **XAD4.A2-B5-C2** did not indicate a clear change in colour after UV-irradiation, the change in absorption spectra due to photochromic action was still apparent, with peaks forming at around 350 nm, 554 nm and 645 nm. **However, XAD4.Ctrl-C1** also demonstrated photochromic phenomena as seen in **Table 4.1**, most likely due to adsorption of the spiropyran molecules on the surface, and absorption of the photochromic compound into the pores. Nonetheless, as seen from its absorption spectra, the change in absorbance for the control was lower than that of the surface modified samples, thus, indicating that photochromic activities of other samples were not due to simple surface adsorption surface or absorption of spiropyran into pores of the polymer.

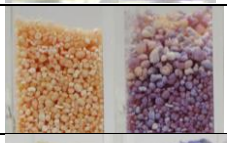
The examination of the UV-Vis spectra of photochromic XAD-4 PS beads with spiropyran immobilized onto surface showed that change in absorption spectra occurred most significantly at 500 – 650 nm due to the ring opening of the spiropyran to give highly coloured MC form. This was similar to the photochromicity of analogue **2.49**, with structure analogous to the surface modification, as the absorption spectra also reflected significant change due to photochromism at around 500 – 650 nm, and peaked at 540 nm, as seen in **Figure 4.9**. In addition, compared to analogues in solution which took only less than 2 min for the MC form to revert back to the more stable SP form, the spiropyran in MC open-ring form seemed to be more stable when immobilised onto surface, as indicated by longer

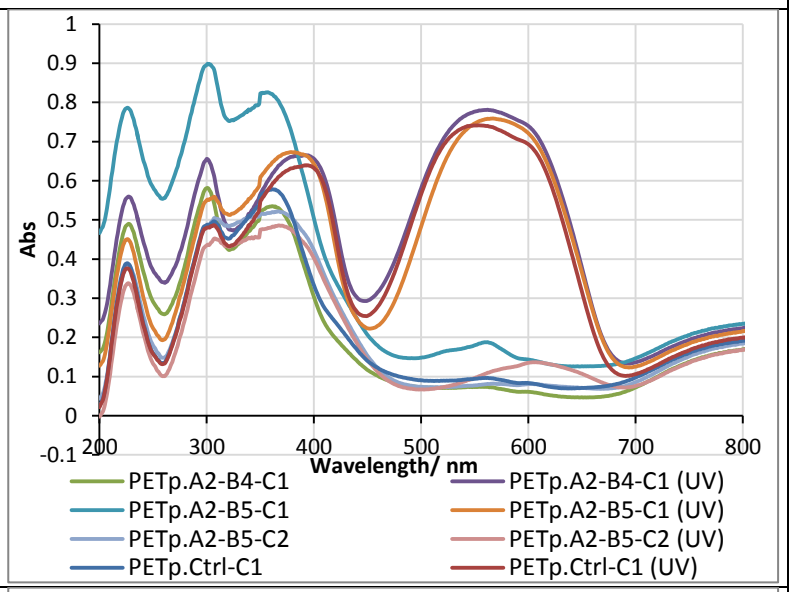
time required for the bleaching to occur, with **XAD4.A2-B5-C1** taking more than 1.5 hours to fully transform back to the original form.

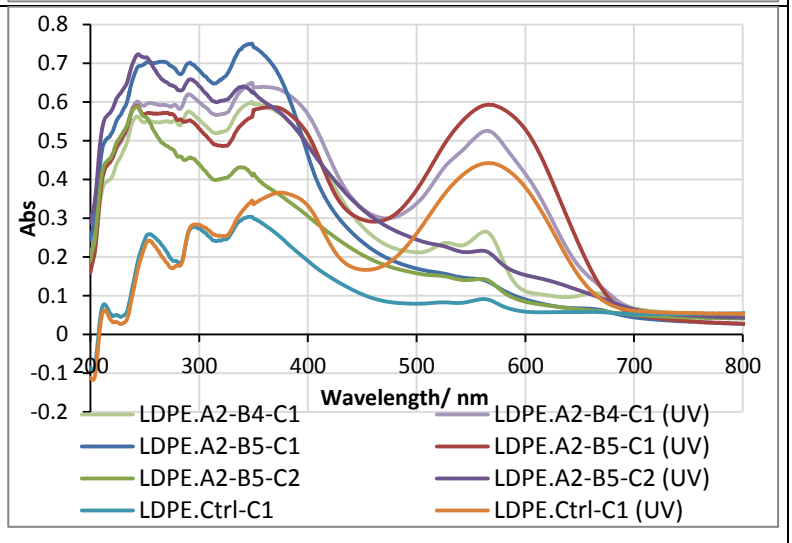
4.2.2.2 Pellets and Powders

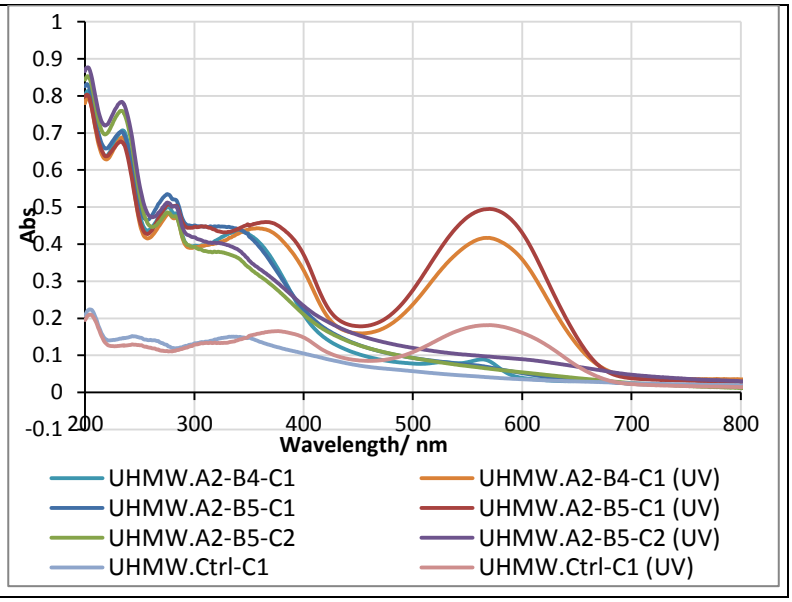
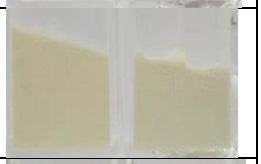
Since the XAD-4 PS beads have a large surface area, significant photochromic activity was observed in surface modified materials. Surface modified PET pellet, LDPE and UHMWPE powders were then investigated to see if a reduction in surface area modified with spiropyran would still yield good photochromic activity.

Table 4.2. Surface modified PET pellet, LDPE power and UHMWPE powder before and after UV-irradiation, with the correspoinding UV-Vis spectra.

Sample	Before UV	After UV	UV-Vis
PETp. A2-B4-C1			
PETp. A2-B5-C1			
PETp. A2-B5-C2			
PETp. Ctrl-C			
LDPE. A2-B4-C1			
LDPE. A2-B5-C1			
LDPE. A2-B5-C2			
LDPE. Ctrl-C1			





UHMW. A2-B4-C1		
UHMW. A2-B5-C1		
UHMW. A2-B5-C2		
UHMW. Ctrl-C1		

As seen from **Table 4.2** above, UV-Vis spectra for PET pellet samples and LDPE powder samples were rather irregular. This was due to the form of the polymer samples and the nature the diffused reflectance instrument, as discussed previously in Chapter 3. Irregularities in UV-Vis absorption spectra for PET pellet and LDPE powder samples between 200 – 400 nm were apparent, unlike UHMWPE powders which were neat and clear. Nonetheless, changes in absorption spectra due to photochromism for all three forms polymers were still apparent between 500 – 680nm, and similar to both the photochromic XAD-4 beads and solution analogue **2.49**.

While **PETp.A2-B4-C1** and **PETp.A2-B5-C1** showed a significant change in colour after UV-irradiation, **PETp.A2-B5-C2** showed only slight change. This was in accordance with the UV-Vis spectra recorded, where a large increase of approximately 0.6 in absorbance was measured for **PETp.A2-B4-C1** and **PETp.A2-B5-C1,** with λ_{max} at around 562 nm and 567 nm respectively, whereas **PETp.A2-B5-C2** only peaked slightly at 615 nm, with about a 0.05 increase in absorbance. Similar to surface-modified PET pellets, surface-modified LDPE and UHMWPE powders also showed that **LDPE.A2-B4-C1**, **LDPE.A2-B5-C1**, **UHMW.A2-B4-C1**

and **UHMW.A2-B5-C1** that had surfaces modified with spiropyran with a NO_2 side group gave stronger photochromic activity when compared to **LDPE.A2-B5-C2** and **UHMW.A2-B5-C2** that was surface-modified with spiropyran with Br side group. As seen from the UV-Vis spectra, photochromic activity of **LDPE.A2-B4-C1** and **LDPE.A2-B5-C1** was higher than **LDPE.A2-B5-C2** by 7 – 9 times in terms of increase in absorbance, similar to **UHMW.A2-B4-C1** and **UHMW.A2-B5-C1** compared to **UHMW.A2-B5-C2**.

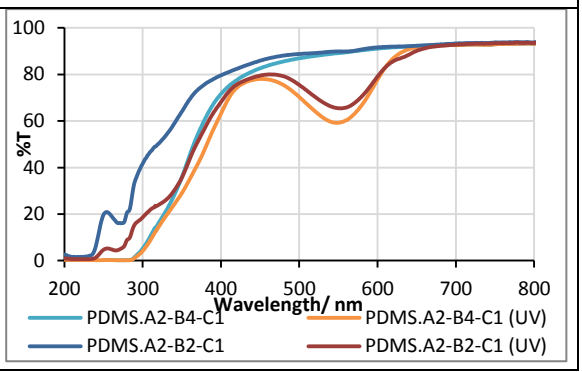
Controls were prepared by refluxing the blank polymers with spiropyran in basic MeCN, analogously to the surface modified polymers which were derivatized with spiropyrans. It was noted that **PET.Ctrl-C1** also showed very strong photochromic activity, similar to that of the surface modified samples. This could be due to the higher reactivity of polyesters to a range of reactions. Though LDPE also showed noticeable photochromic activity as seen from **Table 4.2**, the UV-Vis spectra indicated lower change in absorbance for **LDPE.Ctrl-C1** compared to surface modified LDPE sample **UHMW.A2-B4-C1** and **UHMW.A2-B5-C1**. However, different from PET pellet and LDPE powder samples, the control for UHMWPE powder displayed much lower photochromic activity compared to the UHMWPE surface modified samples **UHMW.A2-B4-C1** and **UHMW.A2-B5-C1** as the surface of UHMWPE are much more inert than PET and LDPE despite having the highest surface area among the three, according to BET measurements as seen in **Table 3.7** in Chapter 3. Photochromicity of the control was due to adsorption of the spiropyran on the surface, and this again showed that photochromic activities of the surface modified samples were not due to simple surface adsorption surface, and the first two steps of surface modification (surface pre-activation followed by azo coupling) prior to derivatizing with spiropyran were essential.

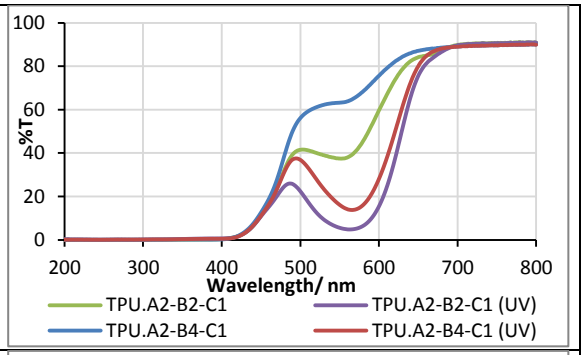
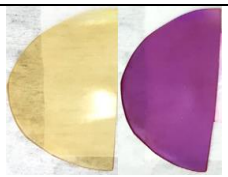
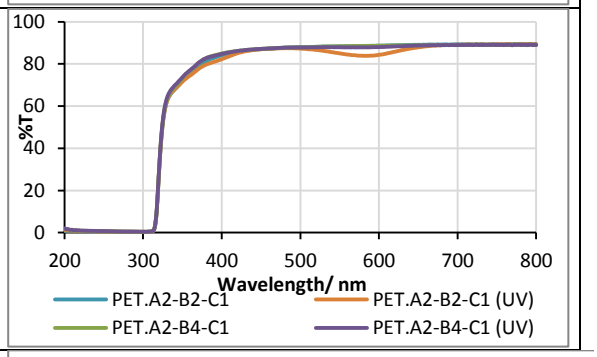
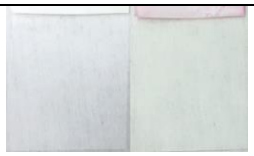
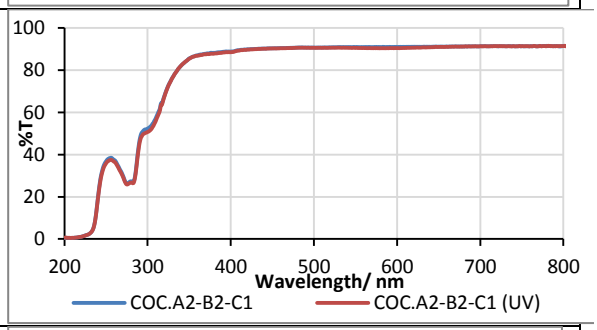
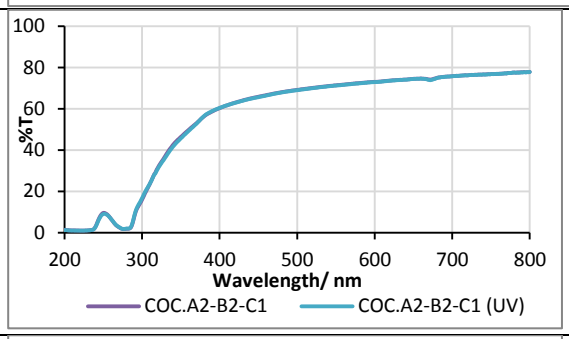
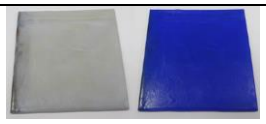
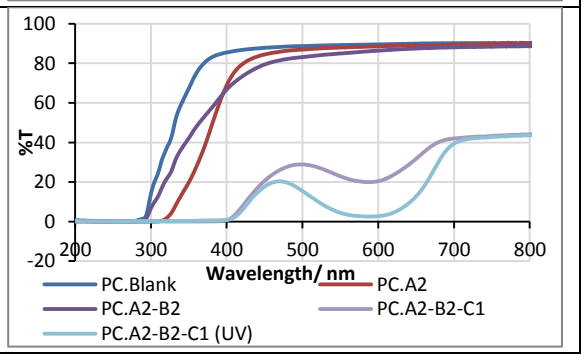
Similar to the photochromic XAD-4 PS beads, these photochromic polymers also took significantly longer to bleach back to their original form, compared to analogues in solution. In addition, this study also showed that despite having much lower surface area than PS XAD-4 beads, and much lower surface modification loading as discussed in Chapter 3, surface modified PET pellets, LDPE and UHMWPE powders still demonstrated good photochromic activities as supported by the UV-Vis absorption data collected.

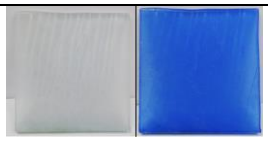
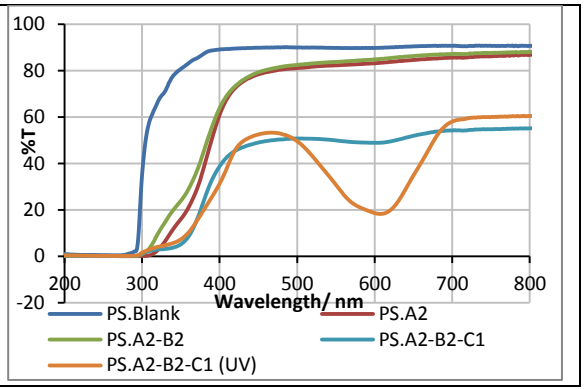
4.2.2.3 Flat polymer substrates

Moving from beads, pellets and powders to flat substrates, surface area was further reduced by one dimension. This section reports the investigation of the photochromic activity on the surface modified flat substrates, whose surface modification process and characterisation was previously discussed in Chapter 3. As seen from **Scheme 4.4**, the open-ring MC form can exist in zwitterionic form, which results in the surface being more hydrophilic. Thus, WCA was also investigated alongside with the photochromic activity.

Table 4.3. Surface modified photochromic flat substrates with their corresponding UV-Vis spectra before and after UV-irradiation.

Sample	Before UV	After UV	WCA/°	UV-Vis
PDMS.A2-B2-C			Before UV: 110.7±0.9 After UV: 106.0±4.6	
PDMS.A2-B4-C1			Before UV: 114.6±0.7 After UV: 112.9±2.0	

TPU. A2-B2-C1		Before UV: 95.7±2.1 After UV: 86.6±5.1	
TPU. A2-B4-C1		Before UV: 85.4±1.8 After UV: 81.6±3.6	
PET. A2-B2-C1		Before UV: 87.2±3.5 After UV: 80.9±2.9	
PET. A2-B4-C1		Before UV: 79.9±1.5 After UV: 78.1±2.2	
COC. A2-B2-C1		Before UV: 92.7±4.1 After UV: 85.2±7.8	
PP.A2-B2-C1		Before UV: 99.5±1.6 After UV: 94.9±2.5	
PC.A2-B2-C1		Before UV: 95.2±2.8 After UV: 89.2±4.1	

PS.A2-B2-C1		Before UV: 115.1±4.0 After UV: 108.1±8.0	

As seen from **Table 4.3** above, the photochromic PDMS and TPU flat substrates showed evident change in colour after UV-irradiation. From the UV-Vis spectra, although both **PDMS.A2-B2-C1** and **PDMS.A2-B4-C1** registered similar decrease in %T of about 30% at around 550 nm due to the photochromic change, WCA measured for **PDMS.A2-B4-C1** had very little change, whereas the WCA for UV-irradiated **PDMS.A2-B2-C1** decreased by 4.6°. The non-uniformity in the surface modification and photochromic transformation was reflected in the large ± error in WCA measured.

On the other hand, photochromicity of **TPU.A2-B2-C1** resulted in a decrease in %T of approximately 35% at around 569 nm, whereas **TPU.A2-B4-C1** registered a decrease of approximately 50% also around 569 nm. With **TPU.A2-B2-C1** being intensely coloured prior to UV-irradiation, but here the extent of photochromic activity measured could be limited by the instrument as it was nearing 0 %T. The photochromic change in the samples also brought about a decrease in WCA, with WCA of **TPU.A2-B2-C1** and **TPU.A2-B4-C1** decreased by 9.1° and 3.8°. This is due to the greater percentage of merocyanine form, which is zwitterionic and hence polar, being present on the surface of the polymer.

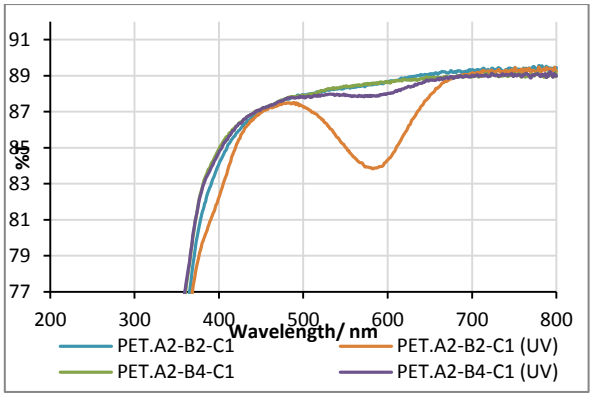


Figure 4.10. Expanded view of UV-Vis spectra for surface modified photochromic PET.

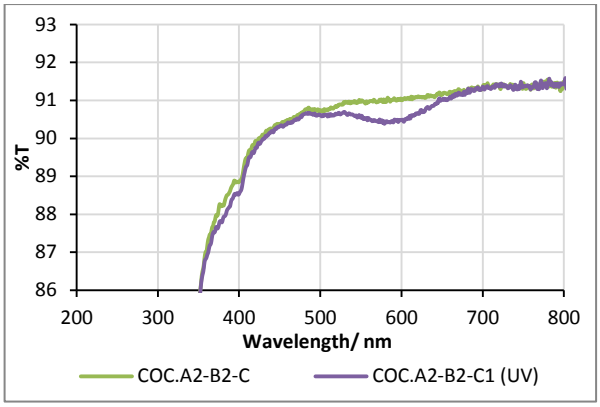


Figure 4.11. Expanded view of UV-Vis spectra for surface modified photochromic COC.

Although the PET and COC samples appeared to remain unchanged visually before and after UV-irradiation seen from **Table 4.3**, upon closer examination of the UV-Vis spectra, it was noted that photochromic changes were still detected via UV-Vis spectrophotometry. As seen in **Figure 4.10**, though the photochromic change in %T for **PET.A2-B4-C1** was only about 0.6, it could still detected by the UV-Vis spectrophotometer. **PET.A2-B2-C1** showed a more noticeable change of about 4.5 decrease %T. Both changes occurred at about 590 nm. Similarly, a small decrease of 0.5 in %T was detected after **COC.A2-B2-C1** UV irradiation (**Figure 4.11**). The change in %T is consistent with the decrease in WCA measured for the photochromic PET sample. With a small change in %T, **PET.A2-B4-C1** registered a small decrease in WCA of about 1.8°, whereas **PET.A2-B2-C1** with a more noticeable change in %T registered a larger decrease of 6.3° in WCA. Similarly, the surface of **COC.A2-B2-C1** also saw a decrease in WCA of about 7.5°. These 2 substrates demonstrated that even though photochromic change might not be sufficient for significant change in colour detectable by eye, the surface modification loading was sufficient to bring about an evident change in macroscopic properties like WCA and UV-Vis absorbance.

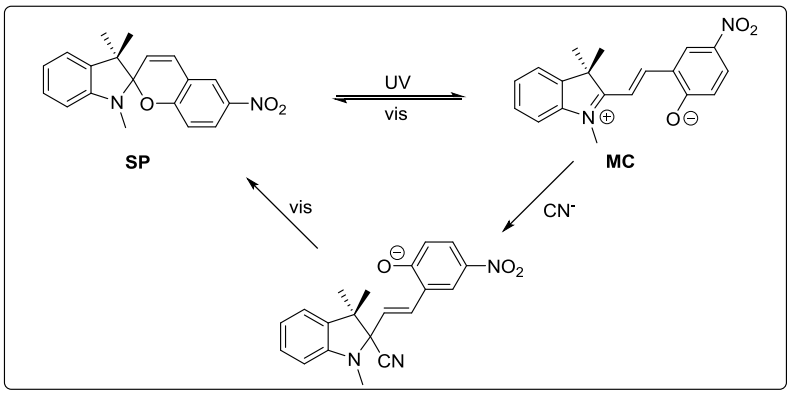
Unlike PET and COC, the UV-Vis spectra of PP appeared to be similar before and after UV-irradiation, and WCA was also fairly constant, thus, indicating that surface modification loading was not sufficient to bring about a detectable photochromic change. For PP, its chemical inertness is high, rendering it more difficult to modify. As seen from **Table 4.3**, surfaces of PC and PS were damaged when immersed overnight in DMSO for derivatization with spiropyran. This was also reflected in their UV-Vis spectra with a significant decrease in %T. Nonetheless, the solvent-melted surface was impregnated with spiropyran and still enabled photochromism, with a change in %T at around 600 nm.

Generally, different flat substrates expressed different extent of photochromic activity, with TPU being the best and PP being the worst, excluding damaged samples of PC and PS. This study showed that despite a significant decrease in surface area when reduce by one dimension from 3D to 2D, surface modification onto the flat substrates was still sufficient to demonstrate a change in macroscopic properties such as colour change and surface wettability, controlled by UV-irradiation.

4.3 Drug delivery

A photochromic change of the spiropyran moiety from spirocyclic closed-ring form to zwitterionic merocyanine open-ring form could result in colour and surface wettability change as investigated previously. There have been reports where the zwitterionic MC was used as receptors for optical detection of transition metal ions[135] or alkali metal ions,[136] or for quantification of amino acids.[137] In particular, work done by Shiraishi *et. al.* was noteworthy since it demonstrated the use of spiropyran (SP) functionality as a reversible cyanide anion receptor and illustrated

the covalent bonding of the cyanide ion to the merocyanine (MC) form (see **Scheme 4.5**).[92]



Scheme 4.5. Structure change of spiropyran in the presence of cyanide ion (CN^-) under UV or visible light. [92]

It was of interest to investigate if the surface modified polymers would be able to bind other anions, and whether having a photochromic spiropyran moiety incorporated onto the polymer surface would enable the surface of the polymer to therefore have controlled drug binding and release. For this purpose, Penicillin V (Pen V) was chosen as an easily detectable system.

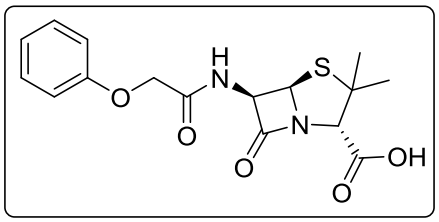


Figure 4.12. Chemical structure of Penicillin V.

4.3.1 Solution UV-Vis study

During the investigation of photochromic activity of the analogues in solution, it was noted that when doped with Pen V, there is change in colour of the solution.



Figure 4.13. Analogue 2.7 MeCN (left) and when doped with Pen V (right) before (top) and after (bottom) UV-irradiation.

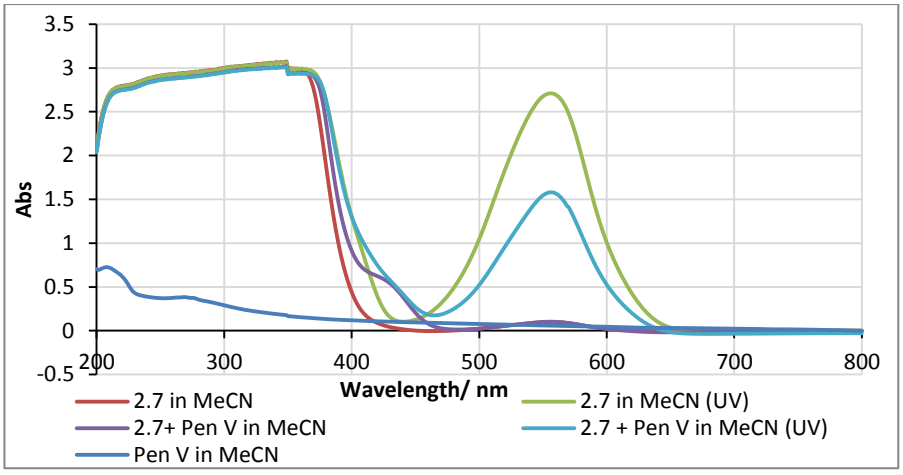


Figure 4.14. UV-Vis spectra of 2.7, Penicillin, 2.7 doped with Penicillin in MeCN before and after UV-irradiation.



Figure 4.15. Analogue 4.2 in DMSO (left) and when doped with Pen V (right) before (top) and after (bottom) UV-irradiation.

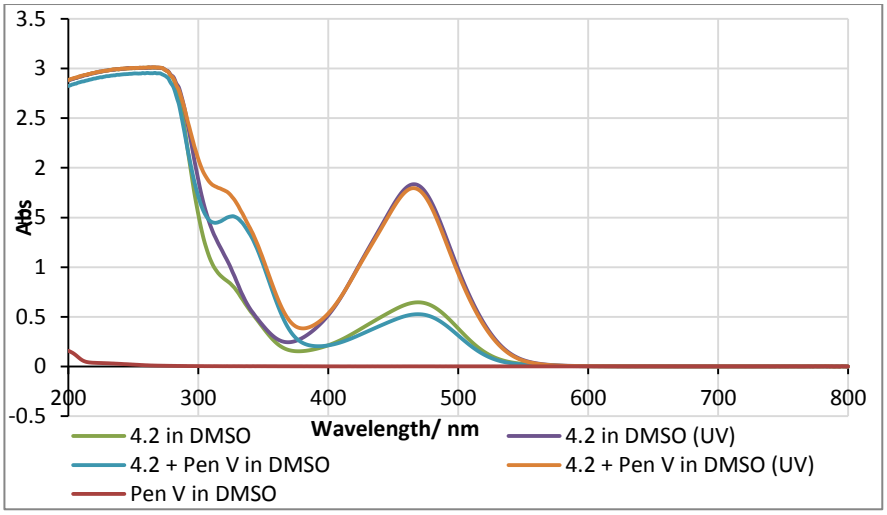


Figure 4.16. UV-Vis spectra of 4.2, Penicillin, 4.2 doped with Penicillin in DMSO before and after UV-irradiation.

When **Pen V** was added to a solution of spiropyran **2.7** or **4.2**, colour changes were observed as depicted in **Figure 4.13** and **Figure 4.15**. These changes in colour were also reflected in the change in UV-Vis absorption spectra at around 370 – 470 nm for spiropyran **2.7**, and around 300 – 400 nm for spiropyran **4.2**. The UV-Vis absorption spectrum of **Pen V** was also recorded in MeCN and DMSO to ensure that these changes were not due to any chromophore in **Pen V**. On the other hand, upon UV-irradiation, reversible photochromic activity was observed, as was indicated by the increase in absorbance at around 557 nm for both samples of spiropyran **2.7**, and at around 467 nm for both samples of spiropyran **4.2**, due to

ring opening of spiropyran, as seen in **Figure 4.14** and **Figure 4.16** respectively. This showed that presence of Pen V in the solutions of both photochromic compounds did not affect their ability to display photochromism.

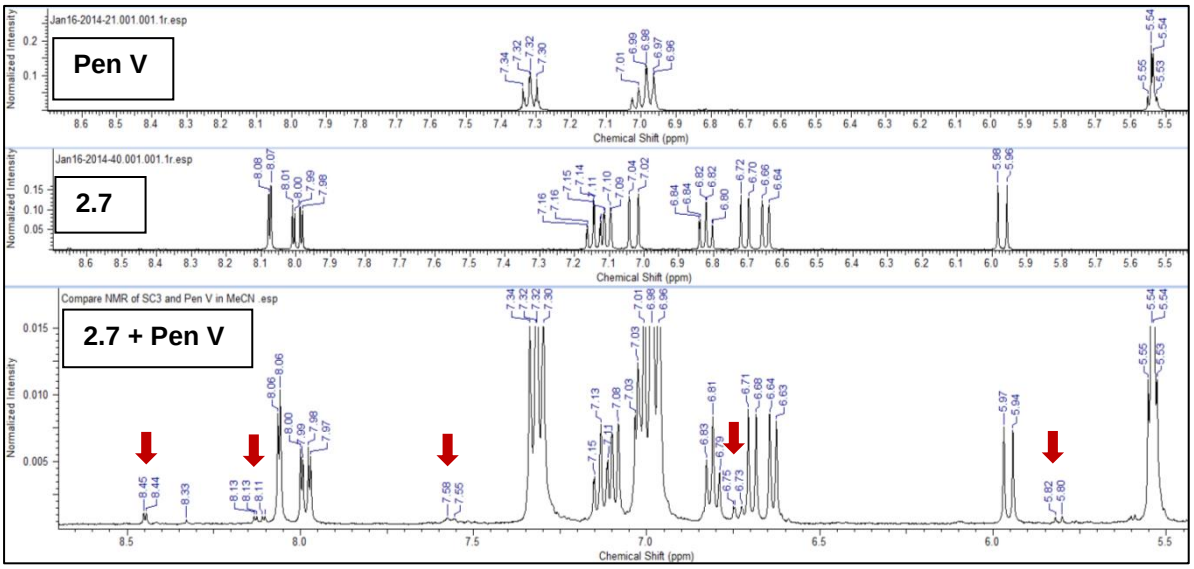


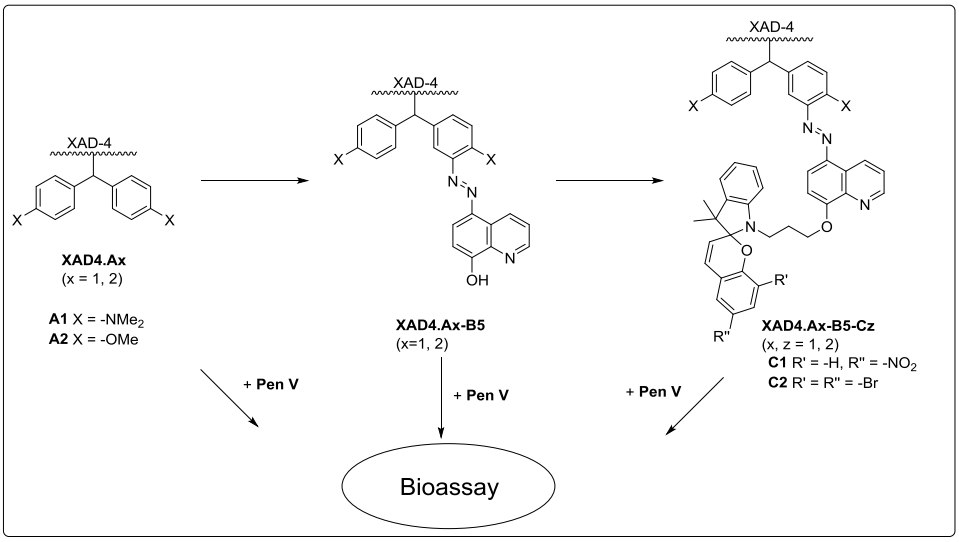
Figure 4.17. NMR spectra of Penicillin V (top), 2.7 (middle) and the mix of both (bottom) in CD_3CN.

In an attempt to investigate possible structural changes in **2.7** due to the addition of **Pen V**, NMR spectra were examined. As seen from **Figure 4.17**, there was no significant change in chemical shifts of **2.7** peaks when mixed with **Pen V,** despite the colour change observed in **Figure 4.13**, although small peaks observed (indicated by small arrows in **Figure 4.17**) could be peaks arising from an alternative structure of **2.7** present in the mixed solution. Therefore, with inconclusive information from NMR, it was uncertain how the presence of **Pen V** might affect structures of **2.7** and **4.2**. Nonetheless, UV-Vis results did suggest possible interactions of **Pen V** with the photochromic compound, thus, forming the basis for further probing of possible controlled drug delivery by a photochromic moiety on a polymer surface.

4.3.2 Hole-plate bioassay

Hole-plate bioassay is a common preliminary screening approach for the determination of antibacterial activities of various compounds synthesized for drug discovery. The traditional protocol involves filling 100 µl wells in bacteria-impregnated agar with solutions of the compounds to be tested, followed by incubation at 37°C for 16 – 18 h, and measuring the inhibition zone (or clear-zone) sizes. The zone sizes can be matched to calibrated known amounts of a control biocidal agent, *Cephalosporin C* (*Ceph. C*), to quantify the antibacterial activity. *S.aureus* (DS267) and *E.coli* (X580) were used as examples of Gram-positive and Gram negative bacteria testing respectively. In contrast to conventional methods where solutions were simply micro-pipetted into agar wells, solid samples were first weighed and then transferred into the wells. These sample-filled wells were then covered with blank agarose gel to aid in diffusion of the biocidal agent from the polymer surface to the bacteria-filled agar. Prior to testing, surface-modified polymers were first loaded with drug. This was done by immersing samples in Pen V solution for 18 h. Blank polymers were subjected to the same procedure and conditions as controls (see in Chapter 6).

4.3.3 XAD-4 beads for drug delivery



Scheme 4.6. Surface modified XAD-4 samples loaded with Pen V for bioassay.

For initial testing, each well on the agar plate was loaded with 10 mg of beads in duplicates. Inhibition zone sizes for all wells were measured and the average for each sample was compiled as shown in **Table 4.4** below.

Table 4.4. Preliminary testing of surface modified XAD-4 beads loaded with Penicillin V.

Sample	Average Inhibition zone size/ mm	
	E.coli	***S.aureus***
XAD4.A1	31.3	42.8
XAD4.A1-B5	28.5	41
XAD4.A1-B5-C1	32.4	42.7
XAD4.A1-B5-C2	31.3	40.5
XAD4.Ctrl-Pen V	32.8	42.8

Inhibition zones beyond 25 mm were considered to be out of accurate calibration range. As seen from **Table 4.4**, surface modified XAD-4 beads samples and their control loaded with Pen V yielded inhibition zones that were much greater than 25 mm, clearly indicating significant levels of antibacterial activity.

As means to improve this testing method, all the surface modified XAD-4 beads and the control (**XAD4.Ctrl-PenV**) that were loaded with Pen V were further ‘diluted’ with

blank XAD-4 beads, by mixing 30 mg of sample beads with 90 mg of blank beads. Then, 6 sets of 10mg of beads were weighed out into 6 vials in preparation for the hole-plate bioassay. Of the 6 sets, 3 sets of 10mg mixed beads were used for *S.aureus* plates as triplicate, and the remaining 3 sets of 10 mg mixed beads were for testing with *E.coli* plates as another set of triplicate. This meant that there were approximately 2.5 mg of surface modified XAD-4 beads or **XAD4.Ctrl-Pen V** in each well. In addition to performing hole-plate bioassay, Pen V loaded control (**XAD4.Ctrl-Pen V)** and other surface modified XAD-4 PS beads loaded with Pen V were sent for combustion analysis. With sulfur (S) present in Pen V, combustion analysis characterisation was employed to give an estimated value of amount of Pen V loaded onto the control and samples.

Table 4.5. Combustion Analysis and average inhibition zone sizes of surface modified XAD-4 beads and its control.

Samples	Combustion Analysis/ % Found	Surface Modifications/ {mol / g of polymer} [molecules. per cm^2] (%Surface Coverage)	Average Inhibition zone size/ mm	
			E.coli	*S.aureus*
XAD4.A1	C: 89.23 ± 0.30 H: 7.99 ± 0.30 N: 0.92 ± 0.20 S: 0.39 ± 0.09	S: {(1.2 ± 0.3) $x10^{-4}$} [(1.0 ± 0.22) $x10^{13}$] (4.9 ± 1.1)	26.2	37.7
XAD4.A1-B5	C: 89.23 ± 0.30 H: 8.23 ± 0.30 N: 0.88 ± 0.19 S: 0.36 ± 0.08	S: {(1.1 ± 0.2) $x10^{-4}$} [(9.3 ± 2.0) $x10^{12}$] (4.5 ± 1.0)	25.3	36.7
XAD4.A1-B5-C1	C: 88.9 ± 0.30 H: 8.14 ± 0.30 N: 0.83 ± 0.18 S: 0.32 ± 0.07	S: {(10 ± 2.2) $x10^{-5}$} [(8.3 ± 1.8) $x10^{12}$] (4.0 ± 0.9)	29.7	38.9
XAD4.A1-B5-C2	C: 88.54 ± 0.30 H: 7.59 ± 0.30 N: 0.74 ± 0.16 S: 0.38±0.08 Br: 0.52 ± 0.11	S: {(1.2 ± 0.3) $x10^{-4}$} [(9.9 ± 2.2) $x10^{12}$] (4.7 ± 1.0)	28.5	39.8
XAD4.A2	C: 88.12 ± 0.30 H: 7.76± 0.30 N: 0.54 ± 0.12 S: 0.56 ± 0.12	S: {(1.8 ± 0.4) $x10^{-4}$} [(1.5 ± 0.3) $x10^{13}$] (7.0 ± 1.5)	31.0	40.5
XAD4.A2-B5	C: 89.77 ± 0.30 H: 7.84 ± 0.30 N: 0.54 ± 0.12 S: 0.6 ± 0.13	S: {(1.9 ± 0.4) $x10^{-4}$} [(1.6 ± 0.4) $x10^{13}$] (7.5 ± 1.7)	30.0	40.8

XAD4.A2-B5-C1	C: 89.59 ± 0.30 H: 7.89 ± 0.30 N: 0.54 ± 0.12 S: 0.53 ± 0.12	S: {(1.7 ± 0.4) x10^{-4}} [(1.4 ± 0.3) x10^{13}] (6.6 ± 1.5)	28.5	39.2
XAD4.A2-B5-C2	C: 89.51 ± 0.30 H: 7.88 ± 0.30 N: 0.58 ± 0.13 S: 0.57 ± 0.13 Br: 0.14 ± 0.03	S: {(1.8 ± 0.4) x10^{-4}} [(1.5 ± 0.3) x10^{13}] (7.1 ± 1.6)	31.5	41.5
XAD4.Ctrl-PenV	C: 90.21 ± 0.30 H: 8.17 ± 0.30 N: 0.44 ± 0.10 S: 0.34 ± 0.07	S: {(1.1 ± 0.2) x10^{-4}} [(8.8 ± 1.9) x10^{12}] (4.3 ± 0.9)	29.0	39.3

Combustion analysis results as seen from **Table 4.5** indicated that XAD-4 beads with surface modification **A1** had similar S content as the control, thus, similar Pen V loading, whereas XAD-4 PS beads with surface modification **A2** had S content higher than **XAD4.Ctrl-PenV**. This meant a 4.0 – 4.5% surface coverage for XAD-4 beads with surface modification **A1** and **XAD4.Ctrl-PenV**, and about 6.6 – 7.5% for XAD-4 beads with surface modification **A2**. In general, this suggested that surface modification **A2** has slightly better Pen V loading efficiency compared to surface modification **A1**. However, this was not reflected in the results of the hole-plate bioassay.

As seen from **Table 4.5**, all surface modified XAD-4 beads and their controls (**XAD4.Ctrl-PenV**) loaded with Pen V again showed average inhibition zone sizes that were too large for accuracy, despite the effort to dilute it with blank XAD-4 beads. This preliminary testing with selected XAD-4 bead samples showed limitations of the form of polymer used; XAD-4 beads are highly porous, and this resulted absorption of Pen V into the pores, and were not suitable for hole-plate bioassay. Moreover, the beads were electrostatic, and it was difficult to handle them in small quantities and neatly pouring them into agar wells. Therefore, there was a need to devise another method to study the drug delivery profile.

4.3.3.1 HPLC-MS

In an attempt to study the drug release profile in solution, which could then be used to estimate total amount to drug release for each sample, a method using HPLC-MS detection was developed. First, surface-modified beads and control that were loaded with Pen V were placed into individual mass spec vials. Then, each vial was filled with 0.5 mL MeOH, followed by 1.5 mL of H_2O, and left to stand under different conditions (**Light**-in presence of fumehood light at room temperature, **Dark**- placed in fumehood covered up by aluminum foil at room temperature, or **Fridge**- placed in the fridge at sub-zero degree Celsius in the dark). After 1h, the whole 2.0 mL aliquot of solution was drawn from each sample vial, into a new mass spec vial, ready for HPLC-MS injection, with the XAD-4 beads left the sample vial). A fresh aliquot of 0.5 mL MeOH and 1.5 mL H_2O was then injected into the sample vial, and left to stand for another 1 h. The aliquots were drawn out at hourly interval for 5 h, and left to stand overnight for 19 h (total of 24 h). MeOH was necessary to allow the XAD-4 beads to fully submerge in the solution, which would otherwise float in solution if only water was used. By using known concentrations of Pen V solution injected into HPLC-MS, a calibration graph was generated using the peak area from the chromatogram. The samples were then injected into the HPLC-MS and peak areas measured were correlated to the calibration graph to give the concentration of Pen V in the sample. By plotting the graph of Pen V released at each hour, the rate of Pen V released was obtained. By plotting the cumulative graph of Pen V released, an approximation of the amount of Pen V released by the beads in total was calculated (see Appendix I for detailed calculations and data).

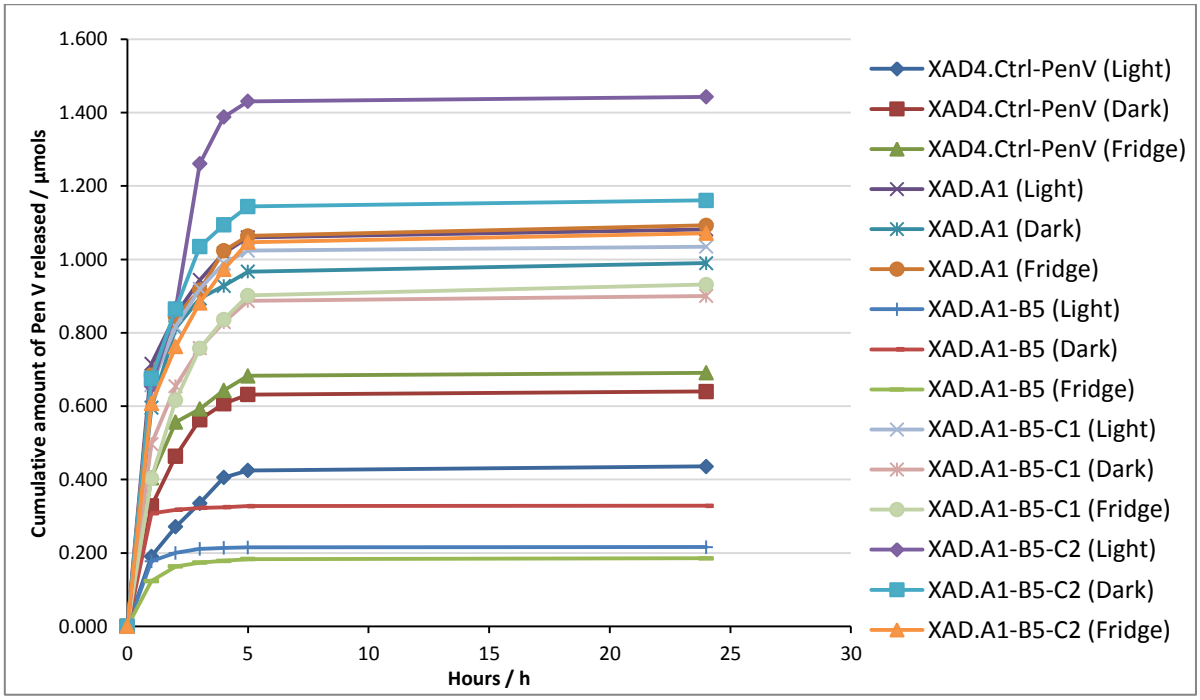


Figure 4.18. Cumulative graph of amount of Pen V released by all XAD-4 beads with surface modification A1 and its controls in various conditions.

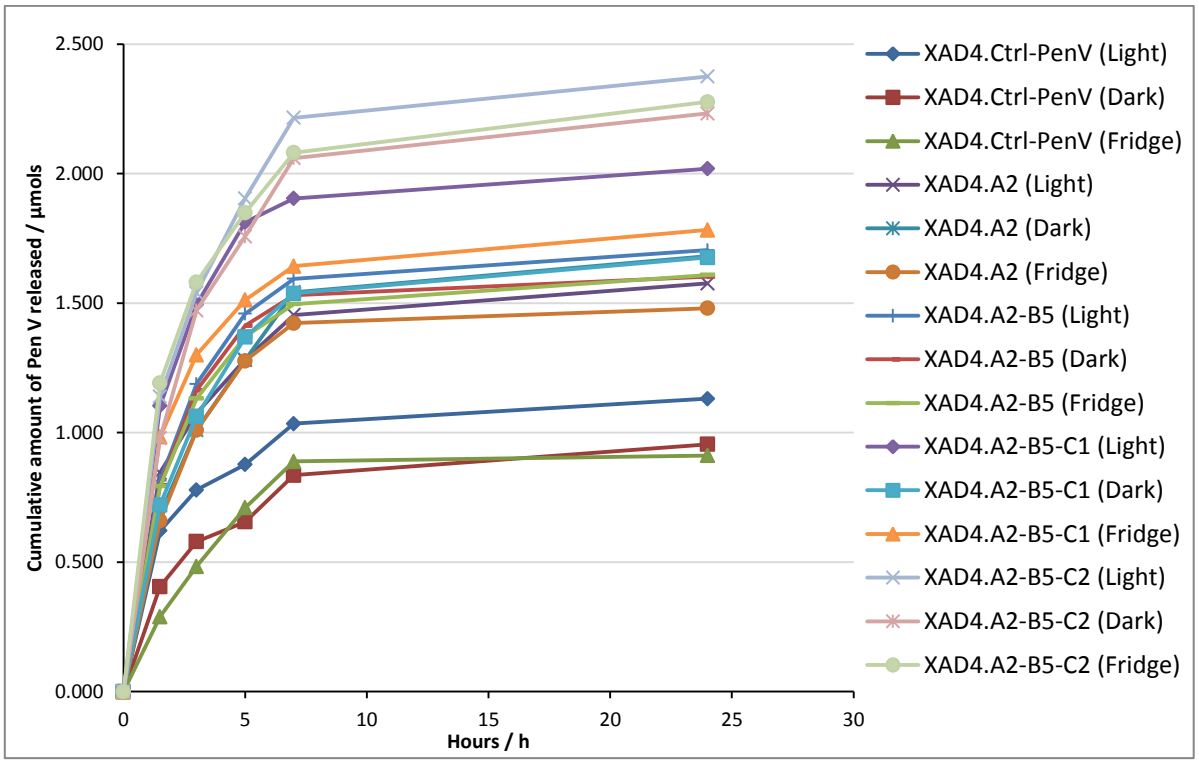


Figure 4.19. Cumulative graph of amount of Pen V released by all XAD-4 beads with surface modification A2 and its controls in various conditions.

The cumulative graph (**Figure 4.18**) showed that **XAD4.A1-B5-C2** beads released the most Pen V, followed by **XAD4.A1** and **XAD4.A1-B5-C1**, then the Controls (**XAD4.Ctrl-PenV**), while **XAD4.A1-B5** beads released the least amount of Pen V in

total. Photochromic samples **XAD4.A1-B5-C1** and **XAD4.A1-B5-C2** seemed to release slightly more Pen V in presence of light than in the dark. Compared to control which released about 0.43 – 0.69 µmol of Pen V in total, **XAD4.A1-B5-C2** released 1.07 – 1.44 µmol of Pen V in all, which was up to 2 times better than control.

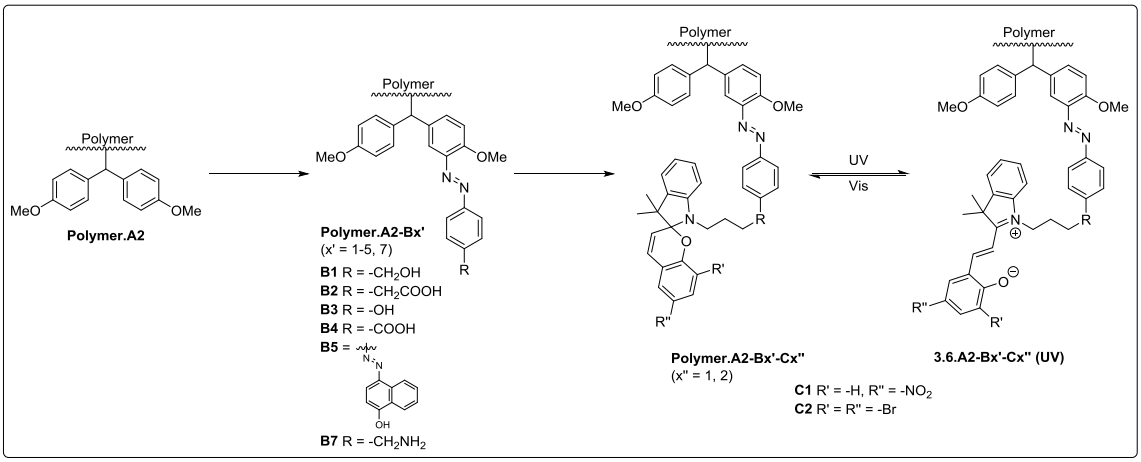
On the other hand, cumulative graph (**Figure 4.19**) showed that **XAD4.A2-B5-C2** beads released the most Pen V, followed by **XAD4.A2-B5-C1,** then **XAD4.A2** and **XAD4.A2-B5**, and lastly**,** the controls (**XAD4.Ctrl-PenV**) released the least amount of Pen V in total. Photochromic samples **XAD4.A2-B5-C1** and **XAD4.A2-B5-C2** also seemed to release slightly more Pen V in presence of light than in the dark. Compared to control which released about 0.91 – 1.13 µmol of Pen V in total, **XAD4.A2-B5-C2** released 2.23 – 2.38 µmol of Pen V in all, which was up to 2 times better than control.

Comparing **Figure 4.18** and **Figure 4.19**, the drug-release profile of XAD-4 beads with surface modification **A1** differed only slightly from XAD-4 beads with surface modification **A2**. Compared to combustion analysis results compiled in **Table 4.5**, results obtained from this study were generally consistent in showing that the surface modified XAD-4 beads were able to bind and release more drugs than the control.

However, this method was very tedious and challenging, when conducting the experiment and when performing the calculations and analysis. As mentioned previously, the XAD-4 beads were rather electrostatic, and measuring them into small mass spec vials was very difficult, and could result in erroneous measurements. In addition, the aliquots measured out had to be analysed as soon as possible since Pen V is unstable to hydrolysis of the β-lactam core. This

challenge was further heightened with the need to handle multiple samples at the same time. Even with staggered timing, and the extraction of aliquots from each sample was not be exactly 1 hour each; some samples from the fridge might have warmed up to room temperature prior to extraction of the aliquots, and some samples might have beads immersed some time longer than the others, thus, resulting in possible errors. Moreover, much time was spent adjusting the pump pressure and flow rate every time when using the instrument. Therefore, subsequent testing of samples for drug delivery reverted to using simple hole-plate bioassay for a quicker and more straight-forward method for preliminary testing of biocidal activity due to drug release.

4.3.4 Pellets and Powders



Scheme 4.7. Pellets and powders surface modified for drug delivery testing.

Using non-porous polymers with lower surface area, it was hoped that that drug blinding and releasing due to surface modification could be more apparent compared to porous XAD-4 beads. Following the protocols mentioned previously, surface modified LDPE and UHMWPE powder samples, and PET pellet samples, alongside with their respective controls, were loaded with Pen V and testing using hole-plate bioassay.

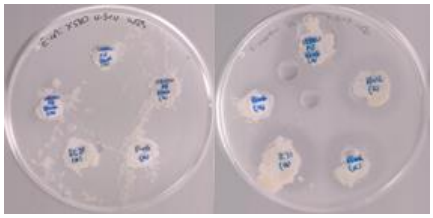


Figure 4.20. Hole-plate bioassay of UHMWPE powder samples using E.coli (left) and S.aureus (right).

The powder samples were difficult to handle, and in particular, the UHMWPE powder samples. As seen from **Figure 4.20**, the UHMWPE powder samples would spill easily on the agar plates. Similar to XAD-4 PS beads, LDPE powder were slightly electrostatic. In addition, both LDPE and UHMWPE samples were very hydrophobic, and did not interact well with blank agarose gel. After loading the samples neatly into the well, attempts to cover the wells with blank agarose would cause the displacement of the powder samples from the well due to incompatible surface tensions, resulting in messy loading on the agar plate. On the other hand, PET pellets were much easier to handle, and could be covered well by the blank agarose gel for diffusion of drug on the surface to the agar impregnated with bacteria.

Hole-plate bioassay for surface modified polymers and its control was conducted with duplicates for a quick qualitative test to determine if surface modification was aiding drug binding and releasing. To test if photochromic moiety was aiding in drug delivery, samples with spiropyran moiety were also set aside and were UV-irradiated prior to immersion in Pen V solution, as indicated by (UV) in labelling.

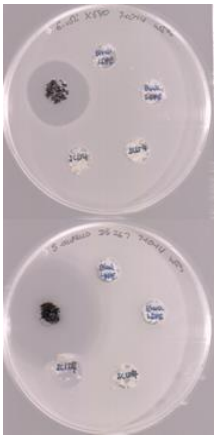


Figure 4.21. Hole-plate bioassay of surface modified LDPE powders and its control in *E.coli* (top) and *S.aureus* (bottom).

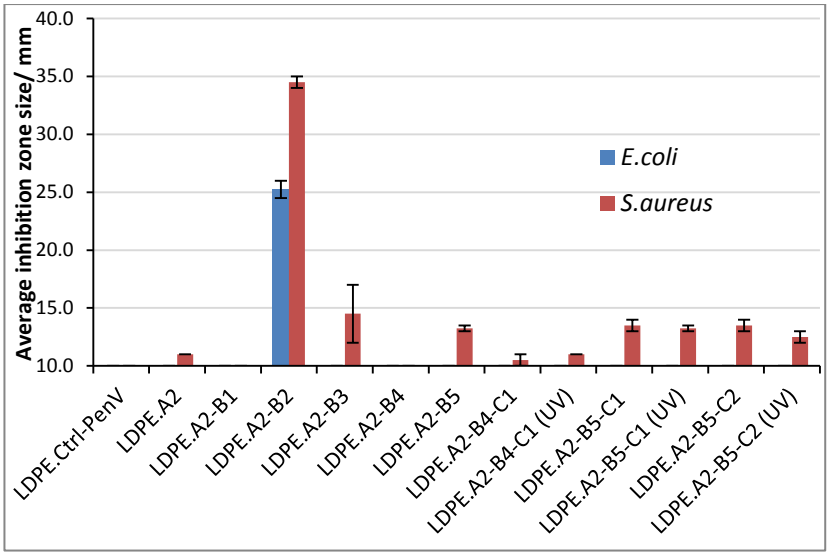


Figure 4.22. Average inhibition zone size of various surface modified LDPE powder and its control

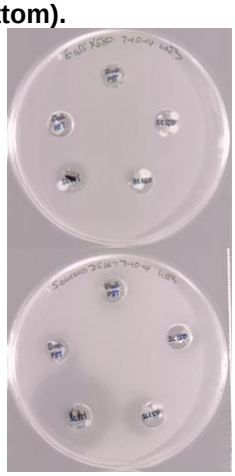


Figure 4.23. Hole-plate bioassay of surface modified PET pellets and its control in *E.coli* (top) and *S.aureus* (bottom).

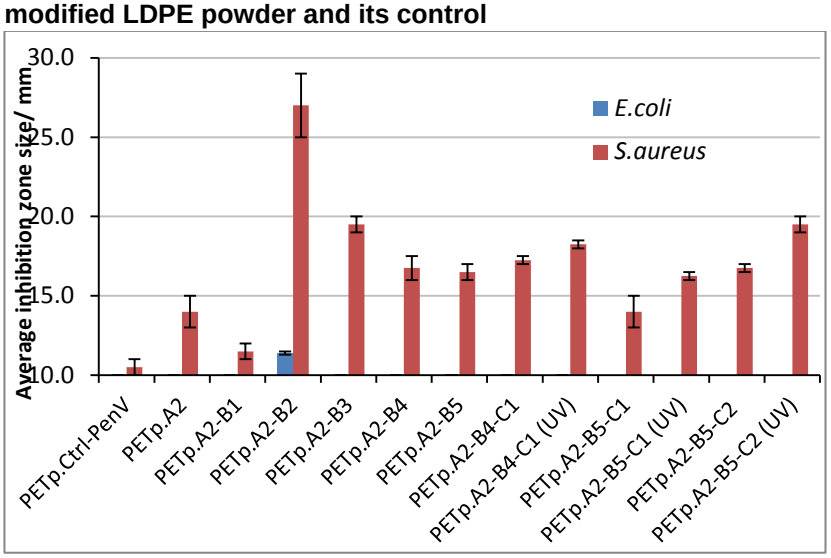


Figure 4.24. Average inhibition zone size of various surface modified PET pellets and its control

Inhibition zones formed by the UHMWPE samples were too irregular for measurement, therefore, were omitted from the results.

<u>*LPDE samples:*</u> Pen V is more susceptible to killing *S.aureus* than *E.coli*. As seen from **Figure 4.22**, all of the surface modified LDPE powder samples displayed some anti-bacterial activity against *S.aureus*, except for LDPE **LDPE.A2-B1** and **LDPE.A2-B4**. **LDPE A2**, **LDPE.A2-B4-C1** only had very slight anti-bacterial activity against *S.aureus*. The inhibition zone measured for **LDPE.A2-B5** was the same after derivatization with spiropyran moiety in **LDPE.A2-B5-C1** and **LDPE.A2-B5-C2**,

and there was no difference observed in anti-bacterial activity with or without UV-irradiation when loading with Pen V. Surprisingly, **LDPE.A2-B2** gave exceptionally high anti-bacterial activity as indicated by the large inhibition zone size. Moreover, while all other LDPE samples did not show any biocidal effect in *E.coli*, **LDPE.A2-B2** gave a large average inhibition zone size of 25.3 mm. **LDPE.A2-B2** without Pen V loading did not show any biocidal effect, thus, indicating that the high biocidal activity was indeed due to good binding and release of Pen V by the polymer surface modification, and not due to possible leaching of the modification. On the other hand, the LDPE control did not register any biocidal activity.

PET Pellets: On the other hand, surface modified PET pellets loaded with Pen V displayed good anti-bacterial activity against *S.aureus*. With the exception of **PETp.A2-B1**, surface-modified PET pellets gave decent average inhibition zone size ranging from 14 mm for **PETp.A2** and **PETp.A2-B5-C1**, to 19.5 mm for **PETp.A2-B3** and **PET Mod B5-C2 (UV)**. Similar to results from LDPE samples, PET pellet with modification **B2** (**PETp.A2-B2**) loaded with Pen V gave excellent biocidal activity with a large average inhibition zone size of 27 mm for *S.aureus* agar plates, with slight biocidal activity against *E.Coli*. To ensure that anti-bacterial activity was indeed due to Pen V loaded onto **PETp.A2- B2**, and not due to modification **B2** itself, **PETp.A2-B2** not loaded with Pen V was tested as well. As expected, no inhibition zone was observed, thus, proving that it was good drug binding onto **PETp.A2-B2** that resulted in large inhibition zone. The control for PET pellets loaded with Pen V (**PETp.Ctrl-PenV**) only showed very slight anti-bacterial activity against *S.aureus*, thus showing that surface modifications on the PET polymer were essential in binding and releasing sufficient Pen V for a macroscopic effect.

Photochromic effect for drug delivery: While results from **Figure 4.22** showed that there was no clear difference between photochromic LDPE samples with or without UV-irradiation prior to Pen V loading, there was slight difference observed for photochromic PET pellets samples. As seen from **Figure 4.24**, **PET.A2-B5-C1(UV)** had a slightly larger inhibition zone size than **PET.A2.B3.C1** of about 2.3 mm, while **PET.A2-B5-C2(UV)** had average inhibition zone size about 2.7 mm larger than **PET.A2-B5-C2**. In addition, results from the drug-release profiling using HPLC-MS method as shown in **Figure 4.18** and **Figure 4.19** also did indicate that the photochromic XAD-4 samples release more Pen V in presence of visible light, compared to when kept in the dark. While these preliminary results suggested possible photochromic effect on controlled drug binding and release, a better sample preparation and testing method would be necessary for a more reliable investigation.

Nonetheless, this work gave preliminary evidence that antibacterially active materials, prepared using surface modifications followed by loading of Pen V, could be prepared. In all, the results gathered from solution drug-release measurement of XAD-4 beads samples, and hole-plate bioassay of LDPE powder and PET pellets, showed that surface modification successfully provided improved Pen V binding and release, compared to unmodified surfaces of the various polymers. In addition, even with a large reduction in surface modification loading due to a significant decrease in surface area of the polymers, macroscopic function of anti-bacterial activity was still effective and evident.

Calibration using Penicillin V: Calibration of Pen V against *S.aureus* and *E.coli* was performed as well as seen in **Figure 4.25** and **Figure 4.26** respectively. Using the calibration graph, and knowing that each agar well was about 100 µL, average

inhibition zone size of the tested samples can be correlated, and amount of Pen V bound and released for anti-bacterial activity could be estimated.

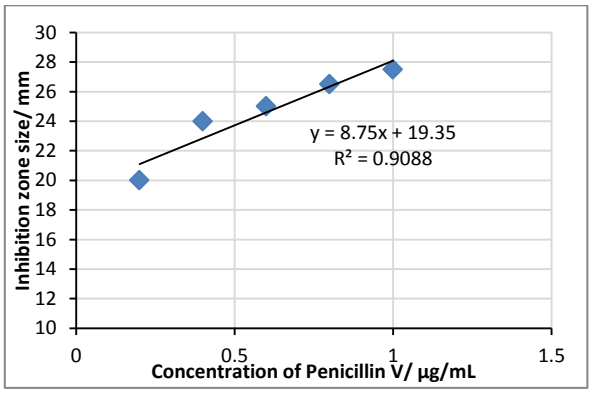


Figure 4.25. Calibration curve of Penicillin V for *S.aureus*.

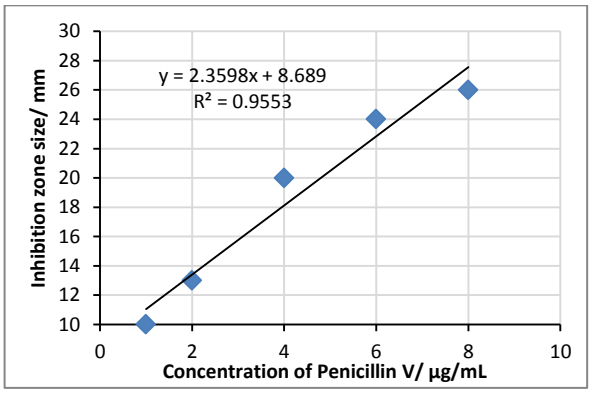


Figure 4.26. Calibration curve of Penicillin V for *E.coli*.

However, as this is a semi-quantitative test, more emphasis was placed on qualitative results than quantitative analysis, thus, corresponding amounts of Pen V eluted by the samples were not further discussed.

4.3.5 Flat substrates

Similar to 3D substrates, hole-plate bioassay was used for the testing of flat substrates loaded with Pen V, for its simplicity and ready availability as a preliminary screening. However, sample preparation was more difficult than the beads, pellets and powders. Before immersion of samples in Pen V solution for loading of Pen V onto the surface, the flat samples had to be cut into 0.5 cm by 0.5 cm pieces to be able to fit into 1 cm diameter agar well on the plate. As such, samples that were too thick or rigid and which could not be cut in this way, like the flat PS substrates, were not tested.

After some experimentation, the protocol for sample preparation for flat samples was refined. Firstly, samples to be tested with *S.aureus* were immersed in 0.5 mg/mL Pen V solution, whereas samples to be tested with *E.Coli* were immersed in 1 mg/mL Pen V solution, both for 18h. The difference in the immersion solution was

due to *S.aureus* being more susceptible to bactericidal effect of Pen V than *E.coli*. Hence, less Pen V was required to be loaded onto the samples. Secondly, different from the previous sample preparation method, instead of drying the samples in batches, all the samples were dried with nitrogen gas individually, piece by piece. The hole-plate bioassay was then repeated in triplicates for each sample.

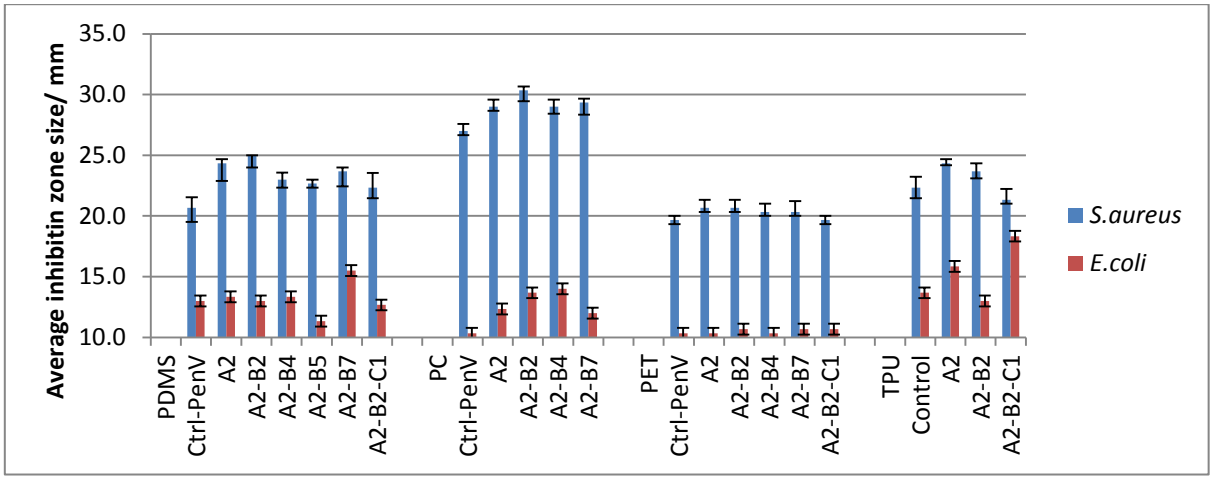


Figure 4.27. Average inhibition zone sizes of various surface modified flat substrates and their controls, using improved sample preparation method.

PDMS samples: All PDMS samples loaded with Pen V showed relatively good biocidal activity against *S.aureus*, with **PDMS.A2-B2** having the largest average inhibition zone size of 25 mm, and **PDMS.Ctrl-PenV** having the lowest of 20.7 mm. The samples also showed biocidal effect against *E.coli* with an average inhibition zone size varying from 11.3 mm to 15 mm. With PDMS being very hydrophobic, surface modification of the polymer not only allowed for better Pen V binding, but also allowed better contact with hydrophilic solution that contained the drugs. However, results from **Figure 4.27** seemed to suggest that the surface modification was not sufficient to bring about a very significant difference between surface modified and unmodified blank PDMS as the difference in average inhibition zone size were not substantial. This could also be due to the limitation of the sample preparation and testing method, which will be discussed at the next section.

PC samples: As seen from **Figure 4.27**, all PC samples loaded with Pen V showed excellent anti-bacterial against *S.aureus*, with **PC.A2-B2** showing the largest average inhibition zone size of 30.3 mm and the **PC.Ctrl-PenV** showing the lowest of 27 mm. On the other hand, the control showed little or no biocidal effect against *E.coli*, whereas all the other samples of PC with surface modification showed decent activity of 12 to 14 mm in average inhibition zone size. This set of results showed that surface modification on PC substrates was sufficient to bring about macroscopic anti-bacterial effect, and that there was a clear difference of this effect between modified and unmodified surface of the polymer.

PET samples: All PET samples loaded with Pen V showed decent anti-bacterial effect against *S.aureus* with only very slight variation in average inhibition zone size of 19.7 mm to 20.7 mm as shown in **Figure 4.27**. The samples showed little or no effect against *E.coli*. However, this set of results from PET film samples demonstrated that surface modifications on the PET films were not sufficient to bring about a macroscopic anti-bacterial effect, as the activity of the samples were similar to that of the control, indicating that any activity was likely to be due to surface adsorption of Pen V on the surface rather than due to preferential binding of the drug due to surface modification.

Similar to the discussion in previous section on photochromism, despite having similar surface area, different polymer surfaces clearly have different reactivity towards the surface modification chemistry, thus, resulting in different surface modification loading. This difference in loading was then reflected in the macroscopic properties of the polymers such as photochromic activity, or in this case, ability to bind and release Pen V. Therefore, even though the samples were subjected to same surface modification process and same hole-plate bioassay

sample preparation and testing, the results of flat PC samples and PET film gave different trends and implications.

TPU samples: The hole-plate bioassay results of TPU samples loaded with Pen V as shown in **Figure 4.27** were somewhat peculiar. While **TPU.A2-B2-C2** showed lowest average inhibition zone size of 21.3 mm against *S.aureus* that was similar to **TPU.Ctrl-PenV**, it also had largest average inhibition zone size of 18.3 mm against *E.coli* compared to all the other TPU samples and control, causing both results to be contradictory. This result, in fact, highlighted the limitation of this hole-plate bioassay method used for testing Pen V loading of flat substrates, which is further discussed in the next section below.

4.3.6 Limitations of the bioassays

Unlike conventional methods where solutions were simply micropipetted into agar wells, hole-plate bioassay of solid samples could be challenging and tedious with various limitations. Prior to loading them into the wells, solid samples needed to be measured into vials for loading into individual wells. In addition, beads and powder samples that were electrostatic could result in messy loading onto the agar, and thus, inaccuracy in the test. Moreover, should the samples be too hydrophobic, blank agarose gel used to cover the solid samples to aid in diffusion of the drugs on the polymer surface to the bacteria agar could displace the sample from the well, causing messy loading onto the agar plate. Uneven agarose gel coverage would also lead to uneven diffusion of the drug, resulting in uneven inhibition zone. In addition, as mentioned above in the sample preparation, it could be difficult and tedious to cut flat samples into very small pieces, and drying them individually for hole-plate bioassay.

Technical difficulties aside, sampling of the surface modified polymers for bioassay provided room for error as well, especially for the flat samples. With low and non-uniform surface modification coverage, cutting out three pieces of 0.5 cm x 0.5 cm sample for bioassay from a 5 cm x 5 cm flat sample meant that only 3% of the whole polymer piece was sampled. This is illustrated, for example, in the results of **TPU.A2-B2-C1** in **Figure 4.27**. Samples used for *E.coli* testing could have very high surface modification coverage which resulted in good Pen V binding and gave large average inhibition zone size, while those used for *S.aureus* testing might have relatively lower surface coverage, or worse, unmodified, thus resulting in average inhibition zone size similar to **TPU.Ctrl-PenV**. A bioassay method that is able to test the surface of the whole flat substrate for biocidal activity would need to be developed for better anti-bacterial testing.

Despite these challenges and limitations with anti-bacterial testing facilities and capabilities, many of the surface modified polymers examined using the hole-plate bioassay did show that surface modification was effective in binding and release of Pen V, compared to unmodified surfaces. Even though the surface modification loading was low, it was still sufficient for enhanced macroscopic function of drug delivery.

4.4 Conclusion

The work in this chapter has demonstrated the capability of the surface modifications on various polymeric substrates to control macroscopic functionalities, namely photochromic activity and drug delivery. Alongside with analogues synthesized in solution as described in Chapter 2, polymers surface derivatized with spiropyran were examined for photochromic activity. While some of the results

obtained from this study suggested possible photochromic control for drug binding and release, more detailed and careful study is required for further probe this area. Nonetheless, most of the surface modified samples showed better drug delivery than unmodified polymer surface. However, limitations of this method were also discussed. Despite these surface modified polymers having low surface modification loading as investigated in Chapter 3, they were sufficient for the demonstration of macroscopic functions.

5 Adhesion Enhancement

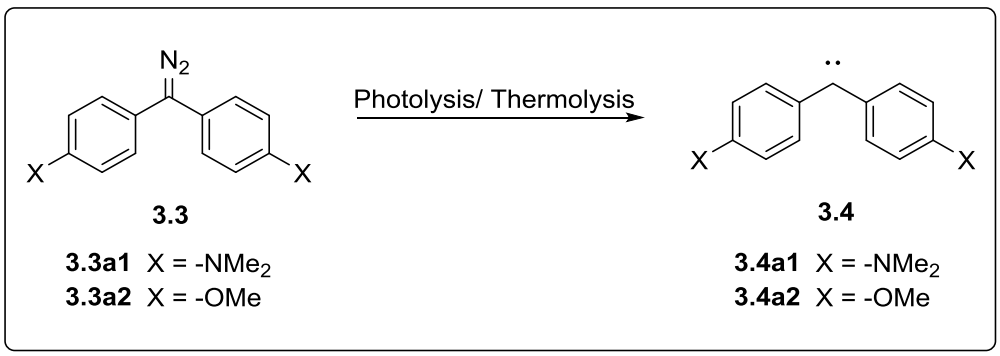
5.1 Introduction

While the previous chapter explored photochromic activity and drug delivery as macroscopic functions tailored by surface modifications of polymers, this chapter further explores another surface macroscopic function - adhesion.

Adhesion can be defined as the state where two surfaces are held together by interfacial forces, which may comprise of valence forces of the same type that give rise to cohesion (specific), or interlocking actions (mechanical), or both.[138] The term “adhesive” refers to the substance that causes two surfaces to adhere to each other. An adherend is the body bonded or to be bonded to another body using the adhesive.[139]

While developing the process for surface modification of flat substrates, a surprising finding led to further investigation of the use diazo **3.3** (see **Scheme 5.1** below) as a possible adhesive, and its adhesion properties. The preliminary findings and feasibility for its application as a primer for sol-gel coating are reported in this section.

5.2 Substrate-to-substrate adhesion



Scheme 5.1. Generation of carbene 3.3.5 from diazo 3.3 via photolysis or thermolysis.

It was observed that after high intensity UV irradiation, **3.3a2** changed from a purple precipitate to a yellow sticky substance. Out of interest, two of the same flat PC substrates with this yellow sticky substance were joined together. Surprisingly, it was found that some effort was required pull the substrates apart after the yellow layer had dried. For PET sheet, much less effort was required to peel the two substrates apart, but unlike the PC substrates, the sticky-ness on the PET sheet could be re-used multiple times. Therefore, preliminary investigations were conducted to better understand this behaviour and to quantify the adhesion properties.

5.2.1 Testing method

The Instron Micro meter was used to measure the extension and load for the adhesive test, which differed for rigid and flexible substrates, as described below.

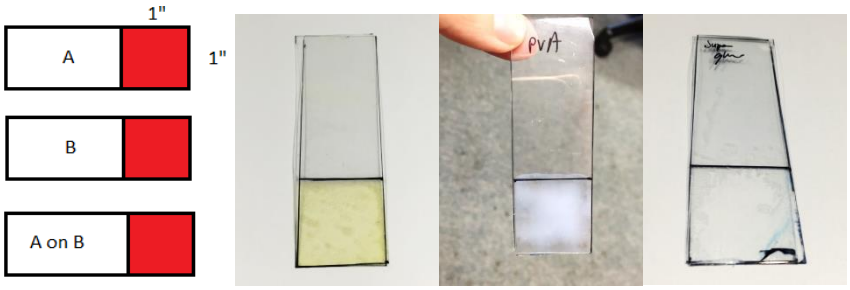


Figure 5.1. Sample preparation for T-peel test. (From right: adhesive used- diazo 3.3a2, PVA and superglue)

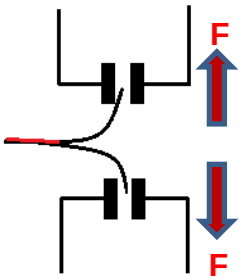


Figure 5.2. T-peel test on Instron micro meter.

The T-peel test is a form of cleavage test that is often used to examine the adhesion of flexible substrates, such as films and sheets, to an adhesive.[139] However, as the angle of peel is determined by the inherent properties of the adherends and the adhesives, the test is less reproducible than other types of peel tests, such as the 180 peel test. Nonetheless, T-peel test is still the most popular amongst all peel tests, and is commonly used when both adherends are flexible. In this study, PET sheets were used as the adherends.

PET film was cut into 3" x 1" strips and masked, but a 1" x 1" section was left uncovered. Diazo **3.3a2** dissolved in Et_2O was then spray coated onto the uncovered area of the sample. The pieces were subject to high intensity UV-irradiation to give the yellow adhesive, and the two PET samples were then pressed together manually.

Figure 5.1 showed the sample bound together by the yellow adhesive generated from diazo **3.3a2**, along with controls with PVA glue and superglue.

The sample was then mounted onto the Instron Micro meter as shown in **Figure 5.2**, and the test was done by exerting force to peel the 2 samples apart; the load required to break the bonded joint was measured.

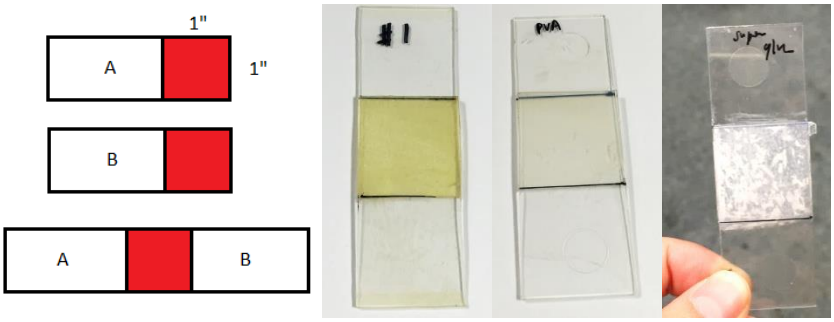


Figure 5.3. Sample preparation for lap shear test. (From right: adhesive used- diazo 3.3a2, PVA and superglue)

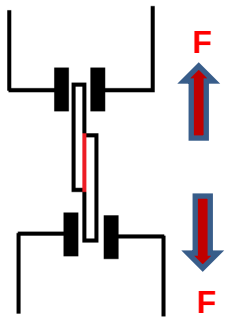


Figure 5.4. Lap shear test on Instron micro meter.

Adhesives display their highest strength in shear mode,[139] and lap shear test is usually performed to measure this strength as it can be easily replicated. PC substrates were first cut into 2" x 1" pieces, half of it was masked and the 1" x 1" unmasked area was spray coated with diazo **3.3a1** or **3.3a2** dissolved in Et_2O. After high intensity UV-irradiation to give the yellow adhesive, the two PC pieces were overlapped and pressed together as shown in **Figure 5.3**, along with control samples bound by PVA adhesive and superglue.

The lap shear test was performed by first mounting the samples onto the Instron Micro meter as shown in **Figure 5.4**, and the test was then run by pulling the two ends of the samples, causing the adhesive to be stressed in shear, thus, breaking the adhesion. The results of both the T-peel test and lap shear test of the samples prepared are discussed in the next section below.

5.2.2 T-peel test for PET-PET film

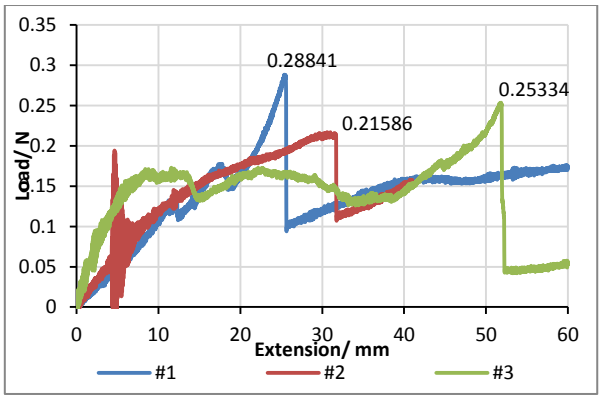


Figure 5.5. T-peel test results of PET-PET sample.

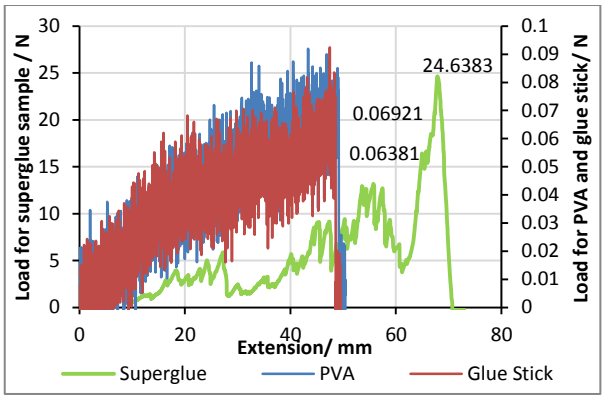


Figure 5.6. T-peel test result of superglue, PVA adhesive and glue stick.

It was noted that peel test results tended to fluctuate as the area subjected to load at any point in time is small.[139] Results of the T-peel test for PET-PET samples showed in **Figure 5.5** gave an average of 0.253 N. This result was benchmarked against 3 other commercial adhesives. The first was SureMark® 'superglue', which is a type of adhesive derived from cyanoacrylates, which dries fast with excellent shear strength.[140] The second was normal white art glue, otherwise known as white polyvinyl acetate (PVA), which is a type of thermoplastic adhesive. And lastly, glue stick, which is generally made up of approximately 40% acrylic and 40% water, commonly used in offices and schools for its low cost and ease of use. As seen from **Figure 5.6**, the T-peel of superglue gave peak peel strength of about 25 N, while performance of PVA adhesive and glue stick was similar with peel value of approximately 0.06 N. With the bench-marking, it appeared that though the peel

strength of the adhesive was not as strong as superglue, it was much stronger than commercial PVA and glue stick.

5.2.3 Lapshear test for PC-PC pieces

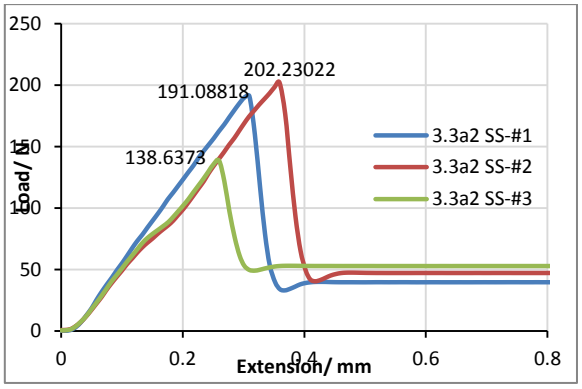


Figure 5.7. Lap shear results of diazo 3.3a2 single side coated PC-PC sample.

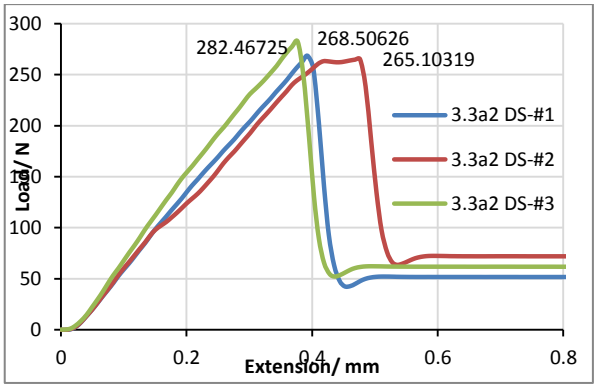


Figure 5.8. Lap shear results of PC-PC samples coated with fresh diazo 3.32a2 on both sides.

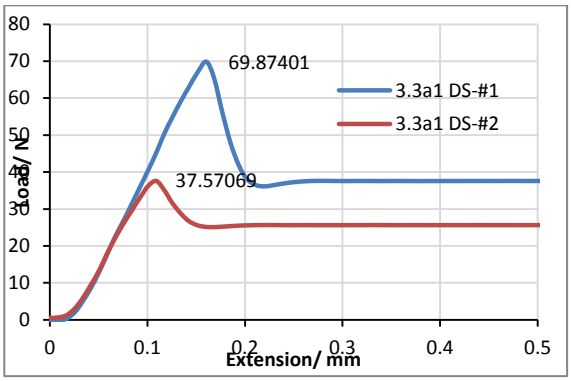


Figure 5.9. Lap shear results of PC-PC samples with diazo 3.3a1 coated on both sides.

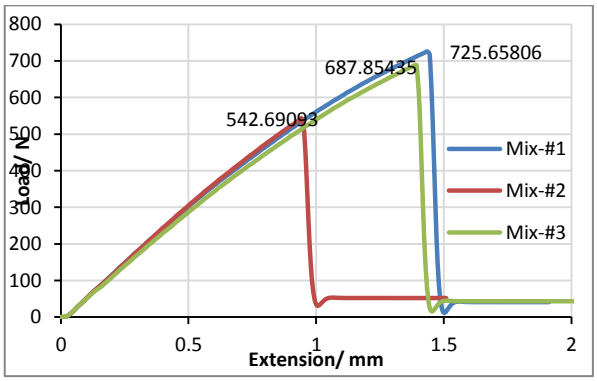
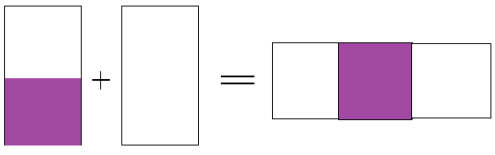
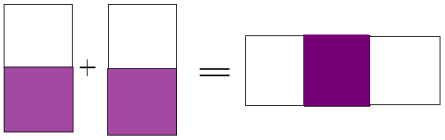
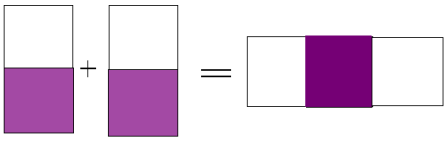
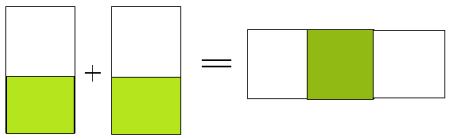
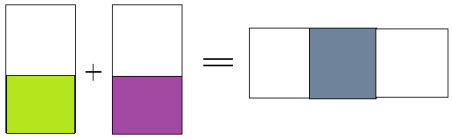
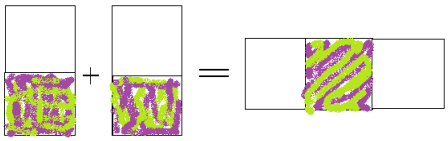


Figure 5.10. Lap shear results of PC-PC samples with mixed diazo coated on both sides.

Table 5.1. Lapshear results of all PC-PC substrates.

Entry	Diazo used	#1	#2	#3	[d]Average load /N
1	**3.3a2** single sided (SS) 	138.64	191.09	202.23	177
2	**3.3a2** double sided (DS) 	282.47	268.51	265.10	272

3	[a]**3.3a2** double sided (DS) 	210.48	238.03	243.09	231
4	[b,c]**3.3a1** double side (DS) 	69.87	37.57	-nil-	54
5	[b]**3.3a1** single sided + **3.3a2** single sided 	241.57	276.84	284.74	268
6	[b,e]**3.3a1** and **3.3a2** Mix 	725.66	542.69	687.85	652

[a] Diazo was used 72 hours after preparation and dissolved in Et_2O.
[b] Diazo was heated instead of UV-irradiated.
[c] Samples were damaged during transportation back to Singapore.
[d] Average load was rounded off to nearest whole number

The average load required to shear the samples were rounded off to the nearest whole number (**Table 5.1)**; comparing results of the lap shear test as shown in **Figure 5.7** and **Figure 5.8**, PC-PC samples coated on both sides (**Entry 2** and **3**) displayed better strength than only one side was coated (**Entry 1**). **Entry 1** and **2** in **Table 5.1** showed that having an additional side coated resulted in a higher load of approximately 95 N. Having both sides covered with the adhesive would increase the amount of adhesive within the boundary layer, where the adhesion and bonding strength are effective. This showed that having more of the UV-irradiated diazo did increase the adhesion strength. Comparing **Entry 2** and **3**, there was a slight decrease of about 41 N when the diazo compound that has been left in solvent for 72 h was used instead of freshly prepared material. This suggested that some diazo

might have decomposed after 72 h, thus, resulted in less carbene formed and hence, weaker adhesive.

On the other hand, it was surprising to note that adhesive formed from diazo **3.3a1** was much weaker than that of **3.3a2** (**Entry 4** of **Table 5.1**). However, when pressed together with another PC substrate covered with adhesive generated from diazo **3.3a2**, the shear load increased by 214 N as seen in **Entry 5**. The best result was obtained when the substrates were sprayed intermittently with both diazo **3.3a1** and **3.3a2** on both pieces, UV irradiated, and pressed together; up to 725 N of shear load was recorded for PC-PC samples coated with a mixed of **3.3a1** and **3.3a2**, as seen in **Figure 5.10**. A possible explanation for the results obtained might be related to how the adhesive was formed, which is discussed later in Section 5.4. These results were also bench-marked against superglue, PVA and glue stick.

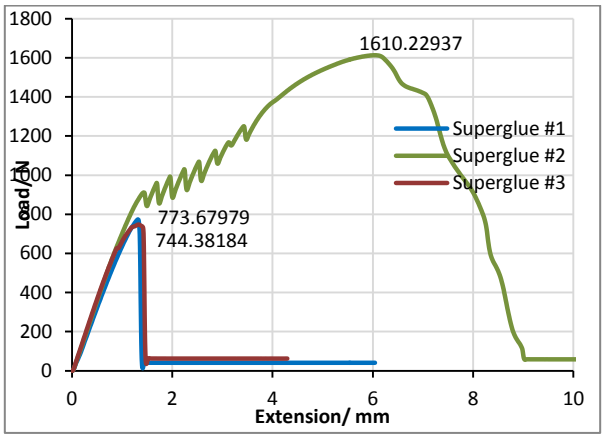


Figure 5.11. Lap shear results for PC-PC samples using cyanoacrylate adhesive (superglue).

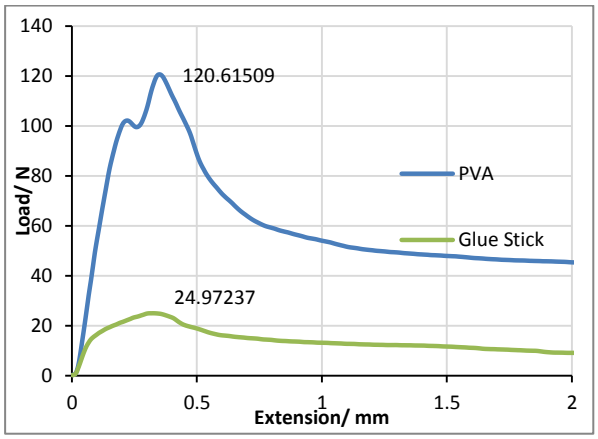


Figure 5.12. Lap Shear test for PC-PC samples using PVA adhesive and glue stick.

As seen from **Figure 5.11**, superglue could reach a shear load ranging from 744 to 1610 N. However, the high shear load recorded of 1610 N might not due to the cyanoacrylates alone, but also due to solvent bonding as the solvent used in the superglue melts the surface of the PC substrate when applying onto its surface. This can be seen from **Figure 5.3**, where the surface of the PC turned white in

colour, indicating that some part of the surface was damaged or melted by the adhesive. On the other hand, as seen from **Figure 5.12**, PVA showed a peak shear strength of approximately 121 N while glue stick resulted in a very low shear strength of about 25 N. Comparing this to the adhesive generated from the diazo, the best result obtained as seen in **Figure 5.10** was somewhat comparable to average superglue shear load of about 750 N.

It was noted that the joint bonded with the adhesive generated from the diazo compound or with the superglue was rather rigid, and upon extension by the Instron Micro meter, the bond became brittle and broke with a ‘snap’. This was indicated by the sharp drop in shear load upon breakage, as seen from the results above. However, for PVA or glue stick, the joints were relatively soft and were much more flexible. As such, their breakage was neither a sudden ‘snap’ nor indicated by a sudden drop in shear load, but rather, the shear load would peak and decrease relatively smoothly.

There are other factors that can affect the performance of the adhesive and bond strength. For example, as the samples were all prepared by pressing the pieces together manually, there might be air or solvent entrapped in the adhesive layer. In addition, the strength exerted for pressing the pieces together might differ for each sample, thus, resulting in different extent of active contact of the adhesive with surface of the adherend. Spraying of the diazo compound was done manually with a simple spray bottle, thus, amount of diazo spray coated onto the surface and thus, the adhesive generated for the samples would vary. As this was a preliminary study, further work needs to be performed to improve adhesion strength.

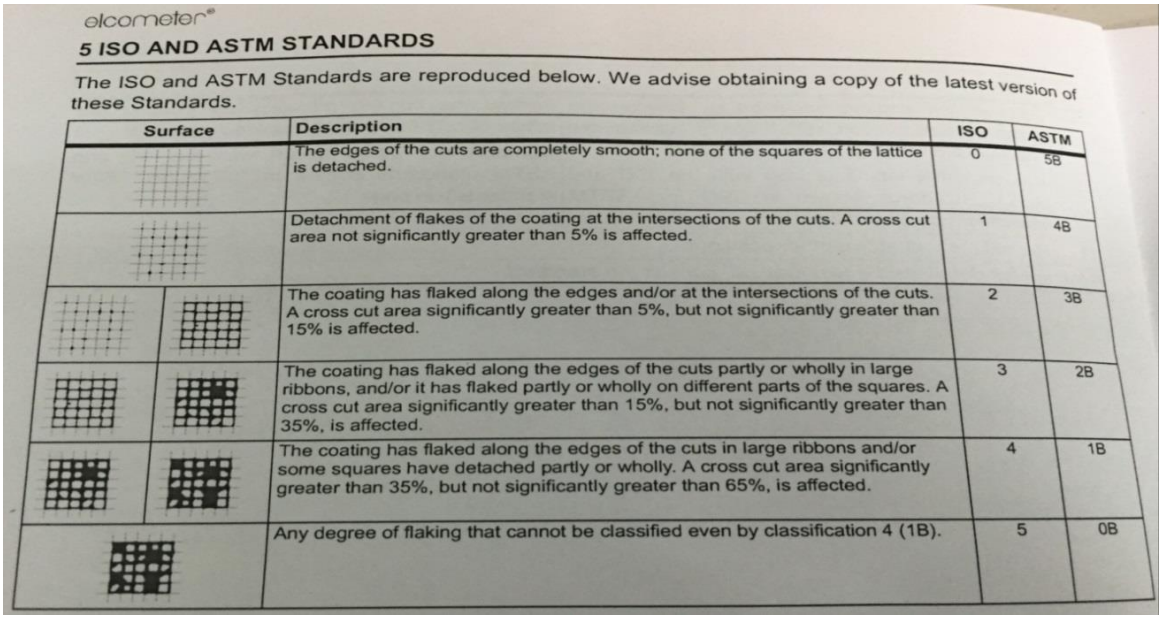
In all, despite the limitations in sample preparation, the preliminary results of this study demonstrated that the yellow adhesive formed post-carbene formation from

diazo **3.3a2** had good adhesion for PC and PET flat substrates. When mixing two different types of diazo **3.3a1** and **3.3a2**, a synergistic effect was observed with greatly enhanced shear strength measured.

5.3 Application with sol-gel as primer

One of the main research areas in the Surface Technology Group of SIMTech focuses on sol-gel formulation for various functional coatings. However, adhesion of the sol-gel coating on a polymer surface has always been an issue of concern as most of the polymer surfaces are relatively inert. Therefore, it was of interest to test if this adhesive found would be useful as a primer for enhanced adhesion of the sol-gel coating. Sample preparation was performed by spraying 5 cm x 5 cm PC substrate or PET film with diazo **3.3a2** that was dissolved in Et_2O, followed by high intensity UV-irradiation. The samples were then immediately spray coated with GLYMO based sol-gel, and heated in the furnace at 100°C for 1 h.

The adhesion of the sol-gel coatings was examined using the cross hatch test, which follows ATSM Standard D3359 - Standard Test Methods for Measuring Adhesion by Tape Test, test method B, using the Elcometer 1542 Cross Hatch Adhesion Tester as shown in **Figure 5.13** below.



elcometer®

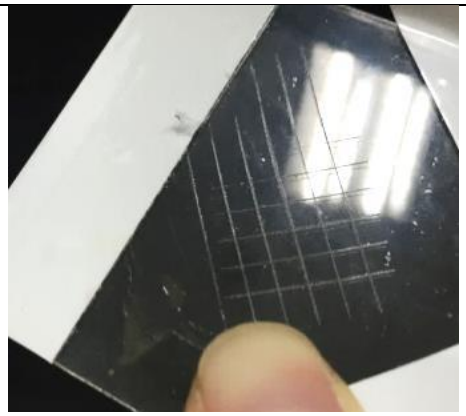
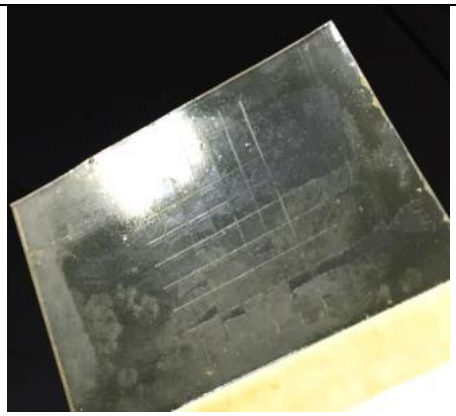
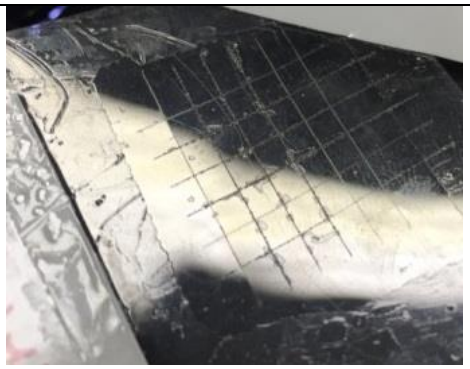
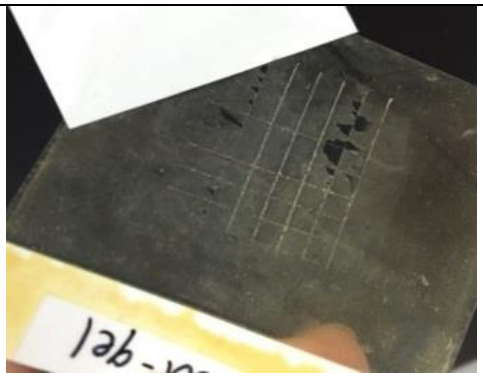
5 ISO AND ASTM STANDARDS

The ISO and ASTM Standards are reproduced below. We advise obtaining a copy of the latest version of these Standards.

Surface	Description	ISO	ASTM
	The edges of the cuts are completely smooth; none of the squares of the lattice is detached.	0	5B
	Detachment of flakes of the coating at the intersections of the cuts. A cross cut area not significantly greater than 5% is affected.	1	4B
	The coating has flaked along the edges and/or at the intersections of the cuts. A cross cut area significantly greater than 5%, but not significantly greater than 15% is affected.	2	3B
	The coating has flaked along the edges of the cuts partly or wholly in large ribbons, and/or it has flaked partly or wholly on different parts of the squares. A cross cut area significantly greater than 15%, but not significantly greater than 35%, is affected.	3	2B
	The coating has flaked along the edges of the cuts in large ribbons and/or some squares have detached partly or wholly. A cross cut area significantly greater than 35%, but not significantly greater than 65%, is affected.	4	1B
	Any degree of flaking that cannot be classified even by classification 4 (1B).	5	0B

Figure 5.13. ASTM standard of the cross hatch test.

Table 5.2. Cross hatch test results for sol gel coating with and without surface modification.

	Without surface modification	With surface modification
PC piece		
PET film		

As seen from **Table 5.2**, without any surface modification prior to sol-gel coating and curing, there is no adhesion of the GLYMO-based coating to the PC piece or PET film; the area covered by the tape had the sol-gel coating totally peeled off.

However, with surface modification, only some flaking was observed along the edges of the cut parts. According to ASTM standard, the adhesion of the coating was between 3B and 2B. Despite the enhanced adhesion for the sol-gel coating, the yellow colouration due to the adhesive formed might pose as in issue should high transparency coating be preferred. Therefore, more development needs to be performed in the direction of improving the adhesion of the sol-gel coating for a better ASTM grading, and developing the process of coating the surface more thinly for improved transparency.

5.4 Proposed cause of adhesion

It was postulated that this adhesion property arose due to polymerisation of carbenes. When irradiated with high intensity UV to generate the carbene from the corresponding diazo, it was likely that the carbenes generated undergo C1 polymerisation.[141] Previously, such adhesion phenomena had never been observed, firstly due to the diazo precursor being very thinly coated on the XAD-4 polystyrene beads when solvent was removed *in vacuo*, and secondly, the modified beads were very small and round, and were washed immediately with water and acetone after modification. However, when the diazo compound was sprayed with some thickness on the flat substrates, layers of carbene generated have the potential to react with each other and polymerise into short chains, thus leading to possible entanglement between the chains. Such entanglement could have resulted in the adhesion phenomenon observed. Certain extent of cross-linking across the network of polymer chains in the adhesive layer could also have aided in the adhesion.

It was noted from

Table 5.1 that adhesive generated from diazo **3.3a1** (with NMe_2 side groups) gave very weak adhesion compared to adhesive using diazo **3.3a2** (with OMe side group). This could be due to carbene generated from diazo **3.3a1** being more reactive and thus more short-lived than those generated from diazo **3.3a2** ones, resulting in shorter polymer chains formed. Moreover, as diazo **3.3a1** is less stable than diazo **3.3a2** as mentioned in Chapter 3, some diazo compound might have decomposed upon exposure to air and light prior to polymerisation. Having lesser diazo undergoing carbene formation for polymerisation, and having shorter chains formed might have led to adhesive being generated from diazo **3.3a1** having much lesser shear strength than adhesive generated from diazo **3.3a2**.

It was also noted that the adhesive generated from mixing the two different types of diazo compound gave much better shear strength than using only one type of diazo compound. When the two different diazo compounds were sprayed intermittently and UV irradiated, copolymer might have been formed instead. Such copolymer was expected to have varied chain length and steric demands, and gave rise to better entanglement, and thus better adhesion property compared to homopolymers formed when using only one type of diazo. The varied carbene philicity might enhance polymerisation.

While it was proposed in this thesis that the adhesion function was observed due to formation of the adhesive via polymerisation of carbenes, more work needs to be performed to verify these results, and for further probing of this mechanism to fully understand this adhesion phenomenon.

5.5 Conclusion

Surface modification that led to macroscopic adhesion between polymer substrates, and enhanced adhesion of sol-gel to polymer substrates, has been explored and discussed. T-peel tests and lap shear tests were conducted to examine the polymer substrate-to-substrate adhesion, with results bench-marked to cyanoacrylate adhesives. In addition, cross-hatch tests were applied to give an indication of adhesion of the sol-gel coating with the aid of the surface modification, with reference to ASTM standard. With potential application as thin layer surface modification, or primers for coatings with limited adhesion to surface-inert substrates, this area of work is worthy of further research and development. The mechanism by which this adhesive adheres to surfaces also remains to be elucidated.

6 Conclusions and Future Work

In all, this thesis set out to explore means to confer functionalities on surface of polymers by wet chemical methods in order to demonstrate macroscopic functions of photochromic activity and drug delivery. This was first done by investigating both the direct and indirect modification of the XAD-4 polystyrene beads surfaces using various functionalised diaryldiazo compounds. The indirect modification strategy was chosen as the preferred method, due to greater ease of synthesis and modification, as well as better surface loading. A shorter route with a more straight-forward diaryldiazo synthesis was then proposed, and the underlying chemistry for azo coupling with diazonium salt and subsequent derivatization with spiropyran was studied by synthesizing the analogous compounds in solution for greater confidence of the chemistry. This is discussed in Chapter 2.

Chapter 3 began with the optimisation of the various diaryldiazo systems syntheses. From commercially available benzophenone derivatives, various diaryldiazo systems were tested for the generation of diarylcarbenes for pre-activation of the polymer surface (Mod **Ax**). A diaryldiazo system with OMe side group was chosen for better stability and ease of handling and replication. The surface pre-activated XAD-4 beads were then azo coupled with diazonium salt with various side groups (Mod B**x'**). This was followed by derivatization with photochromic spiropyran (Mod **Cx''**). The surface modified XAD-4 beads gave excellent photochromic activity and demonstrated better Penicillin V binding and release in solution using the HPLC-MS detection method as discussed in Chapter 4.

The substrate scope was expanded to include PET pellets, LDPE and UHMWPE powders to test the versatility of the surface modification method. Even with a

significant reduction in surface area, and PET type polymers having a more inert surface compared to XAD-4 beads, the beads and pellets still gave great photochromic activities, and showed better biocidal effects with Penicillin V compared to their controls.

Having demonstrated that the surface modification on various beads, pellets and powder polymers can bring about macroscopic functionality, this technology was then transferred to SIMTech, where re-designing of the surface modification processes took place to be made suitable for large surface engineering. A variety of 2D polymeric substrates were used. Despite a further reduction in surface area, photochromic activity was still detectable, and hole-plate bioassay with Penicillin V gave satisfactory results with the surface modified polymers giving larger inhibition zone sizes than their control.

Possible future work would include investigating means to improve on the surface loading using this surface modification method developed, and to explore other macroscopic functions to match various on-demand applications, including the adhesion function that was briefly discussed in this chapter.

7 Experimental

7.1 General

All reactions that required anhydrous conditions were carried out under nitrogen by standard procedures. All reagents and solvents were purchased from commercial suppliers and were used without further treatment, except for dry THF, which was obtained by passing through a dry alumina column.

Analytical thin layer chromatography (TLC) was performed whenever possible with Merck aluminium foil backed TLC sheets, pre-coated with silica gel 60 F254 and layer thickness of 0.2 mm, and visualized under UV fluorescence (λ_{max} = 254 nm). Silica gel flash columns were performed on Merck Geduran 60 (0.040-0.063 mm) mesh silica gel.

^{1}H, ^{13}C, COSY, HSQC and DEPT-135 spectra were recorded on either a Bruker DPX200 (200 MHz) or AVF400 (400 MHz) spectrometer. Chemical shifts (δ) are reported in parts per million (ppm) relative various solvent residual peaks, and coupling constants in hertz (Hz). Low resolution mass spectra were obtained on a Fison Platform spectrometer with electrospray ionisation (ESI). High resolution mass spectra were obtained on a Bruker microTOF spectrometer, all reported in Daltons. For compounds in solid, liquid or oil form, IR spectra were obtained using a Bruker Tensor 27 FT-IR spectrometer. Absorption maxima (ν_{max}) are reported in wavenumbers (cm^{-1}) with selected peaks reported. Melting points were measured using a Stuart Scientific SMP1 melting point instrument.

Surface analyses of various modified substrates were performed through ATR-IR, performed on a Bio-Rad FTS-6000 with a diamond stage accessory. Combustion analysis was performed by MEDAC Ltd (www.medacltd.com).

HPLC-MS was performed on Mass Quattro CTC, comprising of Waters 1525µ Binary HPLC Pump and Micromass® Quattro micro™ API. Column used was Macherey-Nagel Nucleodur® 100-5 18 EC, 125 mm in length, particle size 5 µm.

Solid state diffused reflectance UV-Vis and solution absorbance in UV-Vis performed in University of Oxford was performed on Agilent Cary 4000 UV Vis Spectrophotometer. Pike Veemac Diffuse IR accessory was used with the Spectrometer for Diffused Reflectance UV-Vis measurements. BET Surface Area measurement was conducted using Micromeritics® Microactive for Tristar II Plus Version 2.02.

At SIMTech, diffused reflectance, transmittance and solution absorbance was performed on Perkin Elmer UV/Vis/NIR Spectrometer Lamda 1050, while ATR-IR was performed on a Brunker Vertex 80v FTIR spectroscopy. XPS was done using ThermoScientific ESCA Lab 250X with AlKα source and AFM was performed using Veeco Nanoscope IIIa Scanning Probe Microscopy.

7.2 Substrates used

Material	**Forms**	**Remarks**
Amberlite® XAD-4 Polystyrene	Beads	20-60 mesh from Supelco, Sigma Aldrich. Highly crosslinked polystyrene beads of about xxmm, surface area 725 m^2/g.
LDPE	Powder	From GoodFellow.
UHMWPE	Powder	From GoodFellow
PET	Pellets	From Aldrich, with 30% glass particles as reinforcer
PET	Sheets	Obtained from Roll-to-Roll machine.
COC	Pieces	Injection molded in SIMTech.
PDMS	Pieces	Sylgard 184 (Silicone Elastomer base + Hardener). The Elastomer base and hardener was mixed in 10:1 wt/wt ratio. The mixture was put into a Thinky Mixer ARV-310 to be mixed homogeneously under vacuum (1000 RPM for 1min,2000 RPM for 30s). This helps to remove air bubble when pouring the mixture onto silicon wafer surface to be casted and cured. The

		silicon wafer with Sylgard 184 mixture was heated at 50°C for 4h. The hardened PDMS is then cut into desired size using a pen-knife.
TPU	Sheet	Lubrizol Pellethane 5855-92A TPU resins are dissolved in THF. The viscous mixture is then poured into petri dish to be casted. THF is allowed to evaporate over 48 h. The hardened TPU is removed from the petri dish and heated at 70°C under vacuum for 24 h to remove residual THF. The flat TPU was then cut into desired size.
PC	Pieces	Produced in SIMTech in 10 cm x 10 cm pieces from Panlite L1225L pellets, using Injection Moulding Machine Nestal HP1000
PS	Pieces	Produced in SIMTech in 10 cm x 10 cm pieces from Denka styrol mw1 pellets, moulded using Injection Moulding Machine Nestal HP1000
PMMA		Produced in SIMTech in 10 cm x 10 cm pieces from VRL40 pellets, moulded using Injection Moulding Machine Nestal HP1000.

7.3 General Methods

General Method (A): Diazonium salt formation

The corresponding amine (1.00 eq) was dissolved solvent (EtOH or THF:H_2O=1:1). 3M HCl (2.00 eq) was added into the mixture and this was then stirred in ice-bath for 10 min. $NaNO_2$ (1.20 eq) dissolved in approximately 1 mL H_2O was then added into the cold mixture. The mixture was stirred in ice-bath for 30 - 40 min before H-acid was performed to test for presence of diazonium salt. The diazonium salt reaction mixture was used immediately *in situ*.

Alternative method: The corresponding amine (1.00 eq) was added into a stirring solution of EtOH (15 mL) at 0 °C in the dark. Isopentyl nitrite (1.20 eq) was added, followed by tetrafluoroboric acid (2.00 eq) into the reaction mixture, which was then continued to be stirred at 0 °C in the dark for 50 mins. H- acid test was conducted to detect presence of diazonium functional group. The mixture was used directly.

General Method (B): H-acid test for presence of diazonium functionality

A sample of the diazonium salt solution (adjusted to about pH 4 using NaOAc) was added into a suspension (0.5 mL) of H-acid (4-amino-5-hydroxynaphthalene-2,7-disulfonic acid): H_2O (1:1 v/v). Upon standing for some time, the beige colour suspension turning dark purple would indicate the presence of diazonium functionality.

General method (C): Polymer surface modification using diaryldiazo[25]

For beads, pellets, powders: For a 20 w/w% loading, the intended diaryldiazo derivatives (1.00 g) was dissolved in Et_2O and swirled in the dark. Blank polymer (~5.00 g) was then added into the suspension and swirled for homogenous coverage of the beads with the compound. Solvent was removed carefully and slowly *in vacuo*. The flask was then heated to 120 °C for 30 min (or until all the beads have changed colour) and cooled to room temperature. A change in colour of the beads would indicate successful functionalisation of the beads surface. The beads were washed thoroughly with acetone and water until no colour was observed to be washed out, and dried on a sintered funnel.

For flat substrates: Diaryldiazo derivative **3.3a2** (1 g) was dissolved in Et_2O or AcOH (50 mL) and poured into a spray bottle. The solution was then sprayed evenly onto the flat polymer substrates, and the substrates covered with the diaryldiazo derivative were placed on conveyor belt of the high intensity UV machine to be UV irradiated for about 40 s. A change of colour from purple to transparent with slight tint of yellow would indicate completion of the surface modification. The flat substrates were then washed with copious amount of water and ethanol, and dried using a nitrogen gun.

General method (D): Azo coupling of diazonium salt compounds on modified surface of polymers[28, 30]

For beads, pellets, powders: Functionalised polymers (~2.50 g) were added into the diazonium salt suspension (~375 mg in 10 mL solvent) at 0 °C and swirled in the dark. The mixture was then left in the fridge at 4 °C to stand for 18-20 h. The polymers were then filtered and wash thoroughly with acetone and water until no colour was observed to be washed out, and dried on a sintered funnel. [15w/w% loading, assuming 80% conversion of amines to diazonium salts from **General Method (B)**]

For flat substrates: Surface pre-activated flat polymers were fitted into slots in container and diazonium salt suspension (~500 mg in 80 mL solvent) was then poured into the container. The mixture is left to stand in dark in the fumehood for 18 h, and gradually warmed up to room temperature, with slight stirring using a stir bar at the bottom of the container. The polymers were then washed with copious amount of water and ethanol, and dried using a nitrogen gun.

General method (E): Derivatization of modified polymers with spiropyran

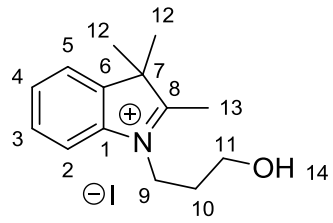
For beads, pellets, powders: For a 10 w/w% loading, functionalised polymers from **General Method (D)** (~1 g) were refluxed with spiropyran **2.8 or 2.9** (100 mg) and K_2CO_3 in MeCN for 3 h. The mixture was then cooled to room temperature. The polymers were then filtered and wash thoroughly with acetone and water until no colour was observed to be washed out. [Alternatively, polymers can be stirred in spiropyran **2.8** with K_2CO_3 for 18 h in acetone or DMSO at room temperature.]

For flat substrates: Surface functionalised flat polymers were fitted into slots in container and a mixture of spiropyran **2.8** (350 mg) with K_2CO_3 (200 mg) in DMSO (80 mL) was then poured into the container. The mixture was left to stand in dark in

the fumehood for at least 5 h, with slight stirring using a stir bar at the bottom of the container. The polymers were then washed with copious amount of water and ethanol.

7.4 Experimental for Chapter 2

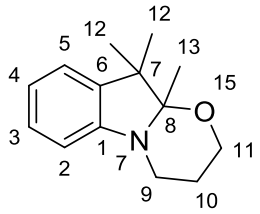
1-(3-Hydroxypropyl)-2,3,3-trimethyl-3H-indol-1-ium iodide. (2.3)[93]



Freshly distilled 2,3,3-trimethylindolenine (1.02 mL, 6.36 mmol, 1.06 eq) was dissolved in $CHCl_3$ (30 mL). 3-Iodo-1-propanol (0.60 mL, 6.00 mmol, 1.00 eq) was added into the mixture, and refluxed for 50h. After the reaction mixture was cooled to room temperature, the solvent was evaporated. The oil was then washed with petrol, and triturated with Et_2O to afford dark red oil (1.96 g, 95% yield).

Dark red oil; IR (neat): 3361 (O-H), 1627(C=N), 1608 (C=C), 1593, 1460, 1124, 1071, 764 cm^{-1}; ^1H NMR (400 MHz, DMSO-d_6): δ 7.88-7.91 (1H, m, H-2), 7.79-7.81 (1H, m, H-5), 7.59-7.61 (2H, m, H-3,4), 4.50 (2H, t, *J*= 6.8 Hz, H-9), 3.52 (2H, t, *J*= 5.4Hz, H-11), 2.80 (3H, s, H-13), 1.99-2.05 (2H, m ,H-10), 1.50 (6H, s, H-12); ^{13}C (100 MHz, DMSO-d_6): δ 196.9, 142.2, 141.4, 129.8 and 129.4 (C-3,4), 123.8 (C-5), 115.7 (C-2), 58.3 (C-11), 54.5, 46.0 (C-9), 29.9 (C-10), 22.2 (C-12), 14.4 (C-13). LRMS (ESI) m/z: $[M-I]^+$: 218.2. HRMS (ESI) calculated for $C_{14}H_{20}NO$ *m/z* $[M-I]^+$: 218.1539 ; found: 218.1543.

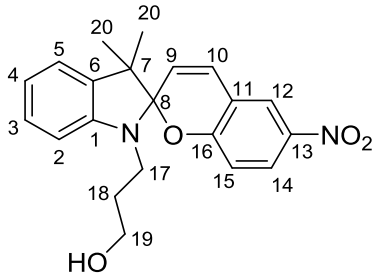
10,10,10a-Trimethyl-3,4,10,10a-tetrahydro-2H-[1,3]oxazino[3,2-a]indole. (2.5) [93]



The indolium iodide **2.3** (1.036 g, 3.00 mmol, 1.00 eq) was suspended in degassed water (10 mL). Finely ground KOH (0.348 g, 6.20 mmol, 2.07 eq) was added, and the mixture was stirred for 3 h at RT. DCM (10 mL) was then added to the mixture and stirred for 1h. The aqueous layer was separated and extracted with DCM. The combined organic layers were washed with brine and dried over anhydrous Na_2SO_4, filtered, and concentrated *in vacuo*. The residue was purified by flash column chromatography (Petrol:EA = 30:1) to yield a yellow-brown oil (145 mg, 47% yield). (R_f: 0.76 in Petrol:EA= 3:1)

Yellow-brown oil; IR (neat): 2959, 1719, 1606 (C=C), 1481, 1456 (C=C), 1267, 1074, 1056, 858, 742 cm^{-1}; ^1H NMR (400 MHz, $CDCl_3$): δ 7.14 (1h, ddd, , *J* = 7.5, 7.5, 1.2 Hz, H-3), 7.09 (1h, d, *J* = 7.3 Hz, H-5), 6.82 (1H, ddd, , *J* = 7.3, 7.3, 0.7 Hz, H-4), 6.60 (1H, d, *J* = 7.6 Hz, H-2), 4.09 (1H, ddd, *J* = 12.7, 12.7, 2.7 Hz, H-11), 3.73 (1H, dddd, *J* = 11.8, 5.4, 1.5, 1.5 Hz, H-11), 3.67 (1H, ddd, *J* = 3.2, 13.8, 13.8 Hz, H-9), 3.54 (1H, ddd, *J* = 13.9, 13.9, 3.2 Hz, H-9), 1.91-2.03 (1H, m, H-10), 1.56 (3H, s, H-13), 1.30 (3H, s, H-12), 1.18-1.22 (1H, m, H-10), 1.07 (3H, s, H-12); ^{13}C (100 MHz, $CDCl_3$): δ 148.0 (C-1), 139.2 (C-6), 127.2 (C-3), 122.0 (C-5), 119.2 (C-4), 108.6 (C-2), 98.3 (C-8), 61.0 (C-11), 48.03 (C-9), 39.1 (C-12), 26.7 (C-12), 21.7 (C-10), 18.6 (C-12), 13.0 (C-13). LRMS (ESI) m/z: $[M+H]^+$: 218.2. HRMS (ESI) calculated for $C_{14}H_{19}NO$ *m/z* $[M+H]^+$: 218.1539 ; found: 218.1544.

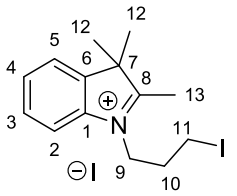
3-(3',3'-Dimethyl-6-nitrospiro[chromene-2,2'-indolin]-1'-yl)propan-1-ol. (2.7) [93]



To a degassed solution of **2.5** (140 mg, 0.64 mmol, 1.00 eq) in EtOH (5 mL), 5-nitrosalicylaldehyde (115 mg, 0.69 mmol, 1.08 eq) was added. The mixture was sonicated for 1h. EtOH was evaporated and the residue was taken up in DCM, washed with water, and dried over anhydrous Na_2SO_4, filtered, and concentrated *in vacuo*. The residue was purified by flash column chromatography (elute at Petrol: EA = 2:1) to yield a dark purple solid. (161 mg, 80% yield). (R_f: 0.71 in Petrol:EA = 1:1).

Purple solid; M.P: 130 °C; IR (neat): 2927, 1651, 1610 (C=C), 1577 (C=C), 1513 (NO_2), 1333 (NO_2), 1273, 1089 (C-O), 954, 745 cm^{-1}; ^1H NMR (400 MHz, $CDCl_3$): δ 8.00-8.04 (2H, m, H-12,14), 7.21 (1H, ddd, *J* = 7.8, 7.8, 1.3 Hz, H-3), 7.10 (1H, dd, *J* = 7.3, 0.9 Hz, H-5), 6.92 (1H, d, *J* = 10.1 Hz, H-10), 6.90 (1H, ddd, , *J* = 7.4, 7.4, 0.7 Hz, H-4), 6.76 (1H, d, *J* = 8.8 Hz, H-15), 6.66 (1H, d, *J* = 7.8 Hz, H-2), 5.90 (1H, d, *J* = 10.5 Hz, H-9), 3.72 (2H, t, *J* = 6.0 Hz, H-19), 3.23- 3.42 (2H, m, H-17), 1.79 – 1.98 (2H, m, H-18), 1.29 (3H, s, H-20), 1.19 (3H, s, H-20); ^{13}C (100 MHz, $CDCl_3$): δ 159.6 (C-13), 147.0 (C-16), 140.09 (C-1), 136.0 (C-11), 128.2 (C-2), 127.8(C-15), 125.9 (C-4), 122.7 (C-9), 121.8 (C-5), 121.7 (C-12/14), 119.6 (C-12/14), 118.4 (C-6), 115.5 (C-3), 106.9 (C-10), 106.8 (C-8), 60.7 (C-19), 52.6(C-7), 40.7 (C-17), 31.6 (C-18), 25.9 (C-20), 19.9 (C-20). LRMS (ESI) m/z: $[M+Na]^+$: 389.1. HRMS (ESI) calculated for $C_{21}H_{22}N_2NaO_4$ *m/z* $[M+Na]^+$: 389.1472; found: 389.1480.

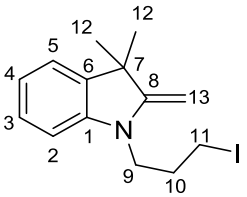
1-(3-Iodopropyl)-2,3,3-trimethyl-3H-indol-1-ium iodide. (2.4) [93]



To a solution of 2,3,3-trimethylindolinine (1.00 mL, 6.23 mmol, 1.00 eq), MeCN (10 mL) was added and degassed with N_2. After adding 1,3-diiodopropane (2.50 mL, 21.77 mmol, 3.49 eq) into the solution, the mixture was refluxed for at least 48h. After cooling to room temperature, the mixture was then filtered, and the residue was washed with minimal amount of MeCN and $CHCl_3$ and collected, giving a golden yellow solid (1.46 g, 51%).

Golden yellow solid; M.P: 216-217 °C. IR (neat): 3434, 2253, 2127, 1665, 1054, 1025, 1004, 823, 761cm^{-1}; ^{1}H NMR (400 MHz, DMSO-d_6): δ7.97-8.00 (1H,m, H-2), 7.82-7.87 (1H, m ,H-5), 7.67 (2H, m, H-3,4), 4.48 (1H, t, *J* = 7.6Hz, H-9), 3.43 (1H, t, , *J* = 7.4, H-11), 2.86 (3H, s, H-13), 2.40 (2G, tt, , *J* = 7.3, 7.6Hz, H-10), 1.55 (6H, s, H-12); ^{13}C (100 MHz, DMSO-d_6): δ197.3 (C-1), 141.8 (C-8), 141.1 (C-6), 129.4 (C-3/4), 128.9 (C-3/4), 123.5 (C-5), 115.2 (C-2), 54.3 (C-7), 48.4 (C-9), 31.0 (C-10), 22.0 (C-12), 14.3 (C-13), 2.3 (C-11). LRMS (ESI) m/z: [M-I]$^+$: 328.1. HRMS (ESI) calculated for $C_{14}H_{19}I_2N$ *m/z* [M-I]$^+$: 328.0557; found: 328.0560.

1-(3-Iodopropyl)-3,3-dimethyl-2-methyleneindoline. (2.6) [93]

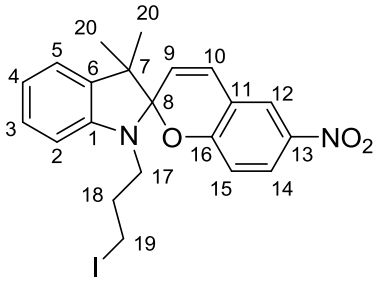


Indolium iodide **2.4** (212 mg, 0.466 mmol, 1.00 eq) was suspended in degassed water (56 mL). Finely ground NaOH (559 mg, 14.0 mmol, 30.0 eq) was added all at one go. The solution was stirred at room temperature for 1 h. Et_2O (60 mL) was

then added and stirred for 30 min. The layers were then separated, and aqueous layer was then extracted with DCM. The organic layers were washed with water separately, then combined, dried over $MgSO_4$ and filtered before concentrating in *vacuo* to give a dark pink gum (crude yield 261 mg, 80%)

Dark pink gum; IR (neat): 2965, 2360, 1707, 1612, 1458, 1207, 745cm^{-1}. LRMS (ESI) m/z: $[M+H]^+$: 218.2. NMR obtained was contaminated with impurities as crude mixture was used directly for the next step in the synthesis without further purification. ^1H NMR (200 MHz, $CDCl_3$): 7.13 – 7.19 (2H, m, H-3, 5), 6.83 (1H, t, *J* =7.3 Hz, H-4), 6.68 (1H, d, *J* =7.6 Hz, H-2), 3.96 (2H, d, *J* = 14.5 Hz, H-13), 3.67 (2H, t, *J* = 6.7 Hz, H-9), 3.26 (2H, t, *J* = 6.6 Hz, H-10), 2.24 (2H, m, H-11), 1.39 (6H, s, H-12). LRMS (ESI) m/z: $[M+H]^+$: 328.1. HRMS (ESI) calculated for $C_{14}H_{19}IN$ *m/z* $[M+H]^+$: 328.0557; found: 328.0568.

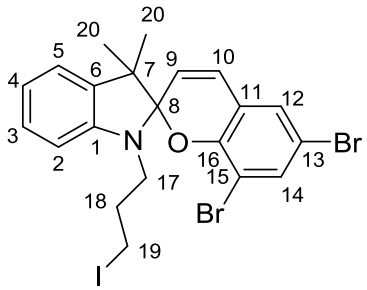
1'-(3-Iodopropyl)-3',3'-dimethyl-6-nitrospiro[chromene-2,2'-indoline]. (2.8) [93]



Indoline **2.6** (190mg, 0.587 mmol, 1.00 eq) was dissolved in EtOH (10 mL), followed by addition of 5-nitrosalicylaldehyde (103 mg, 0.616 mmol, 1.05 eq). The mixture was then sonicated for 2hr, before concentrating *in vacuo* to remove solvent. The residue was then taken up by DCM and washed with water. The organic layer was dried over $MgSO_4$, filtered and concentrated *in vacuo*. Purification by a short flash column chromatography (eluted at Petrol: EA= 45:1) gave a yellow-green oil (161 mg, 58% yield). (R_f: 0.80 in Petrol:Ea = 5:1)

Yellow-green oil; IR (neat): 2964, 2359, 1611 (C=C), 1518 (NO_2), 1481, 1336 (NO_2), 1273, 952, 808, 745 cm^{-1}; ^1H NMR (400 MHz, $CDCl_3$): 8.02-8.05 (2H,m, H-12,14), 7.21 (1H, ddd, *J* =7.6, 7.6, 1.2 Hz, H-3), 7.11 (1H, dd, *J* =7.1, 1.0 Hz, H-5), 6.96 (1H, d, *J* =10.5 Hz, H-10), 6.91 (1H, ddd, *J* =7.6, 7.6, 0.7 Hz, H-4), 6.77 (1H, d, *J* =8.3 Hz, H-15), 6.65 (1H, d, *J* =7.9 Hz, H-2), 5.88 (1H, d, *J* =10.2 Hz, H-9), 3.12-3.38 (4H, m, H-17,19), 2.04-2.27 (2H, m, H-18), 1.30 (3H, s, H-20), 1.20 (3H, s, H-20); ^{13}C (100 MHz, $CDCl_3$): δ159.3 (C-13), 146.8 (C_{quat}), 141.0 (C_{quat}), 136.0(C_{quat}) 128.5 (C-10), 127.8 (C-3), 126.0 (C-12/14), 122.8 (C-12/14), 121.8 (C-5), 121.7 (C-9), 119.8 (C-4), 118.5 (C_{quat}), 115.5 (C-15), 106.8 (C-2), 106.6 (C_{quat}), 52.6 (C-7), 44.1 (C-17), 32.5 (C-18), 26.0 (C-20), 19.9 (C-20), 3.2 (C-19). LRMS (ESI) m/z: $[M+H]^+$: 477.1. HRMS (ESI) calculated for $C_{21}H_{22}IN_2O_3$ *m/z* $[M+H]^+$: 477.0670; found: 477.0669.

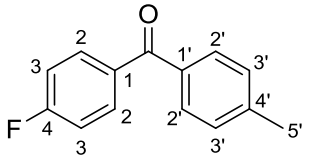
6,8-Dibromo-1'-(3-iodopropyl)-3',3'-dimethylspiro[chromene-2,2'-indoline]. (2.9)[93]



Indoline **2.6** (260 mg, 0.795 mmol, 1.00 eq) was dissolved in EtOH (8 mL), followed by addition of 3,5-dibromosalicylaldehyde (234 mg, 0.832 mmol, 1.05 eq). The mixture was then sonicated for 2hr, before concentrating *in vacuo* to remove solvent. The residue was then taken up by DCM and washed with water. The organic layer was dried over $MgSO_4$, filtered and concentrated *in vacuo*. Purification by a short flash column chromatography (eluted at Petrol:EA= 55:1) gave a green gum (252 mg, 54% yield). (R_f: 0.70 in Petrol:EA=9:1)

Green gum; IR (neat): 2963, 1607 (C=C), 1484, 1446 (C=C), 1262, 893, 746 cm^{-1}; ^{1}H NMR (400 MHz, $CDCl_3$): δ7.47 (1H, d, *J* = 2.2 Hz, H-14), 7.18 (1H, ddd, *J* = 7.6, 7.6, 1.3 Hz, H-3), 7.15 (1H, d, *J* = 2.5 Hz, H-12,), 7.08 (1H, dd, *J* = 7.4, 0.7 Hz, H-5), 6.86 (1H, ddd, *J* = 7.3, 7.3, 0.7 Hz, H-4), 6.77 (1H, d, *J* = 10.3 Hz, H-10), 6.61 (1H, d, *J* = 7.8 Hz, H-2), 5.77 (1H, d, *J* = 10.0 Hz, H-9), 3.14-3.38 (4H, m, H-17,19), 2.01-2.29 (2H, m, H-18), 1.31 (3H, s, H-20), 1.17(3H, s, H-20); ^{13}C (100 MHz, $CDCl_3$): δ 149.62, 146.71 (C-8), 136.07, 134.89 (C-16), 128.32 (C-18), 128.07 (C-13), 127.53 (C-2), 122.07 (C-14), 121.70 (C-6), 121.24, 119.35 (C-1), 111.87, 110.17, 106.56 (C-3), 106.12, 52.27, 43.95 (C-21), 32.30 (C-22), 25.66 (C-19/20), 20.40 (C-19/20), 3.80 (C-23). LRMS (ESI) m/z: $[M+H]^+$: 587.9. HRMS (ESI) calculated for $C_{21}H_{20}{}^{79}Br_2INO$ *m/z* $[M+H]^+$: 587.9029; found: 587.9022.

(4-Fluorophenyl)(4'-tolyl)methanone. (2.12)[95]

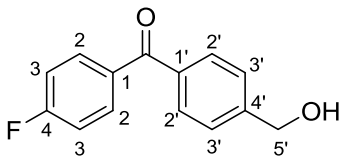


n-BuLi (1.6 M in hexane, 6.88 mL, 11.00 mmol, 1.10 eq) was added drop-wise into the solution of 4-bromotoluene (1.71 g, 10.00 mmol, 1.00 eq) in dry THF (25 mL) at -78 °C and stirred for 30 min. The reddish mixture first turned cyan then cloudy white. 4-fluorobenzaldehyde (1.13 mL, 10.5 mmol, 1.05 eq) was then added drop-wise into the mixture at -78 °C, and stirred at RT for 2 hr, where the solution turned light yellow. After the solvent was evaporated, I_2 (4.06 g, 16.00 mmol, 1.60 eq), K_2CO_3 (4.15 g, 30.00 mmol, 3.00 eq) and *t*-BuOH (25 mL) were added to the mixture, and it was then refluxed for 3 h. The reaction was then quenched with Na_2SO_3, and extracted with EA, washed with brine, dried over anhydrous Na_2SO_4, filtered and concentrated *in vacuo*. The residue was purified by flash column

chromatography (Petrol: EA = 30:1), to yield a light yellow-white solid. (1.67 g, 78% yield). (R_f: 0.76 in Petrol:EA = 3:1).

Light yellow-white solid; M.P: 97-98 °C (lit.[25] mp: 97-98 °C); IR (neat): 2924, 1648 (C=O), 1598 (C=C), 1502 (C=C), 1222, 851, 752 cm^{-1}; ^1H NMR (400 MHz, $CDCl_3$): δ7.81-7.86(2H, m, H-2), 7.70(2H, d, *J* = 8.0 Hz, H-2'), 7.30(2H, d, *J* = 7.8 Hz, H-3'), 7.16 (2H, m, H-3), 2.46 (3H, s, H-5'); ^{13}C (100 MHz, $CDCl_3$): δ 195.0 (C=O), 165.2 (d, J_{C-F} = 165.2 Hz, C-4), 143.3 (C-1'), 143.7 (C-4'), 143.1 (d, J_{C-F} = 3.2 Hz, C-1), 132.5 (d, J_{C-F} = 8.8 Hz, C-2), 130.1 (C-2'), 129.0 (C-3'), 115.3 (d, J_{C-F} = 22.3 Hz, C-3), 21.6 (C-5'). LRMS (ESI) m/z: $[M+Na]^+$: 237.1. HRMS (ESI) calculated for $C_{14}H_{11}FO$ *m/z* $[M+Na]^+$: 237.0686; found: 237.0694.

(4-Fluorophenyl)(4'-(hydroxymethyl)phenyl)methanone. (2.13) [95]

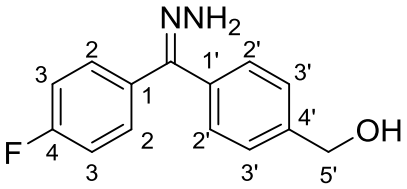


2.12 (1.07 g, 5.00 mmol, 1.00 eq) was added into a stirring solution of benzoyl peroxide (1.26 g, 5.20 mmol, 1.04 eq) and N-bromosuccinimide (1.07 g, 6.00 mmol, 1.20 eq) in $CHCl_3$ (50 mL). The mixture was refluxed for 24 h in the presence of fumehood light. After cooling the reaction mixture to room temperature, the reaction mixture was washed with brine and dried over anhydrous $MgSO_4$, filtered and concentrated *in vacuo* to afford a yellow solid. $CaCO_3$ (2.58 g, 25.8 mmol, 5.16 eq) was then added to it, and the mixture was suspended in 1,4-dioxane (25 mL) and water (25 mL). The mixture was then refluxed for 24 h before it was cooled to room temperature. 3 M HCl was added and stirred for 30 min. The mixture was then extracted with DCM, washed with brine and dried over anhydrous $MgSO_4$. The organic layer was filtered, concentrated and purified on a flash column, eluting the

desired compound at Petrol:EA = 1:1. (383 mg, 33% yield). (R_f: 0.26 in Petrol:EA= 3:1).

Light yellow solid .M.P: 85-86°C. IR (neat): 3428.69 (O-H), 2924.67, 1655.29 (C=O), 1598.47 (C=C), 1279.35, 1156.58, 929.88, 759.80 cm^{-1}; ^1H NMR (400 MHz, $CDCl_3$): δ7.83 (2H, m, H-3), 7.76 (2H, d, *J* = 8.3 Hz, H-2'), 7.48 (2H, d, *J* = 8.1 Hz, H-3'), 7.16 (2H, m, H-2), 4.80 (2H, s, H-5'); ^{13}C (100 MHz, $CDCl_3$): δ195.1 (C=O), 165.3 (d, $J_{C\text{-}F}$= 254.3 Hz, C-4), 145.6 (C-1'), 136.5 (C-4'), 133.7 (d, $J_{C\text{-}F}$ = 3.20 Hz, C-1), 132.6 (d, $J_{C\text{-}F}$ = 9.6 Hz, C-2), 130.2 (C-2'), 126.4 (C-3'), 115.4 (d, $J_{C\text{-}F}$ = 22.3 Hz, C-3), 64.5 (C-5'). LRMS (ESI) m/z: $[M+H]^+$: 253.1. HRMS (ESI) calculated for $C_{14}H_{11}FO_2$ *m/z* $[M+Na]^+$: 253.0635; found: 253.0644.

(4'-((4-Fluorophenyl)(hydrazono)methyl)phenyl)methanol. (2.14) [95]

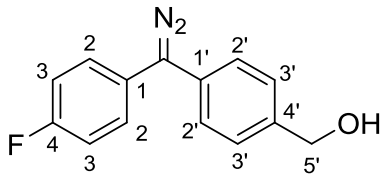


2.13 (500 mg, 2.17 mmol, 1.00 eq) was added into EtOH (10 mL) and stirred. Hydrazine monohydrate (0.6 mL, 12.37 mmol, 5.70 eq) was the added slowly, and the reaction mixture was refluxed for 24h. After the mixture was cooled to room temperature, water (~2 mL) was added and the mixture was concentrated *in vacuo* to remove EtOH. The residue was extracted with in DCM. The organic layer was collected, washed with brine, dried over anhydrous $MgSO_4$, filtered and concentrated *in vacuo* to give a yellow oil (440 mg, 83% yield).

Yellow oil; IR (neat): 3365 (N-H), 1602 (C=N), 1505 (C=C), 1409, 1221, 1013, 838 cm^{-1}; ^1H NMR (400 MHz, $CDCl_3$): δ 7.52-7.54 (2H, m), 7.41-7.45 (3H, m), 7.33-7.35 (2H, m), 7.25-7.29 (5H, m), 7.22-7.23 (1H, m), 6.94-7.03 (3H, m), 4.71 (2H, s), 4.60

(2H, s); ^{13}C (100 MHz, $CDCl_3$): δ 164.0 (C=N), 161.6 (C=N), (148.2, 147.9), (130.9, 130.82), (126.8, 126.6), (116.7, 116.5), (115.2, 115.0), (64.9, 64.7 ($-CH_2$)). LRMS (ESI) m/z: $[M+H]^+$: 245.1. HRMS (ESI) calculated for $C_{14}H_{14}FN_2O$ *m/z* $[M+H]^+$: 245.1085; found: 245.1081.

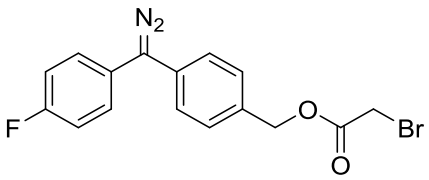
(4-(Diazo(4'-fluorophenyl)methyl)phenyl)methanol. (2.15) [95]



2.14 (280 mg, 1.15 mmol, 1.00 eq) was dissolved in a mixture of KOH (130 mg, 2.32 mmol, 2.02 eq), MnO_2 (402 mg, 4.62 mmol, 4.02 eq), Na_2SO_4 (277 mg, 1.95 mmol, 1.70 eq) and MeOH (15 mL). The mixture was stirred in the dark for 24 h, before filtering it through a celite pad, eluting with EA. The filtrate was then concentrated in *vacuo*. The concentrate was then dissolved in with EA, washed with water and dried over anhydrous $MgSO_4$. After filtering, the filtrate was then concentrated *in vacuo* to give a dark red sticky gum (226 mg, 81% yield).

Dark red sticky gum; IR (neat): 2043 ($=N^+=N^-$), 1698 (C=N), 1598 (C=C), 1508 (C=C), 1224, 832 cm^{-1}. The NMR obtained is impure and not distinguishable. However, from the IR, the absorption band for diazo functional group was still present.

4'-(Diazo(4-fluorophenyl)methyl)benzyl 2-bromoacetate. (2.16) [95]

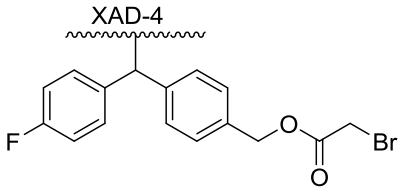


2.15 (120 mg, 0.49 mmol, 1.00 eq) was stirred with with Et_3N (0.21 mL, 1.5 mmol, 3.06 eq) in DCM (15 mL) at 0°C. Bromoacetyl bromide (0.05mL, 0.60mmol, 1.22eq)

was added dropwise into the mixture, and mixture was stirred at at 0°C for 4h. The mixture was then washed with water, dried with $MgSO_4$, filtered and concentrated in *vacuo* to give a brown mixture (271mg).

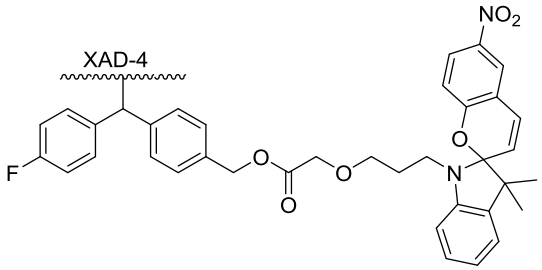
IR (neat): 2341 ($=N^+=N^-$), 1698 (C=O), 1604 (C=C), 1508 (C=C), 1276, 1261, 1158(C-O), 750cm^{-1}. The NMR obtained is impure and not distinguishable. However, from the IR, the absorption band for diazo functional group was still present.

Immobilization of 4'-(diazo(4-fluorophenyl)methyl)benzyl 2-bromoacetate on polystyrene XAD-4. (2.17)



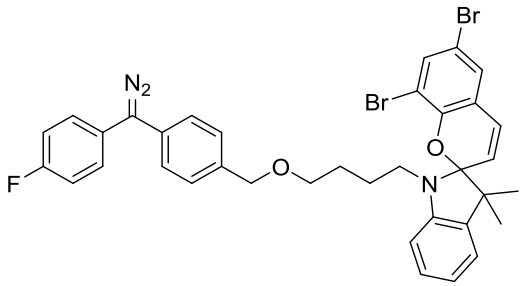
Following General Method (C), diaryldiazo **2.16** (200 mg) and blank XAD-4 polystyrene beads (1.00g) was used, giving brown colour beads. (See Appendix B and C for combustion analyisis data and ATR-IR data).

Derivatization of 4'-(diazo(4-fluorophenyl)methyl)benzyl 2-bromoacetate on polystyrene XAD-4. (2.18)



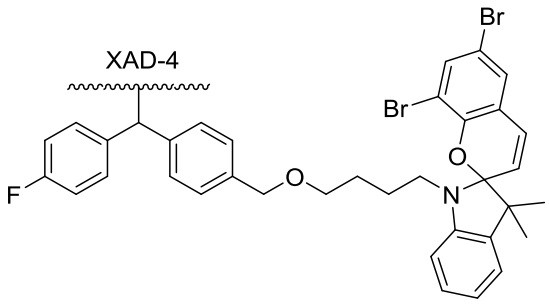
Functionalised XAD-4 beads **2.17** (41 mg, 0.11 mmol) was stirred with K_2CO_3 (55 mg, 0.400 mmol) and MeCN (10 mL). Spiropyran **2.7** (25mg) was then added and stirred at room temperature for 48 h. The beads were washed thoroughly with acetone, and dried (See Appendix B and C for combustion analyisis data and ATR-IR data).

6,8-Dibromo-1'-(4-((4-(diazo(4-fluorophenyl)methyl)benzyl)oxy)butyl)-3',3'-dimethylspiro[chromene-2,2'-indoline] (2.19)



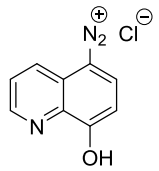
2.15 (120 mg, 0.495 mmol, 1.00 eq) was stirred with NaH (50 mg of 60% NaH in mineral oil, 1.25 mmol, 2.53 eq) in dry THF (15 mL) at -78°C. Spiropyran **2.9** (300 mg, 0.51mmol, 1.03eq) was then added into the suspension and the mixture was stirred for 48 h at RT. The reaction mixture was then quenched by adding Et_2O (10 mL), followed by ice (~5 mL), and extracted with Et_2O. Concentration *in vacuo* yielded a navy blue gum (322 mg, 90% crude yield).). IR (neat): 2925, 2360, 2039 ($=N^+=N^-$), 1606 (C=C), 1508 (C=C), 1447, 1225, 1158, 1029, 830.

Immobilization of 6,8-dibromo-1'-(4-((4-(diazo(4-fluorophenyl)methyl)benzyl)oxy)butyl)-3',3'-dimethylspiro[chromene-2,2'-indoline] onto XAD-4 beads. (2.20)



Following General Method (C), 300 mg of diaryldiazo **2.19** and 1.00g of XAD-4 beads were used, yielding blue coloured modified beads (See Appendix B and C for combustion analysis data and ATR-IR data).

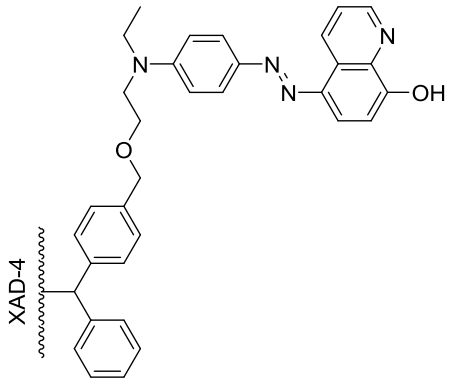
Synthesis of 8-hydroxyquinoline-5-diazonium chloride. (2.28)



Amine used: 5-amino-8-hydroxyquinoline dihydrochloride

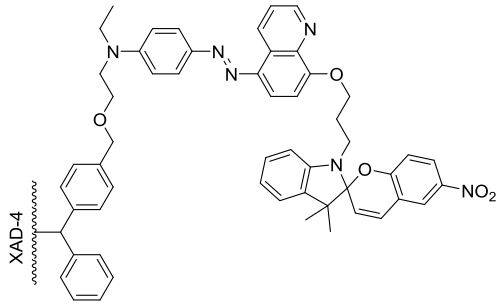
Following General Method (A) for diazonium salt formation: After 30 min of reaction, red solution turned dark brown.

Azo coupling of 8-hydroxyquinoline-5-diazonium to surface modified bead (2.29)



Using General Method (D), 588 mg modified beads **2.26** were used with 12 mg of diazonium salt **22** to give blue beads. (See Appendix B and C for combustion analysis and ATR-IR).

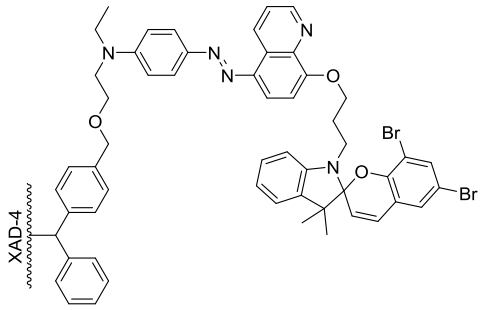
Derivatization of modified beads (2.29) with 1'-(3-Iodopropyl)-3',3'-dimethyl-6-nitrospiro[chromene-2,2'-indoline]. (2.30)



Following General Method (E), spiroypyran **2.8** (30mg, 0.06mmol) was stirred with K_2CO_3 (50mg, 0.36mmol) and MeCN (8mL). Surface functionalised beads **2.29**

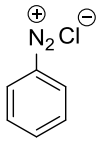
(80mg) was then added and refluxed for 5 h. The beads were washed thoroughly with acetone, and dried to give beige coloured beads (See Appendix B and C for combustion analysis and ATR-IR).

Derivatization of modified bead (2.29) with 6,8-Dibromo-1'-(3-iodopropyl)-3',3'-dimethylspiro[chromene-2,2'-indoline] (2.31).



Following General Method (E), spiropyran **2.9** (40mg, 0.06mmol) was stirred with K_2CO_3 (50 mg, 0.36 mmol) and MeCN (8 mL). Surface functionalised beads **2.29** (80 mg) were then added and refluxed for 5 h. The beads were washed thoroughly with acetone, and dried, giving pale blue-green beads (See Appendix B and C for Combustion Analysis and ATR-IR data).

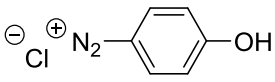
Synthesis of benzenediazonium chloride. (2.45a)



Amine used: Aniline

Following General Method (A): After 30min of reaction, colourless solution would turn bright yellow.

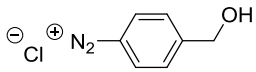
Synthesis of 4-hydroxybenzenediazonium chloride. (2.45b).



Amine used: 4-aminophenol.

Following General Method (A): After 30mins of stirring, the colourless solution turned deep brown.

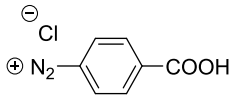
Synthesis of 4-(hydroxymethyl)benzenediazonium chloride (2.45c).



Amine used: 4-aminobenzyl alcohol.

Following General Method (A): After 30min of reaction, the brownish-yellow solution would turn bright yellow.

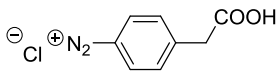
Synthesis of 4-carboxybenzenediazonium chloride. (2.45d)



Amine used: 4-aminobenzoic acid.

Following General Method (A): After 30mins of stirring, the colourless solution turned bright yellow.

Synthesis of 4-(carboxymethyl)benzenediazonium chloride. (37e)



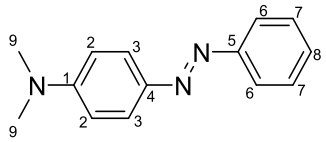
Amine used: 4-aminophenylacetic acid

Following General Method (A): Upon addition of acid, the solution turned yellow. After adding in the nitrite to initiate the reaction, the reaction mixture turned deep red immediately.

Solution Study: Azo coupling method

NaOAc (246 mg, 3.00 mmol, 2.00 eq) was added into the diazonium salt mixture in ice bath and stirred for 5 min, before phenol (141 mg, 1.50 mmol, 1.00 eq) dissolved in 1 mL of THF [or dimenthylaniline (1.50 mmol, 1.00 eq)] was added. The reaction mixture was then stirred for 18 h before THF was removed *in vacuo* .The precipitated product was collected on a Büchner funnel, washed with H_2O and dried. Alternatively, if there were no precipitated product formed, the reaction mixture was extracted with DCM. The combined organic layers were dried over $MgSO_4$, concentrated and purified using flash column chromatography

Synthesis of *N*,*N*-dimethyl-4-(phenyldiazenyl)aniline (2.46a).



Amine used: Aniline (0.14 mL, 1.50 mmol, 1.00 eq)

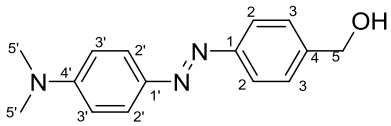
Coupling: *N*,*N*-Dimethylaniline (0.14 mL, 1.50 mmol, 1.00 eq) in 1 mL THF

Purification: Precipitated product collected on Büchner funnel and dried.

Yield: 331mg, 98%.

Orange-yellow solid; M.P: 105 -107 °C (lit.[142] 111 °C); IR (neat): 2914, 1600 (C=C), 1564, 1516, 1407, 1364, 1139, 821 cm^{-1}; ^1H NMR (400 MHz, $CDCl_3$): δ 7.91 (2H, d, *J* = 8.5 Hz, H-3), 7.86 (2H, d, *J* = 7.6 Hz, H-6), 7.48 (2H, t, *J* = 7.3 Hz, H-7), 7.39 (1H, tt, *J* = 7.3, 1.7 Hz, H-8), 6.79 (2H, d, *J* = 9.1 Hz, H-2), 3.11 (6H, s, H-9); ^{13}C (100 MHz, $CDCl_3$): δ153.2 (C_{quat}), 152.4 (C_{quat}), 143.6 (C_{quat}), 128.3 (C-8), 128.9 (C-7), 124.9 (C-3), 122.1 (C-6), 111.4 (C-2), 40.2 (C-9). HRMS (ESI) calculated for $C_{14}H_{15}N_3$ *m/z* $[M+H]^+$: 226.1339; found: 226.1342.

Synthesis of (4-((4'-(dimethylamino)phenyl)diazenyl)phenyl)methanol (2.46c).



Amine used: 4-Aminobenzyl alcohol (185 mg, 1.50 mmol, 1.00 eq)

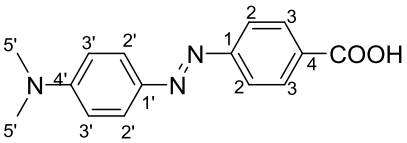
Coupled to: N,N-Dimethylaniline (0.14 mL, 1.50 mmol, 1.00 eq) in 1 mL THF

Purification: Precipitated product collected on Büchner funnel and dried.

Yield: 368 mg, 96%.

Bright orange solid; M.P: 195 – 197 °C; IR (neat): 3352, 1976, 1609 (C=C), 1555 (N=N), 1522, 1442, 1374, 1231, 11588, 1051 (C-O) cm^{-1}; ^{1}H NMR (400 MHz, DMSO): δ7.78 (2H, d, *J* = 9.0 Hz, H-2'), 7.75 (2H, d, *J* = 8.3 Hz, H-2), 7.46 (2H, d, *J* = 8.3 Hz, H-3), 6.83 (2H, d, *J* = 9.1 Hz, H-3'), 5.31 (1H, t, *J* = 5.6 Hz, -OH), 4.57 (2H, d, *J* = 5.6 Hz, H-5), 3.05 (6H, s, H-5') ; ^{13}C (100 MHz, DMSO): δ152.4 (C_{quat}), 151.3 (C_{quat}), 144.3 (C_{quat}), 142.5 (C_{quat}), 127.0 (C-3), 124.6 (C-2'), 121.6 (C-2), 111.5 (C-3'), 62.5 (C-5), 39.8 (C-5'). HRMS (ESI) calculated for $C_{15}H_{17}N_3O$ *m/z* $[M+H]^+$: 256.14444; found: 256.14410.

Synthesis of 4-((4'-(dimethylamino)phenyl)diazenyl)benzoic acid (2.46d).



Amine used: 4-Aminobenzoic acid (206 mg, 1.50 mmol, 1.00 eq)

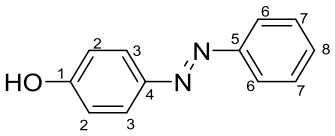
Coupled to: N,N-Dimethylaniline (0.14 mL, 1.50 mmol, 1.00 eq) in 1 mL THF

Purification: Precipitated product collected on Büchner funnel and dried.

Yield: 394 mg, 97%.

Bright red solid; M.P: >250 °C (lit.[142] 300°C); IR (neat): 2822, 1994, 1676 (C=O), 1594 (C=C), 1556 (N=N), 1421, 1361, (C-N), 1252, 1136 cm^{-1}; ^{1}H NMR (400 MHz, DMSO): δ13.07 (1H, broad s, -OH), 8.07 (2H, d, J = 8.5 Hz, H-3), 7.83 (2H, d, J = 8.5 Hz, H-2), 7.82 (2H, d, J = 9.3 Hz, H-2'), 6.84 (2H, d, J = 9.3 Hz, H-3'), 3.07 (6H, s, H-5'); ^{13}C (100 MHz, DMSO): δ166.9 (-COOH), 1555.1 (C_{quat}), 153.0 (C_{quat}), 142.7 (C_{quat}), 130.9 (C_{quat}), 130.5 (C-3), 125.3 (C-2'), 121.7 (C-2), 111.6 (C-3'), 39.8 (C-5').HRMS (ESI) calculated for $C_{15}H_{15}N_3O_2$ *m/z* $[M+H]^+$: 270.12370; found: 270.12344.

Synthesis of 4-(phenyldiazenyl)phenol (2.47a).



Amine used: Aniline (0.14mL, 1.50 mmol, 1.00eq)

Coupled to: Phenol (141 mg, 1.50 mmol, 1.00 eq) in 1 mL THF

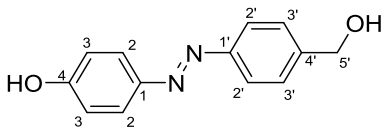
Purification: Flash column chromatography, eluting product at Petrol 40-60: EA = 30:1. R_f= 0.54 in Petrol 40-60:EA = 4:1.

Yields:

- (244mg, 82%) – when 1.00 eq of NaOAc used
- (280 mg, 95%)-when 2.00 eq of NaOAc used.

Orange-yellow solid; M.P: 155 -157 °C (lit.[142] 158 - 160°C); IR (neat): 2161, 1977, 1582, 1503, 1413, 1268, 1219, 1142, 993 cm^{-1}; ^{1}H NMR (400 MHz, MeOD): δ 7.81 – 7.84 (4H, m, H-3, 6), 7.44 – 7.48 (2H, m, H-7) 7.38 – 7.42 (1H, m, H-8), 6,92 (2H, app d, *J* = 8.8 Hz, H-2); ^{13}C (100 MHz, MeOD): δ162.0 (C_{quat}), 154.0 (C_{quat}), 147.4 (C_{quat}), 131.2 (C-8), 130.0 (C-7), 125.9 (C-3/6), 123.3 (C-3/6), 116.7 (C-2). HRMS (ESI) calculated for $C_{12}H_{10}N_2O_2$ *m/z* $[M+H]^+$:199.08659; found: 199.08676.

Synthesis of 4-((4'-(hydroxymethyl)phenyl)diazenyl)phenol. (2.47c)



Amine used: 4-Aminobenzyl alcohol (185 mg, 1.50 mmol, 1.00eq)

Coupled to: Phenol (141 mg, 1.50 mmol, 1.00 eq) in 1 mL THF

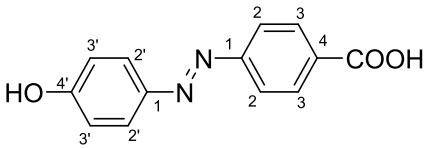
Purification: Precipitated product collected on Büchner funnel and dried.

Yields:

- (264 mg, 77%) – when 1 eq of NaOAc used,
- (297 mg, 87%) – when 2 eq of NaOAc used

Brown solid; M.P: 198 - 200 °C IR (neat): 3385, 2160, 1594 (N=N), 1500, (C=C), 1238, 1199, 1142, 1103 cm^{-1}; ^{1}H NMR (400 MHz, MeOD): δ 7.80 – 7.83 (4H, m, H-2, 2'), 7.50 (2H, d, *J* = 8.6 Hz, H-3'), 6.91 (2H, d, *J* = 9.0 Hz, H-3), 4.68 (2H, s, H-5'); ^{13}C (100 MHz, MeOD): δ162.1 (C_{quat}), 153.4 (C_{quat}), 147.5 (C_{quat}), 145.3 (C_{quat}), 128.5 (C-3'), 125.9 (C-2'), 123.4 (C-2), 116.7 (C-3), 64.8 (C-5'). HRMS (ESI) calculated for $C_{13}H_{12}N_2O_2$ *m/z* $[M+H]^+$: 229.09715; found: 229.09715.

Synthesis of 4-((4'-hydroxyphenyl)diazenyl)benzoic acid (2.47d).



Amine used: 4-Aminobenzoic acid (206 mg, 1.50 mmol, 1.00eq)

Coupled to: Phenol (141 mg, 1.50 mmol, 1.00 eq) in 1 mL THF

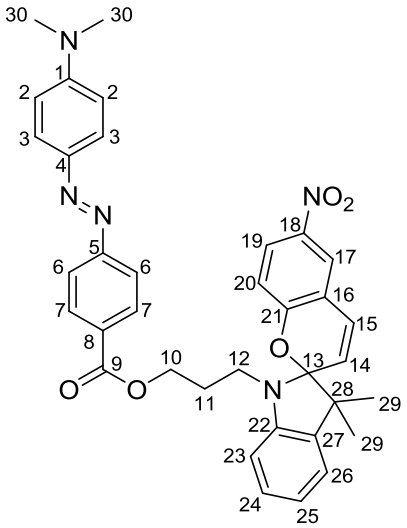
Purification: Precipitated product collected on Büchner funnel and dried.

Yields:

- (318mg, 88%) -when 1 eq of NaOAc used,
- (332mg, 92%)-when 2 eq of NaOAc used

Orange-yellow solid; M.P: >250 °C (lit.[142] 270 -280°C); IR (neat): 3542, 3447, 1663 (C=O), 1588 (N=N), 1500 (C=C), 1429, 1283, 1143, 912 cm^{-1}; ^{1}H NMR (400 MHz, MeOD): δ 8.16 (2H, *J* = 8.8 Hz, H-3), 7.89 (2H, d, *J* = 8.6 Hz, H-2), 7.86 (2H, d, *J*= 8.8 Hz, H-2'), 6.93 (2H, d, *J* = 8.8 Hz, H-3'); ^{13}C (100 MHz, MeOD): δ169.2 (C_{quat}), 162.9 (C_{quat}), 156.8 (C_{quat}), 147.6 9 (C_{quat}) 132.9 (C_{quat}), 131.8 (C-3), 126.4 (C-2'), 123..2 (C-2), 116.8 (C-3'). HRMS (ESI) calculated for $C_{13}H_{10}N_2O_3$ *m/z* $[M+H]^+$:241.06077; found: 241.06173.

Synthesis of 3-(3',3'-dimethyl-6-nitrospiro[chromene-2,2'-indolin]-1'-yl)propyl 4-(dimethylamino)benzoate (2.48).

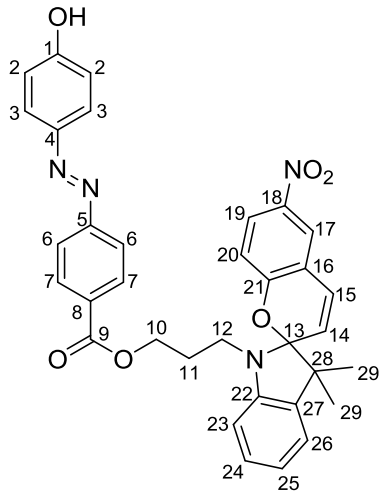


Azo compound **2.46d** (57 mg, 0.21 mmol, 1 eq) was stirred together with spiropyran **2.8** (100m mg, 0.21 mmol, 1.00 eq) and K_2CO_3 (43 mg, 0.32 mmol, 1.50 eq) in DMSO for 6 h. Water was then added into the solution which was then extracted repeatedly with DCM until the water layer turned yellow. The organic layers were dried over $MgSO_4$ concentrated *in vacuo* and purified though using flash column

chromatography. Product eluted at Petrol 40-60: EA = 15:1. (R_f = 0.36 Petrol 40:60:EA = 3:1)

Orange-red solid (79% yield); IR (neat): 2964, 2361, 2341, 1714, 1650, 1599 (C=C), 1519 (NO2), 1481, 1364, 1336 (NO2), 1271 (C-O), 1136, 1093, 955, 746cm-1; ^{1}H NMR (400 MHz, CD_2Cl_2): δ 8.07 – 8.10 (2H, m, H-7), 8.00 (1H, dd, J = 9.1, 2.7 Hz, H-19), 7.86 – 7.95 (5H, m, H-3, 6, 17), 7.19 (1H, ddd, J = 7.6, 7.6, 1.2 Hz, H- 24), 7.12 (1H, dd, J = 7.1, 0.7 Hz H-26), 6.89 (1H, ddd, H = 87.3, 7.3, 0.7 Hz, H-25), 6.78 – 6.83 (4H, m, H-2, 15, 20), 6.66 (1H, d, J = 7.8 Hz, H-23),5.90 (1H, d, J = 10.5 Hz, H-14), 4.36 – 4.40 (2H, m, H-10), 3.28 – 3.50 (2H, m, H- 12), 3.11 (6H, s, H-30), 2.03 – 2.22 (2H, m, H-11), 1.29 (3H, s, H-29), 1.20 (3H, s, H-29); ^{13}C (100 MHz, CD_2Cl_2): δ 166.5 (C_{quat}), 160.0(C_{quat}), 156.6 (C_{quat}), 153.7 (C_{quat}), 147.5 (C_{quat}), 141.6 (C_{quat}), 136.8 (C_{quat}), 130.9 (C-7), 130.7 (C_{quat}), 128.9 (C-20), 128.3 (C-24), 126.3 (C-19), 126.0 (C-6), 123.2 (C-17), 122.5 (C-3), 122.3 (C-26), 122.2 (C-14), 120.2 (C-25), 119.2 (C_{quat}), 116.0 (C-15), 112.0 (C-2), 107.4 (C_{quat}), 107.3 (C-23), 62.9 (C-10), 53.1 (C_{quat}), 40.9 (C-12), 40.6 (C-30), 28.6 (C-11), 26.4 (C-29), 20.1 (C-29). HRMS (ESI) calculated for $C_{36}H_{35}N_5O_5$ *m/z* $[M+H]^+$: 618.27110 ; found: 618.27098.

Synthesis of 3-(3',3'-dimethyl-6-nitrospiro[chromene-2,2'-indolin]-1'-yl)propyl 4-hydroxybenzoate. (2.49).



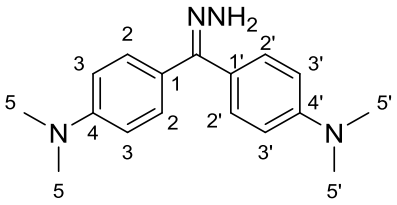
Azo compound **2.47d** (51 mg, 0.21 mmol, 1.00 eq) was stirred together with spiropyran **2.8** (100m mg, 0.21 mmol, 1.00 eq) and K_2CO_3 (43 mg, 0.32 mmol, 1.50 eq) in DMSO for 6 h. Water was then added into the solution which was then extracted repeatedly with DCM. The organic layers were dried over $MgSO_4$ concentrated in *vacuo* and purified though using flash column chromatography. The product eluted at Petrol: EA = 15:1. (R_f = 0.36 in Petrol 40:60:EA = 3:1)

Orange-red solid (72% yield); IR (neat): 3363, 2965, 2360, 1716, 1652, 1605, 1518, 1481, 1381, 1336, 1274, 1165, 1138, 1012, 908, 773cm-1; ^{1}H NMR (400 MHz, $CDCl_3$): δ 8.09 – 8.12 (2H, m, H-7), 8.02 (1H, dd, J = 8.8, 2.7 Hz, H-19), 7.88 – 7.97 (5H, m, H-3, 6, 17), 7.121 (1H, ddd, J = 7.6, 7.6, 1.2 Hz, H- 24), 7.12 (1H, dd, J = 7.1, 0.7 Hz, H-26), 6.97 – 7.01 (2H, m, H-2), 6.92 (1H, ddd, J = 7.6, 7.6, 0.7 Hz, H-25), 6.77 (1H, d, J = 8.8 Hz, H-20), 6.76 (1H, d, J = 10.3 Hz, H-15), 6.65 (1H, d, J = 7.6 Hz, H-23), 5.87 (1H, d, J = 10.5 Hz, H-14), 4.36 – 4.47 (2H, m, H-10), 3.30 – 3.48 (2H, m, H- 12), 2.05 – 2.22 (2H, m, H-11), 1.29 (3H, s, H-29), 1.20 (3H, s, H-29); ^{13}C (100 MHz, $CDCl_3$): δ 166.1 (C_{quat}), 159.4(C_{quat}), 159.2 (C_{quat}), 155.5 (C_{quat}), 147.1 (C_{quat}), 146.8 (C_{quat}), 141.0 (C_{quat}), 136.1 (C_{quat}), 130.9 (C_{quat}), 130.5 (C-7),

128.2 (C-15), 127.8 (C-24), 125.9 (C-19), 125.5 (C-6), 122.7 (C-17), 122.4 (C-3), 121.8 (C-26), 121.6 (C-14), 119.8 (C-25), 118.3 (C_{quat}), 116.0 (C-2), 115.6 (C-2), 106.7 (C_{quat}), 106.6 (C-23), 62.6 (C-10), 52.5 (C_{quat}), 40.4 (C-12), 27.9 (C-11), 26.0 (C-29), 19.9 (C-29). HRMS (ESI) calculated for $C_{34}H_{30}N_4O_6$ *m/z* $[M+Na]^+$: 613.2-576 ; found: 613.20546.

7.5 Experimental for Chapter 3

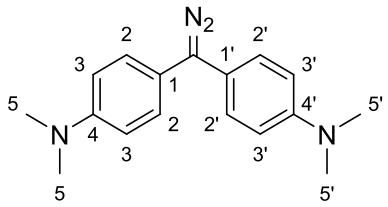
Synthesis of 4,4'-(Hydrazonomethylene)bis(N,N-dimethylaniline) (3.2a1).



Michler's ketone (1.50 g, 5.60 mmol, 1.00 eq) was suspended in EtOH (20 mL). After adding hydrazine monohydrate (4.06 mL, 84.0 mmol, 15.00 eq) into the suspension, the reaction mixture was stirred under reflux condition for 72 h. After cooling the reaction mixture to room temperature, the mixture was cooled in ice bath to crystalize out the products, which were then filtered out, washed with minimal amount of 2-propanol and dried, giving white-yellow soild (1.22 g, 77% yield).

Yellow-white solid. M.P: 153-154°C (lit.[26] m.p 151-152 °C). I.R: 2802, 1608 (C=C), 1519 (C=C), 1341(C-N), 1190, 1166, 1061, 994, 820; ^{1}H NMR (400 MHz, $CDCl_3$): δ7.40 (2H, m, H-2/2'), 7.19 (2H, m, H-2/2'), 6.83 (2H, m, H-3/3'), 6.65 (2H, m, H-3/3'), 3.03 (6H, s, H-5/5'), 2.96 (6H, s, H-5/5'); ^{13}C (100 MHz, $CDCl_3$): δ151.1 (C_{quat}), 150.3 (C_{quat}), 129.9 (C-2,2'), 127.9 (C-2,2'), 127.7 (C_{quat}), 120.5 (C_{quat}), 112.4 (C-3,3'), 111.7 (C-3,3'), 40.4 (C-5,5'), 40.3 (C-5,5'). LRMS (ESI) m/z: $[M+H]^+$: 283.2. HRMS (ESI) calculated for $C_{17}H_{23}N_4$ *m/z* $[M+H]^+$: 283.1917; found: 283.1908.

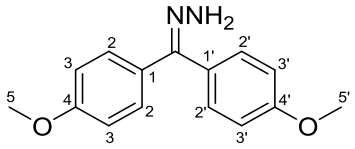
Synthesis of 4,4'-(Diazomethylene)bis(N,N-dimethylaniline) (3.3a1).



Hydrazone **3.2a1** (500 mg, 1.77 mmol, 1.00 eq), MnO_2 (308 mg, 3.54 mmol, 2.60 eq) and Na_2SO_4 (640 mg, 4.42 mmol, 2.50 eq) was added into a RBF wrapped in aluminium foil, and stirred in EtOH (10 mL). KOH saturated in EtOH (3mL) was then added, and the reaction mixture was stirred in the dark for 3 h. After filtering through a celite pad, the filtrate collected was concentrated *in vacuo* in the dark and used immediately. The resulting mixture was a dark green slime (crude 440 mg, 90% yield).

I.R (neat): 3389, 2021 ($=N^+=N^-$ diazo), 1610 (C=C), 1519 (C=C), 1444, 1370, 1226, 1167, 1070, 945, 820 cm^{-1}. No NMR due to compound being too unstable in light.

Synthesis of (Bis(4-methoxyphenyl)methylene)hydrazine (3.2a2).

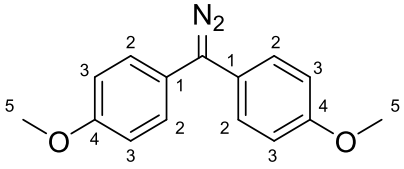


Hydrazine monohydrate (2.00 mL, 20.6mmol, 10.00 eq) was added to a suspension of 4,4'-dimethoxybenzophenone (1.00g, 4.13 mmol, 1.00 eq) in EtOH (20 mL), stirred and refluxed for 24 h. The reaction was then cooled to room temperature, and EtOH was removed *in vacuo*. The reaction mixture was then extracted with DCM. The organic layer was washed with brine and dried over anhydrous Na_2SO_4, filtered, and dried under vacuum. (Alternatively, 10 – 15m L of H_2O was added into reaction mixture and EtOH was removed *in vacuo* until product started to precipitate.

The reaction mixture was then placed in ice bath for an hour before the precipitated white soild (912mg, 86% crude yield) was collected on a Büchner funnel and dried.

White solid; M.P: 83 – 84 °C; IR (neat): 1607 (C=C), 1509 (C=C), 1246 (C-O), 1172, 1031, 834 cm^{-1};^{1}H NMR (400 MHz, $CDCl_3$): δ 7.41 (2H, m, H-2/2'), 7.23 (2H, m, H-2/2'), 7.05 (2H, m, H-3/3'), 6.83 (2H, m, H-3/3'), 3.88 (3H, s, H-5/5'), 3.81 (3H, s, H-5/5'; ^{13}C (100 MHz, $CDCl_3$): δ 159.8 (C_{quat}), 159.6 (C_{quat}), 149.3 (C_{quat}), 130.2 (C-2/2'), 127.9 (C-2/2'), 125.0 (C_{quat}), 114.6 (C-3/3'), 113.4 (C-3/3'), 55.3 (C-5/5'), 55.2 (C-5/5)'. LRMS (ESI) m/z: $[M+H]^+$: 257.1. HRMS (ESI) calculated for $C_{22}H_{24}N_2O_4$ *m/z* $[M+H]^+$: 257.1285 ; found: 257.1278.

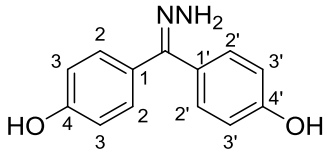
Synthesis of 4,4'-(Diazomethylene)bis(methoxybenzene) (3.3a2).



Hydrazone **3.2a2** (1.00g, 3.90mmol, 1.00 eq) was stirred with MnO_2 (882 mg, 10.14mmol, 2.60 eq) and Na_2SO_4 (776 mg, 5.46 mmol, 1.40 eq) in THF (10 mL). KOH saturated in EtOH (0.20 mL) was then added to the reaction mixture, which was stirred in the dark for 18 h. The mixture is then filtered through a celite pad, eluted using DCM. The filtrate was concentrated and dried *in vacuo* (in the dark) to give a dark purple solid.

Dark purple solid; M.P: 88-90 °C; IR (neat): 2954, 2836, 2027 (N=N), 1606 (C=C), 1507 (C=C), 1466, 1441, 1244, 1178, 1027, 830 cm^{-1}; ^{1}H NMR (200 MHz, $CDCl_3$): δ 7.20 (4H, m, H-2), 6.96 (4H, m, H-3) 3.83 (6H, s, H-5); ^{13}C (50 MHz, $CDCl_3$): δ157.7 (C-4), 126.5 (C-2), 121.5 (C-1), 114.8 (C-3), 53.4 (C-5). HRMS (TOF MS FI+) calculated for $C_{15}H_{14}N_2O_2$ *m/z* $[M+]^+$: 254.1055 ; found: 254.1049.

Synthesis of 4,4'-(hydrazonomethylene)diphenol (3.2a3)

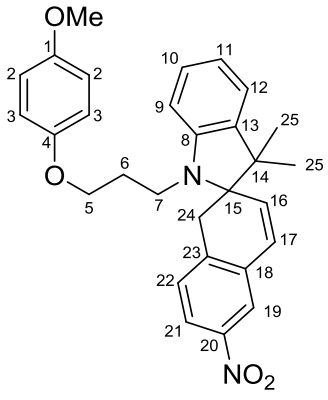


4,4’-Dihydroxybenzophenone was (1.00 g, 4.67 mmol, 1.00 eq) was refluxed with hydrazine monohydrate (2.3 mL, 46.7 mmol, 10.0 eq) in EtOH (15 mL) for 48h. After which, about 5mL of water was added to the hot reaction mixture, and the reaction mixture was cooled down to room temperature before some EtOH was removed *in vacuo*, and the reaction mixture was then placed in ice bath to crystalize out the product as white solid. The white solid was filtered out on a Büchner funnel, washed with cold water and dried (0.972 g, 91% yield).

I.R (neat): 3346 (broad –OH), 2361, 1608 (C=C), 1511 (C=C), 1439, 1335 (C-N), 1241, 1106, 836; ^{1}H NMR (400 MHz, MeOD): δ 7.24 (2H, m, H-2/2’), 7.10 (2H, m, H-2/2’), 6.94 (2H, m, H-3/3’), 6.69 (2H, m, H-3/3’), 4.89 (s, -OH’); ^{13}C (100 MHz, $CDCl_3$): δ 159.5 (C-4/4’), 159.3 (C-4/4’), 153.2 (C_{quat}), 131.9 (C_{quat}), 1301.4 (C-2/2’), 129.6 (C-2/2’), 125.4 (C_{quat}), 117.2 (C-3/3’), 116.0 (C-3/3’). HRMS (ESI) calculated for $C_{13}H_{13}N_2O_2$ *m/z* $[M+H]^+$: 229.0972; found: 229.0976.

7.6 Experimental for Chapter 4:

Synthesis of 1-(3-(4-methoxyphenoxy)propyl)-3,3-dimethyl-6'-nitro-1'H-spiro[indoline-2,2'-naphthalene] (4.2).



4-Methoxyphenol (57 mg, 0.21 mmol, 1 eq) and spiropyran **2.8** (119 mg, 0.25 mmol, 1.2 eq) was dissolved in MeCN (15 mL). K_2CO_3 was added into the mixture and refluxed for 5 h. After cooling reaction mixture to room temperature, the organic solvent was removed *in vacuo*. Water was then added and DCM was used for extraction. The organic layers were collected and combined, dried over MgSO4, concentrated in *vacuo* and purified on flash column. Product was eluted with Petrol 40-60: EA= 35:1. (R_f = 0.36 in Petrol:EA = 9:1).

Red oil; IR (neat): 2963, 1610 (C=C), 1508 (C=C), 1482, 1336 (NO_2), 1272, 1232, 1165, 1090, 1033, 950 cm-1; ^{1}H NMR (400 MHz, $CDCl_3$): δ 7.98 – 8.03 (2H, m, H-18, 20), 7.20 (1H, ddd, J = 7.6, 7.6, 1.2 Hz, H-10), 7.11 (1H, dd, J = 7.1, 0.7 Hz, H-12), 6.89 (1H, dd, J = 7.2, 7.2 Hz, H- 11), 6.78 – 6.86 (5H, m, H-2, 3,16), 6.74 (1H, d, H = 8.8 Hz, H-21), 6.65 (1H, d, J = 7.8 Hz, H-9), 5.77 (1H, d, J = 10.5 Hz, H-15), 3.95 (2H, t, J = 5.9 Hz, H-5), 3.70 (3H, s, H-24), 3.45 – 3.53 (1H, m, H-7), 3.29 – 3.36 (1H, m, H-7), 2.00 – 2.14 (2H, m, H-6), 1.29 (3H, s, H-23), 1.18 (3H, s, H-23);); ^{13}C (100 MHz, $CDCl_3$): δ 159.5 (C-19), 153.8 (C_{quat}), 152.7 (C_{quat}), 147.0 (C_{quat}), 140.9 (C_{quat}), 136.0 (C_{quat}), 128.0 (C-16), 127.8 (C-10), 125.8 (C-18/20), 122.6 (C-18/20), 121.8 (C-15), 121.7 (C-12), 119.5 (C-11), 118.5 (C_{quat}), 115.5 (C-21), 115.1 (C-2/3), 114.6 (C-2/3), 106.7 (C-9), 65.2 (C-6), 55.7 (C-24), 52.6 (C_{quat}), 40.2 (C-7), 28.5 (C-6), 25.9 (C-23), 19.8 (C-23). HRMS (ESI) calculated for $C_{28}H_{28}N_2O_5$ *m/z* $[M+H]^+$: 473.20710 ; found: 473.20638.

Procedure for photochromic activity measurement:

For solution: The photochromic compound was first dissolved in the solvent and leave to stand in light for at least 1 h. After which, the solution was transferred carefully into a quarts vial using a syringe. A UV-Vis absorbance data was measured. After which, the quartz vial containing the solution was carefully

transferred to the UV-box for UV-irradiation at 360 – 375 nm for 1 min. The quartz vial with the photochromic solution was then transferred immediately back to the UV-Vis spectrophotometer for absorbance measurement.

For beads, pellets, powders: The sample was first transferred carefully into the small sample holder made for the diffused reflectance accessary. A UV-Vis diffused reflectance spectrum was recorded. After which, the sample holder was transferred from the UV-Vis spectrophotometer to the UV-box where the photochromic sample was exposed to UV irradiated at 360 – 375 nm for 1 min. The sample holder was then transferred immediately back to the UV-Vis spectrophotometer for diffused reflectance measurement.

For flat samples: UV-Vis transmittance spectrum for photochromic flat substrates was first collected. After which, the sample was UV irradiated at 360 – 375 nm for 1 min, and transferred back to the UV-Vis spectrophotometer for another transmittance measurement (For all UV-Vis spectra, see Appendix D).

Sample preparation for bioassay

For beads, pellets and powders: A stock solution of 5 µmol/mL of Penicillin V K salt solution was prepared. 200 mg of blank (for control experiment) or modified beads were weighed out into a vial. The vial was then filled with 0.5 mL of MeOH, followed by 4.5 mL of the Penicillin V K salt solution. After capping the vial, the beads were submerged for 18 h in the fridge. After which, the beads were rinsed with water (3 x 5 mL) and acetone (3 x 5 mL), and dried for 30 min. The beads were kept refrigerated for further tests and analyses.

For flat samples: Two different stock solutions were prepared. Samples for testing with *S.aureus* were immersed in 0.5 mg/mL Penicillin V K salt solution (stock

solution A), and samples for testing with *E.Coli* were immersed in 1 mg/mL Penicillin V solution (stock solution B). Each vial was filled 4.5 mL of either Penicillin V K salt solution.

Flat substrates were first cut into 0.5 cm x 0.5 cm small pieces. For every sample or control, 6 pieces of the substrate were immersed in a vial with stock solution A, and another 6 pieces submerged in stock solution B, and left to stand in the refrigerator for 18h. The pieces were then dried using nitrogen individually.

Hole-plate bioassay

Agar plates were prepared by Ms Wendy Sobey. Modified beads loaded with Penicillin V were tested again *Escherichia coli* (*E.coli*) and *Staphylococcus aureus* (*S. aureus*). Samples were transferred carefully into various wells, and then covered with liquid agar, which will solidify after some time. The plates were then placed into an incubator for 18h at 37°C in the dark. Inhibition zones were measured in mm. Cephalosporin C was used for calibration as a measure of biocide activity. Calibration by Penicillin V was also conducted (See Appendix H for calibration and bioassay results).

HPLC-MS method

Surface modified beads that were loaded with Penicillin V were placed into individual mass spec vials. After which, each vial was filled with 0.5 mL of MeOH, followed by 1.5mL of H_2O, and left to stand **(Light**: in the fumehood with lights on at room temperature, **Dark**: vials were warpped in aluminium foil and left to stand in fumehood at room temperature, or **Fridge**: vials were warpped in aluminum foil and placed in the refrigerator at sub-zero degree Celsius). After 1h, the whole 2.0mL aliquot of solution was drawn from each sample vial, into a new mass spectrometry

vial, ready for HPLC-MS injection. (Beads are left the sample vial). A fresh aliquot of 0.5mL MeOH and 1.5mL H_2O was then injected into the sample vial, and left to stand for another 1h. The aliquots are drawn at hourly interval for 5 h, and left to stand overnight for 19h (total of 24 h).

Known concentration of Penicillin V solutions were injected into HPLC-MS to generate a calibration graph using the peak area from the chromatogram. Samples were then injected into the HPLC-MS and peak areas measured were correlated to the calibration graph to give the concentration of Penicillin V in the sample. By plotting the cumulative graph of Penicillin V released, amounts of Penicillin V released by the beads in total were estimated. (See calibration and results in Appendix I).

7.7 Experimental for chapter 5:

T-peel test sample preparation

PET sheets were first cut into pieces using a pen-knife, with the dimension of 3" x 1". 1" x 1" area at the end of each piece was marked out for application of adhesive. The two pieces were then manually pressed together for at least 30 s (as shown in **Figure 5.1**), and left to dry in the fumehood for 18 h.

Lapshear test sample preparation

PC sheets were cut into 2" x 1" pieces using a mechanical wet diamond saw. 1" x 1" area at the end of each piece was marked out for application of adhesive. The two pieces were then manually pressed together for at least 30 s (as shown in **Figure 5.3**), and left to dry in the fumehood for 18 h.

Generation of adhesive from diaryldiazo

Area outside the 1" x 1" was first covered with masking. Then diaryldiazo was sprayed on the samples, after which, the masking was removed and the samples were placed onto the conveyor belt for high intensity UV-irradiation. Two sample pieces were then pressed together manually for at least 30 s, and left to dry in the fumehood for 18 h.

Alternatively, sprayed samples were heated on a heat plate, and pressed together immediately for at least 30 s when colour change of the diaryldiazo was observed. The samples were then left in fumehood with lights on for 18 h.

8 References

1. Jensen, W. B., The origin of the polymer concept. *J. Chem. Educ* **2008,** *85* (5), 624.
2. The Polymer Revolution. *New Internationalist* 1 Sep 2008, 2008.
3. Hoffman, A. S. In *Surface modification of polymers: physical, chemical, mechanical and biological methods*, Macromol. Symp., Hüthig & Wepf Verlag: 1996; pp 443-454.
4. Miller, R.; Yang, L.; Shechter, H., Orbital preferences in generation of singlet arylcarbenes. *J. Am. Chem. Soc.* **1977,** *99* (3), 938-939.
5. Miller, R.; Shechter, H., Electronic effects in the unimolecular decomposition of substituted diphenyldiazomethanes. *J. Am. Chem. Soc.* **1978,** *100* (25), 7920-7927.
6. Schuster, G. B., Structure and reactivity of carbenes having aryl substituents. *Adv. Phys. Org. Chem.* **1987,** *22*, 311-361.
7. Clayden, J.; Greeves, N.; Warren, S., *Organic Chemistry*. OUP Oxford: United Kingdom, 2012.
8. Skell, P. S.; Woodworth, R. C., Structure of carbene, CH2. *J. Am. Chem. Soc* **1956,** *78* (17), 4496-4497.
9. Etter, R. M.; Skovronek, H.; Skell, P. S., Diphenylmethylene, (C6H5)2C, A Diradical Species. *J. Am. Chem. Soc.* **1959,** *81* (4), 1008-1009.
10. Tomioka, H.; Tabayashi, K.; Ozaki, Y.; Izawa, Y., The effect of aryl substituents on arylcarbene reactivity. *Tetrahedron* **1985,** *41* (8), 1435-1440.
11. Moss, R. A.; Dolling, U. H., Photolysis of phenyldiazomethane in olefinic matrices. Chemistry of triplet phenylcarbene. *J. Am. Chem. Soc.* **1971,** *93* (4), 954-960.
12. Moss, R. A.; Joyce, M. A., Chemistry of fluorenylidene at low temperatures. *J. Am. Chem. Soc.* **1978,** *100* (14), 4475-4480.
13. Moss, R. A.; Huselton, J. K., Reactions of carbenes at low temperatures. Diphenylcarbene and isobutene. *J. Am. Chem. Soc.* **1978,** *100* (4), 1314-1315.
14. Moss, R. A.; Joyce, M. A., Reactions of methylphenylcarbene and phenylcarbene in isobutene matrices: origins of the" insertion" products. *J. Am. Chem. Soc.* **1977,** *99* (4), 1262-1264.
15. Tomioka, H.; Inagaki, T.; Izawa, Y., Photolysis of α-diazobenzylphosphonates in alcoholic matrices at 77 K. *J. Chem. Soc., Chem. Commun.* **1976,** (24), 1023-1024.
16. Tomioka, H.; Izawa, Y., Photolysis of aryldiazomethanes in alcoholic matrices. Temperature and host dependences of phenylcarbene processes in alcohols. *J. Am. Chem. Soc.* **1977,** *99* (18), 6128-6129.
17. Tomioka, H.; Okuno, H.; Izawa, Y., Carbenes in a rigid matrix. Substituent effects on the temperature dependence of α-carbonylcarbene reactions. *J. Chem. Soc., Perkin Trans. 2* **1980,** (11), 1636-1641.
18. Tomioka, H.; Suzuki, S.; Izawa, Y., Carbene in a rigid matrix. XII. Temperature and substituent effects on regioselectivity in the insertion of arylcarbene into alcohols. *J. Am. Chem. Soc.* **1982,** *104* (11), 3156-3162.
19. Tomioka, H., Reactions of carbenes in solidified organic molecules at low temperature. *Res. Chem. Intermed.* **1994,** *20* (6), 605-634.

20. Braybrook, D. R.; Moloney, M. G.; Osborn, H. M.; Norris, W. J., The preparation and reactivity of some photoactivable reactive dyes. *J. Photochem. Photobiol., A* **1993,** *70* (2), 171-178.
21. Blencowe, A.; Cosstick, K.; Hayes, W., Surface modification of nylon 6, 6 using a carbene insertion approach. *New J. Chem.* **2006,** *30* (1), 53-58.
22. Moloney, M. G.; Ebenezer, W.; Awenat, K. Process for surface functionalization of polymeric substrates using diaryl carbenes as reactive intermediates. 2 Mar, 2004, 2004.
23. Moloney, M.; Griffiths, J. P. Surface Functionalisation Using Arylcarbene Reactive Intermediates. 10 May, 2011, 2011.
24. Awenat, K. M.; Davis, P. J.; Moloney, M. G.; Ebenezer, W., A chemical method for the convenient surface functionalisation of polymers. *Chem. Commun.* **2005,** (8), 990-2.
25. Leonard, D.; Moloney, M. G.; Thompson, C., Chemical modification of materials by reaction with diaryl diazomethanes. *Tetrahedron Lett.* **2009,** *50* (26), 3499-3502.
26. Bagwell, C. L.; Leonard, D. M. L.; Griffiths, J.-P.; Moloney, M. G.; Stratton, N. J.; Travers, D. P., Post-Polymerization Modification of Materials using Diaryldiazomethanes: Changes to Surface Macroscopic Properties. *Macromol. React. Eng.* **2014,** *8* (2), 170 - 180.
27. Choong, C.; Foord, J. S.; Griffiths, J. P.; Parker, E. M.; Luo, B. W.; Bora, M.; Moloney, M. G., Post-polymerisation modification of surface chemical functionality and its effect on protein binding. *New J. Chem.* **2012,** *36* (5), 1187-1200.
28. Nelson, G. W.; Parker, E. M.; Singh, K.; Blanford, C. F.; Moloney, M. G.; Foord, J. S., Surface characterization and in situ protein adsorption studies on carbene-modified polymers. *Langmuir* **2015,** *31* (40), 11086-11096.
29. Choong, C.; Griffiths, J. P.; Moloney, M. G.; Triffitt, J.; Swallow, D., Direct introduction of phosphonate by the surface modification of polymers enhances biocompatibility. *React. Funct. Polym.* **2009,** *69* (2), 77-85.
30. Aphaiwong, A.; Moloney, M. G.; Christlieb, M., Surface functional polymer library by post-polymerisation modification using diarylmethylenes: metal ligand catch and release. *J. Mater. Chem.* **2012,** *22* (47), 24627-24636.
31. Wang, H.; Griffiths, J. P.; Egdell, R. G.; Moloney, M. G.; Foord, J. S., Chemical functionalization of diamond surfaces by reaction with diaryl carbenes. *Langmuir* **2008,** *24* (3), 862-868.
32. Griffiths, J. P.; Maliha, B.; Moloney, M. G.; Thompson, A. L.; Hussain, I., Surface Functional Polymers by Post-Polymerization Modification using Diarylcarbenes: Introduction, Release and Regeneration of Hydrogen Peroxide and Bactericidal Activity. *Langmuir* **2010,** *26* (17), 14142-14153.
33. Griffiths, J.-P.; Leonard, D. M. L.; Moloney, M. G.; Stratton, N. J., Control Of Wetting Behavior Using Post-Polymerization Modifications Of Surface Chemical Functionality. *J. Mol. Eng. Mater.* **2013,** *1* (1), 1250002-1250009.
34. Luksirikul, P.; Ballesteros, B.; Tobias, G.; Moloney, M. G.; Green, M. L. H., pH-triggered release of materials from single-walled carbon nanotubes using dimethylamino-functionalized fullerenes as removable "corks". *Carbon* **2010,** *48* (7), 1912-1917.
35. Luksirikul, P.; Ballesteros, B.; Tobias, G.; Moloney, M. G.; Green, M. L. H., Sidewall functionalisation of carbon nanotubes by addition of diarylcarbene derivatives. *J. Mater. Chem.* **2011,** *21* (47), 19080-19085.

36. Moloney, M. G., Functionalized polymers by chemical surface modification. *J. Phys. D: Appl. Phys.* **2008,** *41* (17), 174006.
37. Moloney, M.; Griffiths, J. P. Carbene precursor compound for producing an adhesive surface on a substrate. 10 Sep 2013, 2013.
38. Bouas-Laurent, H.; Dürr, H., Organic photochromism (IUPAC technical report). *Pure Appl. Chem.* **2001,** *73* (4), 639-665.
39. Bamfield, P.; Hutchings, M. G., *Chromic phenomena: technological applications of colour chemistry*. Royal Society of Chemistry: 2010.
40. Kobatake, S.; Irie, M., 8 Photochromism. *Annu. Rep. Prog. Chem., Sect. C: Phys. Chem.* **2003,** *99* (0), 277-313.
41. Klajn, R., Spiropyran-based dynamic materials. *Chem. Soc. Rev.* **2014,** *43* (1), 148-184.
42. Dürr, H.; Bouas-Laurent, H., *Photochromism: molecules and systems*. Gulf Professional Publishing: 2003.
43. Berkovic, G.; Krongauz, V.; Weiss, V., Spiropyrans and spirooxazines for memories and switches. *Chem. Rev.* **2000,** *100* (5), 1741-1753.
44. Minkin, V., Photo-, thermo-, solvato-, and electrochromic spiroheterocyclic compounds. *Chem. Rev.* **2004,** *104* (5), 2751-2776.
45. Metelitsa, A.; Lokshin, V.; Micheau, J.; Samat, A.; Guglielmetti, R.; Minkin, V., Photochromism and solvatochromism of push–pull or pull–push spiroindolinenaphthoxazines. *Phys. Chem. Chem. Phys.* **2002,** *4* (18), 4340-4345.
46. Fischer, E.; Hirshberg, Y., Formation of coloured forms of spirans by low-temperature irradiation. **1952,** (Nov), 4522-4524.
47. Görner, H., Photochromism of nitrospiropyrans: effects of structure, solvent and temperature. *Phys. Chem. Chem. Phys.* **2001,** *3* (3), 416-423.
48. Krysanov, S.; Alfimov, M., Ultrafast formation of transients in spiropyran photochromism. *Chem. Phys. Lett.* **1982,** *91* (1), 77-80.
49. Irie, M.; Menju, A.; Hayashi, K., Photoresponsive polymers. Reversible solution viscosity change of poly (methyl methacrylate) having spirobenzopyran side groups. *Macromolecules* **1979,** *12* (6), 1176-1180.
50. Song, X.; Zhou, J.; Li, Y.; Tang, Y., Correlations between solvatochromism, Lewis acid-base equilibrium and photochromism of an indoline spiropyran. *J. Photochem. Photobiol., A* **1995,** *92* (1), 99-103.
51. Swansburg, S.; Buncel, E.; Lemieux, R. P., Thermal racemization of substituted indolinobenzospiropyrans: evidence of competing polar and nonpolar mechanisms. *J. Am. Chem. Soc.* **2000,** *122* (28), 6594-6600.
52. Charvat, R. A., *Coloring of Plastics: Fundamentals*. Wiley: 2005.
53. Hirshberg, Y.; Fischer, E., Photochromism and reversible multiple internal transitions in some spiro pyrans at low temperatures. Part I. *J. Chem. Soc.* **1954**, 297-303.
54. Hirshberg, Y.; Fischer, E., Photochromism and reversible multiple internal transitions in some spiro Pyrans at low temperatures. Part II. *J. Chem. Soc.* **1954**, 3129-3137.
55. Suppan, P.; Ghonheim, N., Solvatochromism. The Royal Society of Chemistry: 1997.
56. Radu, A.; Byrne, R.; Alhashimy, N.; Fusaro, M.; Scarmagnani, S.; Diamond, D., Spiropyran-based reversible, light-modulated sensing with reduced photofatigue. *J. Photochem. Photobiol., A* **2009,** *206* (2), 109-115.
57. Adelmann, R.; Mela, P.; Gallyamov, M. O.; Keul, H.; Möller, M., Synthesis of high - molecular - weight linear methacrylate copolymers with spiropyran side

groups: Conformational changes of single molecules in solution and on surfaces. *J. Polym. Sci. A Polym. Chem.* **2009,** *47* (5), 1274-1283.
58. Bertoldo, M.; Nazzi, S.; Zampano, G.; Ciardelli, F., Synthesis and photochromic response of a new precisely functionalized chitosan with “clicked” spiropyran. *Carbohydr Polym.* **2011,** *85* (2), 401-407.
59. Sugiura, S.; Szilágyi, A.; Sumaru, K.; Hattori, K.; Takagi, T.; Filipcsei, G.; Zrínyi, M.; Kanamori, T., On-demand microfluidic control by micropatterned light irradiation of a photoresponsive hydrogel sheet. *Lab Chip* **2009,** *9* (2), 196-198.
60. Sugiura, S.; Sumaru, K.; Ohi, K.; Hiroki, K.; Takagi, T.; Kanamori, T., Photoresponsive polymer gel microvalves controlled by local light irradiation. *Sens. Actuators, A* **2007,** *140* (2), 176-184.
61. Sumaru, K.; Ohi, K.; Takagi, T.; Kanamori, T.; Shinbo, T., Photoresponsive properties of poly (N-isopropylacrylamide) hydrogel partly modified with spirobenzopyran. *Langmuir* **2006,** *22* (9), 4353-4356.
62. Davis, D. A.; Hamilton, A.; Yang, J.; Cremar, L. D.; Van Gough, D.; Potisek, S. L.; Ong, M. T.; Braun, P. V.; Martínez, T. J.; White, S. R., Force-induced activation of covalent bonds in mechanoresponsive polymeric materials. *Nature* **2009,** *459* (7243), 68-72.
63. Ciardelli, F.; Fabbri, D.; Pieroni, O.; Fissi, A., Photomodulation of polypeptide conformation by sunlight in spiropyran-containing poly (L-glutamic acid). *J. Am. Chem. Soc.* **1989,** *111* (9), 3470-3472.
64. Cooper, T. M.; Natarajan, L. V.; Miller, C. G., Control by ring substitution of the conformation change dynamics in photochromic polypeptides. *J. Photochem. Photobiol.* **1999,** *69* (2), 173-176.
65. Aizawa, M.; Namba, K.; Suzuki, S., Light-induced enzyme activity changes associated with the photoisomerization of bound spiropyran. *Arch. Biochem. Biophys.* **1977,** *182* (1), 305-310.
66. Namba, K.; Suzuki, S., Photo-control of enzyme activity with a photochromic spiropyran compound-modification of. ALPHA.-amylase with spiropyran compound. *Chem. Lett.* **1975,** (9), 947-950.
67. Karube, I.; Ishimori, Y.; Suzuki, S., Photocontrol of affinity chromatography: I. Trypsin purification by photosensitive soybean trypsin inhibitor (STI) gel. *Anal. Biochem.* **1978,** *86* (1), 100-106.
68. Karube, I.; Ishimori, Y.; Suzuki, S.; Sato, T., Photocontrol of affinity chromatography: Purification of asparaginase by photosensitive AHA ‐ gel. *Biotechnol. Bioeng.* **1978,** *20* (11), 1775-1783.
69. Odonkor, S.; Addo, K., Bacteria resistance to antibiotics: recent trends and challenges. *Int. J. Biol. Med. Res.* **2011,** *2* (4), 1204-10.
70. Davies, P., Does increased use of antibiotics result in increased antibiotic resistance? *Clin. Infect. Dis.* **2004,** *39* (1), 18-19.
71. Leung, E.; Weil, D. E.; Raviglione, M.; Nakatani, H., The WHO policy package to combat antimicrobial resistance. *Bull. World Health Organ.* **2011,** *89* (5), 390-392.
72. Wise, J., Report calls for $2 bn global fund to kickstart antibiotic development. *BMJ* **2015,** *350*, h2635.
73. Bragginton, E. C.; Piddock, L. J., UK and European Union public and charitable funding from 2008 to 2013 for bacteriology and antibiotic research in the UK: an observational study. *Lancet. Infect. Dis.* **2014,** *14* (9), 857-868.

74. Wang, L. C.; Chen, X. G.; Yu, L. J.; Li, P. W., Controlled drug release through carboxymethyl‐chitosan/poly (vinyl alcohol) blend films. *Polym. Eng. Sci.* **2007,** *47* (9), 1373-1379.
75. Lecomte, F.; Siepmann, J.; Walther, M.; MacRae, R.; Bodmeier, R., Polymer blends used for the aqueous coating of solid dosage forms: importance of the type of plasticizer. *J. Control. Release* **2004,** *99* (1), 1-13.
76. Lecomte, F.; Siepmann, J.; Walther, M.; MacRae, R. J.; Bodmeier, R., pH-sensitive polymer blends used as coating materials to control drug release from spherical beads: elucidation of the underlying mass transport mechanisms. *Pharm. Res.* **2005,** *22* (7), 1129-1141.
77. Siepmann, F.; Siepmann, J.; Walther, M.; MacRae, R.; Bodmeier, R., Polymer blends for controlled release coatings. *J. Control. Release* **2008,** *125* (1), 1-15.
78. Claude, C. D. Controlled morphologies in polymer drug for release of drugs from polymer films. 24 Aug 2004, 2004.
79. Mi, F.-L.; Lin, Y.-M.; Wu, Y.-B.; Shyu, S.-S.; Tsai, Y.-H., Chitin/PLGA blend microspheres as a biodegradable drug-delivery system: phase-separation, degradation and release behavior. *Biomaterials* **2002,** *23* (15), 3257-3267.
80. Hoare, T. R.; Kohane, D. S., Hydrogels in drug delivery: progress and challenges. *Polymer* **2008,** *49* (8), 1993-2007.
81. Bell, T., Surface engineering: a rapidly developing discipline. *Eur. J. Eng. Educ.* **1987,** *12* (1), 27-32.
82. Dong, H., Guest editorial: in memory of Tom Bell. *Surf. Eng.* **2013**.
83. Handbook, A., *Vol. 5: Surface Engineering*. 1994; p 345-347.
84. Kennedy, D.; Xue, Y.; Mihaylova, E. Current and future applications of surface engineering 2005. http://arrow.dit.ie/cgi/viewcontent.cgi?article=1027&context=engschmecart.
85. Strafford, K. N., *Surface Engineering: Processes and Applications*. CRC Press: 1994; p 349.
86. Littlefair, G.; Gibson, I.; Usma, C.; Collins, P.; Hilditch, T.; Mohammed, M. I.; Haswell, S., Proceedings of The 1st International Design Technology Conference, DESTECH2015, GeelongLab-on-a-chip or Chip-in-a-lab: Challenges of Commercialization Lost in Translation. *Procedia Technology* **2015,** *20*, 54-59.
87. Group, S. E. A. C. S. I. *Time for Strategic Change: UK surface engineering and advanced coating Industry*; 2014.
88. Edmondson, G.; Valigra, L.; Kenward, M.; Hudson, R.; Belfield, H., Making Industry-University Partnerships Work. Lessons from Successful Collaborations. *Science Business Innovation Board* **2012**.
89. Lehr, J. H.; Ltd., J. W. S., *Wiley's Remediation Technologies Handbook: Major Contaminant Chemicals and Chemical Groups*. John Wiley & Sons: 2004; p 900.
90. Product Information of Amberlite® XAD-4. In *MSDS No.*, Sigma Aldrich: Saint Louis, Missouri, USA, 1998; Vol. 2016.
91. Singh, K., *Chemistry In Daily Life*. PHI Learning: 2012.
92. Shiraishi, Y.; Adachi, K.; Itoh, M.; Hirai, T., Spiropyran as a Selective, Sensitive, and Reproducible Cyanide Anion Receptor. *Org. Lett.* **2009,** *11* (15), 3482-3485.
93. Beyer, C.; Wagenknecht, H. A., Synthesis of spiropyrans as building blocks for molecular switches and dyads. *J. Org. Chem.* **2010,** *75* (8), 2752 - 2755.

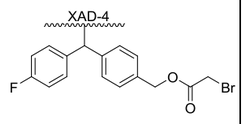
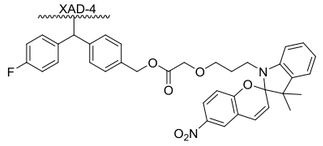
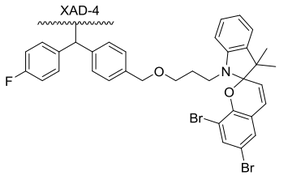
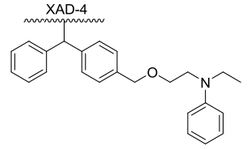
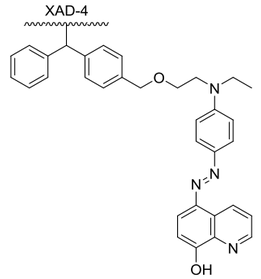
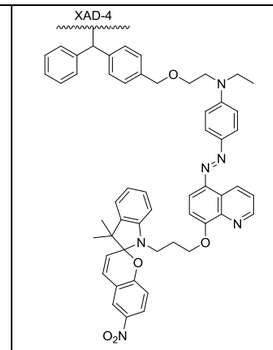
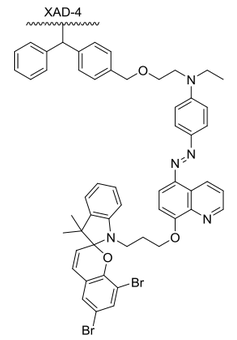
94. Zhang, W.; Cue, B. W., *Green techniques for organic synthesis and medicinal chemistry*. John Wiley & Sons: Chichester, West Sussex, 2012; p 768.
95. Aphaiwong, A. a.; Moloney, M. d. s. Functionalised polymers by surface modification using diaryl carbenes. Thesis (Ph.D.), University of Oxford, 2014.
96. Zollinger, H., *Color chemistry : syntheses, properties, and applications of organic dyes and pigments*. 2nd rev. ed. ed.; VCH: Weinheim ; Cambridge, 1991.
97. Hunger, K., *Industrial Dyes: Chemistry, Properties, Applications*. Wiley: 2003.
98. Fennema, O. R., *Food Chemistry, Third Edition*. Taylor & Francis: 1996.
99. Bishop, E., *Indicators: International Series of Monographs in Analytical Chemistry*. Elsevier Science: 2013.
100. Merino, E., Synthesis of azobenzenes: the coloured pieces of molecular materials. *Chem. Soc. Rev.* **2011,** *40* (7), 3835 - 3853.
101. Szele, I.; Zollinger, H., Azo coupling reactions structures and mechanisms. In *Preparative Organic Chemistry*, Springer Berlin Heidelberg: Berlin, Heidelberg, 1983; pp 1-66.
102. Gardner, J. H.; Joseph, L., Some Coloured Local Anesthetics. *J. Am. Chem. Soc.* **1935,** *57* (5), 901-901.
103. Work, E.; Work, T. S., *Chemical Modification of Proteins*. Elsevier Science: 1976.
104. Oger, N.; d'Halluin, M.; Le Grognec, E.; Felpin, F., Using Aryl Diazonium Salts in Palladium-Catalyzed Reactions under Safer Conditions. *Org. Process Res. Dev.* **2014,** *18* (12), 1786-1801.
105. Banks, R. E.; Thompson, A. R.; Vellis, H. S., Azo-coupling of 2,3,5,6-tetrafluoropyridine-4-diazonium fluoride with mesitylene and anisole. *J. Fluorine Chem.* **1983,** *22* (5), 499-501.
106. Bartle, M. G.; Mackie, R. K.; Tedder, J. M., Reaction of 2,4-dinitrobenzenediazonium ions with thiophens. An acidic Gomberg reaction. *J. Chem. Soc., Chem. Commun.* **1974,** (7), 271-272.
107. Huang, F.; Nie, Y.; Ye, F.; Zhang, M.; Xia, J., Site Selective Azo Coupling for Peptide Cyclization and Affinity Labeling of an SH3 Protein. *Bioconjugate Chem.* **2015,** *26* (8), 1613-1622.
108. Bahulayan, D.; John, L.; Lalithambika, M., - Modified Clays as Efficient Acid–Base Catalyst Systems for Diazotization and Diazocoupling Reactions. *Synth. Commun.* **2003,** *33* (- 6), - 863.
109. Wagner, N.; Theato, P., Light-induced wettability changes on polymer surfaces. *Polymer* **2014,** *55* (16), 3436-3453.
110. Vlassiouk, I.; Park, C.-D.; Vail, S. A.; Gust, D.; Smirnov, S., Control of Nanopore Wetting by a Photochromic Spiropyran: A Light-Controlled Valve and Electrical Switch. *Nano Lett.* **2006,** *6* (5), 1013-1017.
111. Safety Data Sheet for Michler's Ketone. http://www.sigmaaldrich.com/catalog/product/aldrich/147834?lang=en&region=SG.
112. Zarchi, M.; Karimi, M., Diazotization of anilines and diazo coupling with a coupling component mediated by a polymer-supported sodium nitrite and a polymeric acid. *J. Appl. Polym. Sci.* **2012,** *123* (5), 2762-2767.
113. Pavia, D. L.; Lampman, G. M.; Kriz, G. S.; Vyvyan, J. A., *Introduction to Spectroscopy*. Cengage Learning: 2008.
114. Lipp, C., Practical spray technology. *Lake Innovation LLC, Lake Jackson, TX* **2013**.
115. Daniels, C. A., *Polymers: Structure and Properties*. Taylor & Francis: 1989.

116. Zhou, J.; Khodakov, D. A.; Ellis, A. V.; Voelcker, N. H., Surface modification for PDMS-based microfluidic devices. *Electrophoresis* **2012,** *33* (1), 89-104.
117. McDonald, J. C.; Whitesides, G. M., Poly(dimethylsiloxane) as a material for fabricating microfluidic devices. *Acc. Chem. Res.* **2002,** *35* (7), 491-499.
118. Friend, J.; Yeo, L., Fabrication of microfluidic devices using polydimethylsiloxane. *Biomicrofluidics* **2010,** *4* (2), 026502.
119. Abbasi, F.; Mirzadeh, H.; Katbab, A.-A., Modification of polysiloxane polymers for biomedical applications: a review. *Polym. Int.* **2001,** *50* (12), 1279-1287.
120. Goddard, E. D.; Gruber, J. V., *Principles of Polymer Science and Technology in Cosmetics and Personal Care*. CRC Press: 1999.
121. Bélanger, M. C.; Marois, Y., Hemocompatibility, biocompatibility, inflammatory and in vivo studies of primary reference materials low-density polyethylene and polydimethylsiloxane: A review. *J. Biomed. Mater. Res.* **2001,** *58* (5), 467-477.
122. Federation, B. P. The British Plastics Federation (BPF). bpf.co.uk.
123. Reviews, C., *Introduction to Industrial Polyethylene , Properties, Catalysts, and Processes: Chemistry, Chemistry*. Cram101: 2016.
124. Carraher, C. E., *Introduction to Polymer Chemistry, Third Edition*. CRC Press: 2012.
125. Frazer, R. Q.; Byron, R. T.; Osborne, P. B.; West, K. P., PMMA: an essential material in medicine and dentistry. *J. Long Term Eff. Med. Implants* **2005,** *15* (6).
126. Temiz, Y.; Lovchik, R. D.; Kaigala, G. V.; Delamarche, E., Lab-on-a-chip devices: How to close and plug the lab? *Microelectron. Eng.* **2015,** *132*, 156-175.
127. Engineers, N. B. o. C., *Disposable Products Manufacturing Handbook*. NIIR Project Consuntancy Services: 2014.
128. Kumar, K. V.; Safiulla, M.; Ahmed, A. K., An Experimental Evaluation of Fiber Reinforced Polypropylene Thermoplastics for Aerospace Applications. *J. Mech. Eng.* **2014,** *43* (2), 92-97.
129. http://medacltd.com/.
130. Kulkarni, P.; Baron, P. A.; Willeke, K., *Aerosol Measurement: Principles, Techniques, and Applications*. Wiley: 2011.
131. Liu, P.; Chen, G. F., *Porous Materials: Processing and Applications*. Elsevier Science: 2014.
132. What is XPS? Analysis of surfaces and thin films. http://xpssimplified.com/whatisxps.php.
133. Yuan, Y.; Lee, T. R., Contact angle and wetting properties. In *Surface science techniques*, Springer: 2013; pp 3-34.
134. Tyer Jr, N. W.; Becker, R. S., Photochromic spiropyrans. I. Absorption spectra and evaluation of the. pi.-electron orthogonality of the constituent halves. *J. Am. Chem. Soc.* **1970,** *92* (5), 1289-1294.
135. Ko, C.-C.; Yam, V. W.-W., Transition metal complexes with photochromic ligands—photosensitization and photoswitchable properties. *J. Mater. Chem.* **2010,** *20* (11), 2063-2070.
136. Inouye, M.; Ueno, M.; Kitao, T.; Tsuchiya, K., Alkali metal recognition induced isomerization of spiropyrans. *J. Am. Chem. Soc.* **1990,** *112* (24), 8977-8979.
137. Shao, N.; Jin, J.; Cheung, S.; Yang, R.; Chan, W.; Mo, T., A spiropyran-based ensemble for visual recognition and quantification of cysteine and

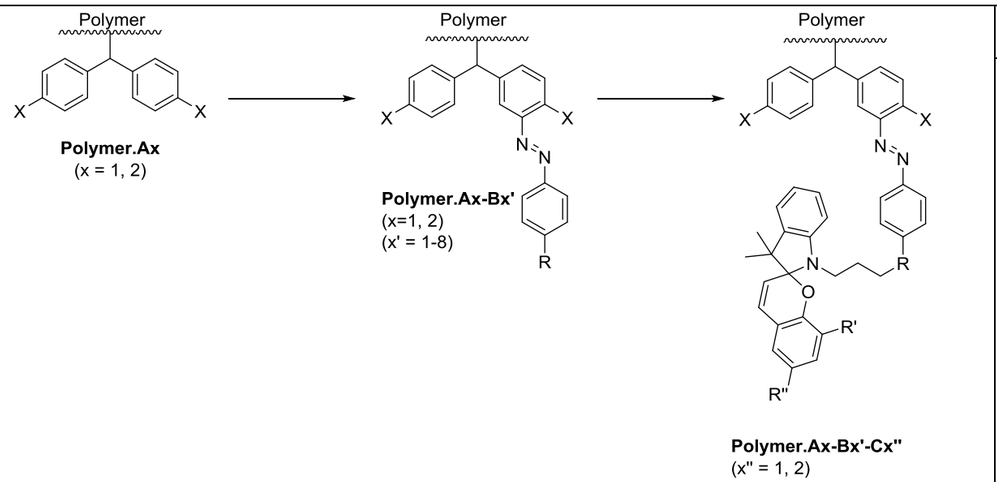
homocysteine at physiological levels. *Angew. Chem. Int. Ed.* **2006,** *45* (30), 4944-4948.
138. Good, R. J., On the definition of adhesion. *J. Adhes.* **1976,** *8* (1), 1-9.
139. Pocius, A. V., *Adhesion and adhesives technology: an introduction*. Carl Hanser Verlag GmbH Co KG: 2012.
140. da Silva, L. F. M.; Öchsner, A.; Adams, R. D., *Handbook of Adhesion Technology*. Springer Berlin Heidelberg: 2011.
141. Jellema, E.; Jongerius, A. L.; Reek, J. N.; de Bruin, B., C1 polymerisation and related C–C bond forming 'carbene insertion'reactions. *Chem. Soc. Rev.* **2010,** *39* (5), 1706-1723.
142. Corporation, S.-A., *Aldrich Chemistry 2012-2014: Handbook of Fine Chemicals*. Milwaukee, Wisconsin : Sigma-Aldrich, ©2011.: 2011; p 3216.

Appendix A: List of surface modified polymers

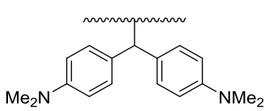
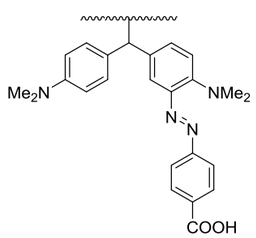
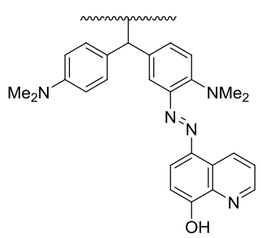
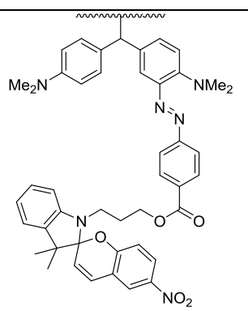
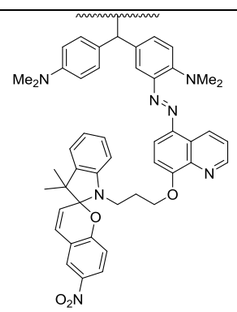
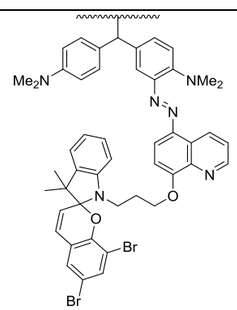
Chapter 2: Surface modifications of XAD-4 beads

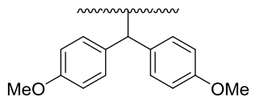
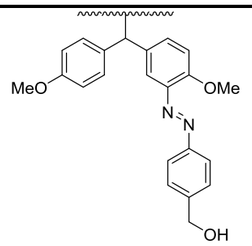
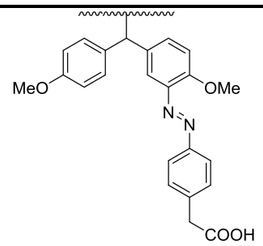
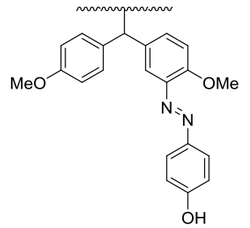
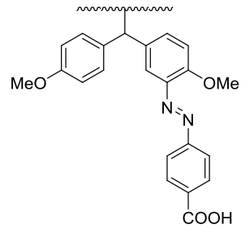
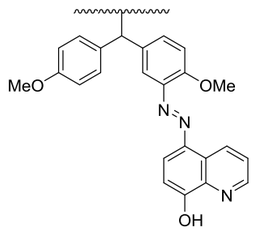
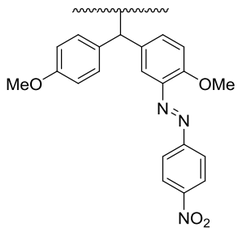
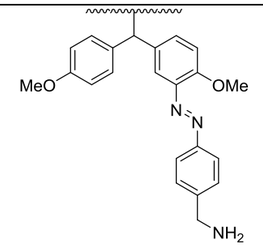
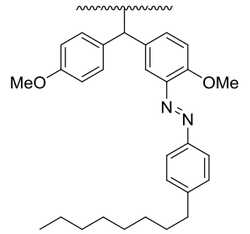
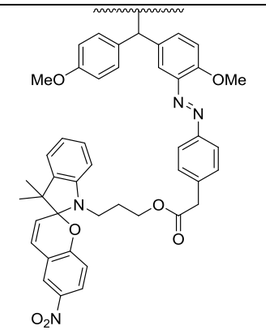
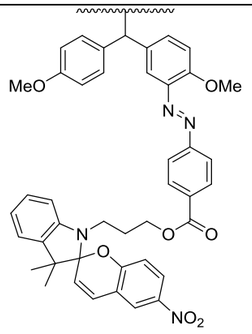
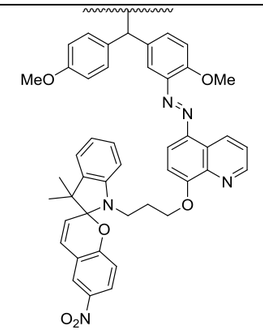
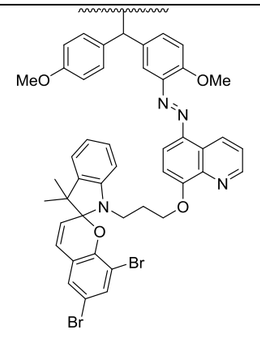
Modification							
Labelling	**2.17**	**2.18**	**2.20**	**2.26**	**2.29**	**2.30**	**2.31**

Chapter 3: Surface modification of various polymers



Polymers	
<u>Beads, pellets, powders</u> **XAD4** = XAD-4 polystyrene beads **PETp** = Polyethylene terephthalate pellets **LDPE** = Low Density Polyethylene powder **UHMW** = Ultra Hight Molecular Weight Polyethylene powder	<u>Flat substrates</u> **PDMS** = Polydimethoxysilane piece **PC** = Polycarbonate piece **PET** = Polyethylene terephthalate film **TPU** = Thermoplastic Polyurethane piece **COC** = Cyclic Olefin Copolymer piece **PMMA** = Poly(methyl methacrylate) piece **PS** = Polystyrene piece **PP** = Polypropylene piece

Modification						
Labelling	**A1**	**A1-B4**	**A1-B5**	**A1-B4-C1**	**A1-B5-C1**	**A1-B5-C2**

Modification					
Labelling	**A2**	**A2-B1**	**A2-B2**	**A2-B3**	**A2-B4**
Modification					
Labelling	**A2-B5**	**A2-B6**	**A2-B7**	**A2-B8**	
Modification					
Labelling	**A2-B2-C1**	**A2-B4-C1**	**A2-B5-C1**	**A2-B5-C2**	

Appendix B: Combustion Analysis Calculations and Results

Calculation method

Using sample **2.17** as an example:

- Given %Br = 0.87, as obtained from combustion analysis. (Outsourced to Medac Ltd)
- No. of mols of Br per g of polymer = $\frac{\%Br}{Mr\ (Br)} \div 100$

  $= \frac{0.87}{79.90} \div 100 = 1.09 \times 10^{-4}\ mols$
- Numbers of moles of surface modification per g of polymer = $\frac{mols\ of\ Br\ per\ g\ of\ polymer}{No.of\ Br\ atoms\ \ per\ molecule}$

  $= \frac{1.39 \times 10^{-4}}{1} = 1.09 \times 10^{-4} mols$
- Number of molecules of surface modification per g of polymer = mols of surface modification x Avogadro's number

  $= (1.05 \times 10^{-4}) \times (6.02214 \times 10^{23}) = 6.56 \times 10^{19}$
- Number of molecule of surface modification per cm^2 (given that lit surface area of XAD-4 is $725m^2/g$)

  $= \frac{No.of\ molecules\ per\ g\ of\ polymer}{725} \div (10000)$

  $= \frac{6.33 \times 10^{19}}{725} \div (10000) = 9.04 \times 10^{12}$
- Maximum number of molecules possible in $1cm^2 = \frac{1}{Ao}$, where Ao is the minimum projection area in cm^2 as calculated using chemistry software on www.chemicalize.org. $= \frac{1}{7.27 \times 10^{-15}} = 1.38 \times 10^{14}$
- % Surface coverage = $\frac{Actual\ number\ of\ molecules\ per\ cm^2}{Max\ number\ of\ molecules\ per\ cm^2} \times 100\% = \frac{9.04 \times 10^{12}}{1.38 \times 10^{14}} \times 100\% = 6.6\%$

Error calculation method

As the sample size is small, t distribution was used: For a confidence interval of 95%,

Sample **XAD4.A1**	%N found
1	0.5
2	0.73
3	0.64
4	0.83
5	0.69

Parameters	**Commands in excel**	**Values**
Number of samples (Count)	5	5
Mean	=average (cell1 : cell 5)	0.678
Standard deviation	=stdev (cell1:cell5)	0.121532
Standard error	= [standard deviation/ (SQRT (count))]	0.054351
Hypothesis mean	0	0
Alpha (probability)	0.05	0.05
Tails	2	2
Degree of freedom	=(count – 1)	4
t stat	$= \frac{Mean - Hypothesis\ mean}{standard\ error}$	12.47454
p value	= TDIST (ABS (T-stat, deg freedom, tails)	0.000238
t critical	=TINV (probability, deg freedom)	2.776445
Confidence Interval	=confidence.T(alpha,stdev,count)	0.150902
Percentage error	= (confidence interval/ mean) x100%	22%

From the error calculations, results of the combustion analysis were thus assumed to have percentage error of 22% of the given value.

Tabulated results

Sample		% Found	Element per g polymer/ mol	Surface Modification per g polymer/mol	No. of molecules of surface modification per g of polymer	No. of molecules of surface mod. per cm	A_0 (min Projection area)/ cm2	$1/A_0$	% Surface Coverage
XAD4. Blank	C	86.47 ± 0.30							
	H	7.99 ± 0.30							
	N	0.12 ± 0.03							
2.17	C	86.19 ± 0.30							
	H	7.77 ± 0.30							
	N	0.12 ± 0.03	(8.6 ± 1.9) $x10^{-5}$						
	Br	0.87 ± 0.19	(1.1 ± 0.2) $x10^{-4}$	(1.1 ± 0.2) $x10^{-4}$	(6.6 ± 1.45) $x10^{19}$	(9.0 ± 2.0) $x10^{12}$	7.27 $x10^{-15}$	1.38 $x10^{14}$	6.6 ± 1.5
2.18	C	85.7 ± 0.30							
	H	7.76 ± 0.30							
	N	0.09 ± 0.02	(6.4 ± 1.4) $x10^{-5}$	(3.2 ± 0.7) $x10^{-5}$	(1.9 ± 0.4) $x10^{19}$	(2.7 ± 0.6) $x10^{12}$	9.87 $x10^{-15}$	1.01 $x10^{14}$	2.6 ± 0.6
	Br	0.19 ± 0.04	(2.4 ± 0.5) $x10^{-5}$	(2.4 ± 0.5) $x10^{-5}$	(1.4 ± 0.3) $x10^{19}$	(2.0 ± 0.4) $x10^{12}$	7.27 $x10^{-15}$	1.38 $x10^{14}$	1.4 ± 0.3
2.20	C	89.97 ± 0.30							
	H	8.02 ± 0.30							
	N	<0.10 ± 0.02							
	Br	0.55 ± 0.12	(6.9± 1.5) $x10^{-5}$	(3.4 ± 0.7)$x10^{-5}$	(2.1 ± 0.5) $x10^{19}$	(2.9 ± 0.6) $x10^{12}$	9.18 $x10^{-15}$	1.09 $x10^{14}$	2.6 ± 0.6
2.26	C	90.52 ± 0.30							
	H	7.82 ± 0.30							
	N	0.22 ± 0.05	(1.6 ± 0.4) $x10^{-4}$	(1.6 ± 0.4) $x10^{-4}$	(9.5 ± 2.1) $x10^{19}$	(1.3 ± 0.3) $x10^{13}$	1.08 $x10^{-14}$	9.22 $x10^{13}$	14 + 3.1
2.29	C	89.69 ± 0.30							
	H	7.73 ± 0.30							
	N	0.46 ± 0.10	(3.3 ± 0.7) $x10^{-4}$	(8.2 ± 1.8) $x10^{-5}$	(5.0 ± 1.1) $x10^{19}$	(6.8 ± 1.5) $x10^{12}$	1.08 $x10^{-14}$	9.22 $x10^{13}$	7.4 ± 1.6
2.30	C	89.5 ± 0.30							
	H	7.56 ± 0.30							
	N	0.42 ± 0.09	(3.0 ± 0.7) $x10^{-4}$	(5.0 ± 1.1) $x10^{-5}$	(3.0 ± 0.7) $x10^{19}$	(4.2 ± 0.9) $x10^{12}$	1.09 $x10^{-14}$	9.18 $x10^{13}$	4.5 ± 1.0

Sample		% Found	Element per g polymer/ mol	Surface Modification per g polymer/mol	No. of molecules of surface modification per g of polymer	No. of molecules of surface mod. per cm	A_0 (min Projection area)/ cm2	$1/A_0$	% Surface Coverage
2.31	C	89.79 ± 0.30							
	H	7.63 ± 0.30							
	N	0.28 ± 0.06	$(2.0 \pm 0.4) \times 10^{-4}$	$(4.0 \pm 0.9) \times 10^{-5}$	$(2.4 \pm 0.5) \times 10^{19}$	$(3.3 \pm 0.7) \times 10^{12}$	1.09×10^{-14}	9.18×10^{13}	3.6 ± 0.8
	Br	1.96 ± 0.43	$(2.5 \pm 0.6) \times 10^{-4}$	$(1.2 \pm 0.3) \times 10^{-4}$	$(7.4 \pm 1.6) \times 10^{19}$	$(1.0 \pm 0.2) \times 10^{13}$	1.09×10^{-14}	9.18×10^{13}	11 ± 2.4
XAD4. A1 (Sample 1)	C	88.55 ± 0.30							
	H	8.02							
	N	0.5± 0.11	$(3.6 \pm 0.8) \times 10^{-4}$	$(1.8 \pm 0.4) \times 10^{-4}$	$(1.1 \pm 0.2) \times 10^{20}$	$(1.5 \pm 0.3) \times 10^{13}$	7.80×10^{-15}	1.28×10^{14}	12 ± 2.6
XAD4. A1 (Sample 2)	C	87.95 ± 0.30							
	H	8.05± 0.30							
	N	0.73 ± 0.16	$(5.2 \pm 1.1) \times 10^{-4}$	$(2.6 \pm 0.6) \times 10^{-4}$	$(1.6 \pm 0.4) \times 10^{20}$	$(2.2 \pm 0.5) \times 10^{13}$	7.80×10^{-15}	1.28×10^{14}	17 ± 3.7
XAD4. A1 (Sample 3)	C	90.61 ± 0.30							
	H	8.44± 0.30							
	N	0.64 ± 0.14	$(4.6 \pm 1.0) \times 10^{-4}$	$(2.3 \times 0.5)\ 10^{-4}$	$(1.4 \pm 0.3) \times 10^{20}$	$(1.9 \pm 0.4) \times 10^{13}$	7.80×10^{-15}	1.28×10^{14}	15 ± 3.3
XAD4. A1 (Sample 4)	C	90.6 ± 0.30							
	H	8.19 ± 0.30							
	N	0.83 ± 0.18	$(5.9 \pm 1.3) \times 10^{-4}$	$(3.0 \pm 0.7) \times 10^{-4}$	$(1.8 \pm 0.4) \times 10^{20}$	$(2.5 \pm 0.6) \times 10^{13}$	7.80×10^{-15}	1.28×10^{14}	19 ± 4.2
XAD4. A1 (Sample 5)	C	90.86 ± 0.30							
	H	7.91 ± 0.30							
	N	0.69 ± 0.15	$(4.9 \pm 1.1) \times 10^{-4}$	$(2.5 \pm 0.6) \times 10^{-4}$	$(1.5 \pm 0.3) \times 10^{20}$	$(2.1 \pm 0.5) \times 10^{13}$	7.80×10^{-15}	1.28×10^{14}	16 ± 3.5
XAD4. A1 (Average)	C	89.71 ± 0.30							
	H	7.98 ± 0.30							
	N	0.68 ± 0.15	$(4.9 \pm 1.1) \times 10^{-4}$	$(2.5 \pm 0.6) \times 10^{-4}$	$(1.5 \pm 0.3) \times 10^{20}$	$(2.1 \pm 0.5) \times 10^{13}$	7.80×10^{-15}	1.28×10^{14}	16 ± 3.5
XAD4. A1-B4	C	88.49 ± 0.30							
	H	7.72 ± 0.30							
	N	1.03 ± 0.23	$(7.4 \pm 1.6) \times 10^{-4}$	$(1.8 \pm 0.4) \times 10^{-4}$	$(1.1 \pm 0.2) \times 10^{20}$	$(1.5 \pm 0.3) \times 10^{13}$	9.92×10^{-15}	1.01×10^{14}	15 ± 3.3
XAD4.	C	90.67 ± 0.30							

Sample		% Found	Element per g polymer/ mol	Surface Modification per g polymer/mol	No. of molecules of surface modification per g of polymer	No. of molecules of surface mod. per cm	A_0 (min Projection area)/ cm2	$1/A_0$	% Surface Coverage
A1-B5 (sample 1)	H	8.1 ± 0.30							
	N	0.47 ± 0.10	$(3.4 \pm 0.7) \times 10^{-4}$	$(6.7 \pm 1.5) \times 10^{-5}$	$(4.0 \pm 0.9) \times 10^{19}$	$(5.6 \pm 1.2) \times 10^{12}$	9.92×10^{-15}	1.01×10^{14}	5.5 ± 1.2
XAD4. A1-B5 (sample 2)	C	90.22 ± 0.30							
	H	8.12 ± 0.30							
	N	0.8 ± 0.18	$(5.7 \pm 1.3) \times 10^{-4}$	$(1.1 \pm 0.2) \times 10^{-4}$	$(6.9 \pm 1.5) \times 10^{19}$	$(9.5 \pm 2.1) \times 10^{12}$	9.92×10^{-15}	1.01×10^{14}	9.4 ± 2.1
XAD4. A1-B5 (sample 3)	C	89.25 ± 0.30							
	H	8.01 ± 0.30							
	N	0.89 ± 0.20	$(6.4 \pm 1.4) \times 10^{-4}$	$(1.3 \pm 0.3) \times 10^{-4}$	$(7.7 \pm 1.7) \times 10^{19}$	$(1.1 \pm 0.2) \times 10^{13}$	9.92×10^{-15}	1.01×10^{14}	11 ± 2.4
XAD4. A1-B5 (sample 4)	C	90.07 ± 0.30							
	H	8.4 ± 0.30							
	N	0.53 ± 0.12	$(3.8 \pm 0.8) \times 10^{-4}$	$(7.6 \pm 1.7) \times 10^{-5}$	$(4.6 \pm 1.0) \times 10^{19}$	$(6.3 \pm 1.4) \times 10^{12}$	9.92×10^{-15}	1.01×10^{14}	6.2 ± 1.4
XAD4. A1-B5 (sample 5)	C	88.88 ± 0.30							
	H	8.09 ± 0.30							
	N	0.81 ± 0.18	$(5.8 \pm 1.3) \times 10^{-4}$	$(1.2 \pm 0.3) \times 10^{-4}$	$(7.0 \pm 1.5) \times 10^{19}$	$(9.6 \pm 2.1) \times 10^{12}$	9.92×10^{-15}	1.01×10^{14}	9.5 ± 2.1
XAD4. A1-B5 (Average)	C	89.82 ± 0.30							
	H	8.14 ± 0.30							
	N	0.70 ± 0.15	$(5.0 \pm 1.1) \times 10^{-4}$	$(1.0 \pm 0.2) \times 10^{-4}$	$(6.0 \pm 1.3) \times 10^{19}$	$(8.3 \pm 1.8) \times 10^{12}$	9.92×10^{-15}	1.01×10^{14}	8.2 ± 1.8
XAD4. A1-B4-C1	C	88.33 ± 0.30							
	H	7.66 ± 0.30							
	N	1.03 ± 0.23	$(7.4 \pm 1.6) \times 10^{-4}$	$(1.2 \pm 0.3) \times 10^{-4}$	$(7.4 \pm 1.6) \times 10^{19}$	$(1.0 \pm 0.2) \times 10^{13}$	1.18×10^{-14}	8.49×10^{13}	12 ± 2.6
XAD4. A1-B5-C1	C	90.13 ± 0.30							
	H	7.75 ± 0.30							
	N	0.79 ± 0.17	$(5.6 \pm 1.2) \times 10^{-4}$	$(8.1 \pm 1.8) \times 10^{-5}$	$(4.9 \pm 1.1) \times 10^{19}$	$(6.7 \pm 1.5) \times 10^{12}$	1.18×10^{-14}	8.49×10^{13}	7.9 ± 1.7
XAD4.	C	90 ± 0.30							

Sample		% Found	Element per g polymer/ mol	Surface Modification per g polymer/mol	No. of molecules of surface modification per g of polymer	No. of molecules of surface mod. per cm	A_0 (min Projection area)/ cm2	$1/A_0$	% Surface Coverage
A1-B5-C2 (sample 1)	H	8.4 ± 0.30							
	N	0.45 ± 0.10	$(3.2 \pm 0.7) \times 10^{-4}$	$(5.4 \pm 1.2) \times 10^{-5}$	$(3.2 \pm 0.7) \times 10^{19}$	$(4.5 \pm 1.0) \times 10^{12}$	1.18×10^{-14}	8.49×10^{13}	5.2 ± 1.1
	Br	0.82 ± 0.18	$(1.0 \pm 0.2) \times 10^{-4}$	$(5.1 \pm 1.1) \times 10^{-5}$	$(3.1 \pm 0.7) \times 10^{19}$	$(4.3 \pm 0.9) \times 10^{12}$	1.18×10^{-14}	8.49×10^{13}	5.0 ± 1.1
XAD4. A1-B5-C2 (sample 2)	C	89.43 ± 0.30							
	H	8.15 ± 0.30							
	N	0.52 ± 0.11	$(3.7 \pm 0.8) \times 10^{-4}$	$(6.2 \pm 1.4) \times 10^{-5}$	$(3.7 \pm 0.8) \times 10^{19}$	$(5.1 \pm 1.1) \times 10^{12}$	1.18×10^{-14}	8.49×10^{13}	6.1 ± 1.3
	Br	1.11 ± 0.24	$(1.4 \pm 0.3) \times 10^{-4}$	$(7.0 \pm 1.5) \times 10^{-5}$	$(4.2 \pm 0.9) \times 10^{19}$	$(5.8 \pm 1.3) \times 10^{12}$	1.18×10^{-14}	8.49×10^{13}	6.8 ± 1.5
XAD4. A1-B5-C2 (Average)	C	89.72 ± 0.30							
	H	8.28 ± 0.30							
	N	0.49 ± 0.11	$(3.5 \pm 0.8) \times 10^{-4}$	$(5.8 \pm 1.3) \times 10^{-5}$	$(3.5 \pm 0.8) \times 10^{19}$	$(4.8 \pm 1.1) \times 10^{12}$	1.18×10^{-14}	8.49×10^{13}	5.7 ± 1.3
	Br	0.97 ± 0.21	$(1.2 \pm 0.3) \times 10^{-4}$	$(6.0 \pm 1.3) \times 10^{-5}$	$(3.6 \pm 0.8) \times 10^{19}$	$(5.0 \pm 1.1) \times 10^{12}$	1.18×10^{-14}	8.49×10^{13}	5.9 ± 1.3
XAD4. A2 (Sample 1)	C	90.53 ± 0.30							
	H	7.98 ± 0.30							
	N	0.15 ± 0.03							
XAD4. A2 (Sample 2)	C	91.09 ± 0.30							
	H	8.35 ± 0.30							
	N	0.15 ± 0.03							
XAD4. A2 (Sample 3)	C	91.09 ± 0.30							
	H	8.29± 0.30							
	N	0.11 ± 0.02							
XAD4. A2 (Average)	C	90.90 ± 0.30							
	H	8.21 ± 0.30							
	N	0.14 ± 0.03							
XAD4.A	C	90.1 ± 0.30							

Sample		% Found	Element per g polymer/ mol	Surface Modification per g polymer/mol	No. of molecules of surface modification per g of polymer	No. of molecules of surface mod. per cm	A_0 (min Projection area)/ cm2	$1/A_0$	% Surface Coverage
2-B1 (iia)	H	7.72 ± 0.30							
	N	0.25 ± 0.06	$(1.8 \pm 0.4) \times 10^{-4}$	$(8.9 \pm 2.0) \times 10^{-5}$	$(5.4 \pm 1.2) \times 10^{19}$	$(7.4 \pm 1.6) \times 10^{12}$	1.19×10^{-14}	8.39×10^{13}	8.8 ± 1.9
XAD4.A 2-B1 (iib)	C	89.71 ± 0.30							
	H	7.75 ± 0.30							
	N	0.32 ± 0.07	$(2.3 \pm 0.5) \times 10^{-4}$	$(1.1 \pm 0.2) \times 10^{-4}$	$(6.9 \pm 1.5) \times 10^{19}$	$(9.5 \pm 2.1) \times 10^{12}$	1.19×10^{-14}	8.39×10^{13}	11 ± 2.4
XAD4. Ctrl-B1	C	91.3 ± 0.30							
	H	8.21 ± 0.30							
	N	0.17 ± 0.04	$(1.2 \pm 0.3) \times 10^{-4}$	$(6.1 \pm 1.3) \times 10^{-5}$	$(3.7 \pm 0.8) \times 10^{19}$	$(5.0 \pm 1.1) \times 10^{12}$	8.47×10^{-15}	1.18×10^{14}	4.3 ± 0.9
XAD4. A2-B2 (iia)	C	89.69 ± 0.30							
	H	7.68 ± 0.30							
	N	0.43 ± 0.09	$(3.1 \pm 0.7) \times 10^{-4}$	$(1.5 \pm 0.3) \times 10^{-4}$	$(9.3 \pm 2.0) \times 10^{19}$	$(1.3 \pm 0.3) \times 10^{13}$	1.26×10^{-14}	7.97×10^{13}	16.0 ± 3.5
XAD4. A2-B2 (iib)	C	87.42 ± 0.30							
	H	7.48 ± 0.30							
	N	1.07 ± 0.24	$(7.6 \pm 1.7) \times 10^{-4}$	$(3.8 \pm 0.8) \times 10^{-4}$	$(2.3 \pm 0.5) \times 10^{20}$	$(3.2 \pm 0.7) \times 10^{13}$	1.26×10^{-14}	7.97×10^{13}	40 ± 8.8
XAD4. Ctrl-B2	C	90.63 ± 0.30							
	H	7.94 ± 0.30							
	N	0.3 ± 0.07	$(2.1 \pm 0.5) \times 10^{-4}$	$(1.1 \pm 0.2) \times 10^{-4}$	$(6.5 \pm 1.4) \times 10^{19}$	$(8.9 \pm 2.0) \times 10^{12}$	8.87×10^{-15}	1.13×10^{14}	7.9 ± 1.7
XAD4. A2-B3 (iia)	C	90.18 ± 0.30							
	H	7.84 ± 0.30							
	N	0.27 ± 0.06	$(1.9 \pm 0.4) \times 10^{-4}$	$(9.6 \pm 2.1) \times 10^{-5}$	$(5.8 \pm 1.3) \times 10^{19}$	$(8.0 \pm 1.8) \times 10^{12}$	1.16×10^{-14}	8.61×10^{13}	9.3 ± 2.0
XAD4. A2-B3 (iib)	C	89.81 ± 0.30							
	H	7.78 ± 0.30							
	N	0.4 ± 0.09	$(2.9 \pm 0.6) \times 10^{-4}$	$(1.4 \pm 0.3) \times 10^{-4}$	$(8.6 \pm 1.9) \times 10^{19}$	$(1.2 \pm 0.3) \times 10^{13}$	1.16×10^{-14}	8.61×10^{13}	14 ± 3.1

Sample		% Found	Element per g polymer/ mol	Surface Modification per g polymer/mol	No. of molecules of surface modification per g of polymer	No. of molecules of surface mod. per cm	A_0 (min Projection area)/ cm2	$1/A_0$	% Surface Coverage
XAD4. Ctrl-B3	C	90.92 ± 0.30							
	H	7.92 ± 0.30							
	N	<0.1 ± 0.02							
XAD4. A2-B4 (iia)	C	89.98 ± 0.30							
	H	7.76 ± 0.30							
	N	0.32 ± 0.07	$(2.3 \pm 0.5) \times 10^{-4}$	$(1.1 \pm 0.2) \times 10^{-4}$	$(6.9 \pm 1.5) \times 10^{19}$	$(9.5 \pm 2.1) \times 10^{12}$	1.24×10^{-14}	8.09×10^{13}	12 ± 2.6
XAD4. A2-B4 (iib)	C	88.75 ± 0.30							
	H	7.6 ± 0.30							
	N	0.47 ± 0.10	$(3.4 \pm 0.7) \times 10^{-4}$	$(1.7 \pm 0.4) \times 10^{-4}$	$(1.0 \pm 0.2) \times 10^{20}$	$(1.4 \pm 0.3) \times 10^{13}$	1.24×10^{-14}	8.09×10^{13}	17 ± 3.7
XAD4. Ctrl-B4	C	90.83 ± 0.30							
	H	7.93 ± 0.30							
	N	<0.1 ± 0.02							
XAD4. A2-B5 (iia)	C	90.49 ± 0.30							
	H	8.29 ± 0.30							
	N	0.24 ± 0.05	$(1.7 \pm 0.4) \times 10^{-4}$	$(5.7 \pm 1.3) \times 10^{-5}$	$(3.4 \pm 0.7) \times 10^{19}$	$(4.8 \pm 1.1) \times 10^{12}$	8.30×10^{-15}	1.21×10^{14}	3.9 ± 0.9
XAD4. A2-B5 (iib)	C	90.94 ± 0.30							
	H	8.35 ± 0.30							
	N	0.24 ± 0.05	$(1.7 \pm 0.4) \times 10^{-4}$	$(5.7 \pm 1.3) \times 10^{-5}$	$(3.4 \pm 0.7) \times 10^{19}$	$(4.8 \pm 1.1) \times 10^{12}$	8.30×10^{-15}	1.21×10^{14}	3.9 ± 0.9
XAD4. Ctrl-B5	C	90.66 ± 0.30							
	H	8.02 ± 0.30							
	N	<0.1 ± 0.02							
XAD4.	C	87.60 ± 0.30							

Sample		% Found	Element per g polymer/ mol	Surface Modification per g polymer/mol	No. of molecules of surface modification per g of polymer	No. of molecules of surface mod. per cm	A_0 (min Projection area)/ cm2	$1/A_0$	% Surface Coverage
A2-B4-C1	H	7.71 ± 0.30							
	N	0.60 ± 0.13	$(4.3 \pm 0.9) \times 10^{-4}$	$(1.1 \pm 0.2) \times 10^{-4}$	$(6.5 \pm 1.4) \times 10^{19}$	$(8.0 \pm 1.8) \times 10^{12}$	1.18×10^{-14}	8.49×10^{13}	11 ± 2.4
XAD4. A2-B5-C1	C	89.41 ± 0.30							
	H	8.21 ± 0.30							
	N	0.23 ± 0.05	$(1.6 \pm 0.4) \times 10^{-4}$	$(3.2 \pm 0.7) \times 10^{-5}$	$(1.9 \pm 0.4) \times 10^{19}$	$(2.7 \pm 0.6) \times 10^{12}$	1.04×10^{-14}	9.63×10^{13}	2.8 ± 0.6
XAD4. A2-B5-C2	C	90.77 ± 0.30							
	H	7.64 ± 0.30							
	N	0.23 ± 0.05	$(1.6 \pm 0.4) \times 10^{-4}$	$(4.1 \pm 0.9) \times 10^{-5}$	$(2.5 \pm 0.6) \times 10^{19}$	$(3.4 \pm 0.7) \times 10^{12}$	1.04×10^{-14}	9.63×10^{13}	3.5 ± 0.8
	Br	0.49 ± 0.11	$(6.1 \pm 1.3) \times 10^{-5}$	$(3.1 \pm 0.7) \times 10^{-5}$	$(1.9 \pm 0.4) \times 10^{19}$	$(2.6 \pm 0.6) \times 10^{12}$	1.04×10^{-14}	9.63×10^{13}	2.6 ± 0.6
XAD4. Ctrl-C1	C	90.71 ± 0.30							
	H	7.93 ± 0.30							
	N	<0.1 ± 0.02							
XAD4. Ctrl-Pen V	C	90.21 ± 0.30							
	H	8.17 ± 0.30							
	N	0.44 ± 0.10	$(3.1 \pm 0.7) \times 10^{-4}$	$(1.6 \pm 0.4) \times 10^{-4}$	$(9.5 \pm 2.1) \times 10^{19}$	$(1.3 \pm 0.3) \times 10^{13}$	4.83×10^{-15}	2.07×10^{14}	6.3 ± 1.4
	S	0.34±0.07	$(1.1 \pm 0.2) \times 10^{-4}$	$(1.1 \pm 0.2) \times 10^{-4}$	$(6.4 \pm 1.4) \times 10^{19}$	$(8.8 \pm 1.9) \times 10^{12}$	4.83×10^{-15}	2.07×10^{14}	4.3 ± 0.9
XAD4. A1 (with Pen V)	C	89.23 ± 0.30							
	H	7.99 ± 0.30							
	N	0.92 ± 0.20	$(6.6 \pm 1.5) \times 10^{-4}$	$(1.6 \pm 0.4) \times 10^{-4}$	$(9.9 \pm 2.2) \times 10^{19}$	$(1.4 \pm 0.3) \times 10^{13}$	7.80×10^{-15}	1.28×10^{14}	11 ± 2.4
	S	0.39±0.09	$(1.2 \pm 0.3) \times 10^{-4}$	$(1.2 \pm 0.3) \times 10^{-4}$	$(7.3 \pm 1.6) \times 10^{19}$	$(1.0 \pm 0.22) \times 10^{13}$	4.83×10^{-15}	2.07×10^{14}	4.9 ± 1.1
XAD4. A1-B5 (with Pen V)	C	89.23 ± 0.30							
	H	8.23 ± 0.30							
	N	0.88 ± 0.19	$(6.3 \pm 1.4) \times 10^{-4}$	$(9.0 \pm 2.0) \times 10^{-5}$	$(5.4 \pm 1.2) \times 10^{19}$	$(7.5 \pm 1.7) \times 10^{12}$	4.83×10^{-15}	2.07×10^{14}	3.6 ± 0.8
	S	0.36±0.08	$(1.1 \pm 0.2) \times 10^{-4}$	$(1.1 \pm 0.2) \times 10^{-4}$	$(6.8 \pm 1.5) \times 10^{19}$	$(9.3 \pm 2.0) \times 10^{12}$	4.83×10^{-15}	2.07×10^{14}	4.5 ± 1.0
XAD4.	C	88.54 ± 0.30							

Sample		% Found	Element per g polymer/ mol	Surface Modification per g polymer/mol	No. of molecules of surface modification per g of polymer	No. of molecules of surface mod. per cm	A_0 (min Projection area)/ cm2	$1/A_0$	% Surface Coverage
A1-B5-C2 (with Pen V)	H	7.59 ± 0.30							
	N	0.74 ± 0.16	$(5.3 \pm 1.2) \times 10^{-4}$	$(6.6 \pm 1.5) \times 10^{-5}$	$(4.0 \pm 0.9) \times 10^{19}$	$(5.5 \pm 1.2) \times 10^{12}$	1.18×10^{-14}	8.49×10^{13}	6.5 ± 1.4
	S	0.38±0.08	$(1.2 \pm 0.3) \times 10^{-4}$	$(1.2 \pm 0.3) \times 10^{-4}$	$(7.1 \pm 1.6) \times 10^{19}$	$(9.9 \pm 2.2) \times 10^{12}$	4.83×10^{-15}	2.07×10^{14}	4.7 ± 1.0
	Br	0.52 ± 0.11	$(6.5 \pm 1.4) \times 10^{-5}$	$(3.3 \pm 0.7) \times 10^{-5}$	$(2.0 \pm 0.4) \times 10^{19}$	$(2.7 \pm 0.6) \times 10^{12}$	1.18×10^{-14}	8.49×10^{13}	3.2 ± 0.7
XAD4. A1-B5-C1 (with Pen V)	C	88.9 ± 0.30							
	H	8.14 ± 0.30							
	N	0.83 ± 0.18	$(5.9 \pm 1.3) \times 10^{-4}$	$(6.6 \pm 1.5) \times 10^{-5}$	$(4.0 \pm 0.9) \times 10^{19}$	$(5.5 \pm 1.2) \times 10^{12}$	1.18×10^{-14}	8.49×10^{13}	6.5 ± 1.4
	S	0.32±0.07	$(10 \pm 2.2) \times 10^{-5}$	$(10 \pm 2.2) \times 10^{-5}$	$(6.0 \pm 1.3) \times 10^{19}$	$(8.3 \pm 1.8) \times 10^{12}$	4.83×10^{-15}	2.07×10^{14}	4.0 ± 0.9
XAD4. A2 (with Pen V)	C	88.12 ± 0.30							
	H	7.76± 0.30							
	N	0.54 ± 0.12	$(3.9 \pm 0.9) \times 10^{-4}$	$(1.9 \pm 0.4) \times 10^{-4}$	$(1.2 \pm 0.3) \times 10^{20}$	$(1.6 \pm 0.4) \times 10^{13}$	4.83×10^{-15}	2.07×10^{14}	7.7 ± 1.7
	S	0.56 ± 0.12	$(1.8 \pm 0.4) \times 10^{-4}$	$(1.8 \pm 0.4) \times 10^{-4}$	$(1.1 \pm 0.2) \times 10^{20}$	$(1.5 \pm 0.3) \times 10^{13}$	4.83×10^{-15}	2.07×10^{14}	7.0 ± 1.5
XAD4. A2-B5 (with Pen V)	C	89.77 ± 0.30							
	H	7.84 ± 0.30							
	N	0.54 ± 0.12	$(3.9 \pm 0.9) \times 10^{-4}$	$(7.7 \pm 1.7) \times 10^{-5}$	$(4.7 \pm 1.0) \times 10^{19}$	$(6.4 \pm 1.4) \times 10^{12}$	4.83×10^{-15}	2.07×10^{14}	3.1 ± 0.7
	S	0.6	$(1.9 \pm 0.4) \times 10^{-4}$	$(1.9 \pm 0.4) \times 10^{-4}$	$(1.1 \pm 0.2) \times 10^{20}$	$(1.6 \pm 0.4) \times 10^{13}$	4.83×10^{-15}	2.07×10^{14}	7.5 ± 1.7
XAD4. A2-B5-C1 (with Pen V)	C	89.59 ± 0.30							
	H	7.89 ± 0.30							
	N	0.54 ± 0.12	$(3.9 \pm 0.9) \times 10^{-4}$	$(5.5 \pm 1.2) \times 10^{-5}$	$(3.3 \pm 0.7) \times 10^{19}$	$(4.6 \pm 1.0) \times 10^{12}$	4.83×10^{-15}	2.07×10^{14}	2.2 ± 0.5
	S	0.53	$(1.7 \pm 0.4) \times 10^{-4}$	$(1.7 \pm 0.4) \times 10^{-4}$	$(10 \pm 2.2) \times 10^{19}$	$(1.4 \pm 0.3) \times 10^{13}$	4.83×10^{-15}	2.07×10^{14}	6.6 ± 1.5
XAD4. A2-B5-C2 (with Pen V)	C	89.51 ± 0.30							
	H	7.88 ± 0.30							
	N	0.58 ± 0.13	$(4.1 \pm 0.9) \times 10^{-4}$	$(6.9 \pm 1.5) \times 10^{-5}$	$(4.2 \pm 0.9) \times 10^{19}$	$(5.7 \pm 1.3) \times 10^{12}$	4.83×10^{-15}	2.07×10^{14}	2.8 ± 0.6
	S	0.57	$(1.8 \pm 0.4) \times 10^{-4}$	$(1.8 \pm 0.4) \times 10^{-4}$	$(1.1 \pm 0.2) \times 10^{20}$	$(1.5 \pm 0.3) \times 10^{13}$	4.83×10^{-15}	2.07×10^{14}	7.1 ± 1.6
	Br	0.14 ± 0.03	$(1.8 \pm 0.4) \times 10^{-5}$	$(8.8 \pm 1.9) \times 10^{-6}$	$(5.3 \pm 1.2) \times 10^{18}$	$(7.3 \pm 1.6) \times 10^{11}$	4.83×10^{-15}	2.07×10^{14}	0.4 ± 0.1

Sample		% Found	Element per g polymer/ mol	Surface Modification per g polymer/mol	No. of molecules of surface modification per g of polymer	No. of molecules of surface mod. per cm	A_0 (min Projection area)/ cm2	$1/A_0$	% Surface Coverage
PETp. Blank	C	44.32 ± 0.30							
	H	3.11 ± 0.30							
	N	<0.1 ± 0.02							
PETp. A2	C	44.03 ± 0.30							
	H	3.09 ± 0.30							
	N	<0.1 ± 0.02							
PETp. Blank	C	44.32 ± 0.30							
	H	3.11 ± 0.30							
	N	<0.1 ± 0.02							
PETp. A2	C	44.03 ± 0.30							
	H	3.09 ± 0.30							
	N	<0.1 ± 0.02							
PETp. A2-B1	C	45.06 ± 0.30							
	H	3.87 ± 0.30							
	N	<0.1 ± 0.02							
PETp. A2-B2	C	44.71 ± 0.30							
	H	3.62 ± 0.30							
	N	0.18 ± 0.04	$(1.3 \pm 0.3) \times 10^{-4}$	$(6.4 \pm 1.4) \times 10^{-5}$	$(3.9 \pm 0.9) \times 10^{19}$	$(3.9 \pm 0.9) \times 10^{15}$	6.20×10^{-15}	1.61×10^{14}	2400 ± 528
PETp. A2-B3	C	44.09 ± 0.30							
	H	4.47 ± 0.30							
	N	<0.1 ± 0.02							
PETp. A2-B4	C	44.15 ± 0.30							
	H	4.30 ± 0.30							

Sample		% Found	Element per g polymer/ mol	Surface Modification per g polymer/mol	No. of molecules of surface modification per g of polymer	No. of molecules of surface mod. per cm	A_0 (min Projection area)/ cm2	$1/A_0$	% Surface Coverage
	N	<0.1 ± 0.02							
PETp. A2-B5	C	44.6 ± 0.30							
	H	3.09 ± 0.30							
	N	<0.1 ± 0.02							
PETp. A2-B4-C1	C	43.32 ± 0.30							
	H	3.84 ± 0.30							
	N	0.27 ± 0.06	$(1.9 \pm 0.4) \times 10^{-4}$	$(4.8 \pm 1.1) \times 10^{-5}$	$(2.9 \pm 0.6) \times 10^{19}$	$(2.9 \pm 0.6) \times 10^{15}$	1.03×10^{-14}	9.71×10^{13}	299 ± 65.8
PETp. A2-B5-C1	C	43.42 ± 0.30							
	H	3.12 ± 0.30							
	N	0.52 ± 0.11	$(3.7 \pm 0.8) \times 10^{-4}$	$(7.4 \pm 1.6) \times 10^{-5}$	$(4.5 \pm 1.0) \times 10^{19}$	$(4.5 \pm 1.0) \times 10^{15}$	5.20×10^{-15}	1.92×10^{14}	2330 ± 512.6
PETp. A2-B5-C2	C	44.15 ± 0.30							
	H	3.08 ± 0.30							
	N	0.57 ± 0.13	$(4.1 \pm 0.9) \times 10^{-4}$	$(1.0 \pm 0.2) \times 10^{-4}$	$(6.1 \pm 1.3) \times 10^{19}$	$(6.1 \pm 1.3) \times 10^{15}$	5.20×10^{-15}	1.92×10^{14}	3190 ± 701.8
	Br	0.15 ± 0.03	$(1.9 \pm 0.4) \times 10^{-5}$	$(9.4 \pm 2.1) \times 10^{-6}$	$(5.7 \pm 1.3) \times 10^{18}$	$(5.7 \pm 1.3) \times 10^{14}$	5.20×10^{-15}	1.92×10^{14}	294 ± 64.7
PETp. Ctrl-C1	C	44.23 ± 0.30							
	H	3.87 ± 0.30							
	N	0.21 ± 0.05	$(1.5 \pm 0.3) \times 10^{-4}$	$(7.5 \pm 1.7) \times 10^{-5}$	$(4.5 \pm 1.0) \times 10^{19}$	$(4.5 \pm 1.0) \times 10^{15}$	9.95×10^{-15}	1.01×10^{14}	4500 ± 990
Blank LDPE	C	85.19 ± 0.30							
	H	14.77 ± 0.30							
	N	<0.1 ± 0.02							
LDPE. A2	C	85.16 ± 0.30							
	H	14.66 ± 0.30							
	N	<0.1 ± 0.02							

Sample		% Found	Element per g polymer/ mol	Surface Modification per g polymer/mol	No. of molecules of surface modification per g of polymer	No. of molecules of surface mod. per cm	A_0 (min Projection area)/ cm2	$1/A_0$	% Surface Coverage
LDPE. A2-B1	C	85.55 ± 0.30							
	H	14.75 ± 0.30							
	N	<0.1 ± 0.02							
LDPE. A2-B2	C	83.78 ± 0.30							
	H	14.00 ± 0.30							
	N	1.21 ± 0.27	$(8.6 \pm 1.9) \times 10^{-4}$	$(4.3 \pm 0.9) \times 10^{-4}$	$(2.6 \pm 0.6) \times 10^{20}$	$(1.9 \pm 0.4) \times 10^{17}$	6.20×10^{-15}	1.61×10^{14}	120000 ± 26400
LDPE. A2-B3	C	85.59 ± 0.30							
	H	14.63 ± 0.30							
	N	<0.1 ± 0.02							
LDPE. A2-B4	C	85.59 ± 0.30							
	H	14.09 ± 0.30							
	N	<0.1 ± 0.02							
LDPE. A2-B5	C	85.37 ± 0.30							
	H	14.41 ± 0.30							
	N	<0.1 ± 0.02							
LDPE. A2-B4-C1	C	85.14 ± 0.30							
	H	14.50 ± 0.30							
	N	<0.1 ± 0.02							
LDPE. A2-B5-C1	C	85.5 ± 0.30							
	H	14.56 ± 0.30							
	N	<0.1 ± 0.02							

Sample		% Found	Element per g polymer/ mol	Surface Modification per g polymer/mol	No. of molecules of surface modification per g of polymer	No. of molecules of surface mod. per cm	A_0 (min Projection area)/ cm2	$1/A_0$	% Surface Coverage
LDPE. A2-B5-C2	C	85.51 ± 0.30							
	H	14.65 ± 0.30							
	N	<0.1 ± 0.02							
	Br	<0.1 ± 0.02							
LDPE. Ctrl-C1	C	85.26 ± 0.30							
	H	14.71 ± 0.30							
	N	<0.1 ± 0.02							
UHMW. Blank	C	84.64 ± 0.30							
	H	15.17 ± 0.30							
	N	<0.1 ± 0.02							
UHMW. A2	C	83.28 ± 0.30							
	H	14.78 ± 0.30							
	N	<0.1 ± 0.02							
UHMW. A2-B1	C	84.19 ± 0.30							
	H	14.62 ± 0.30							
	N	<0.1 ± 0.02							
UHMW. A2-B2	C	83.65 ± 0.30							
	H	14.62 ± 0.30							
	N	0.66 ± 0.15	$(4.7 \pm 1.0) \times 10^{-4}$	$(2.4 \pm 0.5) \times 10^{-4}$	$(1.4 \pm 0.3) \times 10^{20}$	$(7.5 \pm 1.7) \times 10^{15}$	6.20×10^{-15}	1.61×10^{14}	4600 ± 1012
UHMW. A2-B3	C	83.53 ± 0.30							
	H	14.62 ± 0.30							
	N	<0.1 ± 0.02							

Sample		% Found	Element per g polymer/ mol	Surface Modification per g polymer/mol	No. of molecules of surface modification per g of polymer	No. of molecules of surface mod. per cm	A_0 (min Projection area)/ cm2	$1/A_0$	% Surface Coverage
UHMW. A2-B4	C	84.81 ± 0.30							
	H	14.37 ± 0.30							
	N	<0.1 ± 0.02							
UHMW. A2-B5	C	84.05 ± 0.30							
	H	14.97 ± 0.30							
	N	<0.1 ± 0.02							
UHMW. A2-B4-C1	C	84.74 ± 0.30							
	H	14.50 ± 0.30							
	N	<0.1 ± 0.02							
UHMW. A2-B5-C1	C	84.85 ± 0.30							
	H	15.35 ± 0.30							
	N	<0.1 ± 0.02							
UHMW. A2-B5-C2	C	85 ± 0.30							
	H	14.93 ± 0.30							
	N	<0.1 ± 0.02							
	Br	0.46 ± 0.10	$(5.8 \pm 1.3) \times 10^{-5}$	$(2.9 \pm 0.6) \times 10^{-5}$	$(1.7 \pm 0.4) \times 10^{19}$	$(9.1 \pm 2.0) \times 10^{14}$	5.20×10^{-15}	1.92×10^{14}	473 ± 104.1
UHMW. Ctrl-C1	C	84.47 ± 0.30							
	H	14.89 ± 0.30							
	N	<0.1 ± 0.02							

Appendix C: List of ATR-IR peaks for all polymers

For ATR-IR spectra, see soft copy in CD-ROM.

XAD4.Blank	3331, 3019, 2914, 2371, 1602 (C=C), 1511 (C=C), 1486 (C=C), 1445 (C=C), 1357, 988
2.17	3019, 2907, 2450, 1726 (C=O), 1603 (C=C), 1510 (C=C), 1486 (C=C), 1444 (C=C), 1168, 1036, 901, 827, 792
2.18	2968, 2186, 1723 (C=O), 1603 (C=C), 1510 (-NO_2 overlapped with C=C), 1486 (C=C), 1356, 1090, 902, 828
2.20	2931, 2631, 2033, 1659, 1604 (C=C), 1511 ((-NO_2 overlapped with C=C), 1487 (C=C), 1446 (C=C), 1357 (-NO_2), 1234, 1171, 1017, 989, 902, 794
2.26	3074, 2939, 2119, 1487 (C=C), 1320 (C-N), 1179 (C-O), 1087, 903.
2.29	3383 (broad –OH), 2933, 2159, 2025, 1659, 1603 (C=C), 1560, 1511 (C=C), 1487 (C=C), 1445 (C=C), 1345, 1069, 1017, 988, 902, 828.
2.30	2928, 2031, 1700, 1604 (C=C), 1561, 1511 (C=C), 1486 (C=C), 1446 (C=C), 1343 (NO_2), 1261, 1169, 1090, 1017, 989, 903, 828, 794.
2.31	3382, 2931, 2030, 1700, 1604 (C=C), 1563, 1511 (C=C), 1486 (C=C), 1446 (C=C), 1357, 1273, 1171, 988, 902, 830, 794.
XAD4.A1	3019, 2968, 2932, 2160, 1977, 1653, 1603 (C=C), 1512 (C=C), 1487 (C=C), 1445 (C=C), 1349 (C-N), 1228, 1168, 1062, 989, 903, 830, 795
XAD4.A1-B4	3296, 3017, 2923, 1734 (C=O) , 1653, 1603 (C=C), 1509 (C=C), 1447, 1362, 1270 (C-O), 1169, 1017, 988, 830, 794
XAD4.A1-B5	3395, 3019, 2970, 2936, 2161, 1977, 1700, 1631, 1603 (C=C), 1511 (C=C), 1486 (C=C), 1445 (C=C), 1352 (C-N), 1277, 1169, 1064, 989, 903, 829, 794
XAD4.A1-B4-C1	3019, 2924, 1734 (C=O), 1603 (C=C), 1362 (NO_2), 1271 (C-O), 1169, 1086, 1017, 988, 830, 794
XAD4.A1-B5-C1	3400, 3019, 2967, 2932, 2161, 2026, 1977, 1701, 1603 (C=C), 1511 (C=C), 1486 (C=C), 1445 (C=C), 1343 (broad peak overlapping NO_2 and C-N), 1275, 1229, 1169, 1088, 1064, 1017, 989, 903, 829, 794
XAD4.A1-B5-C2	3262, 2973, 2939, 2633, 2323, 1920, 1701, 1605 (C=C), 1512 (C=C), 1488 (C=C), 1446 (C=C), 1351 (C-N), 1279, 1169, 1064, 989, 903, 830, 794
XAD4.A2	3018, 2963, 2932, 2484, 2163, 1981, 1603 (C=C), 1512 (C=C), 1487 (C=C), 1443 (C=C), 1245 (C-O), 1173 (C-O), 1034, 989, 903, 830, 794
XAD4.A2-B1	3021, 2921, 2529, 2161, 2028, 1653, 1604 (C=C), 1511 (C=C), 1445, 1352, 1246 (C-O), 1173 (C-O), 1035, 903, 829, 794
XAD4.A2-B2	2917, 2160, 1978, 1701 (C=O), 1631, 1604 (C=C), 1512 (C=C), 1487 (C=C), 1450, 1246, 1173, 1034, 990, 902, 830.
XAD4.A2-B3	3210, 2916, 2489, 2161, 1978, 1630, 1603 (C=C), 1586, 1563, 1512 (C=C), 1487 (C=C), 1444 (C=C), 1246, 1174, 1116, 1035, 1018, 989, 903, 830, 794
XAD4.A2-B4	2930, 2163, 2040, 1980, 1744 (C=O), 1653, 1604 (C=C), 1512 (C=C), 1487 (C=C), 1445 (C=C), 1246, 1173, 1086, 1035, 989, 903, 830.
XAD4.A2-B5	3332, 3018, 2964, 2932, 2165, 2050, 1981, 1603 (C=C), 1512 (C=C), 1487 (C=C), 1444 (C=C), 1246 (C-O), 1178 (C-O), 1034, 989, 903, 830, 795
XAD4.A2-B4-C1	3018, 2931, 2646, 1974, 1702 (C=O), 1630, 1604 (C=C), 1556, 1511 (C=C), 1485, 1444, 1338 (NO_2), 1273, 1173 (C-O), 1090, 1034, 989, 902, 829, 794
XAD4.A2-B5-C1	3019, 2963, 2932, 2411, 2161, 2019, 1979, 1631, 1604 (C=C), 1512 (C=C), 1487 (C=C), 1444 (C=C), 1341 (NO_2), 1246 (C-O), 1173 (C-O), 1034, 988, 903, 830, 795,
XAD4.A2-B5-C2	2930, 2860, 2400, 2161, 1979, 1942, 1652, 1632, 1604 (C=C), 1512 (C=C), 1487 (C=C), 1445 (C=C), 1285, 1246 (C-O), 1173 (C-O), 1034, 989, 903, 830, 795
Blank + Pen V	3371, 2930, 2446, 2162, 1772 (β-lactam), 1678, 1608 (C=C), 1509 (C=C), 1489 (C=C), 1442, 1332, 1215, 1081, 988, 836, 795.
XAD.A1 (with Pen V)	2929, 2163, 1772, (β-lactam), 1677, 1607 (C=C), 1511 (C=C), 1488 (C=C), 1443 (C=C), 1400, 1334, 1242, 1171, 903, 830.
XAD4.A1-B5	2930, 2164, 1780 (β-lactam), 1602 (C=C), 1512 (C=C), 1487 (C=C), 1445

(with Pen V)	(C=C), 1352, 1170, 1017, 903, 830
XAD4.A1-B5-C1 (with Pen V)	2930, 2162, 1772 (β-lactam), 1678, 1608 (C=C), 1510, 1488, 1443, 1335 (NO_2), 1244, 1080, 990, 903, 830.
XAD4.A1-B5-C2 (with Pen V)	2929, 2164, 1773 (β-lactam), 1680, 1608 (C=C), 1510 (C=C), 1488 (C=C), 1444 (C=C), 1333, 1244, 988, 830.
XAD.A2 (with Pen V)	3371, 2930, 2447, 2163, 1980, 1772 (β-lactam), 1677, 1608 (C=C), 1511 (C=C), 1489 (C=C), 1443 (C=C), 1329, 1245, 1175, 1037, 903, 830.
XAD4.A2-B5 (with Pen V)	3370, 2929, 2474, 2164, 1980, 1771 (β-lactam), 1607 (C=C), 1511 (C=C), 1488 (C=C), 1443 (C=C), 1332, 1245 (C-O), 1174, 1036, 902, 830.
XAD4.A2-B5-C1 (with Pen V)	3370, 2929, 2484, 2163, 1980, 1772 (β-lactam), 1677, 1607 (C=C), 1511 C=C), 1488 (C=C), 1442 (C=C), 1334 (NO_2), 1245 (C-O), 1037, 989, 903, 830.
XAD4.A2-B5-C2 (with Pen V)	3371, 2931, 2473, 1772 (β-lactam), 1678, 1608 (C=C), 1506 (C=C), 1490 (C=C), 1441, 1333, 1244 (C-O), 1051, 903, 837.
PETp.Blank	2928, 2163, 1979, 1714 (C=O), 1579, 1506 (C=C), 1456, 1409, 1341, 1240, 1092, 1017, 872
PETp.A2	2956, 2927, 2854, 2162, 2031, 1979, 1715, 1607 (C=C), 1579, 1507 (C=C), 1457, 1410, 1373, 1341, 1242 (C-O), 1173 (C-O), 1093, 1018, 972, 899, 872, 846
PETp.A2-B1	2955, 2923, 2853, 2489, 2161, 2034, 1978, 1714, 1611 (C=C), 1580, 1506 (C=C), 1453, 1410, 1371, 1341, 1243 (C-O), 1096, 1040, 1018, 972, 872
PETp.A2-B2	2969, 2921, 2852, 2451, 2161, 2033, 1976, 1714, 1609 (C=C), 1580, 1507 (C=C), 1455, 1410, 1370, 1341, 1242, 1174, 1095, 1039, 1018, 972,872
PETp.A2-B3	2968, 2921, 2851, 2490, 2169, 2033, 1977, 1713, 1608 (C=C), 1579, 1506 (C=C), 1454, 1409, 1370, 1340, 1241, 1174, 1095, 1041, 1018, 972, 872
PETp.A2-B4	2972, 2919, 2851, 2488, 2161, 2033, 1978, 1714 (C=O), 1608 (C=C), 1580, 1506 (C=C), 1454, 1409, 1370, 1340, 1242, 1174, 1095, 1040, 1018, 972, 872
PETp.A2-B5	925, 2851, 2160, 2031, 1978, 1713, 1606 (C=C), 1506 (C=C), 1457, 1409, 1340, 1241 (C-O), 1173 (C-O), 1094, 1018, 972, 872, 847
PETp.A2-B4-C1	2970, 2926, 2177, 2021, 1978, 1715 (C=O), 1612, 1580, 1507 (C=C), 1471, 1455, 1410, 1371, 1341 (NO_2), 1242 (C-O), 1175 (C-O), 1096, 1018, 972, 872, 846
PETp.A2-B5-C1	2927, 2854, 2490, 2162, 2031, 1979, 1715, 1610 (C=C), 1579, 1507 (C=C), 1458, 1410, 1373, 1341 (NO_2), 1243, 1175, 1095, 1018, 973, 872, 847
PETp.A2-B5-C2	2926, 2853, 2161, 2034, 1715, 1613 (C=C), 1579, 1506 (C=C), 1456, 1411, 1342, 1243 (C-O) 1175 (C-O), 1096, 1019, 1042, 1019, 973, 872, 847
PET Blank + Pen V	2926, 2161, 2033, 1714, 1579, 1506, 1456, 1409, 1341, 1242, 1094, 1018, 872.
PETp.A2 (with Pen V)	2926, 2161, 2031, 1714, 1613 (C=C), 1578, 1506 (C=C), 1470, 1410, 1341, 1242, 1095, 1018, 872.
PETp.A2-B5 (with Pen V)	3426, 2924, 2160, 2032, 1713, 1611 (C=C), 1579, 1506 (C=C), 1456, 1409, 1341, 1241, 1093, 1017, 872.
PETp.A2-B5-C1 (with Pen V)	3428, 2923, 2161, 2033, 1713, 1611 (C=C), 1579, 1506 (C=C), 1456, 1409, 1341, 1241, 1094, 1018, 872.
PETp.A2-B5-C2 (with Pen V)	3431, 2926, 2161, 2033, 1714, 1613 (C=C), 1579, 1506 (C=C), 1457, 1410, 1340, 1242, 1096, 1018, 872.
LDPE.Blank	2916, 2849, 1473, 1308, 1251, 1176, 1081, 909
LDPE.A2	2915, 2848, 1603 (C=C), 1507 (C=C), 1473, 1324, 1299, 1245 (C-O), 1166, 1027, 953, 832
LDPE.A2-B1	2915, 2848, 2160, 1604 (C=C), 1507 (C=C), 1472, 1326, 1246 (C-O), 1167, 1028, 164, 833
LDPE.A2-B2	2914, 2848, 2161, 1979, 1742 (C=O), 1606 (C=C), 1472, 1303, 1253 (C-O), 1171, 1032, 908,
LDPE.A2-B3	2915, 2848, 2160, 1604 (C=C), 1582, 1507 (C=C), 1473, 1325, 1300, 1245 (C-O), 1167, 1118, 1028, 945, 908, 833, 806

LDPE.A2-B4	2915, 2848, 2160, 2022, 1977, 1687, 1604 (C=C), 1582, 1507 (C=C), 1472, 1326, 1300, 1245 (C-O), 1167, 1118, 1028, 954, 833, 805,
LDPE.A2-B5	2915, 2848, 1604 (C=C), 1472, 1368, 1247, 1169, 1096, 805
LDPE.A2-B4-C1	2914, 2848, 2191, 2136, 2018, 1980, 1472, 1247 (C-O), 1175 (C-O), 1041, 908, 806
LDPE.A2-B5-C1	2915, 2848, 2162, 2020, 1472, 1261, 1091
LDPE.A2-B5-C2	2915, 2848, 2162, 1978, 1473, 1368, 1261, 1096, 1024, 908
UHMW.Blank	2915, 2848, 1472, 1080, 889
UHMW.A2	2916, 2829, 2229, 2158, 2021,1974, 1472, 1304, 1249 (C-O), 1171 (C-O), 1062
UHMW.A2-B1	2915, 2849, 2160, 2019, 1977, 1511 (C=C), 1472, 1302, 1247 (C-O), 1037
UHMW.A2-B2	2916, 2849, 2160, 2028, 1977, 1713 (C=O), 1606 (C=C), 1509 (C=C), 1472, 1368, 1305, 1246 (C-O), 1172, 1101, 1038, 836, 816
UHMW.A2-B3	2916, 2849, 2442, 2160, 2026, 1742, 1511 (C=C), 1472, 1246 (C-O), 1172, 1036
UHMW.A2-B4	2915, 2849, 2160, 2023, 1978, 1609 (C=C), 1511 (C=C), 1472, 1368, 1302, 1247 (C-O), 1173, 1037, 908
UHMW.A2-B5	2916, 2849, 2158, 2021, 1472, 1350, 1304, 1248 (C-O), 1172 (C-O), 1079, 946, 830
UHMW.A2-B4-C1	2915, 2848, 2190, 2165, 2036, 1981, 1720 (C=O), 1472, 1247 (C-O), 1085, 1039
UHMW.A2-B5-C1	2916, 2849, 2158, 2020, 1974, 1472, 1349, 1305, 1175 (C-O), 1080, 952, 829
UHMW.A2-B5-C2	2916, 2849, 2229, 2190, 2157, 1976, 1472, 1351, 1304, 1174 (C-O), 1080, 945, 829
Flat Substrates	
PDMS.Blank	2962, 1446, 1412, 1257, 1010, 788
PDMS.A2	2962, 2905, 1607 (C=C), 1511 (C=C), 1445, 1412, 1257, 1010, 863, 788
PDMS.A2-B2	2962, 2905, 1607 (C=C), 1512 (C=C), 1445, 1412, 1258, 1010, 863, 788
PDMS.A2-B4	1700 (C=O), 1608 (C=C), 1559, 1512 (C=C), 1445, 1412, 1258, 1010, 863, 788
PDMS.A2-B5	2962, 2905, 1606 (C=C), 1510 (C=C), 1445, 1412, 1258, 1010, 863, 788
PDSM.A2-B6	2962, 2905, 1608 (C=C), 1512 (C=C), 1445, 1412, 1258, 1010, 863, 844, 788.
PDMS.A2-B7	2962, 1611 (C=C), 1512 (C=C), 1445, 1412, 1010, 863, 843, 787, 756
PDMS.A2-B8	3317, 2962, 2904, 1608 (C=C), 1510 (C=C), 1446, 1411, 1257, 1010, 843, 788.
PDMS.A2-B2-C1	2964, 2905, 1606 (C=C), 1510 (C=C), 1445, 1412, 1257, 1009, 843
PDMS.A2-B4-C1	2962, 2905, 1606 (C=C), 1509 (C=C), 1446, 1258, 1010, 863, 843, 788
TPU.Blank	3330, 2957, 1700, 1596, 1527, 1413, 1309, 1229, 1073, 816, 770
TPU.A2	3445, 2955, 2838, 1724, 1600 (C=C), 1510 (C=C), 1462, 1413, 1305, 1245, 1217, 1171, 1061, 1032, 816, 769.
TPU.A2-B2	3329, 2960, 1726, 1700 (C=O), 1596 (C=C), 1413, 1309, 1221, 1141, 1075, 847
TPU.A2-B4	3329, 2958, 1700 (C=O) , 1596 (C=C), 1527, 1462, 1413, 1358, 1308, 1229, 1172, 1073, 962, 847, 816, 770.
TPU.A2-B2-C	3329, 2960, 1726, 1700, 1596 (C=C, NO_2), 1527 (NO_2), 1413, 1358 (NO_2), 1309, 1220 ,1172, 1075, 847
TPU.A2-B4-C1	3328, 2957, 1701 (C=O), 1597 (C=C), 1527, 1462, 1413, 1359 (NO_2) , 1308, 1219, 1173, 1065, 955, 816, 770.
COC.Blank	2944, 2866, 1455, 1359, 1294, 1155, 1039, 885
COC.A2	2944, 2866, 1606 (C=C), 1510 (C=C), 1455, 1359, 1294, 1253 (C-O), 1172 (C-O), 1155, 1139, 1039, 929, 885, 809, 788.
COC.A2-B2	2944, 2866, 1607 (C=C), 1508 (C=C), 1455, 1360, 1294, 1254, 1227, 1155, 1139, 1046, 885
COC.A2-B4	2944, 2866, 1455, 1359, 1294, 1254, 1155, 1040, 929, 884, 779
COC.A2-B4-	2943, 2866, 1734, 1717, 1455, 1359, 1293, 1254, 1227, 1155, 1040, 929, 885,

C1	779.
PET.Blank	3430, 2969, 1714, 1505, 1409, 1340, 1245, 1098, 1045, 872
PET.A2	2969, 1713, 1606 (C=C), 1578 (C=C), 1471, 1409, 1341, 1246, 1097, 1018, 970, 872, 847, 723.
PET.A2-B2	3030, 2969, 1713 (C=O) , 1578, 1505 (C=C), 1409, 1341, 1246, 1098, 1044, 847
PET.A2-B4	2969, 2907, 1713 (C=O), 1604 (C=C), 1578 (C=C), 1471, 1409, 1341, 1246, 1098, 1043, 1018, 971, 872, 847.
PET.A2-B6	3430, 2969, 1714, 1603 (C=C), 1506 (C=C), 1455, 1386, 1245, 1098, 1044, 872
PET.A2-B7	2969, 1715, 1603 (C=C), 1506 (C=C), 1409, 1340, 1244, 1098, 1044, 872
PET.A2-B2-C	3430, 2969, 1713, 1578, 1505 (C=C), 1454, 1386 (hidden NO_2), 1245, 1098, 1044, 847
PET.A2-B4-C1	2969, 2907, 1715 (C=O), 1578, 1505 (C=C), 1471, 1455, 1409, 1340, 1245, 1120, 1098, 1018, 970, 872, 847, 793, 723.
PMMA.Blank	2995, 2950, 1723, 1483, 1435, 1387, 1246, 1143, 1063, 986, 912, 841
PMMA.A2	2995, 2950, 2843, 1723, 1636, 1483, 1435, 1387, 1240, 1143, 1063, 986, 966, 912, 841.
PMMA.A2-B4	2994, 2950, 2844, 1723, 1637, 1483, 1435, 1387, 1240, 1190, 1143, 1063, 986, 966, 912, 841.
PC.Blank	2967, 1769, 1602 , 1503, 1465, 1409, 1387, 1219, 1187, 1158, 1080, 1013, 828.
PC.A2	2967, 2937, 2050, 1770, 1605 (C=C), 1584 (C=C), 1505 (C=C), 1409, 1364, 1223, 1189, 1160, 1079, 1013, 813.
PC.A2-B2	2968, 1770, 1605 (C=C), 1503 (C=C), 1409, 1364, 1221, 1188, 1159, 1079, 1013, 828.
PC.A2-B4	2965, 2836, 1769, 1700 (C=O), 1685, 1647, 1604 (C=C), 1505 (C=C), 1463, 1410, 1302, 1224, 1190, 1160, 1079, 1013, 888, 828
PC.A2-B7	2965, 2835, 2051, 1985, 1771, 1604 (C=C), 1584, 1506 (C=C), 1412, 1364,1238, 1191, 1162, 1079, 1012, 811.
PC.A2-B8	2967, 1770, 1604 (C=C), 1503 (C=C), 1409, 1364, 1220, 1188, 1159, 1079, 1013, 828.
PC.A2-B2-C1	2967, 2051, 1764, 1646, 1601 (C=C), 1503 (C=C), 1409, 1365 (NO_2), 1222, 1188, 1159, 1080, 885, 828.
PS.Blank	3025, 2920, 1942, 1869, 1801, 1746, 1601, 1542, 1451, 1322, 1181, 1028, 964
PS.A2	3025, 2920, 1602, 1583, 1507, 1451, 1301, 1242 (C-O), 1167, 1110, 1029, 834
PS.A2-B2	3289, 2915, 1601 (C=C), 1583 (C=C), 1491, 1418, 1363, 1245 (C-O), 1027, 831
PS.A2-B4	3025, 2922, 2836, 1603 (C=C), 1507 (C=C), 1452, 1326, 1301, 1243 (C-O), 1167, 1110, 1028, 832
PS.A2-B6	3024, 2920, 1646, 1601 (C=C), 1583 (C=C), 1302, 1244 (C-O), 1169, 1029, 831
PS.A2-B7	3025, 2921, 1603 (C=C), 1584, 1508 (C=C), 1452, 1301, 1243 (C-O), 1168, 1028, 830
PS.A2-B8	3296, 2921, 1604 (C=C), 1507 (C=C), 1452, 1374, 1242 (C-O), 1028
PS.A2-B2-C1	3735, 3288, 2967, 1559 (C=C), 1508 (C=C), 1252 (C-O), 1172, 1017, 799
PP.Blank	2950, 2917, 1457, 1376, 1167, 998, 973, 841
PP.A2	2916, 1608 (C=C), 1510 (C=C), 1461, 1376, 1303, 1250 (C-O), 1168, 1103, 1041, 998, 973, 899
PP.A2-B2	2917, 1609 (C=C), 1509 (C=C), 1456, 1376, 1303, 1255 (C-O), 1219, 1167, 1103, 1044, 998, 899
PP.A2-B2-C1	2916, 2849, 1734, 1609 (C=C), 1463, 1376, 1303, 1250 (C-O), 1168, 1043, 998, 841

Appendix D: UV-Vis spectra on disc

Appendix E: BET data and analysis on disc

Appendix F: WCA data and analysis on disc

Appendix G: XPS data

Actual XPS spectra on disc

Sample	% Atomic Concentration				Atomic ratio	
	C	N	O	Others	Found	Expected
2.17	76.01	4.67	19.20	Br: 0.07 F: 0.05	N/C: 0.0610 O/C: 0.253 Br/C: 0.000921 F/C: 0.000658	N/C: 0.00 O/C: 0.125 Br/C: 0.0625 F/C: 0.0625
2.20	75.39	5.53	18.74	Br:0.15 F: 0.19	N/C: 0.0734 O/C: 0.249 Br/C: 0.00199 F/C: 0.00199	N/C: 0.0286 O/C: 0.0571 Br/C: 0.0571 F/C: 0.0286
2.31	75.70	5.58	18.51	Br: 0.22	N/C: 0.0737 O/C: 0.245 Br/C: 0.00291	N/C: 0.0909 O/C: 0.0364 Br/C: 0.0364
XAD4. Blank	81.91	4.17	13.91	-	N/C: 0.0509 O/C: 0.170	N/C: 0.00 O/C: 0.00
XAD4. A1	68.41	2.98	28.61	-	N/C: 0.0436 O/C: 0.418	N/C: 0.118 O/C: 0.00
XAD4. A2	85.31	1.08	13.61	-	N/C: 0.0127 O/C: 0.160	N/C: 0.00 O/C: 0.00
XAD4. A1-B4	78.77	6.64	14.59	-	N/C: 0.0843 O/C: 0.185	N/C: 0.167 O/C: 0.0833
XAD4. A1-B5	87.10	1.47	11.43	-	N/C: 0.0215 O/C: 0.131	N/C: 0.192 O/C: 0.0385
XAD4. A2-B2	73.78	7.87	18.34	-	N/C: 0.107 O/C: 0.249	N/C: 0.136 O/C: 0.182
XAD4. A2-B4	76.31	6.86	16.84	-	N/C: 0.0899 O/C: 0.221	N/C: 0.143 O/C: 0.190
XAD4. A2-B5	70.41	4.46	25.13	-	N/C: 0.0633 O/C: 0.357	N/C: 0.125 O/C: 0.125
XAD4. A1-B4-C1	80.88	5.49	13.63	-	N/C: 0.0679 O/C: 0.169	N/C: 0.133 O/C: 0.111
XAD4. A1-B5-C1	83.46	3.58	12.96	-	N/C: 0.0429 O/C: 0.155	N/C: 0.149 O/C: 0.0851
XAD4. A1-B5-C2	80.92	5.90	13.00	Br: 0.18	N/C: 0.0729 O/C: 0.161 Br/C: 0.00222	N/C: 0.128 O/C: 0.0426 Br/C: 0.0426
XAD4. A2-B4-C1	82.38	3.16	14.46	-	N/C: 0.0384 O/C: 0.189	N/C: 0.0930 O/C: 0.163
XAD4. A2-B5-C1	76.16	6.80	17.05	-	N/C: 0.0893 O/C: 0.224	N/C: 0.111 O/C: 0.133
XAD4. A2-B5-C2	73.98	8.45	17.43	Br: 0.13	N/C: 0.114 O/C: 0.236 Br/C: 0.00176	N/C: 0.0889 O/C: 0.0889 Br/C: 0.0444
Blank LDPE	95.49	0.08	4.43		N/C: 0.000838 O/C: 0.0464	N/C: 0.00 O/C: 0.00

Sample	% Atomic Concentration				Atomic ratio	
	C	N	O	Others	Found	Expected
LDPE. A2	95.41	0.23	4.36	-	N/C: 0.00262 O/C: 0.0457	N/C: 0.00 O/C: 0.133
LDPE. A2-B4	90.40	1.32	8.28	-	N/C: 0.0146 O/C: 0.0916	N/C: 0.143 O/C: 0.190
LDPE. A2-B4-C1	92.23	1.59	6.18	-	N/C: 0.0172 O/C: 0.0670	N/C: 0.0930 O/C: 0.163
PDMS. Blank	44.05	0.00	25.31	Si: 30.64	N/C: 0.00 O/C: 0.564	N/C: 0.00 O/C: 0.500
PDMS. A2	52.60	0.00	22.63	Si: 24.77	N/C: 0.00 O/C: 0.430	N/C: 0.00 O/C: 0.133
PDMS. A2-B2	47.50	0.40	29.1	Si: 23.00	N/C: 0.00842 O/C: 0.613	N/C: 0.0870 O/C: 0.174
PDMS. A2-B4	48.46	0.27	26.81	Si: 24.46	N/C: 0.00557 O/C: 0.553	N/C: 0.0909 O/C: 0.182
PDMS. A2-B5	45.27	0.00	30.35	Si: 24.38	N/C: 0.00 O/C: 0.670	N/C: 0.125 O/C: 0.125
PDMS. A2-B6	47.85	0.46	28.67	Si: 23.01	N/C: 0.00961 O/C: 0.599	N/C: 0.143 O/C: 0.190
PDMS. A2-B7	48.20	0.45	28.37	Si: 22.97	N/C: 0.00934 O/C: 0.589	N/C: 0.136 O/C: 0.0909
PDMS. A2-B8	50.06	0.10	28.51	Si: 21.33	N/C: 0.00200 O/C: 0.570	N/C: 0.0690 O/C: 0.0690
PDMS. A2-B2-C1	44.08	0.40	31.51	Si: 24.01	N/C: 0.00907 O/C: 0.715	N/C: 0.0909 O/C: 0.159
PDMS. A2-B4-C1	54.75	0.32	24.71	Si: 20.22	N/C: 0.00585 O/C: 0.451	N/C: 0.0930 O/C: 0.162
PC. Blank	82.23	1.39	16.38	-	N/C: 0.0250 O/C: 0.201	N/C: 0.00 O/C: 0.214
PC.A2	79.17	1.56	19.27	-	N/C: 0.0197 O/C: 0.243	N/C: 0.00 O/C: 0.133
PC. A2-B2	79.34	3.24	17.41	-	N/C: 0.0408 O/C: 0.219	N/C: 0.0870 O/C: 0.174
PC. A2-B4	76.93	4.27	18.81		N/C: 0.0555 O/C: 0.245	N/C: 0.0909 O/C: 0.182
PC. A2-B7	75.55	3.16	21.29	-	N/C: 0.0418 O/C: 0.282	N/C: 0.136 O/C: 0.0909
PC. A2-B8	76.46	1.73	21.82	-	N/C: 0.0226 O/C: 0.286	N/C: 0.0690 O/C: 0.0690
PET. Blank	77.94	1.71	20.35	-	N/C: 0.0230 O/C: 0.262	N/C: 0.00 O/C: 0.00
PET. A2	77.58	1.91	20.51	-	N/C: 0.0323 O/C: 0.266	N/C: 0.00 O/C: 0.133
PET. A2-B2	75.89	1.62	22.49	-	N/C: 0.0213 O/C: 0.296	N/C: 0.0890 O/C: 0.174
PET. A2-B4	72.17	1.11	26.72	-	N/C: 0.0154 O/C: 0.370	N/C: 0.0909 O/C: 0.181
PET. A2-B6	72.38	3.25	24.38	-	N/C: 0.0449 O/C: 0.337	N/C: 0.143 O/C: 0.190

Sample	% Atomic Concentration				Atomic ratio	
	C	N	O	Others	Found	Expected
PET. A2-B7	73.21	3.75	23.04	-	N/C: 0.0512 O/C: 0.315	N/C: 0.136 O/C: 0.0909
PET. A2-B2-C1	76.24	1.77	21.99	-	N/C: 0.0232 O/C: 0.288	N/C: 0.0909 O/C: 0.159
PET. A2-B4-C1	78.97	1.39	19.64	-	N/C: 0.0176 O/C: 0.249	N/C: 0.0930 O/C: 0.162
TPU. Blank	85.02	0.31	14.67	-	N/C: 0.00371 O/C: 0.173	N/C: 0.118 O/C: 0.176
TPU. A2	83.58	0.73	15.69	-	N/C: 0.00873 O/C: 0.188	N/C: 0.00 O/C: 0.133
TPU. A2-B2	83.58	2.03	14.40	-	N/C: 0.0243 O/C: 0.171	N/C: 0.0890 O/C: 0.174
TPU. A2-B2-C1	84.09	0.95	14.97	-	N/C: 0.0198 O/C: 0.178	N/C: 0.0909 O/C: 0.159
TPU. A2-B4	82.27	1.00	16.73	-	N/C: 0.0122 O/C: 0.203	N/C: 0.0909 O/C: 0.182
TPU. A2-B4-C1	82.18	1.13	16.69	-	N/C: 0.0138 O/C: 0.203	N/C: 0.0930 O/C: 0.162
COC. Blank	89.10	0.98	9.92	-	N/C: 0.0110 O/C: 0.111	N/C: 0.00 O/C: 0.00
COC. A2	88.34	1.27	10.39	-	N/C: 0.0144 O/C: 0.118	N/C: 0.00 O/C: 0.133
COC. A2-B2	87.56	1.18	11.26		N/C: 0.0135 O/C: 0.129	N/C: 0.0890 O/C: 0.174
COC. A2-B2-C1	84.46	0.65	14.89	-	N/C: 0.00770 O/C: 0.176	N/C: 0.0909 O/C: 0.159

Appendix H: Bioassay results

Results of hole-plate bioassay

LDPE	Ctrl	A2	A2-B1	.A2-B2	A2-B3	A2-B4	A2-B5	A2-B4-C1	A2-B4-C1 (UV)	A2-B5-C1	A2-B5-C1 (UV)	A2-B5-C2	A2-B5-C2 (UV)
E.coli	10.0	10.0	10.0	26.0	10.0	10.0	10.0	10.0	10.0	10.0	10.0	10.0	10.0
E.coli	10.0	10.0	10.0	24.5	10.0	10.0	10.0	10.0	10.0	10.0	10.0	10.0	10.0
S.aureus	10.0	11.0	10.0	34.0	17.0	10.0	13.5	11.0	11.0	14.0	13.5	14.0	12.0
S.aureus	10.0	11.0	10.0	35.0	12.0	10.0	13.0	10.0	11.0	13.0	13.0	13.0	13.0
Average													
E.coli	10.0	10.0	10.0	25.3	10.0	10.0	10.0	10.0	10.0	10.0	10.0	10.0	10.0
S.aureus	10.0	11.0	10.0	34.5	14.5	10.0	13.3	10.5	11.0	13.5	13.3	13.5	12.5
E.coli													
Standard deviation	0.0	0.0	0.0	1.1	0.0	0.0	0.0	0.0	0.0	0.0	0.0	0.0	0.0
Standard Error	0.0	0.0	0.0	0.8	0.0	0.0	0.0	0.0	0.0	0.0	0.0	0.0	0.0
S.aureus													
Standard deviation	0.0	0.0	0.0	0.7	3.5	0.0	0.4	0.7	0.0	0.7	0.4	0.7	0.7
Standard Error	0.0	0.0	0.0	0.5	2.5	0.0	0.3	0.5	0.0	0.5	0.3	0.5	0.5

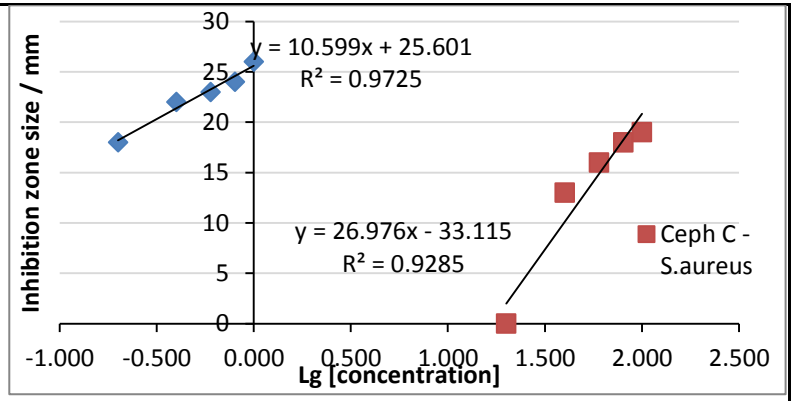
PETp	Ctrl	A2	A2-B1	A2-B2	A2-B3	A2-B4	A2-B5	A2-B4-C1	A2-B4-C1 (UV)	A2-B5-C1	A2-B5-C1 (UV)	A2-B5-C2	A2-B5-C2 (UV)
E.coli	10.0	10.0	10.0	11.3	10.0	10.0	10.0	10.0	10.0	10.0	10.0	10.0	10.0
E.coli	10.0	10.0	10.0	11.5	10.0	10.0	10.0	10.0	10.0	10.0	10.0	10.0	10.0
S.aureus	11.0	13.0	11.0	29.0	19.0	16.0	17.0	17.0	18.5	13.0	16.5	16.5	19.0
S.aureus	10.0	15.0	12.0	25.0	20.0	17.5	16.0	17.5	18.0	15.0	16.0	17.0	20.0
Average													
E.coli	10.0	10.0	10.0	11.4	10.0	10.0	10.0	10.0	10.0	10.0	10.0	10.0	10.0
S.aureus	10.5	14.0	11.5	27.0	19.5	16.8	16.5	17.3	18.3	14.0	16.3	16.8	19.5
E.coli													
Standard deviation	0.0	0.0	0.0	0.1	0.0	0.0	0.0	0.0	0.0	0.0	0.0	0.0	0.0
Standard Error	0.0	0.0	0.0	0.1	0.0	0.0	0.0	0.0	0.0	0.0	0.0	0.0	0.0
S.aureus													
Standard deviation	0.7	1.4	0.7	2.8	0.7	1.1	0.7	0.4	0.4	1.4	0.4	0.4	0.7
Standard Error	0.5	1.0	0.5	2.0	0.5	0.8	0.5	0.3	0.3	1.0	0.3	0.3	0.5

Flat substrates	Inhibition zone size for *S.aureus* / mm						Inhibition zone size for E.coli / mm					
	Sample 1	Sample 2	Sample 3	Ave.	Std.Dev,	Std.Err.	Sample 1	Sample 2	Sample 3	Ave.	Std.Dev.	Std.Err
PDMS												
Ctrl-PenV	22.0	1.5	0.9	20.7	1.5	0.9	11.0	15.0	13.0	13.0	2.0	1.2
A2	24.0	0.6	0.3	24.3	0.6	0.3	11.0	16.0	13.0	13.3	2.5	1.5
A2-B2	25.0	0.0	0.0	25.0	0.0	0.0	12.0	15.0	12.0	13.0	1.7	1.0
A2-B4	24.0	1.0	0.6	23.0	1.0	0.6	14.0	14.0	12.0	13.3	1.2	0.7
A2-B5	23.0	0.6	0.3	22.7	0.6	0.3	11.0	12.0	11.0	11.3	0.6	0.3
A2-B7	24.0	0.6	0.3	23.7	0.6	0.3	17.0		14.0	15.5	2.1	1.2
A2-B2-C1	24.0	2.1	1.2	22.3	2.1	1.2	13.0	11.0	14.0	12.7	1.5	0.9
PC												
Ctrl-PenV	27.0	26.0	28.0	27.0	1.0	0.6	10.0	10.0	11.0	10.3	0.6	0.3
A2	29.0	28.0	30.0	29.0	1.0	0.6	12.0	13.0	12.0	12.3	0.6	0.3
A2-B2	31.0	30.0	30.0	30.3	0.6	0.3	12.0	15.0	14.0	13.7	1.5	0.9
A2-B4	30.0	28.0	29.0	29.0	1.0	0.6	14.0	13.0	15.0	14.0	1.0	0.6
A2-B7	30.0	29.0	29.0	29.3	0.6	0.3	11.0	14.0	11.0	12.0	1.7	1.0
PET												
Ctrl-PenV	19.0	20.0	20.0	19.7	0.6	0.3	10.0	11.0	10.0	10.3	0.6	0.3
A2	20.0	20.0	22.0	20.7	1.2	0.7	10.0	10.0	11.0	10.3	0.6	0.3
A2-B2	20.0	20.0	22.0	20.7	1.2	0.7	11.0	10.0	11.0	10.7	0.6	0.3
A2-B4	21.0	19.0	21.0	20.3	1.2	0.7	10.0	10.0	11.0	10.3	0.6	0.3
A2-B7	20.0	19.0	22.0	20.3	1.5	0.9	10.0	11.0	11.0	10.7	0.6	0.3
A2-B2-C1	20.0	19.0	20.0	19.7	0.6	0.3	11.0	10.0	11.0	10.7	0.6	0.3
TPU												
Ctrl-Pen V	22.0	24.0	21.0	22.3	1.5	0.9	12.0	15.0	14.0	13.7	1.5	0.9
A2	25.0	24.0	24.0	24.3	0.6	0.3	16.0	15.5	16.0	15.8	0.3	0.2
A2-B2	23.0	25.0	23.0	23.7	1.2	0.7	14.0	13.0	12.0	13.0	1.0	0.6
A2-B2-C1	20.0	21.0	23.0	21.3	1.5	0.9	18.0	18.0	19.0	18.3	0.6	0.3

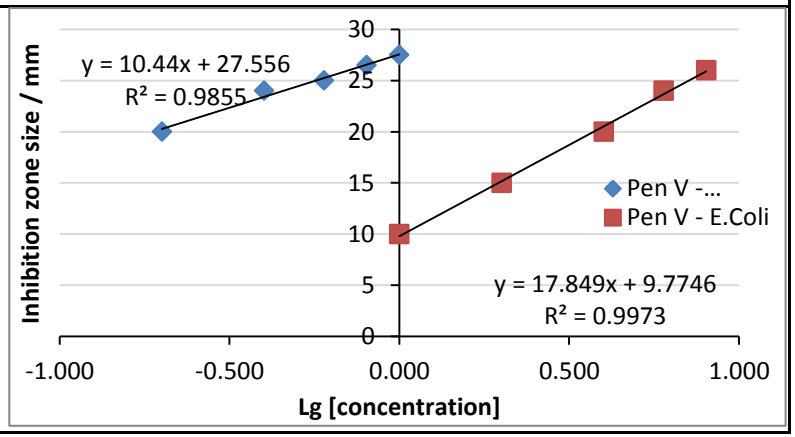
Calibration

Inhibition zones were measured in mm and correlated to the Cephalosporin C calibration as a measure of biocide activity. The calibration curve was drawn with clear zone size against log of molar concentration of Cephalosporin C. In addition, calibration by Penicillin V was also conducted. However, inhibition zones beyond 30mm were considered to be out of accuracy calibration range as the zone sizes would have been affected and limited by the diffusion rates of the antibiotics, resulting in inaccuracy of the correlation.

Conc of *Ceph. C* in µg/100µL	Lg [conc]	Clear zone size for *E.coli*/ mm	Conc of *Ceph. C* in µg/100µL	Lg [conc]	Inhibition zone size for *S.aureus*/ mm
0.2	-0.699	18	20	1.301	0
0.4	-0.398	22	40	1.602	13
0.6	-0.222	23	60	1.778	16
0.8	-0.097	24	80	1.903	18
1	0.000	26	100	2.000	19



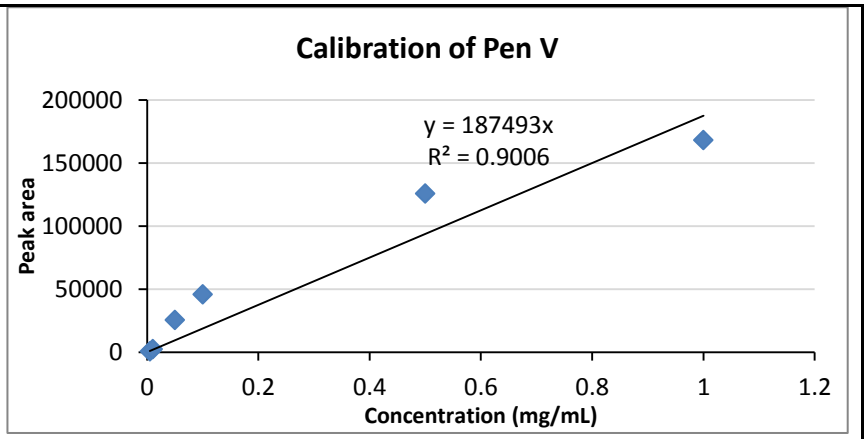
Concentration of Pen V / µg/mL	Lg[conc]	Clearzone size for S.aureus/ mm	µg/mL	Concentration of Pen V / µg/mL	Clearzone size for E.coli / mm
0.2	-0.699	20	1	0.000	10
0.4	-0.398	24	2	0.301	15
0.6	-0.222	25	4	0.602	20
0.8	-0.097	26.5	6	0.778	24
1	0.000	27.5	8	0.903	26



Appendix I: HPLC-MS calculations and results

By plotting the cumulative graph of penicillin V released, amounts of Penicillin V released by the beads in total by the beads were estimated.

Concentration of Pen V in mg/mL	Peak area
0	0
0.005	506
0.01	2426
0.05	25565
0.1	45877
0.5	125764
1	167959



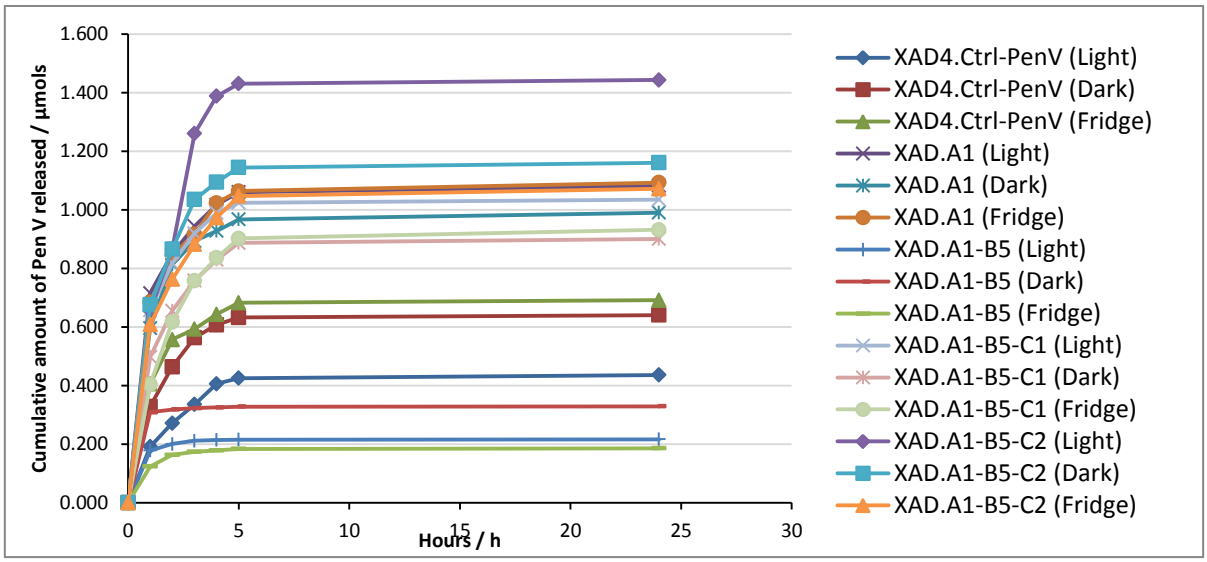
	Peak Area						Cumulative Peak Area					
Time/hr	1	2	3	4	5	24	1	2	3	4	5	24
XAD4.Ctrl-PenV (Light)	6951	2930	2341	2563	689	395	6951	9881	12222	14785	15474	15869
XAD4.Ctrl-PenV (Dark)	11960	4934	3618	1596	906	296	11960	16894	20512	22108	23014	23310
XAD4.Ctrl-PenV (Fridge)	14763	5514	1301	1838	1443	314	14763	20277	21578	23416	24859	25173
XAD.A1 (Light)	26053	4899	3428	2658	1568	802	26053	30952	34380	37038	38606	39408
XAD.A1 (Dark)	21709	7907	2921	1253	1422	837	21709	29616	32537	33790	35212	36049
XAD.A1 (Fridge)	24934	5827	2610	3900	1476	1047	24934	30761	33371	37271	38747	39794
XAD.A1-B5 (Light)	6479	818	394	94	50	39	6479	7297	7691	7785	7835	7874
XAD.A1-B5 (Dark)	11228	347	185	71	111	29	11228	11575	11760	11831	11942	11971
XAD.A1-B5 (Fridge)	4499	1450	376	179	170	91	4499	5949	6325	6504	6674	6765
XAD.A1-B5-C1 (Light)	23931	5821	3743	2526	1261	405	23931	29752	33495	36021	37282	37687
XAD.A1-B5-C1 (Dark)	18097	5760	3764	2574	2098	501	18097	23857	27621	30195	32293	32794
XAD.A1-B5-C1 (Fridge)	14696	7758	5136	2861	2393	1081	14696	22454	27590	30451	32844	33925
XAD.A1-B5-C2 (Light)	23832	7715	14363	4637	1556	455	23832	31547	45910	50547	52103	52558
XAD.A1-B5-C2 (Dark)	24611	6900	6173	2170	1814	606	24611	31511	37684	39854	41668	42274
XAD.A1-B5-C2 (Fridge)	22122	5656	4339	3316	2696	898	22122	27778	32117	35433	38129	39027

Given from the calibration curve:

Peak area = 187493 (Concentration in mg/mL)

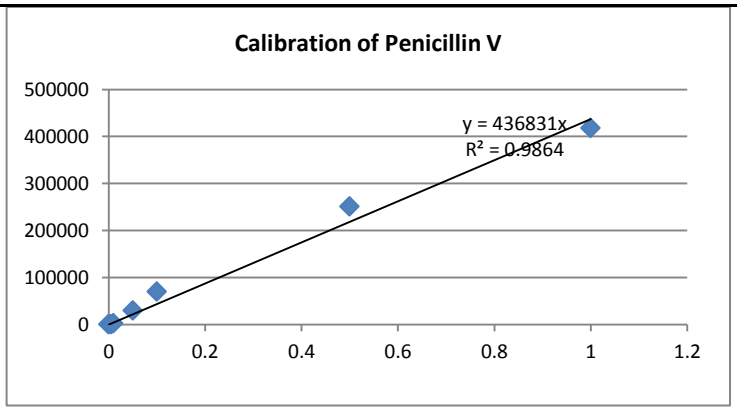
Cumulated peak area can then be converted to concentration in mg/mL, and to cumulative amounts of Penicillin V in mg (2 mL of solution per vial). This can then be converted to cumulative amounts in µmol. (See detailed calculations in soft copy)

	Cumulative amount of Penicillin V in µmols						
Time	0	1	2	3	4	5	24
XAD4.Ctrl-PenV (Light)	0.000	0.191	0.271	0.336	0.406	0.425	0.436
XAD4.Ctrl-PenV (Dark)	0.000	0.328	0.464	0.563	0.607	0.632	0.640
XAD4.Ctrl-PenV (Fridge)	0.000	0.405	0.557	0.592	0.643	0.683	0.691
XAD.A1 (Light)	0.000	0.715	0.850	0.944	1.017	1.060	1.082
XAD.A1 (Dark)	0.000	0.596	0.813	0.893	0.928	0.967	0.990
XAD.A1 (Fridge)	0.000	0.685	0.845	0.916	1.023	1.064	1.093
XAD.A1-B5 (Light)	0.000	0.178	0.200	0.211	0.214	0.215	0.216
XAD.A1-B5 (Dark)	0.000	0.308	0.318	0.323	0.325	0.328	0.329
XAD.A1-B5 (Fridge)	0.000	0.124	0.163	0.174	0.179	0.183	0.186
XAD.A1-B5-C1 (Light)	0.000	0.657	0.817	0.920	0.989	1.024	1.035
XAD.A1-B5-C1 (Dark)	0.000	0.497	0.655	0.758	0.829	0.887	0.900
XAD.A1-B5-C1 (Fridge)	0.000	0.404	0.617	0.758	0.836	0.902	0.932
XAD.A1-B5-C2 (Light)	0.000	0.654	0.866	1.261	1.388	1.431	1.443
XAD.A1-B5-C2 (Dark)	0.000	0.676	0.865	1.035	1.094	1.144	1.161
XAD.A1-B5-C2 (Fridge)	0.000	0.607	0.763	0.882	0.973	1.047	1.072



However, calibration have to be conducted for every new batch of testing as variation in pump pressure, condition of columns can affect the calibration curve, and thus, results obtained.

Concentration of Pen V in mg/mL	Peak Area
0	0
0.005	487
0.01	2256
0.05	29341
0.1	69876
0.5	250672
1	417738



	Peak area					Cumulative				
	1.5	3	5	7	24	1.5	3	5	7	24
XAD4.Ctrl-PenV (Light)	52672	13398	8321	13385	8188	52672	66070	74391	87776	95964
XAD4.Ctrl-PenV (Dark)	34369	14772	6480	15275	10119	34369	49141	55621	70896	81015
XAD4.Ctrl-PenV (Fridge)	24528	16459	19270	15149	1938	24528	40987	60257	75406	77344
XAD4.A2 (Light)	71706	19413	17611	14653	10354	71706	91119	108730	123383	133737
XAD4.A2 (Dark)	57901	27769	23001	22148	11802	57901	85670	108671	130819	142621
XAD4.A2 (Fridge)	55931	29691	22699	12389	4869	55931	85622	108321	120710	125579
XAD4.A2-B5 (Light)	69033	31727	23038	11423	9383	69033	100760	123798	135221	144604
XAD4.A2-B5 (Dark)	67657	31008	21230	9975	6024	67657	98665	119895	129870	135894
XAD4.A2-B5 (Fridge)	67279	28745	20327	10604	9557	67279	96024	116351	126955	136512
XAD4.A2-B5-C1 (Light)	93621	33174	26943	7836	9725	93621	126795	153738	161574	171299
XAD4.A2-B5-C1 (Dark)	61124	29019	26016	14319	11736	61124	90143	116159	130478	142214
XAD4.A2-B5-C1 (Fridge)	83409	26904	17990	11078	11854	83409	110313	128303	139381	151235
XAD4.A2-B5-C2 (Light)	96716	33961	30960	26360	13520	96716	130677	161637	187997	201517
XAD4.A2-B5-C2 (Dark)	83081	41819	24211	25645	14629	83081	124900	149111	174756	189385
XAD4.A2-B5-C2 (Fridge)	101111	33019	22783	19644	16610	101111	134130	156913	176557	193167

From calibration curve: Peak Area = 436831 (Concentration in mg/mL), cumulative amount of Penicillin V can be calculated.

	Cumulative amount of Penicillin V in µmols					
	0	1.5	3	5	7	24
XAD4.Ctrl-PenV (Light)	0.000	0.621	0.779	0.877	1.034	1.131
XAD4.Ctrl-PenV (Dark)	0.000	0.405	0.579	0.656	0.836	0.955
XAD4.Ctrl-PenV (Fridge)	0.000	0.289	0.483	0.710	0.889	0.912
XAD4.A2 (Light)	0.000	0.845	1.074	1.281	1.454	1.576
XAD4.A2 (Dark)	0.000	0.682	1.010	1.281	1.542	1.681
XAD4.A2 (Fridge)	0.000	0.659	1.009	1.277	1.423	1.480
XAD4.A2-B5 (Light)	0.000	0.814	1.188	1.459	1.594	1.704
XAD4.A2-B5 (Dark)	0.000	0.797	1.163	1.413	1.531	1.602
XAD4.A2-B5 (Fridge)	0.000	0.793	1.132	1.371	1.496	1.609
XAD4.A2-B5-C1 (Light)	0.000	1.103	1.494	1.812	1.904	2.019
XAD4.A2-B5-C1 (Dark)	0.000	0.720	1.062	1.369	1.538	1.676
XAD4.A2-B5-C1 (Fridge)	0.000	0.983	1.300	1.512	1.643	1.782
XAD4.A2-B5-C2 (Light)	0.000	1.140	1.540	1.905	2.216	2.375
XAD4.A2-B5-C2 (Dark)	0.000	0.979	1.472	1.757	2.060	2.232
XAD4.A2-B5-C2 (Fridge)	0.000	1.192	1.581	1.849	2.081	2.277

